ANALYZING THE IN VIVO ROLES OF HISTONE ACETYLTRANSFERASES GCN5 AND ESA1 IN RSC RECRUITMENT AND REMODELING ACTIVITY GENOME-WIDE IN *SACCHAROMYCES CEREVISIAE*

by

EMILY R. BIERNAT

A dissertation submitted in partial fulfillment of the
requirements for the degree of

DOCTOR OF PHILOSOPHY IN BIOLOGICAL AND BIOMEDICAL SCIENCES

2023

Oakland University
Rochester, Michigan

Doctoral Advisory Committee:

Chhabi K. Govind, Ph.D., Chair
G. Rasul Chaudhry, Ph.D.
Sara Blumer-Schuette, Ph.D.

To my mother, Lori Biernat, for all of your love and support

ACKNOWLEDGMENTS

I want to thank my advisor, Dr. Chhabi K. Govind, for giving me the opportunity to work on this project, encouraging me to present some of these findings at several conferences, and providing strong foundational support during the challenging parts of this project. I would also like to thank my committee members, Dr. Rasul Chaudhry and Dr. Sara Blumer-Schuette, for their insights on this work. I would especially like to thank Dr. Blumer-Schuette for also giving me the opportunity to present these findings at the American Society for Microbiology Michigan Branch Meeting.

I would like to give special thanks to Dr. Joseph Reese for his gracious donation of the TBP antibody for ChIP-seq experiments, Dr. Frank Uhlmann for donating the RSC catalytic strains, and the National Institutes of Health and Oakland University for funding. I would also like to thank the Govind Lab, especially Mansi Verma, Matthew Werick, Uzair Khan, and Sama Joseph, for encouraging a supportive and collaborative work environment. Special thanks to Uzair Khan for performing the Western Blot included in this work.

Lastly, I would like to thank my brother, Brandon, and my father, Michael, for their love and understanding before and during this project. Special thanks to my mother, Lori, for encouraging my academic development. I know you would have supported me during this project, and you will be forever loved and missed.

Emily R. Biernat

ABSTRACT

ANALYZING THE IN VIVO ROLES OF HISTONE ACETYLTRANSFERASES GCN5 AND ESA1 IN RSC RECRUITMENT AND REMODELING ACTIVITY GENOME-WIDE IN *SACCHAROMYCES CEREVISIAE*

by

Emily R. Biernat

Adviser: Chhabi K. Govind, Ph.D.

Transcription is important for gene expression and is a tightly-controlled process involving multiple mechanisms of regulation, including regulation by chromatin structure. Chromatin consists of nucleosomes, which are comprised of DNA wrapped around histone proteins. Chromatin remodelers such as the Remodels the Structure of Chromatin (RSC) complex play important roles in controlling DNA accessibility to the transcriptional machinery and organizing chromatin throughout the genome. Mutations in yeast and mammalian RSC orthologs have been linked to dysregulated cell cycle progression, chromosome segregation, stress response, and developmental processes.

In this study, we investigated the mechanisms by which RSC associates with chromatin on a genome-wide scale and the impact of disrupted RSC-chromatin interactions on transcription. Previous studies have suggested that nucleosome acetylation via histone acetyltransferases (HATs) may facilitate RSC binding to chromatin. To explore this, we examined the effects of removing HATs Gcn5 and Esa1 on RSC occupancy. Surprisingly, our results revealed distinct effects of HAT loss on RSC occupancy at promoters and gene bodies. In promoters, the loss of HATs increased RSC

association with promoter nucleosomes, particularly in promoters containing partially-unwrapped fragile nucleosomes. Additionally, we found that HAT-mediated acetylation is crucial for maintaining nucleosome depletion at promoters. Conversely, HAT loss decreased RSC occupancy in gene bodies of highly transcribed genes. This reduction in RSC binding was dependent on histone tails, as cells lacking these tails also showed a significant loss of RSC binding to gene bodies.

High-resolution mapping and analyses demonstrated that RSC-bound nucleosomes, particularly in gene bodies, were highly accessible. Consistent with these findings, loss of HAT functions resulted in widespread transcriptional changes, impacting both transcription initiation and elongation. This work provides valuable insights into how HAT-mediated histone modifications regulate RSC association with chromatin and the consequent impact on global transcription.

TABLE OF CONTENTS

TABLE OF CONTENTS—Continued

TABLE OF CONTENTS—Continued

LIST OF TABLES

LIST OF FIGURES

LIST OF ABBREVIATIONS

-1_Nuc	-1 Nucleosome position
'-1_Nuc-T10	10% genes with the highest RSC occupancies at the -1 nucleosome position
-1, NDR, +1	average occupancies at the promoter region
ΔH3 Occ.	Change in H3 Occupancies
ΔNuc Occ.	Change in Nucleosome Occupancies
ΔRpb3 Occ.	Change in Nucleosome Occupancies
ΔRSC Occ.	Change in RSC Occupancies
ΔTBP Occ.	Change in TBP Occupancies
+1_Nuc	+1 Nucleosome position
3-IAA	3-Indoleacetic Acid, auxin
A	Alanine
AA	Anchor-Away
Ac	Acetylation
AID	Auxin-Inducible Degradation
B10	10% genes with the lowest Pol II occupancies
bp	base pair
BrD	Bromodomain
CDS	Coding Sequences
ChIP	Chromatin Immunoprecipitation
ChIP-seq	Chromatin Immunoprecipitation followed by Sequencing

Esa1	Essential Sas2-related Acetyltransferase 1
FN	Fragile Nucleosome
FN_NDR	genes containing Fragile Nucleosomes within NDRs
Gcn5	General Control Non-repressible 5
GRF	General Regulatory Factor
H3	histone H3
H3Ac	Acetylated histone H3
H4	histone H4
H4Ac	Acetylated histone H4
HAT	Histone Acetyltransferase
HS	Heat Shock
HS-WT	Wild Type cells that have been Heat Shocked
K	Lysine
kb	kilobase pair
MNase	Micrococcal Nuclease
MNase ChIP-seq	Chromatin Immunoprecipitation followed by Sequencing using MNase-digested chromatin
MPDF	MNase-Protected DNA Fragments
NDR	Nucleosome-Depleted Region
NS	Not Significant
NTT	N-Terminal Tail

NuA4	Nucleosomal Acetylation of H4 complex
Nuc	Nucleosome
Occ.	Occupancies
PIC	Pre-Initiation Complex
Pol II	RNA Polymerase II
Pol II-B10	10% genes with the lowest Pol II occupancies
Pol II-T10	10% genes with the highest Pol II occupancies
Pol II-T20	20% genes with the highest Pol II occupancies
Rapa	Rapamycin
Rep	Replicate
Rpb3	RNA Polymerase B3, the third largest subunit of RNA Polymerase II
RPG	Ribosomal Protein Gene
RSC	Remodels the Structure of Chromatin complex
RSC-T10	10% genes with the highest RSC occupancies
SAGA	Spt-Ada-Gcn5-Acetyltransferase complex
SN	Stable Nucleosome
SN_NDR	genes containing Stable Nucleosomes at the -1 nucleosome position
Sth1	Snf2 Homolog 1, the catalytic subunit of RSC
T10	10% genes with the highest Pol II occupancies
TBP	TATA-Binding Protein

TF	Transcription Factor
TSS	Transcription Start Site
WT	Wild Type
WT (H3)	Cells containing WT histone H3 tails
YPD	Yeast, Peptone, Dextrose media

CHAPTER ONE

INTRODUCTION

1.1 Overview of Transcription

Transcription is critical for gene expression and for the viability of all organisms. It is the cellular process in which ribonucleic acid (RNA) molecules are synthesized from deoxyribonucleic acid (DNA) templates via RNA polymerase (Clancy, 2008; Greber and Nogales, 2019). Many of the RNA products can be translated into proteins needed for cellular function, while many of the non-coding RNA products are used to facilitate translation and protein production (Avcilar-Kucukgoze and Kashina, 2020; Hoagland et al., 1958; Karakas and Ozpolat, 2021; Loveland et al., 2017; Ramakrishnan, 2002). Transcription is tightly regulated to allow for accurate gene expression, which is critical for the development of an organism and for the rapid and appropriate response to environmental changes within or outside of the organism. Dysregulation of transcription has been linked to many developmental diseases and other diseases, such as cancer, highlighting the importance of understanding this fundamental process. (Bradner et al., 2017; Cox and Goding, 1991; Izumi, 2016; Liao et al., 2018; Loveland et al., 2017; Mark and Rape, 2021; Sun et al., 2023; Wu et al., 2020)

1.1.1 RNA Polymerase is Required for Transcription

RNA polymerase is an essential enzyme complex that reads the DNA template and transcribes it into RNA (Greber and Nogales, 2019). Even though RNA polymerase is present in all organisms and even in some viruses (Greber and Nogales, 2019), the composition of RNA polymerase tends to increase in complexity as lifeforms become

more complex. For instance, viral RNA polymerases typically consist of a single subunit, whereas prokaryotic RNA polymerases generally are composed of 5 subunits (Minakhin et al., 2001). These five core subunits are conserved in eukaryotic RNA polymerases, which can harbor up to 12 additional subunits (Ehara et al., 2017). Additionally, eukaryotic cells utilize three distinct polymerases that produce different RNA products (Roeder and Rutter, 1969, 1970; Sklar et al., 1975). RNA polymerase I (Pol I) synthesizes ribosomal RNA (rRNA) precursors, which are later processed into the 25S/28S, 18S, and 5.8S rRNA molecules, while RNA polymerase III (Pol III) is responsible for synthesizing 5S rRNA, transfer RNAs (tRNAs) involved in translation, and small non-coding RNAs (snRNAs) (Roeder and Rutter, 1970; Weinmann and Roeder, 1974). RNA polymerase II (Pol II) produces the messenger RNAs (mRNAs) that are later translated for protein synthesis and is the polymerase responsible for transcribing the ~6000 protein-coding genes in *Saccharomyces cerevisiae*, commonly known as budding yeast. These three eukaryotic polymerases are highly conserved from yeast to humans and are essential for the viability of organisms.

Despite the variation in subunit composition, the basic process of RNA synthesis is highly conserved in prokaryotes and eukaryotes. With the help of different factors, RNA polymerase binds to the template DNA strand. Helicase activity by one of the transcription factors melts 10-15 base pairs of DNA in an ATP-dependent manner to form a transcription bubble, in which the template strand will be free to hybridize with the complementary RNA strand that will be transcribed. The template strand is fed through the polymerase's active site, and ribonucleotides (rNTPs) access the active site via a separate channel. The rNTPs are incorporated into the RNA strand as the

polymerase catalyzes the formation of phosphodiester bonds between the rNTPs, where the 3' hydroxyl of the previously-added rNTP on the RNA strand undergoes nucleophilic attack by the α-phosphate of the rNTP to be added to the strand. The β and γ phosphates of the newly-added rNTP are released as pyrophosphate (PPi). The RNA polymerase then repeats this process of rNTP incorporation, synthesizing an RNA strand complementary to the template strand in the 5' → 3' direction until the RNA polymerase encounters elements that cause it to disassociate from the template DNA, terminating transcription (Cramer et al., 2001; Gnatt et al., 2001; Kaplan, 2013; Svetlov and Nudler, 2013).

1.1.2 General Structure of Eukaryotic Genes

The basic layout of transcribed genes in eukaryotes can be divided into three regions, regardless of the RNA polymerase that transcribes them (Figure 1.1). The coding sequence (CDS) or open reading frame (ORF) of a gene is the sequence that contains all of the information required to synthesize the protein product and is part of the region transcribed by RNA polymerase. Upstream of the 5' end of the coding sequence is the transcription start site (TSS), where RNA polymerase begins synthesizing the RNA strand. Approximately 35 bp upstream of the TSS lies the core promoter, which contains the DNA elements necessary to recruit general transcription factors (GTFs) and RNA polymerase to the gene to initiate transcription at a basal level. The terminator region is located towards the end of the gene, downstream of the 3' end of the CDS. It contains the transcription termination site (TTS), where the RNA polymerase dissociates from the DNA to end transcription. In addition to these three main areas of a gene, other genomic features help regulate transcription or are important for processes downstream of transcription. Upstream activating sequences (UAS; enhancers in higher eukaryotes)

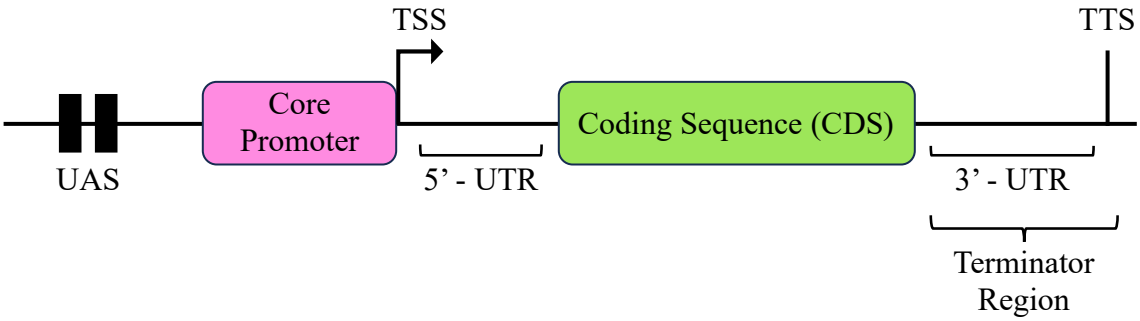

Figure 1.1. Organization of a typical protein-coding gene. The core promoter of the gene contains DNA elements that recruit transcription factors and RNA polymerase II (Pol II) to the gene, which allows for the initiation of transcription. Proximal to the promoter is the transcription start site (TSS), where transcription begins. Upstream of the core promoter lies the upstream activating sequence (UAS), which contains DNA elements that transcriptional activators and coactivators can recognize and bind to in order to further enhance transcription. The Coding Sequence (CDS) is the sequence of DNA that encodes for the protein. When the DNA from the CDS is transcribed into mRNA, this region of the mRNA will be read by the ribosome and translated into protein. In between the core promoter and the CDS is a stretch of DNA encoding for the 5'- untranslated region (UTR) that will be transcribed and processed to include the 5'- methyl guanylate cap, but does not encode for protein and is not translated. Downstream of the CDS lies the terminator region that consists of the 3' - UTR and the transcription termination site (TTS). The 3' - UTR also does not encode for protein and includes the poly-A tail that is important for transcription termination.

are cis-acting elements in *S. cerevisiae* localized upstream of the core promoters of genes (Butler and Kadonaga, 2002). Coactivators and other factors can bind to UASs to induce gene transcription at a level higher than that of the promoter alone (Clancy, 2008; Hahn and Young, 2011). Additionally, for protein-coding genes, there are untranslated regions (UTRs) that flank the CDS of a gene. While these sequences, along with the CDS, are transcribed to produce messenger RNA (mRNA), unlike the CDS of the mRNA, these regions are not translated into protein but are instead post-transcriptionally processed (Schuster and Hsieh, 2019). The 5' - UTR is capped with methyl guanylate and is involved in translation initiation (Hinnebusch, 2014), whereas the 3' - UTR includes the poly-A tail (Tanguay and Gallie, 1996). Both UTRs are important for mRNA stability (Leppek et al., 2018; Schuster and Hsieh, 2019; Tanguay and Gallie, 1996).

Even though this gene layout holds true for a majority of eukaryotic genes, it is important to note that there are differences in the structures of genes transcribed by each polymerase (Greber and Nogales, 2019). Indeed, there is even variation in structure between protein-coding genes, and the majority of genes are unique in terms of structure.

1.2 The Stages of Pol II Transcription are Regulated by Cis- and Trans-Regulatory Elements

The mechanisms by which Pol I, Pol II, and Pol III transcribe their respective genes are distinct from one another (Arimbasseri et al., 2014; Paule and White, 2000). Nonetheless, the process of transcription by these polymerases can be broken down into three basic steps: initiation, elongation, and termination. Transcription initiation occurs when transcription factors and RNA polymerase are recruited to the promoter to form the Pre-Initiation Complex (PIC). During Pol II initiation, these recruited factors are called

general transcription factors (GTFs), but Pol I and Pol III utilize factors that are structurally or functionally similar to GTFs (Vannini, 2013; Vannini and Cramer, 2012). During the elongation phase, DNA in the coding sequence is unwound and RNA polymerase synthesizes RNA complementary to the template DNA strand. Transcription termination differs slightly between the three eukaryotic polymerases, but all involve a termination site, dissociation of the polymerase, and release of the RNA transcripts. Because the majority of *S. cerevisiae's* genes (~6000 vs. 428 RNA genes) encode for proteins and are transcribed by Pol II (Belda et al., 2019; Steinmetz et al., 2006), the details of Pol II transcription and regulation of transcription will be discussed below.

1.2.1 Promoter DNA Sequences Regulate Transcription Initiation

The core promoters of Pol II-transcribed genes have been shown to contain up to four characterized elements in yeast: the TATA-box, the TFIIB recognition element (BRE), the initiator recognition element (Inr), and downstream core promoter element (DPE) (Butler and Kadonaga, 2002; Roy and Singer, 2015; Weis and Reinberg, 1992). These elements can appear in core promoters in varying combinations, but not one native promoter contains all of them (Carninci et al., 2006; Sandelin et al., 2007). Historically, yeast promoters have been assigned to one of two distinct classes based on the elements present within the promoter, including the presence or absence of a consensus TATA sequence (Huisinga and Pugh, 2004). Many Pol II promoters within *S. cerevisiae* lack a TATA box. The TATA-box is the primary binding site for the TATA-binding protein (TBP), a subunit of the transcription factor TFIID (Buratowski et al., 1989). Despite this, TFIID can still be recruited to these promoters via the recognition of other elements and factors interacting with those promoters (Cianfrocco et al., 2013; Patel et al., 2018; Pugh

and Tjian, 1991) so that the recruitment of Pol II and other PIC components can still occur. These genes are referred to as "TFIID-dominant" genes and are predominantly housekeeping genes that are constitutively transcribed (Huisinga and Pugh, 2004). In contrast, Pol II promoters containing more defined TATA-boxes are described as "SAGA-dominant" genes, since these genes are more dependent on the SAGA coactivator complex for initiation and show reduced levels of TFIID within their promoters (Huisinga and Pugh, 2004). These genes are typically stress response genes and their expression is highly regulated. Other researchers have attempted to classify genes based on core promoter content and have found that other factors, such as the poly-T content upstream of the transcription start site (TSS), can fine-tune promoter activity (Lubliner et al., 2015). Overall, core promoter DNA elements impact the recruitment of different factors to the promoter to regulate transcription initiation.

1.2.2 General Transcription Factors are Involved in Transcription Initiation

As stated above, transcription initiation of Pol II genes occurs when general transcription factors (GTFs) bind to promoter DNA and interact with other GTFs to form the Pre-Initiation complex (PIC) (Buratowski et al., 1989; Sainsbury et al., 2015). These factors coordinate with each other in a step-wise fashion. Transcription initiation begins when the TATA-binding protein (TBP) is recruited to the core promoter, either by itself or as part of the TFIID complex (Cormack and Struhl, 1992). TFIID can also be recruited to the core promoter via interaction with TFIIA (Lee et al., 2005; Verrijzer et al., 1995). TBP binding bends the DNA at a 90° angle so that the minor groove is accessible to TFIID binding (He et al., 2016), and the bound TFIID can then act as a platform for TFIIB (Sainsbury et al., 2013). TBP can then bind to the C-terminus of TFIIB, and the N-

terminus of TFIIB can interact with Pol II complexed with TFIIF. After TFIIF-Pol II binds, TFIIE is recruited to the complex and recruits TFIIH (Li et al., 1994; Maxon et al., 1994; Ohkuma et al., 1995). Once TFIIH binds, the PIC is fully assembled.

Up until the point of TFIIF-Pol II complex binding, the PIC is kept in a "closed complex" configuration, where the DNA contained within the PIC is linear except for the bend where it is bound by TBP (He et al., 2016). Structural studies of PIC have shown that both TFIIB and TFIIF are critical for the transition of the PIC from the closed complex to an "open complex," where the DNA is separated into single strands at the TSS and RNA synthesis can begin (Fishburn and Hahn, 2012; He et al., 2016; Treutlein et al., 2012). TFIIE is also important in forming and stabilizing the initial transcription bubble, along with TFIIB and TFIIF (Cabart and Luse, 2012; Grunberg et al., 2012). It is important to note that, unlike Pol I and Pol III, Pol II requires ATP hydrolysis for the PIC to transition from a closed to an open complex (Dvir et al., 1997b; Egly and Coin, 2011; Kim et al., 2000; Rimel and Taatjes, 2018). TFIIH is a 10-subunit complex that contains two ATP-dependent helicases (Ssl2 and Rad3 in yeast), and the ATP hydrolysis activity of Ssl2 is essential for promoter opening (Lin et al., 2005; Rimel and Taatjes, 2018). After TFIIH binds, TFIIB, E, F, and H stabilize the PIC and facilitate the melting of DNA surrounding the TSS (Fishburn and Hahn, 2012; Sainsbury et al., 2015). This induces a conformational change in the complex and allows the template DNA to be properly positioned in the active cleft of Pol II. At this stage, the PIC complex is now considered to be an "open complex" (Conaway et al., 2000; Dvir, 2002; Dvir et al., 1997a; Dvir et al., 1997b; Fishburn and Hahn, 2012; Grunberg et al., 2012; Sainsbury et al., 2013; Spangler et al., 2001; Wang et al., 2003). The TFIIB core domain is now positioned

differently than in closed complexes, and TFIIF is integral for this positioning (Fishburn and Hahn, 2012; Treutlein et al., 2012; Vannini and Cramer, 2012). The B-reader loop of TFIIB allows for the recognition of initiator sequences and the positioning of the TSS, allowing RNA polymerase to begin RNA synthesis (Sainsbury et al., 2013).

In order for transcription elongation to occur, the initiated polymerase must be released from the PIC and dissociate from the promoter. Termed promoter escape, this is the rate-limiting step in elongation. TFIIB, TFIIF, and TFIIH (including its helicase activity) are involved in promoter escape (Lin et al., 2005; Rimel and Taatjes, 2018; Yan et al., 1999). When the RNA becomes longer than six nucleotides, the TFIIB B-reader loop directs RNA to the exit tunnel of the PIC. When the synthesized RNA strand reaches 12-13 nucleotides in length, TFIIB is released from the transcription complex, which facilitates the release of Pol II from the promoter to continue the elongation of the RNA strand (Sainsbury et al., 2013). The helicase activity of TFIIH is also required for promoter escape (Lin et al., 2005; Rimel and Taatjes, 2018), and TFIIF has been shown to support TFIIH activity (Yan et al., 1999).

1.2.3 Coactivators Play a Role in PIC Formation

It has been shown that the binding of activators and co-activators such as Mediator and SAGA to UASs signals the assembly of the PIC and enhances transcription activation (Garcia-Molinero et al., 2018; Govind et al., 2005; Grunberg et al., 2016; Larschan and Winston, 2001; Yarrington et al., 2020). Additionally, the core module of SAGA is composed of TBP-associated factors (TAFs, also found in TFIID) and is involved in PIC assembly by recruiting TBP to a subset of genes via the interaction of its Spt3 and Spt8 subunits with TBP (Cheon et al., 2020; Sermwittayawong and Tan, 2006).

Indeed, the process of transcription initiation, and transcription as a whole, is incredibly complex, and researchers are still working to elucidate the precise mechanisms and interactions of each factor involved.

1.2.4 Phosphorylation of the Pol II C-Terminal Domain is Required for Promoter Escape and Elongation

Promoter escape and the transition from transcription initiation to elongation are mediated by phosphorylation of the C-terminal domain (CTD) of Pol II. Pol II consists of twelve subunits, including the largest subunit Rpb1 (Komarnitsky et al., 2000). Rpb1 possesses an unstructured CTD comprised of heptad repeats of the consensus sequence $Y_1S_2P_3T_4S_5P_6S_7$. The number of heptad repeats contained within the CTD varies between species, where the Pol II CTD of *S. cerevisiae* contains 26 repeats and the human Pol II CTD has 52 repeats (Buratowski, 2009; Egloff, 2012; Egloff and Murphy, 2008; Kim et al., 2004). All CTD residues except the proline residues can be phosphorylated (Buratowski, 2009; Kim et al., 2004; Komarnitsky et al., 2000).

Pol II is recruited to promoters in a hypophosphorylated state. After PIC assembly, the Kin28 subunit of TFIIH phosphorylates Ser5 and Ser7 of the CTD before the formation of the first phosphodiester bond in the RNA strand (Akhtar et al., 1996; Bataille et al., 2012; Kanin et al., 2007; Smolle and Workman, 2013). The Ser5 phosphorylation allows Pol II to dissociate from the other transcription factors, escape the promoter, and begin transcribing through the coding regions. Ser5 phosphorylation (Ser5P) also facilitates the recruitment of cyclin-dependent kinases Bur1/Bur2, which in turn phosphorylate Ser2 of the CTD when Pol II is at the 5' ORF of the gene (Bataille et al., 2012; Qiu et al., 2009). Additional Ser2P throughout the coding sequence is carried

out by the kinase Ctk1 and is necessary for sustained Pol II elongation (Bataille et al., 2012; Kim et al., 2010; Mayer et al., 2012; Mayer et al., 2010). Ser5P and Ser7P levels peak at around the 5' end of the CDS and decrease towards the 3' end of the gene, due to dephosphorylation by Rtr1 and Ssu72 (Mosley et al., 2009; Werner-Allen et al., 2011), while Ser2P levels are minimal at the 5' and increase towards the 3' end (Bataille et al., 2012; Mayer et al., 2012; Mayer et al., 2010). Ser2P is regulated by phosphatase Fcp1, which dephosphorylates Ser2P at the end of the gene and controls the rate at which Ser2P accumulates throughout the gene (Bataille et al., 2012; Mayer et al., 2012; Mayer et al., 2010). Additionally, Tyr1P has been shown to occur (Mayer et al., 2012), and its dephosphorylation at the 3' ends of genes by the CPF termination complex is needed to recruit Pcf11 and Rtt103 for proper termination (Schreieck et al., 2014).

1.2.5 Multiple Trans-Acting Factors Regulate Transcription Elongation

Transcription elongation is a highly-regulated process controlled by multiple factors, including general transcription factors TFIIF and TFIIS (Saunders et al., 2006). In addition to promoter release, the phosphorylated Pol II CTD can act as a scaffold for the recruitment of many different factors, such as the Elongator complex, Spt4/Spt5, and Paf1, to fine-tune Pol II processivity (Jeronimo et al., 2013; Otero et al., 1999). The Elongator complex was initially isolated as a part of an elongating Pol II complex and has been shown to increase the catalytic rate of elongating Pol II (Luo et al., 2012; Otero et al., 1999). Genetic screening studies revealed the interactions of Spt4/Spt5 with genes involved in transcription elongation (Fish and Kane, 2002; Hartzog et al., 1998; Wada et al., 1998), and Spt4/Spt5 has also been shown to affect Pol II processivity (Mason and Struhl, 2005; Quan and Hartzog, 2010). Both the Elongation complex and Spt4/Spt5 are

thought to facilitate elongation by reducing Pol II pausing or arrest in higher eukaryotic organisms and possibly in *S. cerevisiae*, though polymerase pausing has not been observed in the budding yeast (Bourgeois et al., 2002; Otero et al., 1999; Zhu et al., 2007).

Paf1 was identified as a Pol II-associated factor and was shown to facilitate elongation in vitro and in in vivo reporter assays. It regulates elongation by mediating co-transcriptional histone modifications of chromatin that Pol II encounters during elongation to facilitate Pol II passage through the chromatin (Chu et al., 2007; Dover et al., 2002; Krogan et al., 2003; Wood et al., 2003). Other factors such as the co-activator SAGA also regulate the chromatin structure at a gene to control elongation. These factors will be discussed in more detail in 1.3.5-1.3.9.

1.2.6 Factors that Regulate Transcription Termination

The RNA polymerase must dissociate from the template DNA after transcribing a gene and release the RNA transcript to terminate the transcription process. While Pol I and Pol III both recognize termination sites in the RNA and cleave the RNA to release the transcript themselves (Braglia et al., 2005; Jeong et al., 1995), additional protein factors are required for Pol II termination (Mischo and Proudfoot, 2013). Two major complexes mediate mRNA transcript cleavage in *S. cerevisiae*. The cleavage factor 1 (CF1; composed of Rna14, Rna15, Pcf11, Clp1, and Hrp1) and the cleavage and polyadenylation (CPF) complexes bind to the poly(A) site in the pre-mRNA and pre-mRNA cleavage is performed by the enzymatic activity of the CPF complex (Keller and Minvielle-Sebastia, 1997). Termination of Pol II elongation is thought to be controlled by the rate of elongation and the stability of the RNA/DNA hybrid within the complex

(Mischo and Proudfoot, 2013). Elongation complexes tend to slow down when encountering the poly-A signal on the mRNA due to the binding of factors to the Pol II CTD that decrease the speed of elongating Pol II (Kim et al., 2004; Mayer et al., 2010). The reduced elongation rate allows termination complexes to bind to the complex and act on the nascent RNA. The stability of the RNA/DNA hybrid is thought to be regulated by the binding of destabilizing factors. Rat1 and Pcf11 are being studied as destabilizing factors, as mutations in these proteins cause termination defects, and Rat1 and Pcf11 homologs have been shown to destabilize RNA/DNA hybrids in other organisms (Grzechnik et al., 2015; Mischo and Proudfoot, 2013). Sen1 is also a good candidate for RNA/DNA hybrid destabilization, as Sen1 has been shown to restrict the occurrence of RNA/DNA hybrids by preventing R-loop accumulation created by the hybrids (Mischo et al., 2011). However, it has also been shown that, unlike CF1 and CPF, Rat1 does not act at all genes (Dhoondia et al., 2021), suggesting that other destabilizing factors have yet to be identified.

1.3 Chromatin Structure Plays a Crucial Role in Regulating Transcription

1.3.1 Genomic DNA is Packaged into Chromatin

Eukaryotic DNA within the nucleus is packaged into chromatin. The fundamental unit of chromatin is the nucleosome, which consists of ~147 bp DNA wrapped 1.67 times around an octamer of histone proteins composed of two copies each of histone proteins H3, H4, H2A, and H2B (Luger et al., 1997a; Luger et al., 1997b). Each histone protein consists of a globular C-terminal body that interacts with other histone proteins and an N-terminal tail that extends from the body (Li, 1975; Wolffe and Hayes, 1999). The only exception is the H2A protein, which also has a relatively short C-terminal tail extending

from the globular body. Histones H3 and H4 dimerize with each other, and two H3-H4 dimers interact to form the H3-H4 tetramer of the nucleosome. X-ray crystallography has shown that the central 80 bp of nucleosomal DNA interacts with the H3-H4 tetramer. H2A and H2B form heterodimers with each other, and two H2A-H2B dimers bind to each side of the tetramer to form the disk-shaped body of the nucleosome from which the N-terminal tails can extend from the nucleosome body and interact with other factors (Eriksson et al., 2012). Nucleosomes are stabilized by linker histone H1 and are organized into repeating units on genomic DNA, with stretches of linker DNA separating the nucleosomes. This state of uncondensed chromatin has been observed as the 10 nm "beads on a string" motif, named for its appearance observed under an electron microscope under low salt conditions (Li, 1975). In-vitro studies suggested that chromatin condensed into higher-order structures at physiological conditions, forming 30 nm chromatin fibers and even fully-condensed chromosomes (Finch and Klug, 1976). In vivo studies, however, suggest that chromatin compaction results from the association of multiple 10 nm fibers with each other rather than the formation of higher chromatin structures (Fussner et al., 2012; Pepenella et al., 2014; Razin and Gavrilov, 2014). The regulation of chromatin structure is highly dependent on the life cycle of the cell, as well as the type and severity of stress that a cell is exposed to (Govind et al., 2005; Shi et al., 2021; Udvardy and Schedl, 1984; Xu and Zhu, 2010).

1.3.2 General Organization of Nucleosomes within a Typical Gene

Chromatin contained within a chromosome can be classified into euchromatin and heterochromatin (Tamaru, 2010). Heterochromatin consists of highly-condensed chromatin, is gene-poor, and is largely transcriptionally silent. In contrast, euchromatin is

less condensed, transcriptionally more active, and contains more genes than heterochromatin. In vitro assays in which nucleosomes were reconstituted on defined stretches of DNA, as well as in vivo assays involving digestion of chromatin using micrococcal nuclease (MNase), have provided researchers valuable insights as to how nucleosomes are positioned at a typical gene (Jiang and Pugh, 2009; Krietenstein et al., 2016). At the promoter, there is a region that is generally depleted of nucleosomes termed the nucleosome-depleted region (NDR) or nucleosome-free region (NFR) (Cui et al., 2012; Jiang and Pugh, 2009; Krietenstein et al., 2016). Two well-positioned nucleosomes flank either side of the NDR and are defined as the -1 and +1 nucleosomes. The -1 nucleosome is positioned immediately upstream of the NDR, while the +1 nucleosome is located downstream of the NDR, where the transcription start site (TSS) resides just inside the nucleosome border (Jiang and Pugh, 2009; Tsankov et al., 2010). Nucleosomes downstream of the +1 nucleosome (+2, +3, +4, and so on) are located in the coding region of the gene (Jiang and Pugh, 2009; Krietenstein et al., 2016). Nucleosomes more proximal to the TSS are evenly spaced apart, with stretches of linker DNA of equal length separating them (Krietenstein et al., 2016). Farther down the gene, away from the TSS, the nucleosomes become less well-positioned, with the linker DNA between them consisting of varying lengths.

1.3.3 Nucleosomes are Important Regulators of Transcription

Initially, it was thought chromatin had little effect on regulating transcription and other DNA-dependent processes. However, both in vitro and in vivo studies have shown that nucleosomes inhibit transcription (Knezetic et al., 1988; Lorch et al., 1987; Luse and Jacob, 1987). At NDRs, the +1 nucleosome inhibits transcription initiation by occluding

the TSS from Pol II (Jiang and Pugh, 2009; Oruba et al., 2020), and even though it has been demonstrated in vitro that Pol II is capable of transcribing through an individual nucleosome (Kireeva et al., 2002; Kulaeva et al., 2013), each nucleosome within the coding sequence (CDS) of a gene can act as a physical barrier to transcribing polymerase (Knezetic et al., 1988; Knezetic and Luse, 1986). Additionally, nucleosomes within the promoter have been shown to block other transcription factors from binding to their recognition sequences, inhibiting transcription initiation (Hieb et al., 2014). While the impact of nucleosomes on transcription has been extensively studied, nucleosomes are also inhibitory to other DNA-dependent processes. In particular, nucleosomes can also act as barriers to the machinery involved in DNA replication, and many of the same factors involved in regulating chromatin structure during transcription are also involved in replication (Lai and Pugh, 2017).

1.3.4 Trans-Acting Factors Tightly Regulate the Dynamic Organization of Chromatin

Similar to the thought that nucleosomes played no role in transcription initiation, researchers originally proposed that nucleosomes were static entities within the genome whose positions remained largely unchanged during DNA-dependent processes. Current studies have proven this notion as demonstrably false, as nucleosomes have to be evicted from the DNA, moved along the DNA strand, or otherwise altered to facilitate PIC assembly and Pol II traversal along the DNA (Clapier and Cairns, 2009; Clapier et al., 2016). Additionally, nucleosomes must either be replaced or returned to their original positions/composition to prevent cryptic transcription of naked DNA left after Pol II passage (Schwabish and Struhl, 2004).

The histone proteins within nucleosomes contain unstructured N-terminal tails

(NTTs) that protrude from the globular body of the nucleosome (Eriksson et al., 2012). The residues of these tails can be post-translationally modified (PTMs) to include many different marks, including acetylation, methylation, ubiquitination, phosphorylation, and sumoylation (Figure 1.2) (Andrews et al., 2016; Bannister and Kouzarides, 2011; Jaiswal et al., 2017; Jiang and Pugh, 2009; Li et al., 2007; Robzyk et al., 2000; Ryu et al., 2020; Slaughter et al., 2021; Strahl and Allis, 2000). Three types of factors are involved in the post-translational-modifications of histone proteins: writers, readers, and erasers (Xu et al., 2017). Writers add these PTMs to residues within the histone proteins. Histone acetyltransferases and histone methyltransferases are some of the most well-studied writers, and they add marks of active or repressive transcription to histone residues (Andrews et al., 2016; Briggs et al., 2001; Fuchs et al., 2009; Keogh et al., 2005; Marmorstein, 2001). Readers such as chromatin remodelers can recognize these modifications. They also function as effector proteins, where they act on the nucleosome accordingly to alter its histone composition, slide the nucleosome on the DNA or remove it completely (Carey et al., 2006; Lai and Pugh, 2017; Prajapati et al., 2020). Erasers can remove the marks to change the factors that interact with the nucleosome or return the nucleosome to its original composition or position (Xu et al., 2017). Histone deacetylases, histone demethylases, and phosphatases are erasers that remove histone acetylation, methylation, and phosphorylation, respectively (Rando and Winston, 2012; Tu et al., 2007). The dynamic organization of the chromatin structure by these factors has led to the proposal of a "histone code," which postulates that histone modifications act as a "code" and are deciphered by various factors to regulate chromatin structure (Jenuwein and Allis, 2001; Strahl and Allis, 2000). Several of the major readers, writers, and erasers

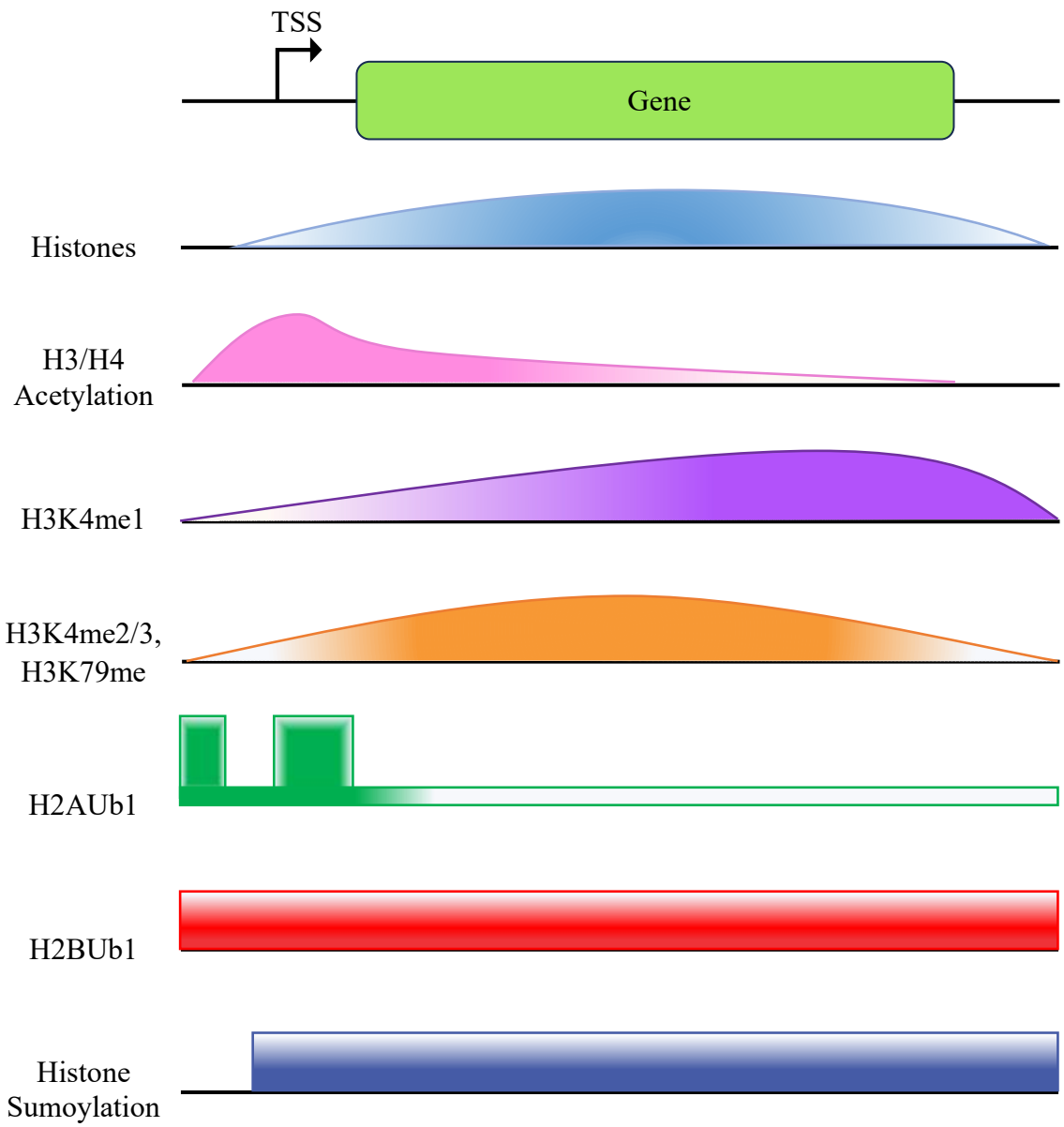

Figure 1.2. Genome-wide distribution pattern of histone modifications. Schematic showing the genome-wide average of several histone modifications across an area containing the transcription start site (TSS) and gene body. Ub, ubiquitination; me, methylation. Photo reprinted and adapted from (Li et al., 2007).

will be discussed in detail in sections 1.3.5-1.3.9.

1.3.5 Histone Methyltransferases Regulate Transcription by Methylating Histone Tails

Lysine and arginine residues within histone tails can be methylated in vivo (Jaiswal et al., 2017). Histone methyltransferases (HMTs) catalyze the transfer of up to three methyl groups to specific lysine and arginine residues on histone N-terminal tails (NTTs). In eukaryotes, the location of the methylation and the number of methyl groups added can indicate whether the modification marks transcriptionally active or repressive chromatin. However, the indication is not as strong as the presence of acetylation. This is because methylation was shown to be important in recruiting various factors to the modified nucleosome, including those involved in either active or repressive transcription (Fuchs et al., 2009).

Set1, Set2, and Dot1 are the three known HMTs in *S. cerevisiae*. Set1 is the catalytic subunit of the COMplex of Proteins Associated with Set1 (COMPASS) and is responsible for the mono-, di-, and tri-methylation of the 4th lysine residue of the histone H3 tail (H3K4; mono-, di-, and tri-methylation labeled as H3K4me1, H3K4me2, and H3K4me3, respectively) (Briggs et al., 2001; Miller et al., 2001). H3K4me3 levels peak near the 5' end of the ORF, while H3K4me2 and H3K4me1 are found further downstream of the ORF, towards the 3' end of transcribed genes (Liu et al., 2005). In yeast, H3K4 methylation, especially trimethylation, can be a mark of active transcription, though in some cases, H3K4 methylation is found in repressed genes (Ramakrishnan et al., 2016). Set1 recruitment requires the activity of several factors, including Paf1 and Bur1, as well as several modifications such as Rad6/Bre1-mediated H2B123 ubiquitination and phosphorylated Ser2 of the Pol II CTD (Dover et al., 2002; Krogan et

al., 2003; Laribee et al., 2005; Rando and Winston, 2012; Sun and Allis, 2002; Wood et al., 2003).

Set2 catalyzes the mono-, di- and trimethylation of H3K36 (Strahl et al., 2002). In contrast to H3K4me3, H3K36me3 levels peak at the 3' end transcribed ORFs and are minimal at the 5' end (Krogan et al., 2003; Liu et al., 2005). Set2 recruitment is less complex than Set1 recruitment and is mediated by the phosphorylation of Ser2 of the Pol II CTD (Kizer et al., 2005; Xiao et al., 2003). Even though H3K36 di- and trimethylation are found on transcriptionally-active genes, it has repressive functions. Consistent with this, Set2 deletion results in increased histone acetylation and cryptic transcription within ORFs (Carrozza et al., 2005; Govind et al., 2010; Joshi and Struhl, 2005; Kim and Buratowski, 2007).

Dot1 catalyzes H3K79 methylation, which is found throughout the coding regions of genes (Rando and Winston, 2012). However, H3K79 methylation does not correlate with active transcription and has been associated with transcriptional silencing of telomeres (Takahashi et al., 2011). Like Set1, Dot1 recruitment requires H2B123 ubiquitination, Rad6, Paf1, and Bre1 (Briggs et al., 2001; Rando and Winston, 2012; Sun and Allis, 2002; Wood et al., 2003).

1.3.6 Histone Acetyltransferases Acetylate Histone Tails to Activate Transcription

Histone acetylation is generally considered a strong marker for active transcription. Histone acetyltransferases (HATs) utilize acetyl CoA to catalyze the transfer of the acetyl group to lysine residues present in both histone NTTs and in the core body of histones (Marmorstein, 2001; Shahbazian and Grunstein, 2007). Histone acetylation of NTTs is thought to promote transcription in two major ways. The first way

involves the intrinsic charge of the acetylated residues. Lysine and arginine possess a positive charge and are thought to interact with the negatively-charged nucleosomal DNA to create a more compact, less accessible nucleosome. When these residues are acetylated, the positive charges are neutralized, allowing the NTTs to interact less with nucleosomal DNA (Berndsen and Denu, 2008; Lee and Workman, 2007). This results in a more accessible nucleosome, where the NTTs are free to interact with and be modified by other factors. The second way histone acetylation can promote transcription is by the recruitment of other factors such as chromatin remodelers that can alter chromatin structure and promote transcription (Carey et al., 2006; Hassan et al., 2007; Lai and Pugh, 2017; Spain et al., 2014).

Histone acetyltransferases can be divided into two major families based on the sequence similarities between the family members (Berndsen and Denu, 2008; Marmorstein, 2001). The GNAT (Gcn5-related-N-acetyltransferase) family is a functionally-diverse family that shares limited sequence homology in their conserved HAT domains, termed motifs A, B, C, D, and generally contain an acetylation-binding bromodomain in addition to their HAT domain (Berndsen and Denu, 2008; Neuwald and Landsman, 1997; Roth et al., 2001). This family includes Gcn5, Elp3, Hpa2, and Hat1 in yeast (Marmorstein, 2001; Neuwald and Landsman, 1997). The MYST (MOZ-Ybf3/Sas3-Sas2-Tip60) family is composed of Sas2, Sas3, and Esa1 in yeast, and its members are characterized by the presence of a methylation-binding chromodomain and a Zinc finger domain (Marmorstein, 2001). Several MYST members, including Esa1, contain motif A in their HAT domains (Marmorstein, 2001). Both GNAT mad MYST family members have been shown to regulate transcription. For instance, Elp3 is part of

the Elongator complex, and the Elongation complex has been shown to possess HAT activity important for the removal of histones in front of the elongation polymerase (Dauden et al., 2017; Winkler et al., 2002). Gcn5 and Esa1 have also been shown to be important for transcription and will be discussed below.

S. cerevisiae also contains two other HATs that are not easily classified into either HAT family. Rtt109 is a fungal-specific HAT that has been shown to acetylate H3K56 in a manner that is stimulated by the histone chaperone Asf1 (Lercher et al., 2018), and is also found at transcriptionally active genes (Schneider et al., 2006). H3K56 acetylation is important for DNA replication and surviving replication stress (Voichek et al., 2016). The Taf1 subunit of TFIID also shows HAT activity in vitro, but in-vivo studies have suggested that this activity is relatively minor (Durant and Pugh, 2006; Hilton et al., 2005).

General Control Non-repressible 5 (Gcn5) is a member of the GNAT family of HATs and is the major H3 HAT in *S. cerevisiae* (Carre et al., 2005; Haque et al., 2021). It can associate with TAFs and other factors to become part of the Spt-Ada-Gcn5 acetyltransferase (SAGA) and Ada2/Gcn5/Ada3 (ADA) complexes, which influence the specific lysine residues that Gcn5 will acetylate (Carre et al., 2005; Cheon et al., 2020; Eberharter et al., 1999; Haque et al., 2021; Marmorstein, 2001). For instance, recombinant Gcn5 has been shown to preferentially acetylate H3K14, but will also acetylate H4K8 and H4K16. However, Gcn5 that is present within the SAGA complex will acetylate lysine residues at positions 9, 14, 18, and 23 of histone H3, as well as residues on H2B (Cheon et al., 2020; Marmorstein, 2001). Likewise, Gcn5 present within the Ada complex will acetylate the same residues as Gcn5/SAGA, except for H3K9

(Eberharter et al., 1999). In addition to histone acetylation, Gcn5 has been shown to acetylate other proteins such as the Rsc4 subunit of the chromatin remodeler RSC and contains a bromodomain, indicating that acetylation may play a role in recruiting Gcn5 (Marmorstein, 2001; VanDemark et al., 2007).

Gcn5 plays a major role in transcription regulation. It has been found in the promoters and CDSs of many genes (Govind et al., 2007; Pascual-Garcia et al.; Robert et al., 2004) and has been shown to aid in the recruitment of TBP, Pol II, and other co-activators (Geng and Laurent, 2004; Qiu et al., 2004; Robert et al., 2004), possibly by being complexed with the multi-subunit, multi-functional SAGA co-activator complex. The 19-subunit SAGA complex has been extensively studied and is a major player in transcription (Chen and Pugh, 2021; Cheon et al., 2020; Huisinga and Pugh, 2004). It regulates transcription elongation in the *GAL1* gene by H3 acetylation to promote histone eviction, recruits TBP and other co-activators to promoters via interactions with its subunits such as Tra1, and is involved in recruiting Ctk1 to promote elongation via the deubiquitination of H2B by its subunit Ubp8 (Cheung and Diaz-Santin, 2019; Govind et al., 2007; Wyce et al., 2007). Gcn5 can also be part of the ADA complex, which is smaller compared to SAGA and lacks several activities that SAGA possesses, such as the deubiquitination of other proteins (Cheon et al., 2020; Eberharter et al., 1999). It is composed of 6 subunits, 4 of which are also found in SAGA, in addition to two subunits (Ach1 and Ach2) that SAGA does not possess. Following the differences in structure, the ADA complex has distinct protein interactions from SAGA. For instance, SAGA can interact with *S. cerevisiae* transcription activators Gcn4, Hap4, and Gal4 via the Tra1 subunit (Cheon et al., 2020; Cheung and Diaz-Santin, 2019; Natarajan et al., 1998).

However, the ADA complex cannot interact with Gcn4 (Eberharter et al., 1999).

Esa1 (Essential Sas2-related Acetyltransferase 1) is a member of the MYST family and is the only essential HAT to be discovered in *S. cerevisiae* (Smith et al., 1998; Wang et al., 2018). While related MYST family member Sas2 (something about silencing 2) can acetylate H4K16, Esa1 is the only HAT with H4 as their primary target, as Sas2 is unable to acetylate nucleosomal histones (Rando and Winston, 2012; Sutton et al., 2003). In addition to H4, Esa1 can acetylate H2A and the histone variant H2A.Z (Cheung and Diaz-Santin, 2019; Marmorstein, 2001; Noguchi et al., 2019). Like other MYST family members, Esa1 contains a chromodomain that can recognize histone methylation, though the exact residue is unknown (Kim and Buratowski, 2009). Esa1 is generally found as the catalytic subunit to the 13-subunits Nucleosomal Acetylation of H4 (NuA4) complex, though it can also exist in the smaller Piccolo subcomplex of NuA4 (Chittuluru et al., 2011; Wang et al., 2018). When Esa1 is present in the full NuA4 complex, it has a strong preference for acetylating H4, specifically residues at positions 5, 8, 12, and 16 (Marmorstein, 2001). Additionally, the Eaf3 and Yng2 subunits in the NuA4 complex can recognize H3K36 methylation and K3K4 methylation, respectively (Kim and Buratowski, 2009). Thus, H3 methylation may serve as a possible mechanism for NuA4 recruitment. The Piccolo subcomplex is the HAT module of NuA4, which contains additional modules and has been shown to make direct contact with the nucleosome (Chittuluru et al., 2011). NuA4 is critical for transcription. Like SAGA, NuA4 has also been shown to promote transcription elongation in *GAL1*, as it is required for H4 acetylation and nucleosome eviction (Ginsburg et al., 2009; Govind et al., 2007). Additionally, the TINTIN module of NuA4 interacts with phosphorylated Pol II and is

important for elongation (Ginsburg et al., 2009; Wang et al., 2018). NuA4 also contains a Tra1 complex that is important in recruiting NuA4 to promotors and for NuA4 interaction with other transcriptional activators (Cheung and Diaz-Santin, 2019; Ginsburg et al., 2009; Wang et al., 2018). NuA4 has also been implicated in DNA replication and repair, as cells containing mutations in Esa1 or Eaf1 (NuA4 subunit) are susceptible to DNA damaging agents, and Esa1 is required for repairing double-stranded breaks in DNA via the homologous recombination and non-homologous end-joining pathways (Cheung and Diaz-Santin, 2019; Noguchi et al., 2019). Furthermore, Eaf1 interacts with the Swi1-Swi3 replication fork protection complex in the fission yeast *Schizosaccharomyces pombe* and is thought to repair broken DNA replication forks (Noguchi et al., 2019).

Both Gcn5 and Esa1 have been shown to recruit chromatin remodelers such as SWI/SNF and RSC to both the promoters and coding sequences of genes (Ginsburg et al., 2009; Qiu et al., 2016; Spain et al., 2014; Zheng et al., 2023). These chromatin remodelers profoundly impact chromatin structure and can position or evict nucleosomes to allow for PIC assembly and Pol II transcription. These complexes will be discussed in more detail in 1.3.9, but nevertheless, highlight the importance of acetylation and HAT complexes in fine-tuning transcription.

1.3.7 Histone Deacetylases Remove Acetylation to Control Transcription

Histone acetylation is a mark of active transcription whose presence facilitates transcription, and the regulation of acetylation marks on genic nucleosomes is critical for fine-tuning transcription and gene expression. For instance, during elongation, HATs are thought to acetylate nucleosomes in front of Pol II and these nucleosomes are then remodeled to facilitate Pol II passage (Govind et al., 2010; Spain and Govind, 2011).

However, once Pol II has passed, if the acetylation is not removed, these nucleosomes could still be recognized by remodelers and other bromodomain-containing factors, resulting in the nucleosomes not being returned to their original position/conformation. This would lead to increased levels of transcription and cryptic transcription at exposed sites that resemble alternate TSSs (Carrozza et al., 2005; Kim et al., 2012; Lickwar et al., 2009). Histone deacetylases (HDACs) remove acetylation and have two major roles in transcription: they remove acetylation marks at promoters to promote gene repression, and they deacetylate ORF nucleosomes that elongating Pol II has cleared, returning the nucleosome to its pre-transcribed state (Rando and Winston, 2012). There are ten known HDAC complexes present in *S. cerevisiae* that are divided into three major classes. Class I HDACs include Rpd3, Hos1, and Hos2; Class II contains Hda1 and Hos3; and Class III consists of Sir2 and its homolog (Yang and Gregoire, 2005). Since Class I and II HDACs lack DNA binding activity, they depend on histone modifications and interactions with other factors for their recruitment/activity (Yang and Gregoire, 2005). For instance, both Rpd3 and Hos2 are recruited coding regions by the phosphorylated Pol II CTD, and both require histone methylation for activity (Carrozza et al., 2005; Drouin et al., 2010; Govind et al., 2010; Joshi and Struhl, 2005; Kim and Buratowski, 2009). However, Rpd3 requires H3K36 methylation (Carrozza et al., 2005; Joshi and Struhl, 2005; Keogh et al., 2005), while Hos2 recognizes H3K4 methylation to deacetylate H3 and H4 residues (Kim and Buratowski, 2009; Rando and Winston, 2012). Loss of both Rpd3 and Hos2 in cells led to reduced histone occupancies in the coding region of ARG1, suggesting that the hyperacetylated histones remaining after HDAC loss are either efficiently recognized and removed by bromodomain-containing remodelers or are inefficiently reassembled after

Pol II passage (Govind et al., 2010). This, combined with the finding that loss of HDACs results in cryptic transcription, highlights the strict mechanisms that regulate histone acetylation and how acetylation can regulate transcription.

1.3.8 Histone Chaperones Regulate Chromatin Structure During and After Transcription

The complex interplay between HATs, HDACs, HMTs, chromatin remodelers (see 1.3.9), and other factors allow nucleosomes to be positioned for PIC assembly and Pol II elongation regulation. During Pol II passage, nucleosomes can be evicted entirely from the DNA or have dimers ejected to yield subnucleosomal particles (Cairns, 2007; Carey et al., 2006; Kulaeva et al., 2013). These nucleosomes and histone proteins must be replaced to restore the chromatin architecture to the state before transcription (Kaplan et al., 2003; Schwabish and Struhl, 2004). Histone chaperones can interact with histones and chromatin to facilitate histone eviction, deposition, and exchange (Eitoku et al., 2008). Asf1, Nap1, FACT, and Spt6 are all histone chaperones found in *S. cerevisiae* and are conserved in higher eukaryotes. Histone chaperones can be found at promoters and coding regions of a gene, and some have been shown to interact with Pol II, chromatin modifiers, and remodelers (Avvakumov et al., 2011). Asf1 binds both to promoters and CDSs of genes (Schwabish and Struhl, 2004). It is required for promoter nucleosome eviction during gene activation and is involved in H3 disassembly in CDSs of a large subset of genes (Adkins et al., 2004; Korber et al., 2006; Schwabish and Struhl, 2004). In contrast, Nap1 favors nucleosome assembly by disfavoring the excessive binding of H2A-H2B to DNA (Andrews et al., 2010). It also associates with the chromatin remodeler RSC, where RSC transfers histone octamers to Nap1 in a histone tail-

dependent manner (Lorch et al., 2023). The FACT complex consists of two subunits, Spt16 and Pob3 in yeast, and has important roles in both transcription initiation and elongation, as FACT depletion leads to reduced Pol II levels genome-wide (Belotserkovskaya et al., 2003; Pathak et al., 2018). Interestingly, the H3 tail contributes to FACT recruitment to CDSs in a Gcn5-dependent manner (Pathak et al., 2018). While the majority of recent studies have characterized the ability of FACT to reassemble histones in the CDSs during transcription, earlier findings have suggested that FACT might play a role in histone disassembly during transcription initiation via the eviction of H2A-H2B (Belotserkovskaya et al., 2003). Spt6 is recruited to CDSs via the phosphorylated Pol II CTD in a Bur1-, Ctk1-, Hos2-, and Rpd3-dependent manner (Burugula et al., 2014). It facilitates histone assembly in the wake of transcribing Pol II to promote transcription and prevents cryptic transcription (Cheung et al., 2008; Ivanovska et al., 2011; Kaplan et al., 2003; Pathak et al., 2018; Perales et al., 2013).

1.3.9 Chromatin Remodelers Regulate Chromatin Organization and Transcription

Chromatin writers and erasers coordinate with each other to tightly regulate the marks that are present on histone residues. Still, they are generally not the factors that directly move nucleosomes or alter the composition of histone proteins within the nucleosome. Chromatin readers/effectors are the factors that recognize the marks on histones and physically act on the nucleosome. One such type of effector protein is chromatin remodelers, which utilize ATP hydrolysis to modify histone-DNA interactions (Prajapati et al., 2020; Tyagi et al., 2016). There are four families of chromatin remodelers: ISWI, CHD, INO80, and SWI/SNF. These complexes vary in composition, with some consisting of only a single catalytic subunit while others contain up to 17

subunits and several distinct modules (Prajapati et al., 2020). All remodelers contain a catalytic subunit containing an ATPase domain, where the DExx and HELICc loops of the ATPase domain are involved in DNA binding and ATP hydrolysis (Langst and Manelyte, 2015; Prajapati et al., 2020). In addition to the ATPase domain, the catalytic subunit of each family differs in the distinct domains that flank the ATPase domain (Langst and Manelyte, 2015). As such, it is expected that each family recognizes different nucleosomes and acts on their targets in a distinct manner.

Members of the Imitation SWItch (ISWI) family of remodelers contain HAND, SANT, and SLIDE domains, in addition to their ATPase domains within their catalytic subunits (Clapier et al., 2017; Langst and Manelyte, 2015). HAND, SANT, and SLIDE domains have been shown to recognize nucleosome and inter-nucleosomal DNA (Clapier et al., 2017). There are two members of the ISWI family in *S. cerevisiae*. Isw1 can exist as two complexes termed ISW1a and ISW1b and contain 2 (Isw1 and Ioc3) and 3 (Isw1, Ioc2, and Ioc4) subunits, respectively, whereas the ISW2 complex contains 4 subunits (Isw2, Itc1, Dls1, and Dpb4) (Prajapati et al., 2020). In vivo, ISWI members have been shown to regulate nucleosome spacing within coding sequences with respect to the +1 nucleosome, though ISW1 makes a stronger contribution to this than ISW2 (Ocampo et al., 2016). Surprisingly, the loss of these factors results in minor effects on gene expression, though the loss of ISW1 has been implicated in premature transcription termination by Pol II (Ocampo et al., 2019; Prajapati et al., 2020). Additionally, ISW1 is involved in the repression of certain stress response genes during normal growth (Lindstrom et al., 2006), and ISW2 suppresses cryptic transcription (Whitehouse et al., 2007).

The Chromodomain-Helicase-DNA-binding (CHD) family members each contain a pair of N-terminal chromodomains along with their ATPase domain in their catalytic subunits, one of which has been implicated in recognizing H3K4 methylation (Langst and Manelyte, 2015; Pray-Grant et al., 2005). However, studies of yeast Chd1 have not been able to demonstrate this (Okuda et al., 2007; Sims et al., 2005). There is only one member of the CHD family in budding yeast, a single-subunit protein termed Chd1 (Prajapati et al., 2020). Chd1 is also involved in nucleosome spacing, where it may coordinate with ISW1 to fine-tune this spacing (Ocampo et al., 2016). It has also been suggested that ISW1 and Chd1 may prevent or resolve the formation of closely-packed di-nucleosome structures (Ocampo et al., 2019). Chd1 also plays a role in transcription, where it has been shown that Chd1 associates with Pol II elongation factors and that Chd1 suppresses cryptic transcription (Simic et al., 2003; Smolle et al., 2012).

There are two members of the INOsitol-requiring 80 (INO80) family in yeast: INO80C and Swr1. Both members possess an N-terminal HSA domain that can interact with actin-related proteins, as well as contain a long insertion in between the DExx and HELICc domains of their ATPase domains (Langst and Manelyte, 2015; Prajapati et al., 2020). Compared to the previously-discussed families, these complexes are large, where INO80C is comprised of 14 subunits and Swr1 is composed of 17 subunits (Prajapati et al., 2020). Swr1 can catalyze the exchange of a canonical H2A-H2B dimer with the histone variant H2A.Z-H2B dimer (Lin et al., 2017). The +1 nucleosome is enriched for H2A.Z, and +1 nucleosomes that contain H2A.Z are preferentially evicted from promoters during gene activation, compared to +1 nucleosomes that contain H2A (Santisteban et al., 2000; Zhang et al., 2005). Even though Swr1 contains an ATPase

domain similar to the INO80 complex (INO80C), Swr1 cannot mobilize nucleosomes in the same manner as INO80C (Lin et al., 2017). Swr1 has also been implicated in maintaining genome stability during DNA replication (Srivatsan et al., 2018).

The INO80 complex has been associated with a wide array of activities that regulate chromatin organization on a gene, including nucleosome sliding, maintenance of the NDR, and nucleosome editing (Prajapati et al., 2020; Qiu et al., 2020). INO80C is important for the positioning of the -1 and +1 nucleosomes to maintain the NDR, where it has been shown in vivo that cells lacking the INO80C catalytic subunit displayed +1 nucleosomes that were shifted downstream compared to nucleosomes in wild-type cells (Qiu et al., 2020). Additionally, loss of INO80C results in the shifting of nucleosomes located downstream of the +1 nucleosome towards the TSS, shortening the spacing in between nucleosomes (Udugama et al., 2011; van Bakel et al., 2013; Yen et al., 2012). It has been found that INO80C is required for nucleosome eviction at protomers of genes induced by the transcriptional activator Gcn4 and that this eviction can occur independently of its role in H2A.Z editing (Qiu et al., 2020). Unsurprisingly, given that cells lacking INO80C show defects in histone eviction, TBP is also reduced in INO80C-deficient cells, highlighting the role that INO80C plays in organizing promoter structure to facilitate PIC assembly (Qiu et al., 2020). Interestingly, INO80C has also been shown to restore promoter nucleosomes in osmotic stress response genes following the rapid eviction of those nucleosomes in response to stress (Klopf et al., 2017), in contrast to its role at other genes in promoting histone eviction. INO80C has also been implicated in nucleosome editing, where it catalyzes the replacement of a histone variant H2A.Z-H2B dimer with a canonical H2A-H2B dimer (Brahma et al., 2017; Clapier et al., 2017;

Papamichos-Chronakis et al., 2011). It has been proposed that +1 nucleosomes containing H2A.Z are inherently susceptible to eviction and that the removal of the H2A.Z-H2B dimer by INO80C renders the partially-disassembled nucleosome even more susceptible to eviction (Lai and Pugh, 2017; Yen et al., 2013). However, other evidence exists that conflicts with this hypothesis, including the finding that H2A.Z occupancies did not change at promoters when the *INO80* gene was either deleted or the INO80C protein was depleted (Jeronimo et al., 2015; Tramantano et al., 2016; Wang et al., 2016).

RSC and SWI/SNF are part of the SWItching/Sucrose Non-Fermenting (SWI/SNF) family of remodelers in *S. cerevisiae*. Members of this family contain an N-terminal HSA domain and a C-terminal bromodomain in addition to their ATPase domain within their catalytic subunits (Langst and Manelyte, 2015; Prajapati et al., 2020). These protein complexes are also large, with the SWI/SNF complex containing 11 subunits and the RSC complex containing 17 subunits (Langst and Manelyte, 2015; Prajapati et al., 2020). Both remodeling complexes are composed of 3 modules: the ATPase module containing the catalytic subunit (Sth1 in RSC or Snf2 in SWI/SNF), and ARP module containing actin-related proteins (consists of Arp7, Arp9, and Rtt102 in both complexes), and a body module (composed of various proteins that are distinct to each complex) (He et al., 2021; Ye et al., 2019). RSC and SWI/SNF have semi-redundant functions. In-vitro studies have shown that the ATPase of both RSC and SWI/SNF utilize ATP hydrolysis to translocate DNA in order to slide and evict nucleosomes (Clapier et al., 2017; Harada et al., 2016; Lorch and Kornberg, 2017; Saha et al., 2002). Additionally, both have been shown to convert canonical nucleosomes into alternative conformation states, where the conformations differ depending on the remodeler (Shukla et al., 2019; Shukla et al.,

2010). Both interact with the -1 and +1 nucleosomes to maintain the NDR, where they coordinate with other chromatin remodelers to properly position the -1 and +1 nucleosome (Ganguli et al., 2014; Rawal et al., 2018). When RSC or SWI/SNF have been depleted in vivo, the -1 and +1 nucleosomes encroach into the NDR, resulting in narrower NDRs than in wild-type cells (Ganguli et al., 2014; Klein-Brill et al., 2019; Kubik et al., 2018; Rawal et al., 2018). This is opposite to what was seen in cells lacking INO80C, indicating that the interplay between RSC and SWI/SNF with INO80C is a major contributor to +1 nucleosome positioning and NDR width (Qiu et al., 2020; Rawal et al., 2022; Udugama et al., 2011; van Bakel et al., 2013; Yen et al., 2012). However, RSC has been shown to maintain NDRs and regulate transcription at a global level, whereas SWI/SNF has a more modest effect and is found in highly-expressed genes (Rawal et al., 2018; Rawal et al., 2022). Additionally, RSC is essential in *S. cerevisiae* while SWI/SNF is not (Cairns et al., 1996; Ganguli et al., 2014), indicating that RSC performs critical roles that SWI/SNF is unable to recapitulate.

RSC and SWI/SNF complexes are highly conserved from yeast to humans and are linked to various developmental disorders including neurodevelopmental and autism spectrum-like disorders, as well as cancers (Bogershausen and Wollnik, 2018; Kadoch et al., 2013). Genetic screening has revealed that over 20% of human tumors contained mutations in the genes encoding for mammalian SWI/SNF complexes, making SWI/SNF the most frequently mutated chromatin-related cancer genes (Kadoch et al., 2013). These findings underline the importance of understanding the roles that SWI/SNF remodelers, specifically RSC, play in cellular processes such as transcription, as well as elucidating the impact on these processes when RSC function is impaired (Rawal et al., 2022).

1.4 RSC is an Essential Remodeler Critical for Chromatin Structure and Transcription

1.4.1 Overview of the RSC Complex

The Remodels the Structure of Chromatin (RSC) complex is a 1.1 mega-Dalton complex composed of 17 subunits and is the only essential chromatin remodeler in *S. cerevisiae* (Cairns et al., 1996; Cairns et al., 1999). It was originally identified in early biochemical studies based on the homology of its subunits to the closely-related SWI/SNF complex (Cairns et al., 1996; Cairns et al., 1999). Four components of the SWI/SNF complex, including the SWI/SNF catalytic subunit, were found to have essential homologs, and these members were further characterized and found to be members of the distinct RSC complex (Cairns et al., 1996; Laurent et al., 1992). In vitro, RSC has been shown to slide and evict nucleosomes reconstituted on a DNA template (Clapier et al., 2017; Harada et al., 2016; Lorch and Kornberg, 2017). RSC is important for several DNA-dependent processes, including cell cycle progression and transcription (Munoz et al., 2022; Munoz et al., 2019; Ocampo et al., 2019; Qiu et al., 2020; Van de Vosse et al., 2013). RSC has been shown to regulate the transcription of various Pol II and Pol III transcribed genes (Ng et al., 2002; Parnell et al., 2008; Qiu et al., 2020), and mutations in RSC result in transcriptional defects of genes involved in mitochondrial function, cell wall synthesis, metabolism, and stress response (Imamura et al., 2015; Wilson et al., 2006). In humans and other mammals, mutations within the BAF and PBAF complexes (mammalian RSC orthologs) are strongly correlated with such as cancer, where it is thought that the misregulation of chromatin structure due to the loss of RSC function results in aberrant gene expression, as well as defects in chromosome segregation and repair of DNA damage (Bohm et al., 2021; Kadoch et al., 2013; Munoz

et al., 2022; Pulice and Kadoch, 2016; Wagner et al., 2020).

1.4.2 RSC is a Large Complex that Contains Multiple Essential Subunits

RSC is a multi-subunit complex organized into three core modules: the ATPase module, the Actin-Related Protein (ARP) module, and the body module (Patel et al., 2019; Ye et al., 2019). The ATPase module consists of the catalytic subunit Sth1, which is responsible for translocating nucleosomal DNA in an ATP-dependent manner (Clapier et al., 2016). It is an essential subunit homologous to the SWI/SNF catalytic subunit Snf2 and contains a helicase-SANT-associated (HSA) domain, a SnAC domain that interacts with the nucleosome, and a C-terminal bromodomain in addition to its ATPase domain (Cairns et al., 1996; Cairns et al., 1999; Langst and Manelyte, 2015; Wagner et al., 2020). The ARP module contains the HSA domain of Sth1, Rtt102, and actin-related proteins Arp7 and Arp9. The Arp subunits interact with the HSA domain of Sth1 via Rtt102 to regulate ATPase activity (Szerlong et al., 2008; Wagner et al., 2020). The body module consists of Sfh1, Rsc7, two copies of Rsc8, Rsc9, Rsc58, Rsc6, Rsc4, Rsc3, Rsc30, Rsc14, Htl1, and either Rsc1 or Rsc2 (Patel et al., 2019; Ye et al., 2019). Rsc1 and Rsc2 are structurally similar and have semi-redundant functions, as loss of both subunits is lethal, but cells survive when only one of these subunits is lost (Cairns et al., 1999). These subunits contain tandem bromodomains and are mutually exclusive members of the complex, resulting in two RSC complex variants within *S. cerevisiae* (Cairns et al., 1999). The C-terminal tail of Sfh1 was found to contact the nucleosome opposite of the Sth1 SnAC domain (Wagner et al., 2020). Rsc8 is a structural protein that contains DNA-(SWIRM and zinc finger) and protein-binding (SANT) domains (Wagner et al., 2020). It interacts with Sfh1 and Sth1 to form the core complex that is sufficient for remodeling

activity (Phelan et al., 1999). Rsc4 contains tandem bromodomains and is important for the interactions between RSC and histone proteins, as well as with RNA polymerase (Kasten et al., 2004; Soutourina et al., 2006; VanDemark et al., 2007; Wagner et al., 2020). Rsc58 stabilizes the body module and also contains a bromodomain that attaches to the top of the module (Wagner et al., 2020). Rsc3 and Rsc30 contain DNA-binding domains and form a heterodimer important for efficient recruitment, though each subunit may have distinct roles (Wagner et al., 2020). Rsc3 is essential and is important for establishing NDRs and suppressing cryptic transcription from target promoters (Badis et al., 2008; van Bakel et al., 2013). Additionally, the zinc-binding domain has DNA binding capabilities and is thought to aid in recruiting RSC to chromatin (Angus-Hill et al., 2001; Badis et al., 2008). Rsc30 is not essential; however, it is important in RSC recruitment to double-stranded breaks to repair DNA damage (Shim et al., 2005). Rsc7 and Rsc14 stabilize Rsc3 association with the complex, with Rsc7 providing additional structural integrity to the complex (Wilson et al., 2006) and Htl1 being important for Rsc8 association with the complex (Florio et al., 2007; Wang and Cheng, 2012).

1.4.3 RSC is Important for Cell Cycle Progression

Sth1, Sfh1, Rsc3/30, Rsc4, Rsc8, Rsc58, Rsc9, Rsc6, and Htl1 are all important for mitotic cell cycle progression (Angus-Hill et al., 2001; Campsteijn et al., 2007; Cao et al., 1997; Hsu et al., 2003; Romeo et al., 2002). Sth1 and Sfh1 mutations are shown to cause cell cycle arrest at the G2/M checkpoint (Cao et al., 1997), most likely due to defects in chromatin remodeling around centromeres resulting in impaired kinetochore function (Tsuchiya et al., 1998). G2/M arrest is thought to be mediated by the DNA damage or spindle checkpoint pathways (Straight and Murray, 1997; Weinert and

Hartwell, 1988). Sth1, Rsc3, and Rsc7 are important for the spindle checkpoint pathway (Angus-Hill et al., 2001; Wilson et al., 2006). Depletion of Rsc8, Rsc9, Rsc58, and Rsc6 also induced cell cycle arrest at the G2/M checkpoint, with the loss of Rsc58 and Rsc8 also resulting in G1/S arrest (Campsteijn et al., 2007). RSC has also been implicated in quiescence exit to promote re-entry into the cell cycle (Cucinotta et al., 2021) and regulates cohesion loading to regulate sister chromatid cohesion (Munoz et al., 2022; Munoz et al., 2019). Overall, these findings provide insight into the role of RSC in regulating multiple stages of cell cycle progression.

1.4.4 RSC is Critical for Transcription Regulation

Genome-wide studies show that RSC is important for regulating the transcription of both Pol II and Pol III genes (Ng et al., 2002; Parnell et al., 2008; Rawal et al., 2018). RSC binds to and positions the -1 and +1 nucleosomes at the majority of genes and is involved in the positioning of these nucleosomes to maintain NDR width (Ganguli et al., 2014; Krietenstein et al., 2016; Rawal et al., 2018; Yen et al., 2012). Depletion of Rsc8 or Sth1 results in the shift of +1 nucleosomes into the NDRs genome-wide, forming NDRs that are narrower than their wild-type counterparts (Kubik et al., 2018; Ocampo et al., 2019; Rawal et al., 2018; Yen et al., 2012). This NDR shift was associated with reduced PIC assembly and transcription (Kubik et al., 2018; Rawal et al., 2018). Mutations in RSC also corresponded to reduced Pol II and TBP levels at the promoter of the Gcn4 target gene *ARG1*, which is induced by the transcriptional activator Gcn4 during amino acid starvation (Govind et al., 2005). RSC was also shown to promote rapid transcription upon quiescence exit, as RSC depletion resulted in a global decrease in Pol II loading at promoters and Pol II accumulation at TSSs (Cucinotta et al., 2021). Furthermore,

evidence suggests that RSC cooperates with other chromatin remodelers to regulate NDR width at promoters. For instance, it was found that RSC cooperates with SWI/SNF to evict promoter nucleosomes at a subset of highly transcribed genes (Rawal et al., 2018) and that RSC and INO80 act more broadly to position promoter nucleosomes at a majority of genes (Qiu et al., 2020; Rawal et al., 2022). These findings highlight the role RSC plays in regulating transcription initiation, though the exact mechanisms of these processes are not well understood.

Recent evidence has implicated RSC in regulating transcription elongation. In vitro, RSC promoted Pol II elongation through a nucleosomal template (Carey et al., 2006). SWI/SNF, CHD1, and ISW1 also stimulated elongation at far lower levels than RSC, establishing RSC as the predominant remodeler during elongation. In addition to its cooperation with histone chaperone Nap1 in nucleosome eviction (Lorch et al., 2023), RSC was shown to coordinate with Nap1 in vitro to facilitate Pol II progression and to maintain nucleosome density in the wake of transcribing Pol II (Kuryan et al., 2012). In vivo, RSC has also been shown to localize to the transcribed coding sequences of Gcn4-activated genes in a SAGA- and NuA4-dependent manner, which led to reduced histone occupancies across transcribed regions (Spain et al., 2014). RSC is also shown to be co-transcriptionally recruited to coding regions of osmotic stress genes (Mas et al., 2009). Cells deficient for both RSC and SWI/SNF displayed reduced Pol II occupancies at Gcn4 targets under amino acid starvation conditions (Rawal et al., 2018; Spain et al., 2014). Furthermore, depleting Rsc8 altered the Pol II distribution along coding regions (Ocampo et al., 2019). Taken together, these results suggest that RSC promotes elongation, where it might remodel nucleosomes immediately downstream of transcribing Pol II.

1.4.5 RSC is thought to Interact with a Largely-Uncharacterized Complex within NDRs

Recent genome-wide studies using micrococcal nuclease (MNase) to digest chromatin before sequencing have uncovered the existence of a previously uncharacterized complex in the NDRs of ~1/3 of Pol II-transcribed genes (Kubik et al., 2015). The signals for these complexes are detectable within NDRs when low amounts of MNase are used to digest chromatin but are undetectable when higher MNase amounts are used (Brahma and Henikoff, 2019; Kubik et al., 2015; Xi et al., 2011). Due to the inherent susceptibility of the complexes to MNase, these complexes were termed "fragile nucleosomes." The exact characteristics of these complexes are unclear, other than they are bound by RSC (Brahma and Henikoff, 2019), are found in genes that generally have wide NDRs, and may be composed of 6 or 8 histone proteins (Klein et al., 2023). Studies have purported to detect these nucleosomes both *in S. cerevisiae* and in mammalian cells, where they are also present at sites specific to the transcription factor CTCF and interact with mammalian IWSI (Brahma and Henikoff, 2019; Klein et al., 2023). However, the nature and existence of these complexes are highly controversial, as some studies could not detect the presence of histones at fragile nucleosome sites (Chereji et al., 2017). An alternative explanation has been proposed that the signals at these NDRs originated from a non-histone complex binding and stabilizing NDRs. Indeed, this is observed for tRNA (Pol III) genes, which are characterized by a wide NDR occupied by a stable complex of transcription factors (Nagarajavel et al., 2013). It could be that the fragile nucleosome signal detected at fragile nucleosome NDRs could be due to the binding of Pol II transcription factor or other general regulatory factors (Abf1, Reb1, Rap1; GRFs), which bind to specific sequences within the promoter to regulate transcription. However, further

research has shown that upon depleting these GRFs and other transcription factors, the signal detected at NDRs did not change, or if it did, it was more likely due to the result of NDR shrinkage, as GRFs have also been shown to help maintain NDR width (Kubik et al., 2017). Nevertheless, the presence of RSC at these sites indicates a possible role for RSC in interacting with these complexes, and further investigation is needed.

1.4.6 RSC is Recruited to Chromatin by Multiple Mechanisms

There is a body of evidence to suggest that multiple different mechanisms are used to recruit RSC to its target nucleosomes. For instance, it has been shown that transcription factors can interact with RSC to recruit it to promoter regions. RSC is known to be recruited to the *ARG1* promoter by interacting with the transcriptional activator Gcn4 (Swanson et al., 2003), and histone chaperone Rtt106 also recruits RSC to the promoters of HIR-dependent histone genes (Ferreira et al., 2011). It was also speculated that RSC could interact with GRFs to target promoters, but more recent evidence suggests that RSC and GRFs are recruited independently to promoters but may coordinate with each other to position the +1 nucleosome (Kubik et al., 2018). There is also evidence that RSC can be targeted to coding sequences by ORF-specific factors. RSC is shown to be recruited to osmotic stress response genes by interacting with the MAP kinase and elongation factor Hog1 (Mas et al., 2009). RSC may also be recruited to its target genes by interacting with Pol II, as the Rsc4 subunit physically interacts with Rpb5, a conserved subunit shared by the three eukaryotic RNA polymerase (Soutourina et al., 2006; Spain et al., 2014). Furthermore, a small portion of the cellular pool of RSC has been shown to interact with the hypophosphorylated Pol II CTD (Soutourina et al., 2006). This specific interaction could allow RSC to be recruited directly to coding

regions in a way that is not dependent on other coactivators and factors. However, it is unclear if this is the predominant way RSC is recruited to coding regions.

In addition to the different factors that may recruit RSC to target genes, multiple subunits within the RSC complex itself facilitate RSC recruitment to nucleosomes. For instance, the zinc cluster DNA binding domains of Rsc3/Rsc30 have been implicated in binding to CGCG motifs located in promoter regions (Badis et al., 2008; Wagner et al., 2020). Rsc1 and Rsc2 possess A-T hook motifs that could stabilize RSC-DNA interactions through their non-specific DNA binding activity (Cairns et al., 1999). Rsc8 may bind to DNA via its SWIRM DNA binding domain, and the SANT domain might allow it to interact with histones and other proteins to be recruited to nucleosomes (Wagner et al., 2020). Furthermore, poly(A) regions are thought to enhance RSC activity, with the poly(A) orientation and position to both GC-rich motifs and GRF binding sites influencing RSC activity (Kubik et al., 2018). However, it is still unclear if the poly(A) sites recruit RSC directly and if any specific domains in RSC recognize this motif.

One type of domain of particular interest is the RSC bromodomains. There are eight bromodomains present in 5 RSC subunits (2 in Rsc1, 2 in Rsc2, 2 in Rsc4, 1 in Rsc58, and one in Sth1), meaning that there are six bromodomains present in any RSC complex (Patel et al., 2019; Wagner et al., 2020). In vitro experiments have shown that bromodomains have been shown to bind to acetylated lysine residues (Dhalluin et al., 1999; Zeng and Zhou, 2002), RSC binds to acetylated nucleosomes, and that the presence of HATs SAGA and NuA4 enhance RSC binding (Chatterjee et al., 2011; Hassan et al., 2001). Interestingly, the second of the Rsc4 tandem bromodomains binds preferentially to H3K14 (Kasten et al., 2004; VanDemark et al., 2007; Wagner et al., 2020), a known

substrate of the SAGA HAT subunit Gcn5. Additionally, RSC has been shown to physically interact with both Gcn5 and Esa1, the catalytic subunits of SAGA and NuA4, respectively (Kasten et al., 2004; Mitchell et al., 2013; VanDemark et al., 2007). In-vivo experiments have shown that RSC binds to coding sequences of transcribed genes in a manner that is dependent on SAGA and NuA4 (Spain et al., 2014; Zheng et al., 2023). Despite these insights into to possible roles of histone acetylation and HATs in recruiting RSC, the exact mechanisms behind these interactions, such as the individual bromodomains involved in recognizing acetylated nucleosomes, are not completely understood.

1.5 Significance and Specific Aims

The regulation of transcription is vital to the growth and overall health of all organisms, as dysregulation has been linked to the development of various diseases including developmental disorders and cancer. Transcription is tightly regulated by multiple factors, including those that regulate chromatin structure. The Remodels the Structure of Chromatin (RSC) complex is the only essential chromatin remodeler in *Saccharomyces cerevisiae* and is important for regulating chromatin structure at a majority of genes. It is highly conserved in eukaryotes, and mutations in human RSC orthologs have been associated with multiple diseases, including autism spectrum disorder and various cancers. At the cellular level, misregulation of chromatin structure leads to the aberrant expression of genes involved in cell cycle progression, chromosome segregation, and responses to DNA damage and other forms of stress. X-ray crystallography, cryo-EM imaging, and in vitro and in vivo experiments have provided insights into the overall structure of RSC, its activity, and how it is possibly recruited to

chromatin. Despite these insights, the exact mechanisms by which RSC is recruited to chromatin in vivo and how exactly RSC remodels nucleosomes within the cell are not completely clear. The overall goal of this work focuses on how histone acetyltransferases (HATs) possibly coordinate with RSC to regulate chromatin structure in the budding yeast *S. cerevisiae*. *S. cerevisiae* has been used extensively as a model organism for decades, as it is a relatively simple eukaryotic organism that can be used to generate mutant strains quickly. Additionally, the mechanisms involved in regulating chromatin structure and transcription are highly conserved from yeast to mammals, allowing researchers to use findings uncovered in yeast as a blueprint to discover novel mechanisms in mammalian cells. The specific aims of this project were to: i) determine the roles of RSC in remodeling nucleosomes in promoters and at coding sequences, ii) determine the effects of histone acetyltransferases and histone acetylation on RSC recruitment, and iii) determine the roles of HATs and RSC on transcription in vivo. Through the experiments outlined in this proposal, this project shows that HATs, especially Esa1, modulate RSC association with promoter nucleosomes; that RSC-bound nucleosomes are more accessible than canonical nucleosomes, indicating that these nucleosomes are being remodeled; that genes thought to contain fragile nucleosomes show stronger effects when RSC or HATs are lost than genes without fragile nucleosomes; and that the loss of HATs or RSC correlates with defects in PIC assembly and transcription. This information will provide a greater understanding as to how RSC coordinates with HATs to regulate chromatin structure and transcription at a genome-wide scale, shows possible RSC remodeling for the first time in vivo, and provides new insights into the possible interactions between RSC and HATs with fragile nucleosomes.

CHAPTER TWO

MATERIALS AND METHODS

2.1 Yeast Strain Construction

All *Saccharomyces cerevisiae* strains used in this study are listed in Appendix A. Sth1-myc tagged strains were generated as described previously (Longtine et al., 1998). Briefly, the plasmids pFA6a-13Myc-His3MX6 or pFA6a-13Myc-TRP1 were used as a template to PCR amplify the 13xMyc region using primers containing sequences homologous to the regions flanking the stop codon of *STH1*. The amplified DNA was used for transformation, and colonies were selected for on synthetic complete plates deficient for histidine (SC/His^-) or tryptophan (SC/Trp^-). Successful integration and expression of the tagged Sth1 protein were determined by Western Blot using a primary antibody specific to the myc tag. Mutants lacking the Sth1 bromodomain (*sth1ΔBrD*) were generated and screened for as described above, with the exception that the forward primer used was homologous to the sequence upstream of the region encoding bromodomain of *STH1*, generating a myc-tagged Sth1 protein that also lacked its bromodomain. The primers and plasmids used for PCR of all myc-tagged Sth1 strains are listed in more detail in Tables 2 and 3 of Appendix B. Y4810 (*Sth1-AID*) and Y4855 (*sth1-KR*) were kindly provided by Dr. Frank Uhlmann of the Francis Crick Institute in London and are described in (Munoz et al., 2019).

2.2 Growth, Crosslinking, and Harvesting of Cell Cultures

Cells were grown in YPD at 30°C to an absorbance A_{600} of 0.7-0.8 before being crosslinked and harvested. Strains containing the temperature-sensitive *ESA1* (L254P)

allele were grown to an A_{600} of 0.6 before being heat-shocked at 37°C for 1 hour to inactivate Esa1 before crosslinking and harvesting. Y4810 and Y4855 were grown in Synthetic Complete media deficient for methionine (SC/Met-) to an A_{600} of 0.7 before being treated with methionine and 3-indole acetic acid (3-IAA, auxin) to repress transcription of the endogenous Sth1 copy and to deplete any endogenous Sth1 present due to leaky expression via auxin-induced degradation as described previously (Haruki et al., 2008; Morawska and Ulrich, 2013; Munoz et al., 2019; Nishimura et al., 2009). Briefly, methionine and 3-IAA were added to final concentrations of 250 μM and 500 μM, respectively, and cultures were incubated at 30°C for 1 hour before crosslinking and harvesting. Spike-in was performed by growing *Schizosaccharomyces pombe* cells to an A_{600} of 10, then adding enough *S. pombe* to the *S. cerevisiae* cultures so that the final A_{600} of *S. pombe* added would be 10% of the A_{600} of *S. cerevisiae*. Spike-in was performed after cell growth but prior to crosslinking and harvesting. Crosslinking was performed as described previously: crosslinking solution (50 mM HEPES-KOH [pH 7.5], 1 mM EDTA, 100 mM NaCl, 11% formaldehyde) was added to cultures to a final concentration of 1% formaldehyde and the cultures were swirled to mix. Cultures were then incubated at room temperature with intermittent shaking, and glycine solution was added to a final concentration of 350 mM to quench the crosslinking. Cells were then collected via centrifugation at 4000 rpm at 4°C for 5 mins, then washed twice with chilled 1X Tris-Buffered Saline solution before being stored at -70°C until ready for sonication or MNase digestion.

2.3 Sonication of Crosslinked Chromatin

Crosslinked cell pellets consisting of ~100 ml of crosslinked cell cultures were thawed on ice and resuspended in 500 µl of FA lysis buffer (50 mM HEPES-KOH [pH 7.5], 1 mM EDTA, 140 mM NaCl, 1% Triton X-100, 0.1% sodium deoxycholate) containing protease inhibitors (Pepstatin, Leupeptin, and PMSF, added to final concentrations of 0.729 mM, 1 µg/m, and 100 mM, respectively). 500 µl of acid-washed glass beads were added to the resuspended cells and cells were disrupted for 45 mins in a 4°C cold room. The cell extracts were then collected by centrifugation at 1000 rpm at 4°C for 2 mins, then glass beads were washed with 500 µl FA lysis buffer, and the washes were pooled with the collected cell extracts. The pooled extracts were centrifuged at 4000 rpm at 4\C for 5 mins to collect the chromatin pellet. The pooled extracts were then sonicated at 4°C using a Branson Sonifier set at 60% Duty Cycle and an Output Control of 2 to shear the chromatin into smaller fragments. The chromatin was sonicated for twelve one-minute cycles, where each cycle consisted of active sonication on ice for 30 seconds, followed by a 30-second rest period to prevent DNA degradation due to friction-generated heat buildup. The chromatin was centrifuged at 15,000 rpm at 4\C for 30 mins, and the supernatant containing sheared chromatin was collected. 100 µl of chromatin combined with 150 µl of Elution Buffer II (10 mM Tris-HCl pH 8.0, 1 mM EDTA, 0.67% SDS) to generate an input for sonicated chromatin, which can be used to check the extent of DNA shearing and to normalize sequencing data. Proteinase K (Ambion, catalog # AM2546) was added to a final concentration of 0.4 mg/ml and the inputs were incubated at 65°C overnight to reverse the formaldehyde crosslinks and

degrade any remaining protein. Input DNA was then purified and collected as described in 2.6. Sonicated chromatin was stored at 70°C until ready for chromatin immunoprecipitation. Sonicated chromatin samples were prepared in replicates (either duplicates or triplicates for each strain and treatment.

2.4 Digestion of Crosslinked Chromatin using Micrococcal Nuclease (MNase)

Crosslinked cell pellets consisting of ~100 ml of crosslinked cell cultures were thawed on ice and resuspended in 500 µl of FA lysis buffer (50 mM HEPES-KOH [pH 7.5], 1 mM EDTA, 140 mM NaCl, 1% Triton X-100, 0.1% sodium deoxycholate) containing protease inhibitors (Pepstatin, Leupeptin and PMSF, added to final concentrations of 0.729 mM, 1 µg/m, and 100 mM, respectively). 500 µl of acid-washed glass beads were added to the resuspended cells and cells were disrupted for 45 mins in a 4°C cold room. The cell extracts were then collected by centrifugation at 1000 rpm at 4°C for 2 mins, then glass beads were washed with 500 µl FA lysis buffer, and the washes were pooled with the collected cell extracts. The pooled extracts were then centrifuged at 4000 rpm at 4°C for 5 mins to collect the pellet containing the chromatin. The pellet was then washed once with FA lysis buffer and once with NP-S buffer (0.5 mM spermidine, 0.075% IGEPAL, 50 mM NaCl, 10 mM Tris-HCl [pH 7.5], 5 mM $MgCl_2$, 1 mM $CaCl_2$) before being resuspended in 300 µl NP-S buffer containing 1 mM of β-mercaptoethanol. 15 kU of micrococcal nuclease (MNase; Worthington Biochemical, catalog # LS004798) was added to the resuspended chromatin and the chromatin was incubated at 30°C for 4 mins on a thermomixer set to 1100 rpm to facilitate even distribution of MNase within the samples. The digestion was quenched by

adding EDTA to a final concentration of 15.7 mM and incubating the samples on ice for 10 mins. The samples were then centrifuged at 15,000 rpm at 4°C for 10 mins and the supernatant containing the digested chromatin was collected. The pellet was then washed with 300 µl NP-S buffer containing 0.2 mM SDS to collect any remaining digested chromatin and centrifuged at 15,000 rpm for 10 mins at 4°C. The supernatant was then collected and pooled with the previously-collected digested chromatin. 100 µl of chromatin was combined with 150 µl of NP-S buffer, 2 µl of 0.5M EDTA, 4 µl of 1M Tris-HCl pH 8.0, 10 µl of 10% SDS to create inputs to be used to determine the extent of MNase digestion and for data normalization. Proteinase K (Ambion, catalog # AM2546) was added to a final concentration of 0.37 mg/ml and the inputs were incubated at 65°C overnight to reverse the formaldehyde crosslinks and degrade any remaining proteins. The input DNA was then purified and quantified to determine the extent of MNase digestion (see 2.6) before being stored at -70°C. The MNase-digested chromatin was stored at -70°C until ready to proceed with chromatin immunoprecipitation. MNase-digested chromatin samples were prepared in replicates (either duplicates or triplicates for each strain and treatment.

2.5 Chromatin Immunoprecipitation (ChIP) of Sonicated and MNase-Digested Chromatin

Chromatin immunoprecipitation was performed using a slightly modified protocol (Govind et al., 2012). Dynabeads were washed twice with PBS containing 5 mg/ml BSA, resuspended in 150 µl PBS/BSA, and conjugated with the appropriate antibody for three hours at 4°C on a nutator. 60 µl of anti-mouse Dynabeads (Thermofisher Scientific, catalog # 11-041) and 3.5 µl of anti-myc antibody (Roche, catalog # 11667203001) per

ChIP were used for myc ChIPs, 50 µl of anti-mouse Dynabeads and 3 µl of anti-Rpb3 antibody (Neoclone, catalog # W0012) per ChIP were used for Rpb3 (Pol II) ChIPs, 40 µl of anti-rabbit Dynabeads (Thermofisher Scientific, catalog # 11-204-D) and 2 µl of anti-H3 antibody (Abcam, catalog # ab1791) per ChIP were used for H3 ChIPs, and 40 µl of anti-rabbit Dynabeads and 0.5 µl anti-TBP antibodies (gift from Dr. Joseph Reese, Penn State University) were used per ChIP for TBP ChIPs. After antibody conjugation, the beads were washed twice with PBS/BSA. 60 µl of PBS/BSA and 40 µl of FA lysis buffer were added to the beads and either sonicated or MNase chromatin was added to the beads. For H3 ChIPs, 100 µl of chromatin per ChIP was used, 110 µl of chromatin per ChIP was used for Rpb3 ChIPs, and 130 µl of chromatin per ChIP was used for TBP or myc ChIPs. The antibody-conjugated Dynabeads were then resuspended in the chromatin solution using a pipette and the conjugated beads were incubated with the chromatin on a nutator at 4°C for either 3.5 hours for H3 or Rpb3 ChIPs or overnight for TBP and myc ChIPs. After incubation, beads were washed once with PBS/BSA, then twice (once for H3 and Rpb3 ChIPs) with the following buffers: FA lysis buffer, Wash Buffer II (50mM HEPES-KOH, 500 mM NaCl, 1 mM EDTA, 0.1% sodium deoxycholate, 1% Triton-X 100), and Wash Buffer III (10mM Tris-HCl [pH8.0], 250 mM LiCl, 1mM EDTA, 0.5% sodium deoxycholate, 0.5% NP-40 substitute). Beads were then washed once with Ultrapure Water before being resuspended in 100 µl of Elution Buffer I (50mM Tris-HCl, 10mM EDTA, 1% SDS) and incubated at 65°C for 15 mins. The eluate was collected and the beads were resuspended in 150 µl of Elution Buffer II (10mM Tris-HCl, 1mM EDTA, 0.67% SDS) before being incubated at 65°C for 10 mins to elute any remaining

chromatin. The ChIP eluates were combined and then incubated at 65°C for at least 4 hours (overnight for H3 and Rpb3 ChIPs, 4 hours for TBP and myc) to reverse the formaldehyde crosslinks. Proteinase K (Ambion, catalog # AM2546) was added to a final concentration of 0.4 mg/ml and the eluates were further incubated at 65°C for 2 hours to degrade any remaining protein. ChIP DNA was then purified as described in 2.6, and the purified DNA was stored at -70°C until ready for library preparation. ChIPs were prepared in replicates for each strain/treatment using one replicate of sonicated or MNase-digested chromatin per ChIP.

2.6 DNA Purification and Quantification of Input or ChIP DNA

After the crosslinks were reversed and Proteinase K digestion was complete, KOAc was added to the input or ChIP DNA to a final concentration of 143 mM before DNA was extracted using an equal volume of chloroform: isoamyl alcohol and the aqueous phase containing the DNA was collected. The DNA for each input or ChIP was re-extracted by adding 100 µl Ultrapure water to the chloroform. The aqueous phase was collected and combined with the previously extracted aqueous phase. The DNA was extracted once more using an equal volume of chloroform: isoamyl alcohol and the aqueous phase was collected. Glycogen and molecular grade ethanol were added to final concentrations of 52 µg/ml and 70%, respectively, before the purified input or ChIP DNA was stored at -70°C overnight to precipitate the DNA. Inputs and ChIPs were then centrifuged at 15,000 rpm at 4°C for 30 mins to pellet the precipitated DNA, and the pellets were washed once with 70% ethanol before being centrifuged on a vacufuge warmed to room temperature for 4 to 7 mins with the vacuum applied to dry the pellets.

DNA pellets were then resuspended in 1X TE/RNase A (To make 10X TE stock: combine 5 ml of 1M Tris-HCl pH 8.0, 1 ml of 0.5M EDTA pH 8.0, and 44 ml diH_2O. Dilute to 1X and add RNase A [Fisher Scientific, catalog # 12091-021] to a final concentration of 200 μg/ml before use) and incubated at 37°C for 1 hour to degrade RNA and resuspend DNA. Purified input DNA was then run on a 2% agarose gel to determine the extent of DNA digestion or shearing. Sonicated chromatin samples that had average fragment sizes were 300-400 bp in length were used for chromatin immunoprecipitation and library preparation, while MNase-digested chromatin samples that showed approximately 80% DNA fragments corresponding to ~150 bp were used for ChIP and library preparation. Inputs and ChIP DNA to be used for library preparation were purified using AMPure XP beads (Beckman Coulter, catalog # A63881) to remove the salt the input or ChIP DNA was precipitated in, where the volume of beads added was 0.9X of the input or ChIP volume to prevent size selection of the fragments during bead cleanup. Input or ChIP DNA was then eluted in 50 μl of 0.1X TE and the yield of DNA was determined using the Qubit 3 fluorometer.

2.7 Library Preparation of Purified Input or ChIP DNA

Library preparation was performed using the NEBNext Ultra II DNA Library Kit (New England Biolabs, catalog # E7645S) and a protocol modified from the manufacturer's instructions for the kit. Briefly, 100 ng of input DNA or 1-10 ng of ChIP DNA resuspended in 50 μl 0.1X TE was thawed on ice and then combined with 7 μl of End Prep Buffer and 3 μl End Prep enzyme before being incubated on the thermocycler according to the manufacturer's instructions to clean up the ends of the DNA fragments for adapter ligation. 1 μl of diluted NEXTFlex DNA barcode (PerkinElmer, catalog #

514104, diluted to 0.24 μM using Ultrapure water) was then added to each prepped input or ChIP and the volume was made up to 62.5 μl using Ultrapure water. 30 μl of Ligation Master Mix and 1 μl of Ligation Enhancer were then added to the end-prepped DNA, and the samples were incubated at 20°C for 15 mins to ligate the DNA barcodes to the end-prepped DNA. Bead cleanup of the adapter-ligated DNA was then performed using AMPure XP beads (Beckman Coulter, catalog # A63881), where the volume of beads added was 0.9X that of the input or ChIP volume to prevent size selection of the fragments during bead cleanup. The DNA was then eluted in 22.5 μl 0.1X TE, and 2.5 μl of universal primers and 25 μl Q5 master mix were added to the DNA. The libraries were amplified according to the manufacturer's instructions, where the ChIP libraries were amplified for 9-15 cycles and the input libraries were amplified for 9-10 cycles. The amplified libraries underwent one more round of bead cleanup without size selection using AMPure XP beads before being eluted in 0.1X TE and loaded onto a 2% E-Gel EX (Thermofisher Scientific, catalog # G401002) and run according to the E-Gel manufacturer's instructions. Gel pieces containing the DNA for the ChIP and input libraries were then excised, and the library DNA was extracted from the gel using the Qiaex II Gel Extraction Kit (Qiagen, catalog # 20051) according to the manufacturer's instructions. Gel slices containing fragments ranging from ~100 bp to 600 bp were excised for libraries from sonicated chromatin. In contrast, gel slices containing fragment sizes ranging from ~100-450 bp were excised for MNase-digested chromatin-containing libraries. DNA yield for the libraries was obtained using the Qubit 3 fluorometer, and the libraries were sequenced on the Illumina HiSeq platform in paired-end mode at

GENEWIZ in South Plainfield, NJ, USA. One library was prepared for each ChIP or input replicate for each strain.

2.8 Analysis of Sequencing Data

Sequences were trimmed to remove adapters using the Cutadapt package (parameter: -m 20) and were aligned to the *S. cerevisiae* genome (SacCer3) using Bowtie2 (parameters: -X 1000 –very-sensitive –no- mix –no-unal). Samtools was used to sort, index, and remove PCR duplicates from the resulting bam files. The data downloaded from the previous studies (Klein-Brill et al., 2019; Kubik et al., 2018; Ocampo et al., 2019; Petrenko et al., 2019) were similarly processed and analyzed as described below. The bam files were then analyzed using BamR (https://github.com/rchereji/bamR) to generate heatmaps and data files. The reads for each chromosome were set to 1 during normalization, and the data values of the replicates for each strain/treatment were averaged before generating heatmaps, metagene profiles, boxplots, and Venn diagrams. The 2 D-occupancy heatmaps were generated using the plot2DO.R and the fragments were aligned to their 5' ends. Transcription start sites were taken from a previous study (Xu et al., 2009). The single-end reads TBP and Pol II (Kubik et al.2018; Petrenko et al.2019) were normalized (106 reads) and analyzed using HOMER (v4.11, 10-24-2019). TBP occupancies were calculated from +/- 200 bp of the TSS, and Pol II occupancies were calculated from –100/+1000 bp from the TSS. For strains in which endogenous Sth1 was depleted using auxin (Y4810 and Y4855), the Pol II ChIP-seq data was normalized using *S. pombe* spike-in reads to visualize the differences in Pol II occupancies better. The spike-in factor was calculated by dividing the average of *S. pombe* reads for all the samples by the average *S. pombe* reads for the

replicate samples. Metagene profiles and scatterplots were generated in JMP (https://www.jmp.com/en_us/software/predictive-analytics-software.html). Boxplots were generated using the BoxplotR website (http://shiny.chemgrid.org/boxplotr/). Venn diagrams were made using the Biovenn website (http://www.biovenn.nl/).

CHAPTER THREE

RSC REMODELS NUCLEOSOMES IN TRANSCRIBED CODING SEQUENCES

3.1 Introduction

It is important to know how RSC functions to regulate chromatin and transcription. The key mechanistic insights into RSC recruitment and activity have been provided through biochemical experiments. For instance, in-vitro studies have shown that RSC can slide, evict, and remodel nucleosomes into alternate conformations to allow for PIC assembly and Pol II elongation (Clapier et al., 2017; Harada et al., 2016; Lorch and Kornberg, 2017; Saha et al., 2002; Shukla et al., 2019; Shukla et al., 2010). These studies use reconstituted nucleosomes assembled on DNA sequences containing strong nucleosomal positioning elements. However, these DNA sequences do not represent the heterogeneity of the sequences found in an organism's genome, and these reconstituted nucleosomes are often missing the epigenetic marks present on nucleosomes in vivo. As such, RSC remodeling activity and the mechanisms that regulate it might be slightly different in vivo than what has been observed so far in vitro. Unfortunately, it is very difficult to visualize remodeling activities in vivo. An ex vivo system was developed to study RSC remodeling in which nucleosomes were isolated from cells via MNase digestion before being purified and subjected to RSC remodeling in vitro in the presence of histone chaperone Nap1, where the resulting naked DNA (remodeling product) was then sequenced and quantified (Cakiroglu et al., 2019). This system has advantages over in vitro remodeling assays using reconstituted nucleosomes in that the purified nucleosomes still retain most, if not all, of the epigenetic marks present on them when

they were still inside the cell. However, it is still limited in that it cannot test for any other physiological players within the cell that could interact with RSC and modulate its remodeling activities in vivo.

Conventional in vivo methods are primarily utilized to map nucleosomes and other factors, such as RSC, to the genome. One such method, MNase-seq, exploits the endo- and exo- nuclease properties of micrococcal nuclease (MNase) to digest the linker DNA in between nucleosomes (Prajapati et al., 2020). DNA that is wrapped around the nucleosome is more resistant to digestion by MNase and can be isolated and sequenced to produce high-resolution mapping of nucleosomes across the genome. Additionally, antibodies specific to transcription factors, coactivators, and chromatin modifiers can be used during chromatin immunoprecipitation (ChIP) (Govind et al., 2012) to isolate factors bound to chromatin from the digested chromatin and map them to the genome. In this work, MNase digestion was coupled to ChIP (MNase-seq) to map RSC and other factors at nucleosomal resolution and to determine RSC-bound nucleosome accessibility genome-wide. For this chapter, to gain more insights into how RSC is recruited to the genome and its activity in vivo, MNase-seq and MNase ChIP-seq were performed using wild-type cells and in cells deficient for RSC. This chapter focuses primarily on where RSC localizes at a genome-wide level and provides a possible method of studying RSC remodeling in vivo and investigating how RSC localization correlates with transcription.

3.2 RSC Localizes to the Coding Sequences of Highly-Transcribed Genes

RSC has been shown to play important roles in maintaining NDR regions at promoters and has also been implicated in facilitating transcription elongation (Badis et al., 2008; Brahma and Henikoff, 2019; Ganguli et al., 2014; Klein-Brill et al., 2019;

Kubik et al., 2015; Rawal et al., 2018; Spain et al., 2014). In agreement with this, multiple studies have shown that RSC localizes to the coding sequences (CDSs) of transcribed genes (Ganguli et al., 2014; Spain et al., 2014). Considering that RSC has been shown to slide, evict, or otherwise remodel nucleosomes in vitro, this work sought to provide insight into the role RSC might play in remodeling nucleosomes within CDSs in vivo. To this end, MNase digestion was performed on chromatin harvested from *S. cerevisiae* cells to digest the linker DNA in between nucleosomes, and the resulting digested chromatin was used to perform chromatin immunoprecipitation (ChIP) using an antibody specific to myc. The *S. cerevisiae* strain used in this work expressed Sth1 protein fused with a myc tag (Sth1-myc). Since Sth1 is the catalytic subunit of RSC, the myc ChIP would isolate any RSC-bound nucleosomes from the chromatin, and the DNA purified from the RSC-bound nucleosomes could then be sequenced to determine where RSC localized on the genome (Ramachandran et al., 2017). In agreement with previous studies (Ganguli et al., 2014; Spain et al., 2014), RSC localized to the coding regions of transcribed genes. Figures 3.1-3.3 depict genome browser snapshots of six genes showing high RSC occupancies in their CDSs. The red peaks indicating RSC enrichment were found largely at regions encoding introns or exons, denoted by thin blue lines (introns) or thick blue boxes (exons) located at the bottom of the snapshot. In addition to RSC ChIP, Rpb3 (Pol II) ChIP was also performed using the same MNase-digested chromatin, and the resulting DNA was sequenced to determine the levels of Pol II genome-wide. Pol II enrichment is generally regarded as a good indicator for transcription, and since Pol II is also enriched in the coding sequences of these genes as indicated by the green peaks, these snapshots suggest that these genes are also transcribed. DNA was also isolated from

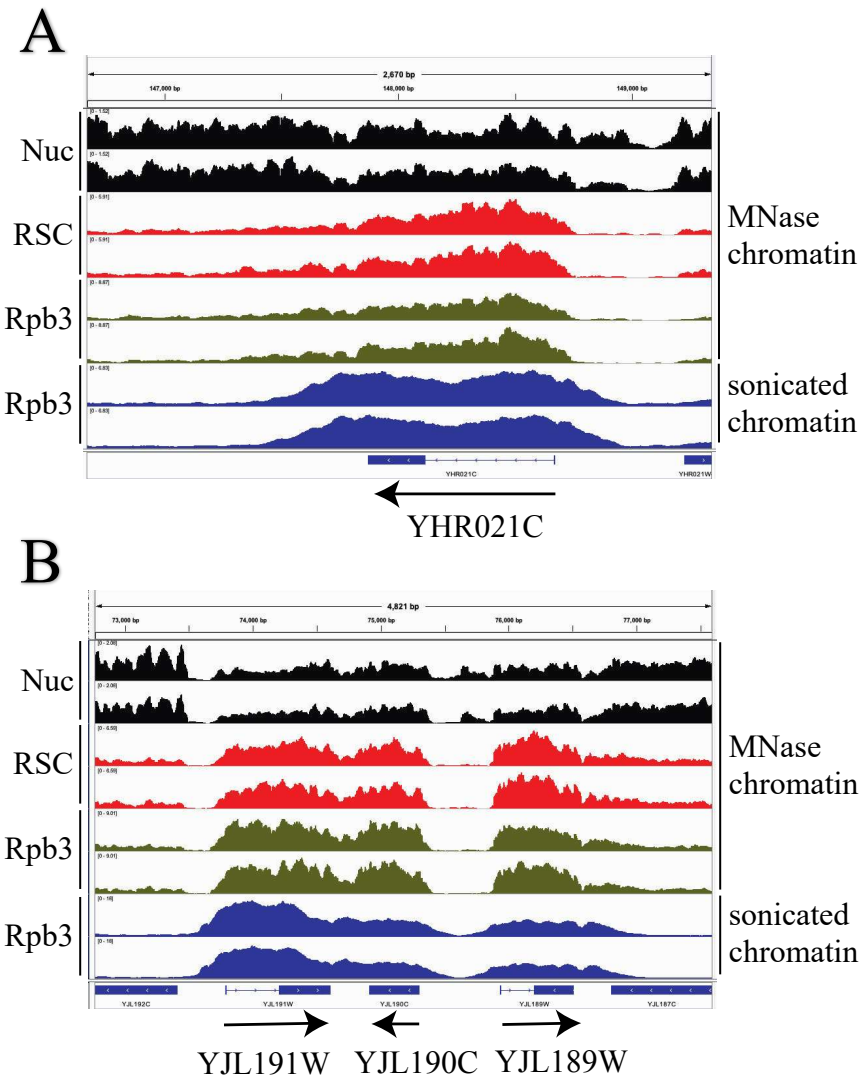

Figure 3.1. RSC localizes to the coding sequences (CDSs) of ribosomal protein genes (RPGs). (A-B) Genome browser snapshots of RPGs YHR021C, YJL191W, YJL189W, and YJL189W. These genes have RSC enriched in their CDSs. Nucleosomes (Nuc, black), RSC MNase ChIP-seq (red), Rpb3 MNase ChIP-seq (green), and Rpb3 ChIP-seq data from sonicated chromatin (blue) are shown. Arrows denote the 5'→ 3' direction of the gene.

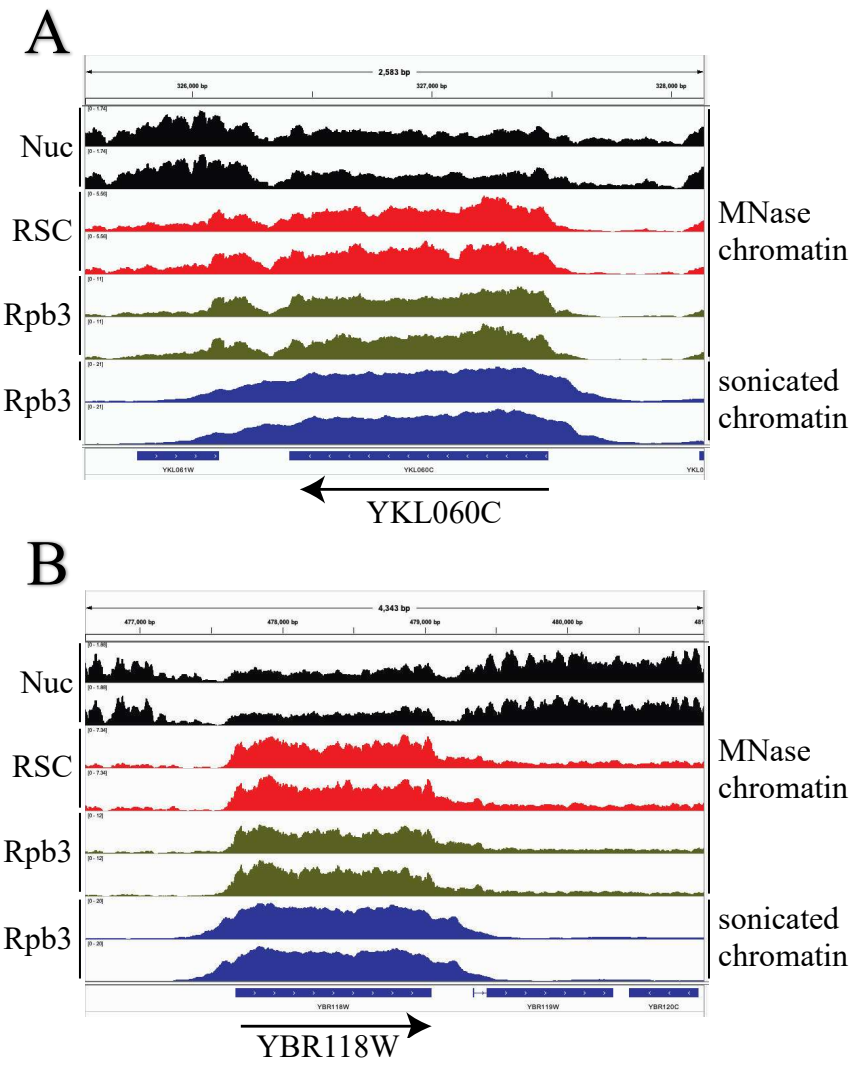

Figure 3.2. RSC localizes to the coding sequences (CDSs) of genes involved in metabolism and translation. (A-B) Genome browser snapshots of YKL060 (involved in glucose metabolism), and TBR118W (encodes for translation elongation factor EF-1 alpha). These genes have RSC enriched in their CDSs. Nucleosomes (Nuc, black), RSC MNase ChIP-seq (red), Rpb3 MNase ChIP-seq (green), and Rpb3 ChIP-seq data from sonicated chromatin (blue) are shown. Arrows denote the 5'→ 3' direction of the gene.

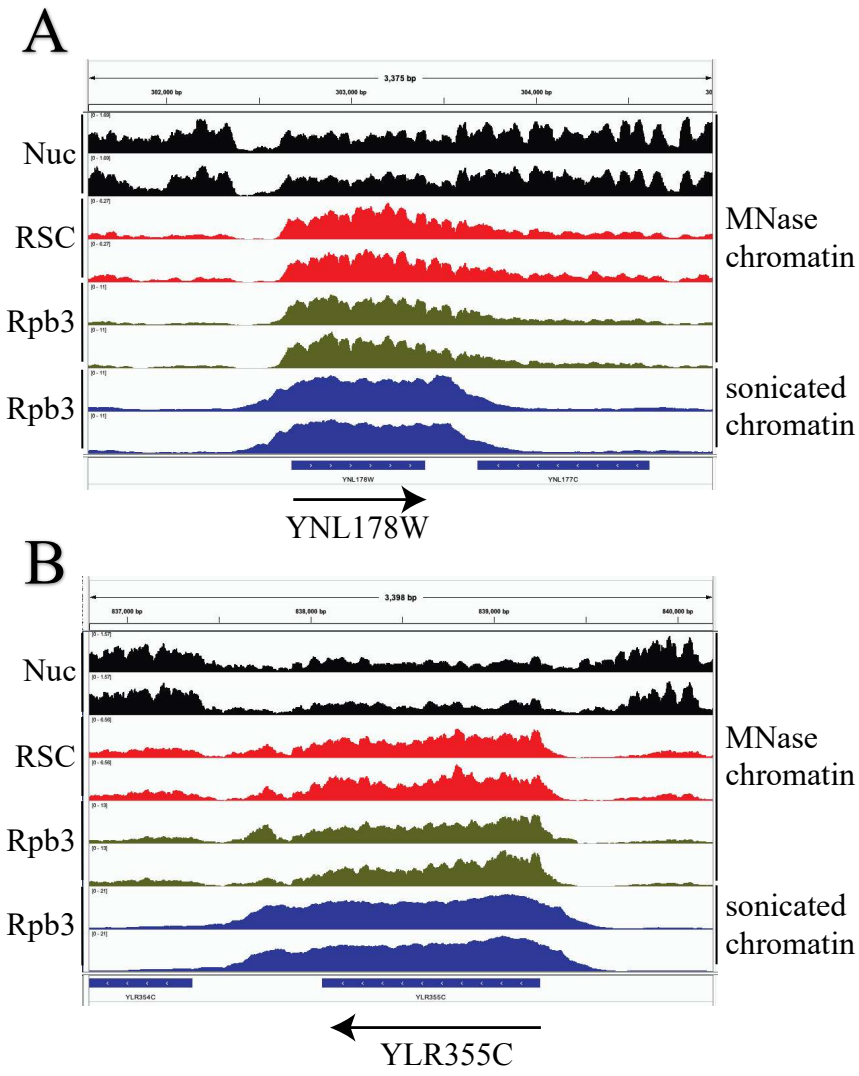

Figure 3.3. RSC localizes to the coding sequences (CDSs) of genes encoding ribosomes and mitochondrial proteins. (A-B) Genome browser snapshots of YNL178W (ribosomal protein) and YLR355C (maintains mitochondrial DNA). These genes have RSC enriched in their CDSs. Nucleosomes (Nuc, black), RSC MNase ChIP-seq (red), Rpb3 MNase ChIP-seq (green), and Rpb3 ChIP-seq data from sonicated chromatin (blue) are shown. Arrows denote the 5'→ 3' direction of the gene.

the MNase-digested chromatin and subjected to sequencing to determine where nucleosomes localized on the genome. RSC was enriched in areas where nucleosomes were also enriched, indicating that RSC was indeed bound to nucleosomes and not to naked DNA.

While the gene snapshots yielded interesting observations regarding RSC localization, these snapshots only represent a very small subset of the ~6000 protein-coding genes present in *S. cerevisiae*. To determine where RSC localizes to genes at a genome-wide level, heatmaps depicting RSC occupancies at all genes (n=5700), genes with high levels of Pol II (Pol II-T10; n=576), genes with low levels of Pol II (Pol II-B10; n=576), and genes with high levels of RSC in the promoter regions (-1_Nuc-T10) were generated using the RSC MNase ChIP-seq data (Figure 3.4 top panels). Genes were sorted by decreasing average Pol II levels within their CDSs and were centered at the transcription start site (TSS). The list to sort the genes was determined by separate Pol II ChIP-seq data that was also used to determine the 10% of genes with the highest Pol II levels (highly-transcribed genes, Pol II-T10) and the 10% of genes with the lowest Pol II levels (lowly transcribed genes, Pol II-B10). To determine the genes with high levels of RSC in their promoter regions, genes with divergent promoters were removed from the data set containing all genes, and the 576 genes with the greatest RSC occupancies at the -1 nucleosome (-1_Nuc) location were selected. The top 10% of Pol II-occupied genes showed high levels of RSC in their CDSs, as demonstrated by the red shading after the TSS at the top of the heatmap for all genes and in the heatmap of the Pol II-T10 genes. Genes containing high levels of RSC in the promoter regions also showed RSC enrichment in their CDSs, though not to the same extent as that observed for Pol II-T10

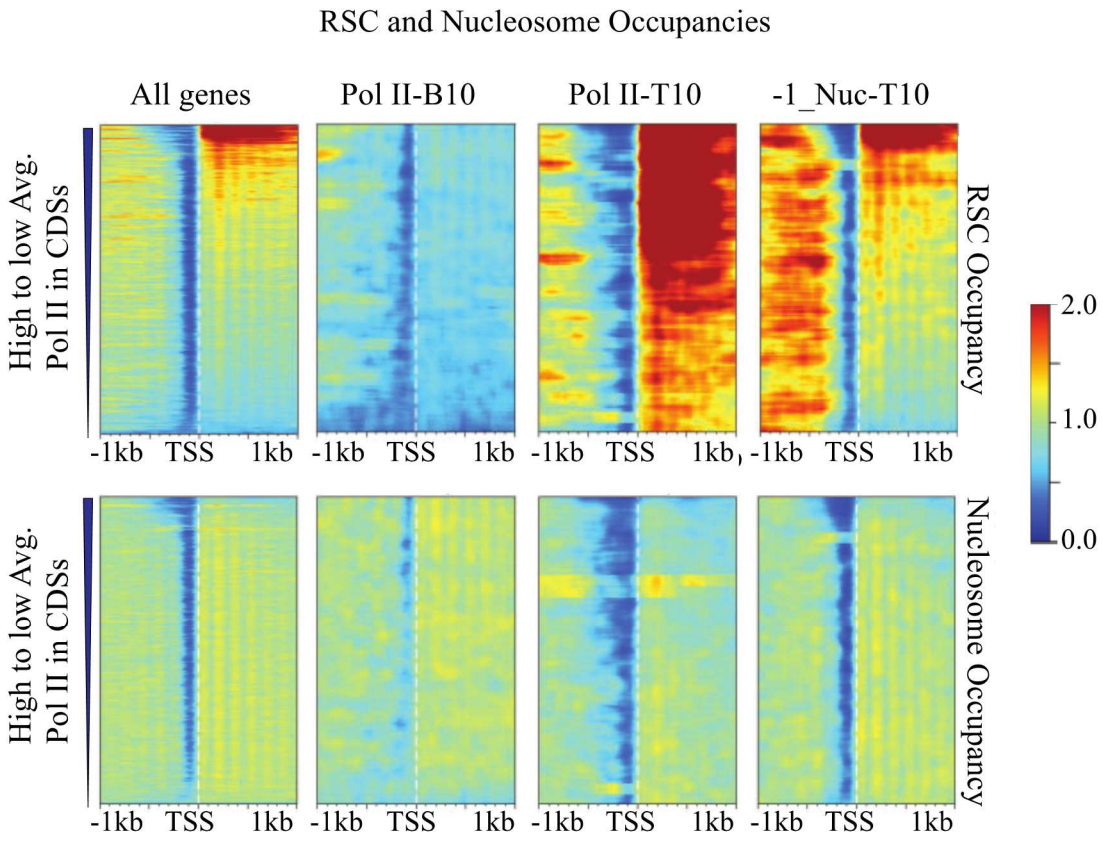

Figure 3.4. RSC is enriched in the CDSs of Pol II-containing genes. Heatmaps showing RSC (top panels) and nucleosome (bottom panels) occupancies for all genes (n=5700), Pol II-B10 genes (n=576), Pol II-T10 genes (n=576), and -1_Nuc-T10 genes (n=576). Pol II-B10 and Pol II-T10 genes were selected by taking the 10% of genes with the lowest and highest average Pol II levels, respectively, from Rpb3 ChIP-seq data. -1_Nuc-T10 were selected by removing genes from divergent promoters and selecting the top 10% genes with the highest RSC levels at the -1 nucleosome position. Genes were sorted by decreasing average Pol II levels in their CDSs and are centered at the transcription start site (TSS).

genes. In contrast, genes with low Pol II levels showed modest RSC levels in the CDSs, shown by the light blue shading after the TSS.

To show that RSC is indeed enriched at CDS nucleosomes and that this enrichment was not simply due to an increased presence of nucleosomes in the CDSs of transcribed and -1_Nic-T10 genes, heatmaps were generated depicting the nucleosome occupancies at all genes, Pol II-B10 genes, Pol II-T10 genes, and -1_Nuc-T10 genes (Figure 3.4 bottom panels). Despite the RSC enrichment at CDSs of Pol II-T10 and -1_Nuc-T10 genes, nucleosome occupancies for these genes were slightly lower for these genes compared to the CDSs of Pol II-B10 genes, suggesting that RSC is enriched in CDSs of transcribed genes. Indeed, the metagene profile showing normalized RSC occupancies for Pol II-B10 genes, Pol II-T10 genes, -1_Nuc_T10 genes, and the 10% genes containing the highest RSC levels (RSC-T10) showed that genes containing high levels of RSC were significantly enriched for RSC in the CDSs (see orange trace, Figure 3.5A, left profile). Interestingly, RSC levels were similar in the RSC-T10 genes compared to those in the Pol II-T10 genes, indicating that RSC presence in CDSs correlates with transcription. -1_Nuc-T10 genes showed higher levels of RSC in their CDSs compared to Pol II-B10 genes, but the enrichment was not as great as in Pol II-B10 or RSC-T10 genes. In contrast, the nucleosome occupancies for -1_Nuc-T10, RSC-T10, and Pol II-T10 genes are all slightly lower than Pol II-B10 occupancies in CDSs (Figure 3.5A, right panel, compare orange and red traces to black trace after the TSS). Ribosomal Protein genes (RPGs) also contained high RSC and Pol II levels in their CDSs (Figure 3.5B). RPGs are highly expressed and undergo high levels of transcription (Petibon et al., 2021), supporting the idea that RSC enrichment in CDSs is linked to transcription.

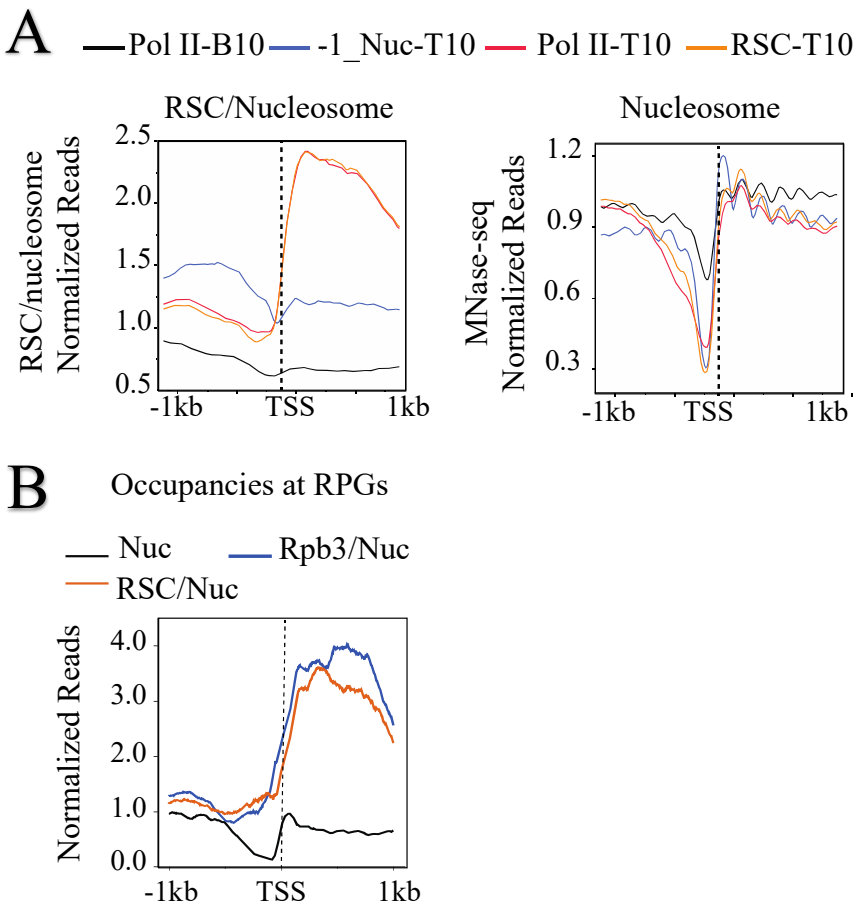

Figure 3.5. RSC is enriched in the CDSs of highly-transcribed genes, including RPGs. A) Metagene profiles showing the normalized occupancies for RSC (left profile) and nucleosomes (right profile) for Pol II-B10, Pol II-T10, -1_Nuc-T10, and RSC-T10 genes. RSC-T10 genes were found by selecting the 10% genes with the highest RSC levels. RSC occupancies were normalized to nucleosome occupancies before the ratio was plotted. B) Metagene profile depicting the nucleosome, Rpb3 and RSC occupancies at ribosomal protein genes (RPGs). The RSC and Rpb3 occupancies were normalized to nucleosome occupancies before the ratios were plotted. All profiles are centered at the TSS.

Collectively, the data suggest that RSC localizes to CDSs of highly transcribed genes and that this recruitment is likely linked to transcription, as previous studies have shown that RSC was enriched in the CDSs of Gcn4 targets (Rawal et al., 2018; Spain et al., 2014). Gcn4 is a transcription factor that is translationally activated upon amino acid starvation conditions and induces transcription of its targets, specifically amino acid biosynthesis genes. In these studies, when amino acid starvation conditions were induced, RSC was only enriched at Gcn4 targets in WT cells. This was not seen in cells lacking Gcn4, even when the cells were subjected to amino acid starvation, supporting the idea that RSC is enriched in CDSs at transcriptionally active genes.

3.3 RSC is Enriched at the Promoters of many Genes, including Transcribed Genes

Several studies have shown that RSC is enriched at the promoters and upstream regulatory regions of many genes (Badis et al., 2008; Brahma and Henikoff, 2019; Kubik et al., 2018; Spain et al., 2014; Yen et al., 2012). Considering that RSC has been shown to position the -1 and +1 nucleosomes to maintain nucleosome-depleted regions (NDRs) (Rawal et al., 2018) and that RSC slides and evicts nucleosomes in vitro (Carey et al., 2006), it is possible that RSC might play a role in transcription initiation by unwrapping the TSS from the +1 nucleosome to facilitate PIC assembly (Kubik et al., 2018). To begin to address the role of RSC in transcription initiation, the RSC MNase ChIP-seq data were analyzed to identify genes where RSC localized to the promoters of transcribed genes. Despite having RSC enriched within their CDSs, the RSC-T10 and Pol II-T10 genes showed very little enrichment within their promoter regions (Figures 3.5 left profile, compare the red and orange traces with the black trace in the region upstream of the TSS). This was surprising, given that RSC is thought to promote transcription initiation

and that a high level of Pol II present in CDSs is generally seen as an indicator of active transcription. However, MNase has been shown to preferentially digest DNA within NDRs (Chereji et al., 2019), so it is possible that the RSC-protected regions within the NDRs might have been lost during MNase digestion. To try to address this possibility, genes that harbored RSC at the -1 nucleosome position (-1_Nuc) were identified to see if the association of RSC with this promoter nucleosome correlated with transcription. Genes that contained divergent promoters were excluded due to the difficulty in identifying the -1 nucleosome for each gene that utilizes the promoter, and the top 10% of genes with the highest RSC occupancies at the -1 nucleosome (-1_Nuc-T10, n=576) were used for analysis. RSC was enriched upstream of the TSS for the -1_Nuc-T10 genes, showing that RSC binds to the promoter regions of these genes (Figures 3.4 and 3.5, compare blue trace in 3.5 before and after TSS). The enrichment also extended further upstream of the -1 nucleosome, beyond the NDRs of these genes (Figure 3.4, -1_Nuc-T10 top panel). The genes with the highest levels of Pol II within this subset of genes also showed RSC enrichment in their CDSs, indicating that these genes might also be transcribed. To see if RSC enrichment in promoters was linked to transcription, scatterplots were generated showing the correlations of Pol II occupancies to normalized RSC occupancies at either -1 or +1 nucleosome positions for all genes or at genes with non-divergent promoters. Whereas RSC occupancies at -1 nucleosome positions correlated weakly with Pol II, RSC occupancies at +1 nucleosome positions correlated strongly with Pol II (Figure 3.6, compare R-squared values of -1 Nuc to those of +1 Nuc). Altogether, the data suggest that RSC recruitment to the +1 nucleosome is tightly linked to Pol II levels and transcription at a genome-wide level.

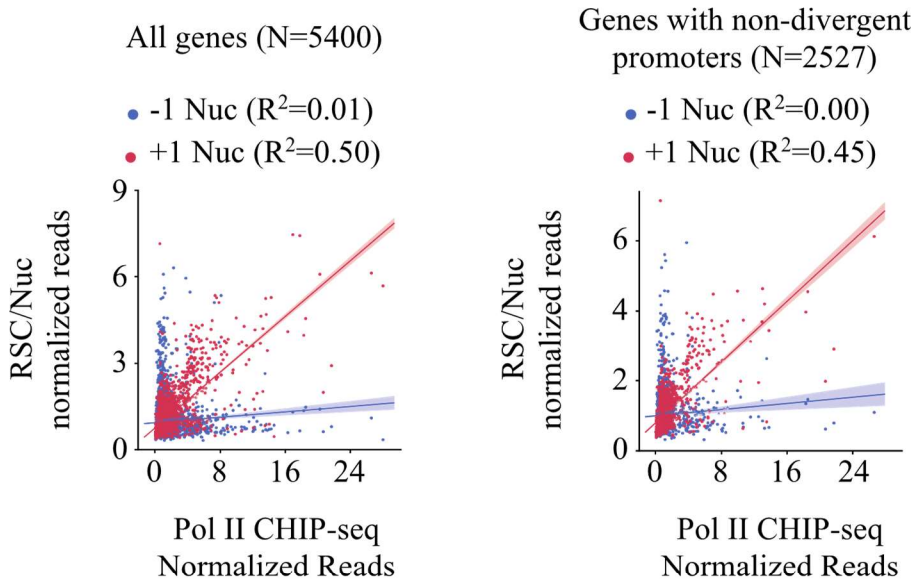

Figure 3.6. RSC enrichment at the +1 nucleosome correlates with Pol II occupancies. Scatterplots showing the correlations between normalized Pol II ChIP-seq reads with the normalized RSC MNase ChIP-seq reads at -1 and +1 nucleosome positions for all genes (N=5400) and for the subset of genes that do not contain divergent promoters (N=2527).

3.4 Nucleosomes in Transcribed Coding Sequences are Sensitive to Digestion by Micrococcal Nuclease (MNase)

In-vitro studies have shown that RSC can slide, evict, and remodel nucleosomes into alternate conformations to allow for PIC assembly and to facilitate Pol II passage (Clapier et al., 2017; Harada et al., 2016; Lorch and Kornberg, 2017; Saha et al., 2002; Shukla et al., 2019; Shukla et al., 2010). However, these methods have limitations in predicting the exact mechanisms of RSC remodeling in vivo, as these assays are often missing other factors found inside the cell that may modulate RSC activity. Additionally, many of these techniques use reconstituted nucleosomes which lack many of the modifications observed on nucleosomes in vivo. However, it is challenging to study RSC activity in vivo, as each nucleosome within the cell is unique in terms of the DNA sequences it binds to and the combination of modifications it possesses. RSC, in turn, may interact with each nucleosome in a slightly different fashion compared to other nucleosomes, and this may affect how RSC remodels each nucleosome (sliding vs ejecting, etc.). In addition, RSC has been shown to interact with many different factors inside the cell that may further modulate RSC recruitment and activity (Ferreira et al., 2011; Kubik et al., 2018; Swanson et al., 2003), making it extremely difficult to measure RSC activity in an in vivo setting directly.

Despite this, current nucleosome mapping techniques might provide insights into RSC remodeling in vivo. MNase-seq and MNase ChIP-seq exploit the aggressive nuclease properties of MNase to digest the linker DNA between nucleosomes. Because nucleosomal DNA is resistant to MNase digestion, these MNase-protected DNA fragments (MPDFs) can be isolated and sequenced to determine the occupancies and

positioning of nucleosomes and factor-bound nucleosomes (Ramachandran et al., 2017). Since nucleosomes wrap 147 bp of DNA (Henikoff et al., 2011; Ramachandran et al., 2017; Ramachandran and Henikoff, 2016), canonical nucleosomes should yield MPDFs ~150 bp in size after MNase digestion. However, if the DNA is unwrapped or if H2A/H2B dimers are ejected from the nucleosome by factors such as remodelers (Brahma and Henikoff, 2019; Ramachandran et al., 2017), the DNA of that nucleosome should be more accessible to MNase, generating MPDFs that are shorter than 147 bp (Figure 3.7A).

To determine the accessibility of nucleosomes at a genome-wide level, MNase digestion was performed using wild-type cells and the isolated DNA was subjected to deep sequencing, where 20-30 million reads were generated per sample. The reads (henceforth fragments) were then aligned to the genome to determine each fragment's location, and the fragments' sizes were then analyzed. The fragment sizes for each wild-type replicate were nearly identical to each other, indicating that the extent of digestion did not vary between the replicates. Most of the fragment sizes for the digested chromatin were between 100 bp to 200 bp, with the peak centered at around 150 bp, consistent with the length of DNA wrapped around a canonical nucleosome (Figure 3.7B). The metagene profiles showing the nucleosome dyad densities also matched each other (Figure 3.7C). Each peak on the density profile represents the average location of the center of each nucleosome, and the large trough directly upstream of the TSS represents the NDR. The peaks immediately upstream and downstream of the NDR represent the -1 and +1 nucleosomes, respectively, and the peaks downstream of the +1 nucleosome peak represent the +2 nucleosome, +3 nucleosome, and so forth. The profiles in Figure 3.8,

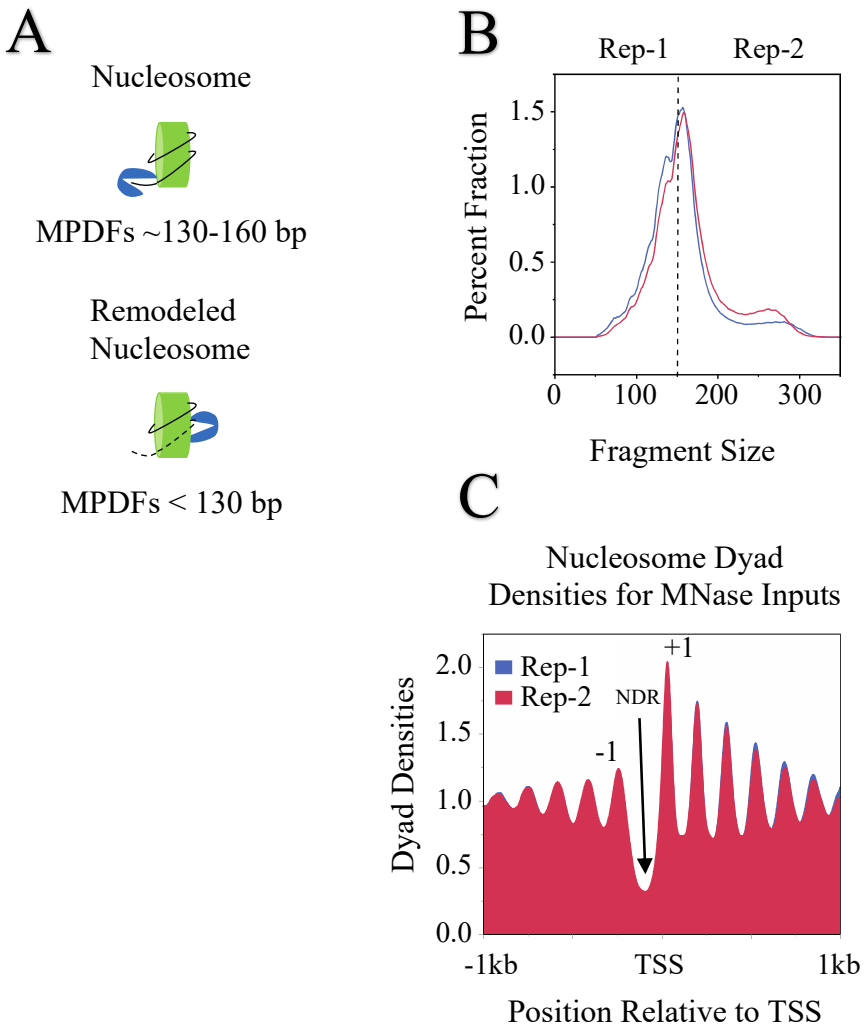

Figure 3.7. Chromatin replicates digested with MNase show similar digestion patterns. A) Schematic showing the potential generation of MNase-protected DNA fragments (MPDFs) from nucleosomes. MNase digestion of canonical nucleosomes generally yields fragments ~130-160 bp in length, while accessible nucleosomes that may have been remodeled might yield MPDFs shorter than 130 bp. B-C) Profiles showing fragment length distribution (B) and nucleosome dyad densities (C) of MNase-digested chromatin produced from two biological replicates (Rep-1 and Rep-2). Dyad density profiles are centered at the TSS.

as well as all other profiles in this work depicting nucleosome occupancies, show a similar pattern in terms of nucleosome positioning, even if the height of each peak is different in each profile. Therefore, for all profiles depicting nucleosome occupancies or MPDFs in this work, the valley that is observed upstream of the TSS henceforth represents the NDR, the peaks flanking the NDR represent the -1 and +1 nucleosomes, and peaks downstream of the +1 nucleosome peak represent the +2, +3, +4 and further downstream nucleosomes located in the coding sequences.

To determine whether nucleosomes at different locations differed in accessibility, the abundance of shorter MPDFs was determined genome-wide by analyzing the MNase-seq data for all genes according to different MPDF lengths. Even though canonical nucleosomes should be largely resistant to MNase digestion and yield fragments ~150 bp in length (Figure 3.7A), there is the possibility that MNase might have been able to access the DNA at the entry and exit points of some of these nucleosomes, yielding MPDFs slightly shorter than 150 bp. Alternately, it is possible that small regions of linker DNA remained undigested on some of the nucleosomes, yielding MDPFs slightly longer than 150 bp. As such, MDPFs ~130-160 bp were considered to have originated from canonical nucleosomes, while MPDFs shorter than 130 bp were considered to be derived from more accessible nucleosomes.

A smaller enrichment for MPDFs shorter than those of canonical nucleosomes (~130-160 bp) was evident for all nucleosomes (Figure 3.8A, compare black trace to colored traces), where enrichment for MPDFs shorter than 120 bp was highest at the -1 and -2 nucleosome positions. The shorter MDPFs at these positions might reflect the chromatin remodeling in the promoter-proximal regions upstream of NDRs that ensues

during transcription. The -1 and +1 nucleosomes are also enriched in the histone variant H2A.Z. Since H2A.Z-containing nucleosomes are inherently less stable than canonical nucleosomes (Weber et al., 2014), the enrichment of shorter MPDFs might be partly due to the presence of H2A.Z. Shorter MPDFs were also enriched at positions downstream of the +1 nucleosome position, indicating that nucleosomes within coding sequences are accessible to MNase digestion.

Since shorter MPDFs were enriched in CDSs and that nucleosomes in CDSs of highly transcribed genes might be remodeled to facilitate Pol II elongation during transcription, it is possible that the CDSs of highly transcribed genes might display a greater abundance of shorter MPDFs than non-transcribed genes. To test this, MPDF fragment lengths were analyzed for the subsets of genes containing the highest levels of Pol II (top 10% Pol II-occupied genes, T10, N = 576) or the lowest levels of Pol II (bottom 10% Pol II-occupied genes, B10, N = 576) (Figure 3.8B). MPDFs greater than 130 bp, representing canonical nucleosome MPDFs, were compared to fragments shorter than 130 bp for each subset of genes. B10 genes displayed higher levels of canonical nucleosome MPDFs than T10 genes (Figure 3.8B, compare dark red and dark blue traces) and showed a greater enrichment of MPDFs > 130 bp than shorter fragments at nucleosome positions downstream of the +1 nucleosome position (compare light and dark blue traces). In contrast, T10 genes showed a higher enrichment of shorter fragments than canonical nucleosome fragments at both promoters and CDSs. The greater proportion of shorter MPDFs in T10 genes suggests that nucleosomes in highly transcribed genes might be more susceptible to MNase digestion than lowly transcribed genes (B10), indicating that nucleosomes in CDSs of transcribed genes are more accessible than non-transcribed

genes.

3.5 RSC-bound Nucleosomes are Susceptible to MNase Digestion

Considering that nucleosomes in promoters and coding sequences both showed the presence of MPDFs shorter than those of canonical nucleosomes and that remodeled nucleosomes should be more susceptible to MNase digestion (Ramachandran et al., 2017), it is possible that these accessible nucleosomes are bound and remodeled by RSC. To determine if RSC-bound nucleosomes are more accessible than other nucleosomes, RSC ChIP-seq was performed using MNase-digested chromatin, and the resulting reads were then aligned to the genome, where the fragment sizes were then analyzed. Because a greater fraction of shorter MPDFs were enriched for nucleosomes in transcribed CDSs versus lowly transcribed CDSs (Figure 3.8B), and RSC preferentially binds to CDSs of genes containing high levels of Pol II (Figures 3.4 and 3.5), fragment length analysis was conducted for the 10% genes with the highest levels of Pol II (Pol II-T10) and the 10% genes with the lowest levels of Pol II (Pol II-B10). At Pol II-B10 genes, both RSC-bound nucleosomes and total nucleosomes (all nucleosomes including RSC-bound nucleosomes) had fragments sizes ranging from ~75 bp to 200 bp in length, with a peak centered at 150 bp in length, indicating that the majority of fragments were the size of canonical nucleosomes (Figure 3.9A). However, there were a proportion of fragment sizes below 150 bp in length before the signal dropped off at around 75 bp for both RSC-bound nucleosomes and total nucleosomes. There were slightly more fragments with sizes ranging from ~75 – 120 bp in length for RSC-bound nucleosomes compared to total nucleosomes (compare orange trace with blue trace). In contrast, RSC-bound nucleosomes at Pol II-T10 genes showed a broader range of fragment lengths than total

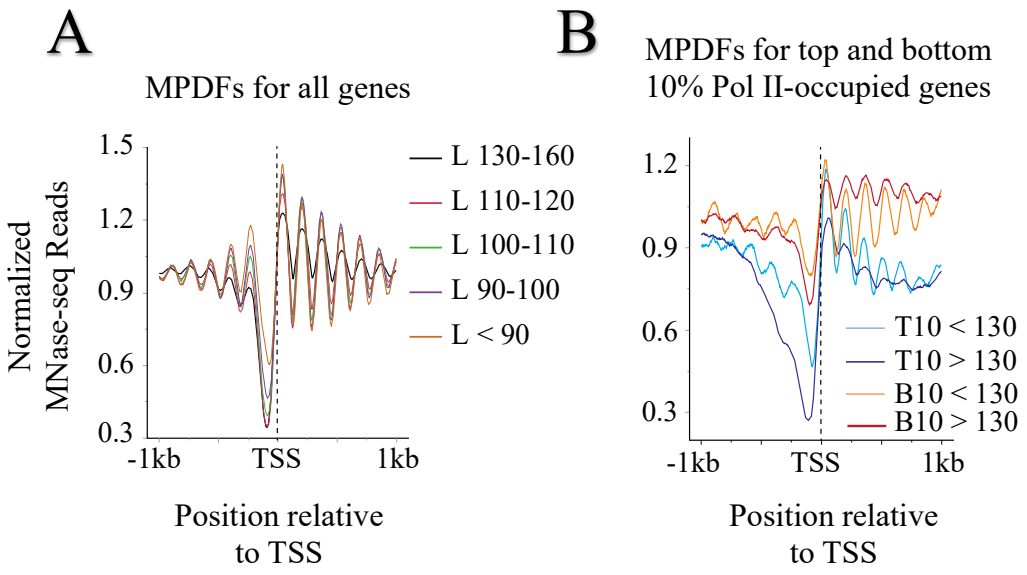

Figure 3.8. Nucleosomes in CDSs are susceptible to MNase digestion. A) Metagene profile showing the MPDF lengths for all genes. Fragment lengths were grouped into categories based on size. The first group has MPDFs ranging from those of canonical nucleosomes (130-160 bp), the second group contains fragments from 110-120 bp in length, the third group from 100-110 bp, the fourth group 90-100 bp, and the last group containing fragments shorter than 90 bp. B) Metagene profile depicting the average occupancies of MPDFs for the top 10% (T10) and bottom 10% (B10) of Pol II-occupied genes. MPDFs for both gene subsets were divided into two categories based on fragment sizes, where one category consists of fragments > 130 bp (dark traces), and the other category contains fragments < 130 bp (light traces). Profiles are centered around the TSS for each figure.

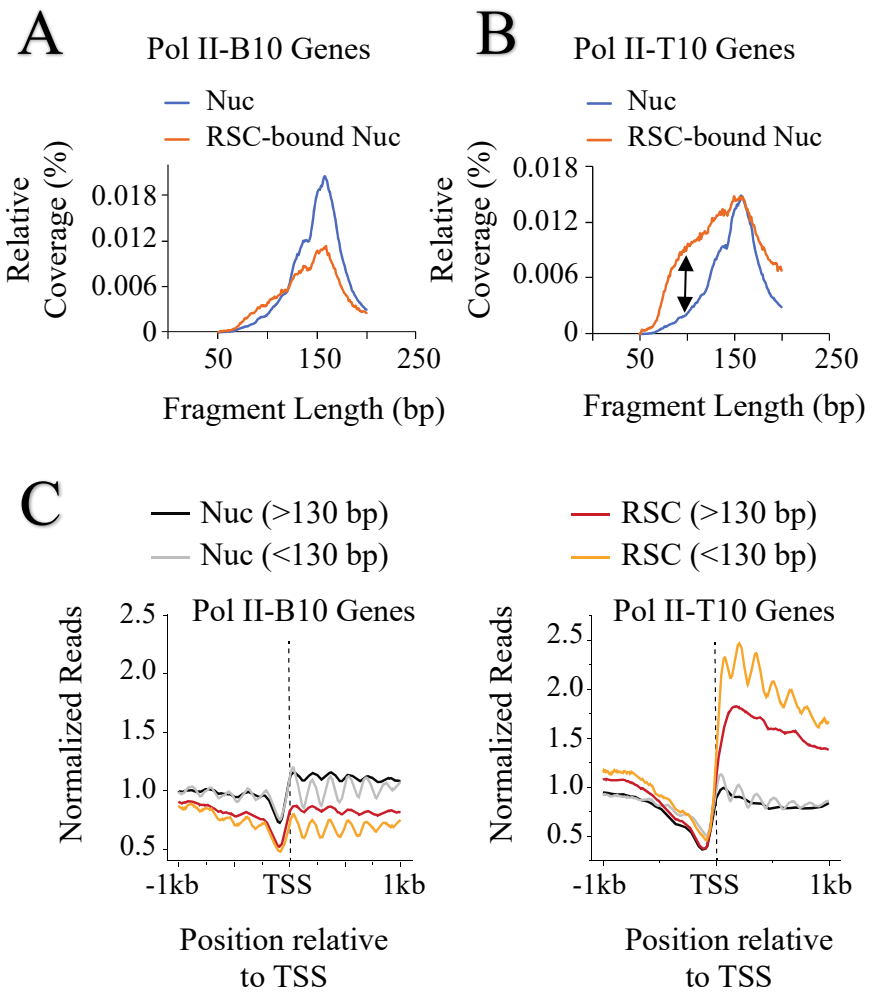

Figure 3.9. RSC associates with full-length and shorter MPDFs. A-B) Metagene profiles depicting the relative coverage of MPDF lengths of RSC-bound nucleosomes and total nucleosomes for the Pol II-B10 (A) and Pol II-T10 (B) genes. C) Metagene profiles showing the average occupancies of MPDFs for the Pol II-B10 (left panel) and Pol II-T10 (right panel) genes. MPDFs for both gene subsets were divided into two categories based on fragment sizes, where one category consists of fragments > 130 bp (dark traces), and the other category contains fragments < 130 bp (light traces). Profiles are centered around the TSS for each figure. Nuc, nucleosome; Pol II-B10, 10% genes with the lowest Pol II occupancies; Pol II-T10, 10% genes with the highest Pol II occupancies.

nucleosomes, where the smallest fragments for RSC-bound nucleosomes were ~50 bp in size compared to ~75 bp for total nucleosomes (Figure 3.9B, compare blue and orange traces). Additionally, there was a substantial proportion of fragments shorter than 150 bp for RSC-bound nucleosomes, much higher than the proportion of shorter fragments observed for total nucleosomes (see double-ended arrow for comparison). This difference in the abundance of shorter fragments between RSC-bound nucleosomes and total nucleosomes is greater in the Pol II-T10 genes than in Pol II-B10 genes (compare traces in Figure 3.9B to those in 3.9A). Overall, these data suggest that RSC-bound nucleosomes, especially RSC-bound nucleosomes in Pol II-occupied genes, are more susceptible to MNase digestion than the general nucleosome population.

Since RSC binds to the CDSs of transcribed genes, we wondered if the shorter MPDFs associated with RSC-bound nucleosomes were found in the CDSs of Pol II-occupied genes. To this end, the RSC MNase ChIP-seq and MNase-seq data were analyzed according to MPDF lengths for Pol II-T10 and Pol II-B10 genes (Figure 3.9C). MPDF profiles were plotted for both RSC-bound nucleosomes and total nucleosomes, and the MPDF lengths were separated into two categories for each data set: fragment sizes >130 bp (dark traces) and sizes < 130 bp (lighter traces). At Pol II-B10 genes, the level of reads was slightly higher for total nucleosomes than RSC-bound nucleosomes for both MPDFs > 130 bp and < 130 bp (compare black/grey and red/orange traces in the left panel). The proportion of fragments > 130 bp for RSC-bound nucleosomes is also larger than that of shorter fragments, indicating limited enrichment for shorter MPDFs for RSC-bound nucleosomes at lowly transcribed genes (compare red with orange traces). In contrast, the level of RSC-bound MPDFs at Pol II-T10 genes is higher than in total

nucleosomes, especially in the regions downstream of the TSS, providing further evidence that RSC associates with nucleosomes in transcribed CDSs (compare traces in the righthand panel). Furthermore, the proportion of MPDFs < 130 bp was substantially higher than MPDFs > 130 bp for RSC-bound nucleosomes, particularly in the CDSs of Pol-T10 genes (compare red trace to orange trace in the righthand panel). While there were also slightly more reads for MPDFs < 130 bp than those > 130 bp for total nucleosomes, this increase was not nearly as pronounced as that seen for RSC-bound nucleosomes. The positioning of RSC-bound nucleosomes also seemed to be more diffuse at Pol II-T10 genes than total nucleosomes, suggesting that RSC-bound nucleosomes could be more dynamically positioned compared to canonical nucleosomes, especially those at highly transcribed genes.

The higher proportion of shorter MPDFs in RSC-bound nucleosomes suggests that the higher levels of RSC and attendant remodeling might make these nucleosomes more susceptible to MNase digestion. To provide more clarity as to the distribution of fragments sizes in RSC-bound nucleosomes versus total nucleosomes, 2-Dimensional (2-D) occupancy analysis of fragment length distributions was performed for RSC-bound nucleosomes and total nucleosomes at Pol II-T10 genes, Pol II-B10 genes, and RPGs (Figure 3.10 A-B). These analyses generated heatmaps displaying fragment size densities in relation to the location on a typical gene, where the y-axis represents the length of the fragment and the x-axis shows the location of the fragment relative to the TSS. For total nucleosomes, the sizes of the MPDFs at all gene sets were slightly longer than 150 bp, as indicated by the red and yellow hues concentrated at a line towards the top of the heatmaps (Figure 3.10A). The red is most intense at the Pol II-B10 genes. In contrast, the

red signal in Pol II-T10 and RPGs becomes fainter and transitions to more orange/yellow, especially after the TSS, indicating an inherently lower nucleosome level at highly transcribed genes than in lowly transcribed genes. Despite this difference in nucleosome densities, the 2D fragment size distribution profiles look similar for all three gene sets, indicating that nucleosomes at these gene sets show similar susceptibility to MNase digestion.

At Pol II-B10 genes, the 2D fragment distribution profile for RSC-bound nucleosomes appears similar to the profiles for total nucleosomes, though the nucleosome density is less than the total nucleosome profiles (Figures 3.10A and B, compare yellow hues of Pol II-B10 profile in 3.10B to redder hues in profiles of 3.10A). In stark contrast, the Pol II-T10 profile shows a much more varied distribution of fragment sizes than nucleosome profiles or the Pol II-B10 RSC-bound profile, especially after the TSS, in which a substantial proportion of fragments were below 150 bp (Figure 3.10B). This variation in fragment sizes observed after the TSS is even more pronounced for RSC-bound nucleosomes in RPGs, where a larger percentage of fragments are shorter than 100 bp. There is a significant fraction of fragments in the RSC-bound nucleosome Pol II-T10 and RPG profiles that are longer than 150 bp. This could indicate the protective properties provided by the formation of the RSC-nucleosome complex (Shukla et al., 2010), where bound RSC could physically shield the DNA of some nucleosomes from MNase digestion. The shorter fragments, in turn, could represent partially-unwrapped nucleosomes or hexasomes (Brahma and Henikoff, 2019). Indeed, the fragment length analyses conducted for RSC-bound nucleosomes and total nucleosomes at these gene sets reveal that the profiles for RSC-bound nucleosomes, especially the profiles for Pol II-T10

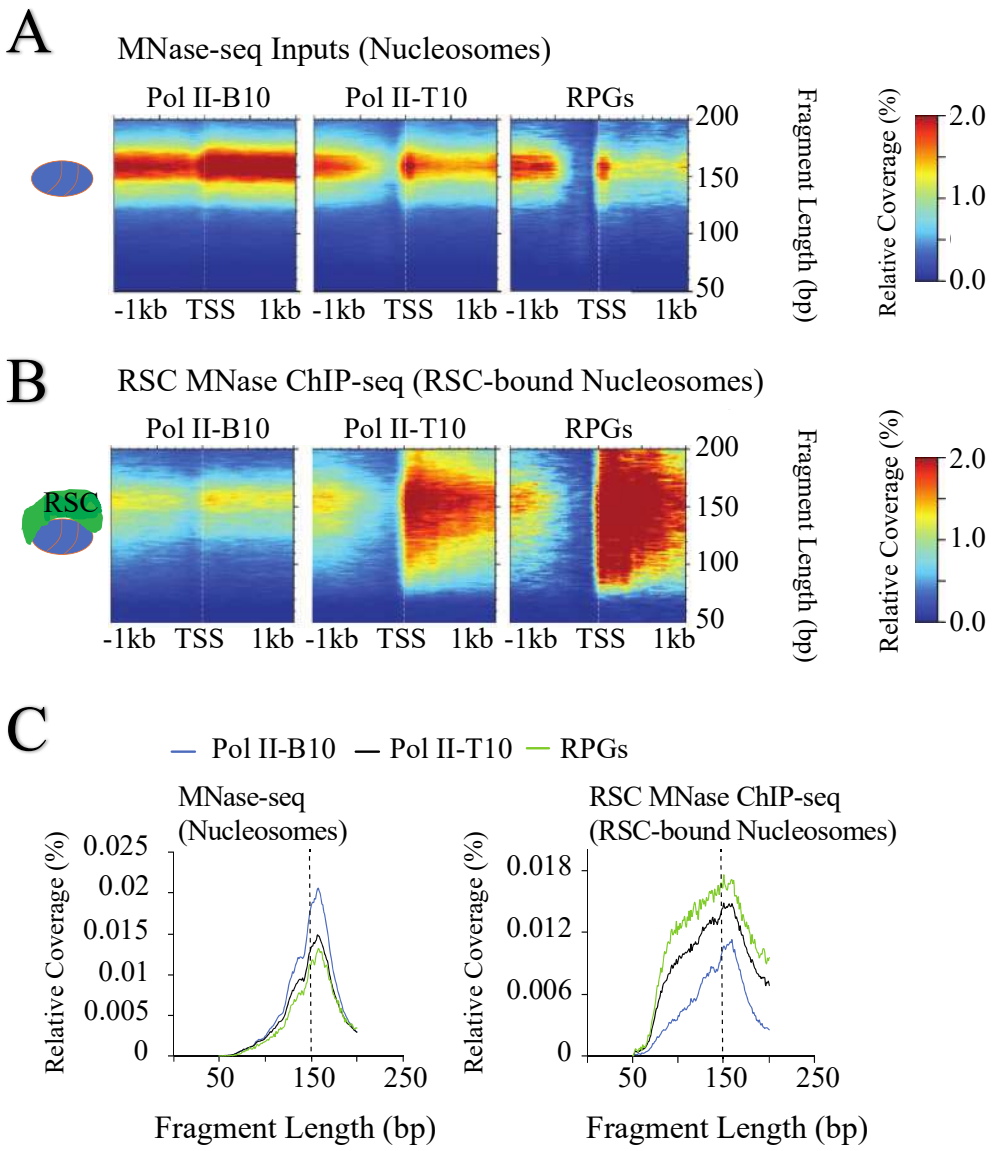

Figure 3.10. RSC MDPFs are more heterogenous in CDSs of transcribed genes. A-B) Heatmaps depicting the 2-D occupancies of MPDFs from nucleosomes (A) and RSC-bound nucleosomes (B) at Pol II-B10 genes, Pol II-T10 genes, and at RPGs. Heatmaps are centered at the TSS, and the fragment lengths are shown on the y-axis. C) Metagene profiles depicting the relative coverage of MPDF lengths of total nucleosomes and RSC-bound nucleosomes for Pol II-B10 genes, Pol II-T10 genes, and RPGs. Pol II-B10, 10% genes with the lowest Pol II occupancies; Pol II-T10, 10% genes with the highest Pol II occupancies; RPG, Ribosomal Protein Genes.

genes and RPGs, are broader than the profiles for total nucleosomes (Figure 3.10C, compare profiles in the lefthand panel to those in the righthand panel). The broad profiles of the Pol II-T10 genes and the RPGs are relatively smooth compared to the discrete-sized fragments observed when MNase is over-digested (Chereji et al., 2018) and fit with the observed remodeling activity of RSC, which gradually exposes nucleosomal DNA through its translocase activity (Clapier et al., 2016). Over-digestion by MNase occurs when either an excessive amount of MNase is used or the digestion is allowed to proceed for too long, allowing the MNase to begin unwrapping and digesting nucleosomal DNA. Because the fragment length profiles do not match the profiles observed from over-digested chromatin, this suggests that RSC-bound nucleosomes are truly more accessible than canonical nucleosomes rather than simply being an artifact caused by over-digestion.

Since the fragment size profiles for total nucleosomes are similar for lowly transcribed genes and highly transcribed genes (Figures 3.10A and 3.10C, lefthand panel), the differences in the RSC-bound nucleosome profiles (Figures 3.10B and 3.10C, righthand panel) suggest that unwrapped nucleosomes might only represent a small fraction of the total nucleosomes present within CDSs, even in transcribed genes. Altogether, these data show that RSC-bound nucleosomes, especially those in transcribed regions, are more susceptible to MNase digestion than canonical nucleosomes.

3.6 Pol II also Interacts with MNase-Susceptible Nucleosomes in vivo

Earlier studies have shown that Pol II tends to localize extremely close to nucleosomes in coding sequences (Churchman and Weissman, 2011) and has been shown to interact with nucleosomes (Koerber et al., 2009). Considering that RSC-bound nucleosomes in CDSs of transcribed genes display heterogenous fragment sizes and that

the presence of RSC enhanced transcription through acetylated chromatin templates in vitro (Carey et al., 2006), Pol II-bound nucleosomes might also display heterogenous fragment lengths. To determine the MPDF lengths of Pol II-bound nucleosomes, Rpb3 ChIP-seq was performed using MNase-digested chromatin. Rpb3 is one of the core subunits of Pol II (Cramer, 2002), so using an antibody specific to this subunit should isolate any RSC-bound nucleosomes in formaldehyde-crosslinked chromatin. The resulting DNA isolated after ChIP was then sequenced, and the reads were then aligned to the genome and subjected to fragment size analysis. In accordance with previous studies, Pol II largely localized to the CDSs of genes with high levels of Pol II, represented by the red hues located after the TSS in the region towards the top of the heatmap (Figure 3.11A). To ensure that nucleosomal-length fragments were associated with Pol II, Rpb3 MNase ChIP-seq signals were analyzed for fragment sizes between 130-160 bp, as these fragments are unlikely to be generated by MNase protection from the elongating Pol II itself. Since Pol II can interact with naked DNA, the Rpb3 ChIP-seq occupancies were compared to Rpb3 ChIP-seq reads from sonicated chromatin (Figure 3.11B). Sonication utilizes ultrasonic waves to shear the linker DNA between chromatin, yielding fragment sizes between 200-400 bp long. While the mapping resolution of sonicated ChIP-seq data is lower than that of MNase ChIP-seq data, it does not suffer from the sequence bias produced from MNase (Lee and Keung, 2018), making ChIP-seq data a useful tool to confirm the observations from MNase ChIP-seq data. The Pol II MNase ChIP-seq occupancies correlated with the Pol II ChIP-seq occupancies from sonicated chromatin (Figure 3.11B, $R^2 = 0.7116$). Since there was a strong Rpb3 signal for 130-160 bp MPDFs in the MNase ChIP-seq data, this suggests that Pol II interacts

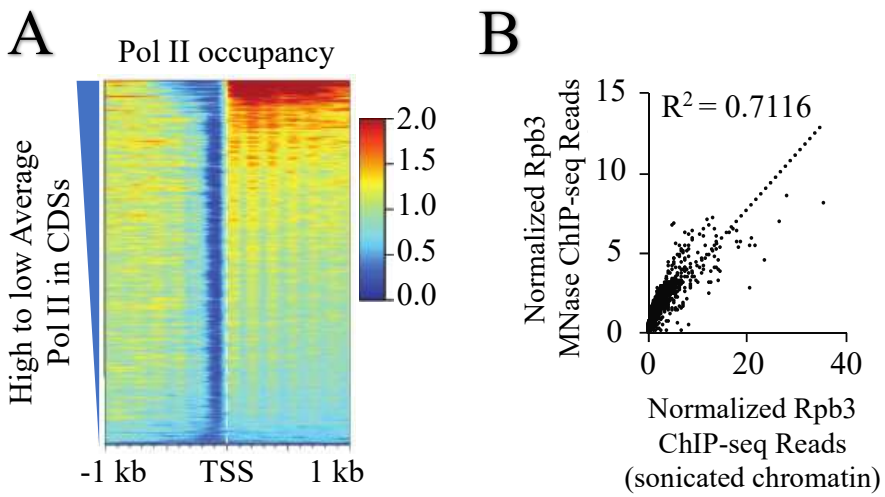

Figure 3.11. Pol II interacts with nucleosomes genome-wide. A) Heatmap depicting Pol II occupancies generated from Rpb3 MNase ChIP-seq data. Genes are sorted by decreasing Pol II occupancies determined from Rpb3 ChIP-seq from sonicated chromatin and are centered at the TSS. B) Scatterplot showing the correlation between normalized Rpb3 ChIP-seq occupancies from MNase and sonicated chromatin.

with nucleosomes in CDSs as opposed to naked DNA, in agreement with previous studies (Bondarenko et al., 2006; Ujvari et al., 2008) (Kireeva et al., 2002) (Kulaeva et al., 2013).

To determine the fragment size distribution of Pol II-bound nucleosomes, 2-D occupancy profiles depicting the fragment length distribution densities for Pol II-bound nucleosomes were generated and examined (Figure 3.12A). Because the majority of Pol II is found in highly transcribed (Pol II-occupied) genes, only the top 10% of Pol II-occupied genes were selected for analysis. The replicates showed very similar profiles and resembled the highly heterogenous fragment profiles of RSC-bound nucleosomes, especially at regions after the TSS (compare 3.12A to 2-D profiles of RSC-bound nucleosomes at the Pol II-T10 and RPGs in 3.10B). A substantial population of the MPDFs had lengths below 130 bp, indicating that MNase ChIP-seq might be able to detect Pol II that is interacting with or traversing through nucleosomes. This in vivo data would be consistent with cryo-EM structures that show Pol II transcribing through nucleosomes (Farnung et al., 2018; Kujirai et al., 2018). To determine if Pol II-bound nucleosomes overlapped with the positions of RSC-bound nucleosomes, the dyad density profiles for RSC-bound and Pol II-bound nucleosomes were generated and analyzed (Figure 3.12B). The dyad positioning of canonical nucleosome MPDFs (> 130) of total nucleosomes (Nuc) largely overlapped those obtained from Rbp3 and RSC MNase ChIP-seq. The shorter MPDFs (< 130 bp) of Pol II-bound nucleosomes also overlapped the Nuc profile and were not exclusively present within the inter-nucleosomal regions, indicating that these shorter MPDFs originated, at least in part, from accessible nucleosomes. The similarity between the size distribution of RSC-bound and Pol II-bound nucleosomes (Figures 3.10B and 3.12), as well as the strong correlation between

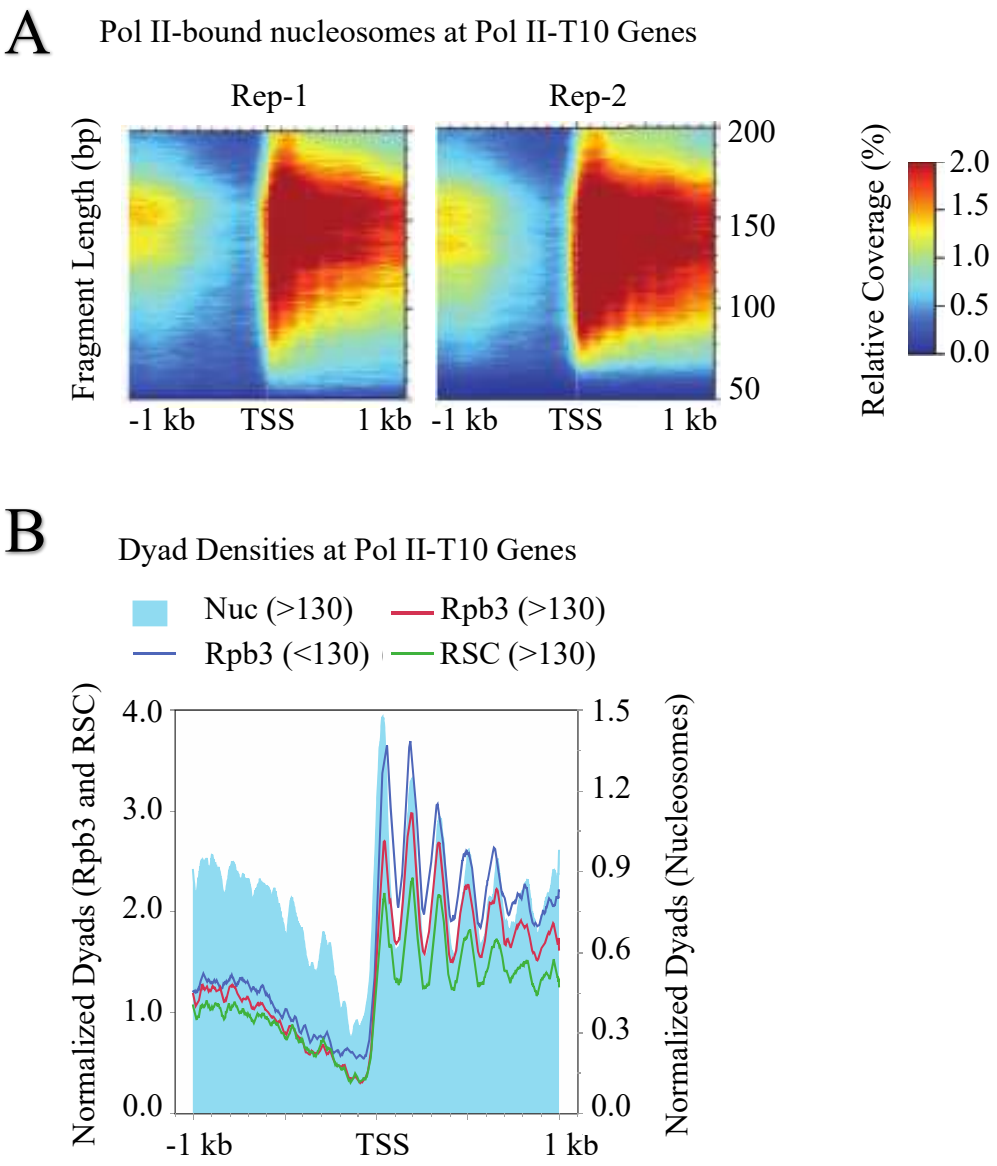

Figure 3.12. Pol II-bound nucleosomes display shorter MPDFs. A) 2-D occupancy profile showing MPDF distribution of Pol II-bound nucleosomes for the top 10% of transcribed genes (Pol II-T10). The profiles for the two replicates (Rep-1 and Rep-2 are shown. B) Profile depicting the dyad densities for Rpb3-bound (Rpb3), RSC-bound (RSC), and total nucleosomes (nucs). Profiles are centered around the TSS. MPDFs < 130 bp and >130 bp are shown for Rpb3, whereas MPDFs > 130 bp are shown for RSC and nucs.

RSC and Pol II occupancies (Figure 3.6), suggest that RSC might help Pol II during transcription elongation by increasing the accessibility of nucleosomal DNA in coding sequences. However, given that Pol II has been shown to transcribe through nucleosomes, it is also possible that the partial unwrapping of accessible nucleosomes by Pol II might facilitate the RSC recruitment to CDSs to further aid in the remodeling of nucleosomes. Due to the interconnected roles of RSC and Pol II in coding sequences, it is challenging to tease out the individual effects of Pol II and RSC in possibly generating these accessible nucleosomes. Indeed, this difficulty demonstrates why remodeling activity in RSC has not been elucidated in vivo. Nevertheless, these findings provide further insight into the accessibility of RSC-bound nucleosomes in vivo and may be an indirect observation of RSC remodeling at a genome-wide scale.

3.7 RSC Plays a Role in Generating Accessible Nucleosomes

Given that both Pol II and RSC are associated with the generation of MPDFs shorter than those of canonical nucleosomes within transcribed CDSs, it is imperative, though difficult, to determine if RSC might generate any of these fragments. To attempt to tweeze out some of the effects of RSC on nucleosome accessibility from those of Pol II, MNase-seq data was analyzed from a previous study in which RSC was depleted (Klein-Brill et al., 2019). Because several subunits of RSC, including Sth1, are essential (Cairns et al., 1996), these proteins must be rapidly depleted before crosslinking. In the study, Sth1 was depleted using the auxin-inducible degradation strategy (Morawska and Ulrich, 2013; Nishimura et al., 2009). Cells encoding for a TIR1 F-box protein and Sth1 tagged with an auxin-inducible degron (AID) were treated with the plant hormone auxin 1 hour before harvesting. Within the cells, TIR1 forms a complex with SKP1–CULLIN–

F-box (SCF) to form an E3 ligase, and the addition of auxin facilitates the interaction of TIR1 with the AID-tagged Sth1. TIR1-SCF then ubiquitinates the AID-tagged Sth1 to mark it for degradation by the 26S proteasome, resulting in depletion of Sth1 within 1 hour after auxin addition. MNase-seq data from untreated (WT, 0 min) cells and Sth1-depleted (60 min) cells underwent MPDF analysis where fragments were grouped into sizes > 130 bp (representing canonical nucleosomes) or < 130 bp (representing more accessible nucleosomes) and plotted as MPDF profiles (Klein-Brill et al., 2019) (Figure 3.13). Since RSC localizes to the CDSs of highly transcribed genes (Figures 3.4-3.5), the MPDFs were analyzed at RPGs and the top 10% of transcribed genes. At RPGs, Sth1 led to a decrease in the ratio of shorter MPDFs to nucleosomal fragments at both promoters and at CDSs (Figure 3.13A, compare dotted red trace to solid red trace) and an increase in nucleosomal MPDFs in CDSs (compare yellow and blue traces). Similar reductions in shorter MPDFs and increases in nucleosomal fragments in CDSs were observed in the top 10% of transcribed genes (Figure 3.13B). These results are consistent with the idea that RSC might remodel nucleosomes within CDSs to generate accessible nucleosomes that yield shorter MPDFs. Since RSC depletion has also been associated with a reduction in Pol II (Klein-Brill et al., 2019; Kubik et al., 2018; Ocampo et al., 2019), it is possible that MPDFs might be reduced upon RSC depletion. However, it was found that Pol II occupancies actually increased when Sth1 was depleted for the genes analyzed in Figure 3.13 (the effects of RSC on Pol II occupancies are detailed in Chapter 5). If Pol II were primarily responsible for the generation of shorter MPDFs at these genes, then the proportion of shorter fragment sizes should be higher in the Sth1-depleted cells at these genes, not lower, due to higher levels of Pol II in the CDSs. These findings suggest that

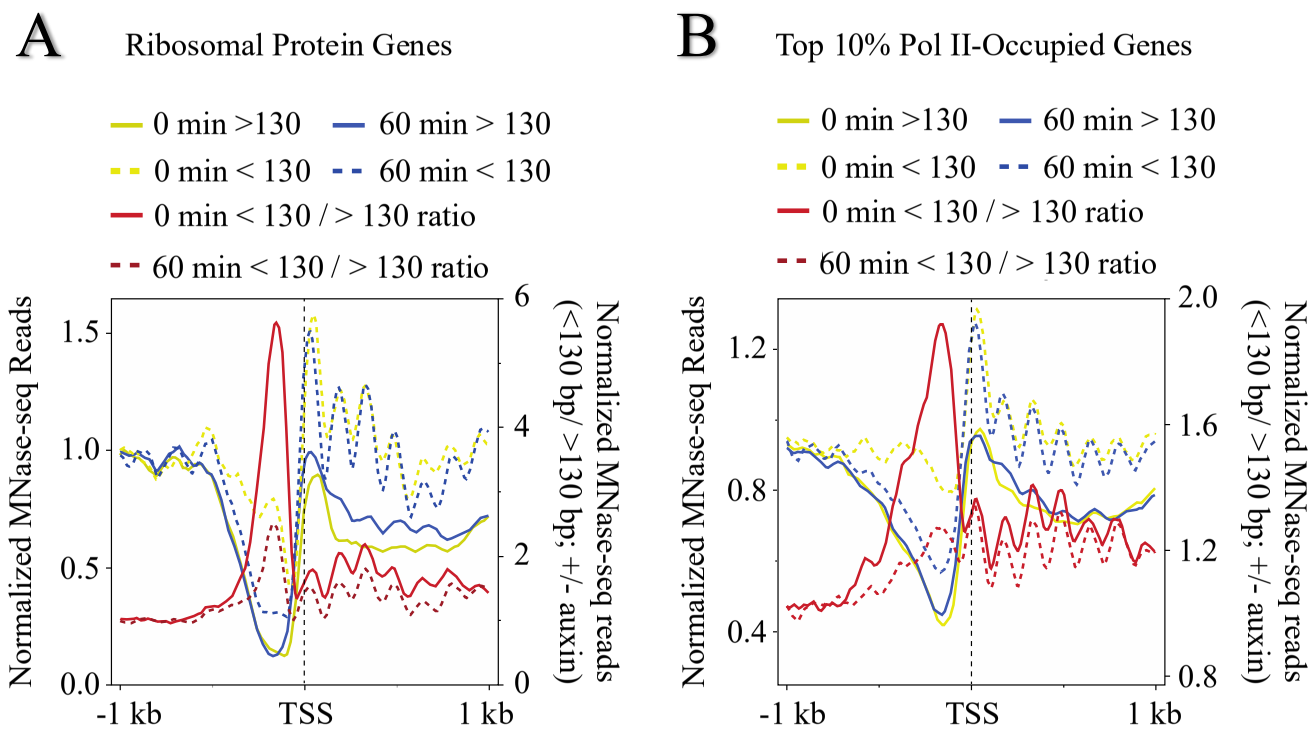

Figure 3.13. RSC contributes to nucleosome accessibility in the CDSs of transcribed genes. A-B) Profiles depicting the MPDF analysis at Ribosomal Protein Genes (RPGs) (A) and at the top 10% of Pol II-Occupied genes (B) at 0 and 60 minutes after treatment of *sth1AID* with auxin to rapidly deplete Sth1. Data obtained from (Klein-Brill et al., 2019).

RSC plays a role in generating shorter MPDFs within the CDSs of transcribed genes. There was also an increase in nucleosomal fragments at the promoters within these genes, which is consistent with transcription initiation defects observed in previous studies II (Klein-Brill et al., 2019) (Kubik et al., 2018; Ocampo et al., 2019). Overall, the data show that the proportion of MPDFs representing accessible nucleosomes is reduced in CDSs of highly-transcribed genes in cells depleted of RSC despite the lack of reduction in Pol II at these genes, suggesting that RSC might affect the ability of elongating polymerases to navigate nucleosomes. Further studies, such as determining nascent RNA levels in RSC-depleted cells, will be needed to provide more direct evidence for the role of RSC in regulating Pol II elongation. Nevertheless, the MPDF analyses conducted for this project might provide in vivo evidence for remodeling, which has been notoriously difficult to obtain.

3.8 Discussion

Collectively, the data suggest that RSC is recruited to transcribed CDSs and makes the nucleosomes within those CDSs more accessible to other factors, such as elongating polymerase. This is supported by the finding that RSC-bound nucleosomes are highly susceptible to MNase digestion (Figure 3.10), suggesting the possibility that RSC might remodel these nucleosomes and makes the nucleosomal DNA more accessible to factors such as elongating Pol II. Consistent with this, Pol II-bound nucleosomes were also more susceptible to MNase digestion than canonical nucleosomes within CDSs of transcribed genes (Figure 3.12).

Since nucleosomes are physical barriers to elongating Pol II (Lorch et al., 1987), mechanisms must exist that render nucleosomes within CDSs accessible to Pol II. The

presence of MPDFs shorter than 130 bp in the CDSs of transcribed genes indicates that MNase-susceptible or accessible nucleosomes might be generated in a transcription-dependent manner (Figure 3.8). Even though elongating Pol II has been shown to disrupt chromatin structure and to transcribe through nucleosomes (Kireeva et al., 2002; Ramachandran and Henikoff, 2016), it is likely chromatin remodelers and other factors help in generating accessible nucleosomes to facilitate Pol II elongation. However, it is unclear which remodelers may participate in this process. Both RSC and SWI/SNF can slide and evict histones (Boeger et al., 2004; Clapier et al., 2017; Montel et al., 2011) and are enriched in transcribed CDSs (Ganguli et al., 2014; Rawal et al., 2018; Spain et al., 2014; Yen et al., 2012). Additionally, in-vitro experiments have demonstrated that RSC promotes Pol II elongation through acetylated nucleosomes (Carey et al., 2006). It has also been reported that RSC also binds to "fragile nucleosomes," located in the promoters of some genes, suggesting that RSC might expose nucleosomal DNA to make these fragile nucleosomes more susceptible to MNase digestion (Brahma and Henikoff, 2019; Kubik et al., 2015). Even though there is controversy regarding the exact nature of these MNase-sensitive complexes within nucleosome depleted regions (NDRs) (Chereji et al., 2017; Kubik et al., 2017; Prajapati et al., 2020), the findings of this project and other studies have collectively shown that RSC makes nucleosomes more susceptible to MNase digestion (Cakiroglu et al., 2019; Clapier et al., 2017). Considering that promoter nucleosomes are highly accessible, this work proposes that RSC generates accessible "promoter-like" nucleosomes in the CDSs of transcribed genes to promote transcription. This is supported by data showing that the RSC-bound nucleosomes in transcribed CDSs are associated with a more heterogenous range of MPDF lengths (Figure 3.10), which

might represent nucleosome remodeling intermediates. Pol II has also been associated with shorter MPDF fragments in CDSs of transcribed genes (Figure 3.12), suggesting that accessible nucleosomes are generated during transcription. In vitro, Pol II has been shown to displace H2A/H2B dimers as it transcribes through nucleosomes (Izban and Luse, 1991; Kireeva et al., 2002), which could contribute to the shorter MPDFs observed in the in vivo experiments of this project. Consistent with the idea that nucleosomes within highly transcribed genes might require more frequent remodeling, a higher proportion of shorter MPDFs was observed at very highly transcribed genes, including RPGs (Figure 3.10C).

It is important to note that the nucleosome profile did not show the fragment heterogeneity observed for RSC-bound nucleosomes. This implies that only a small fraction of nucleosomes within a gene are accessible at any given time. Considering that RSC and Pol II were enriched at similar regions within CDSs of transcribed genes (Figures 3.5B and 3.12B) and that RSC- and Pol II-bound nucleosomes were more accessible in CDSs (Figures 3.10 and 3.12A), it is possible that nucleosomes immediately downstream of elongating Pol II might be targeted and made accessible by RSC. In contrast, other nucleosomes within CDSs would be in the less-accessible canonical conformation (Figures 3.10 and 3.14). Additionally, the shorter fragments of Pol II-bound nucleosomes suggest that Pol II either makes these nucleosomes more accessible directly or interacts with these nucleosomes. This work favors a model in which the initial disruption of nucleosomes by elongating Pol II facilitates RSC recruitment to CDSs, where RSC then remodels nucleosomes to promote more efficient transcription. Consistent with this model, RPGs show high levels of RSC-bound accessible

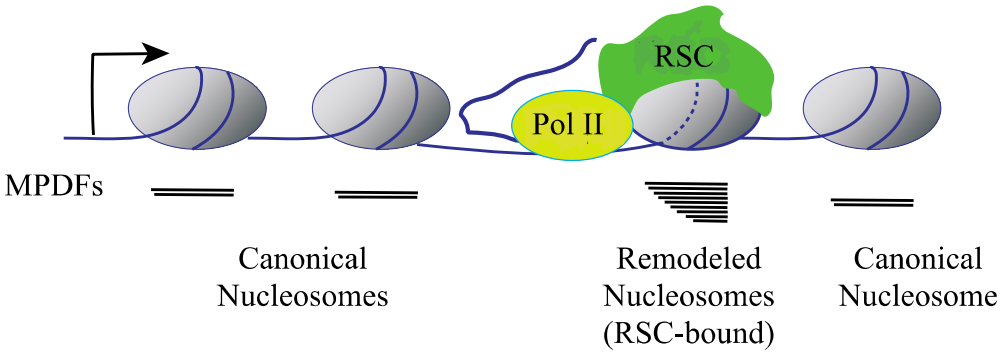

Figure 3.14. RSC remodels nucleosomes downstream of Pol II in transcribed CDSs. Model depicting RSC targeting nucleosomes downstream and in close proximity of elongating Pol II for remodeling. The remodeling status of each nucleosome is indicated by the presence of a dashed (remodeled) or solid line (canonical) on the nucleosome. Nucleosomes undergoing RSC-mediated remodeling would have DNA that is more susceptible to MNase digestion, yielding heterogenous MPDFs ranging in size from 80-160 bp. Nucleosomes not undergoing active remodeling or otherwise returned to a pre-remodeled state would have MPDFs ~150 bp. RSC recruitment could be facilitated by direct interaction with Pol II, via the hypophosphorylated Pol II CTD, or by transient histone acetylation by SAGA or NuA4. After Pol II passage, the nucleosome would have to be returned to its pre-remodeled state to prevent cryptic transcription. This reset could be achieved by deacetylation by Rpd3 or Hos2/Set3 in a histone methylation-dependent manner.

nucleosomes (Figure 3.10) and reduced nucleosome accessibility when RSC was depleted (Figure 3.13).

Previous studies have supported the idea that RSC interacts with elongating Pol II via the Rsc4 subunit or with the hypophosphorylated Pol II CTD (Soutourina et al., 2006; Spain et al., 2014). Additionally, RSC might also be able to recognize Pol II-proximal nucleosomes via the recognition of histone acetylation by RSC bromodomains, as Pol II-proximal nucleosomes are transiently acetylated by SAGA and NuA4 (Ginsburg et al., 2009; Govind et al., 2007; Kasten et al., 2004). Nucleosome acetylation has also been implicated in enhanced remodeling by RSC and has been shown to promote RSC recruitment to transcribed CDSs (Chatterjee et al., 2015; Spain et al., 2014). Thus, RSC-bound nucleosomes might resemble promoter nucleosomes in that they might be hyperacetylated and highly susceptible to MNase digestion. RSC remodeling might be limited to nucleosomes immediately downstream of elongating Pol II, as nucleosomes upstream of Pol II would be deacetylated by Hos2/Set3 and Rpd3 complexes in a histone methylation-dependent manner (Carrozza et al., 2005; Govind et al., 2010; Kim and Buratowski, 2009). The idea that RSC provides transient access to nucleosomal DNA in an acetylation-dependent manner would also offer an explanation as to why cryptic transcription within CDSs is prevalent in cells deficient in histone deacetylase or histone methyltransferase functions since these nucleosomes would still be acetylated and thus remain as targets for further remodeling (Carrozza et al., 2005; Govind et al., 2010; Kim and Buratowski, 2009). Altogether, the findings of this project provide insight into RSC function at transcribed CDSs and indirect in vivo evidence of RSC remodeling of nucleosomes within transcribed CDSs.

CHAPTER FOUR

RSC COORDINATES WITH HISTONE ACETYLTRANSFERASES GCN5 AND ESA1 TO REGULATE CHROMATIN STRUCTURE

4.1 Introduction

To understand how chromatin and transcription are regulated, it is important to know the mechanisms by which chromatin and transcription factors recognize and bind to chromatin. Histone acetylation by histone acetyltransferases (HATs) promotes transcription by recruiting factors such as chromatin remodelers (Carey et al., 2006; Hassan et al., 2007; Lai and Pugh, 2017; Spain et al., 2014). Gcn5 is the HAT subunit of the SAGA complex and is the major HAT that acetylates histone H3 of the nucleosome (Cheon et al., 2020; Cheung and Diaz-Santin, 2019; Marmorstein, 2001), whereas Esa1 is part of the NuA4 complex and is the major HAT for histone H4 (Cheung and Diaz-Santin, 2019; Marmorstein, 2001; Wang et al., 2018). In vitro and in vivo experiments have demonstrated that these HATs can acetylate lysine residues on their respective histone tails (Cheon et al., 2020; Govind et al., 2007; Marmorstein, 2001), and RSC can recognize acetylated histone tails in vitro. Specifically, RSC contains bromodomains that recognize acetylated lysine residues (Dhalluin et al., 1999; Zeng and Zhou, 2002). For instance, the RSC catalytic subunit Sth1 contains a bromodomain that binds to acetylated H3K14 in vitro and in vivo (Blus et al., 2019; Chen et al., 2020; Jain et al., 2020; Patel et al., 2019; Wagner et al., 2020). Additionally, RSC has been shown to bind to coding sequences of transcribed genes in a manner dependent on SAGA and NuA4 (Spain et al., 2014). These HATs have also been implicated in the organization of chromatin structure

at the promoter and in regulating transcription. For instance, transcriptional activators such as Gcn4 recruit SAGA and NuA4 to promoters (Ginsburg et al., 2009; Govind et al., 2005; Govind et al., 2007; Qiu et al., 2016), and this recruitment was associated with increased histone eviction and transcription. Despite these insights, the exact mechanisms by which SAGA and NuA4 coordinate with RSC to regulate RSC recruitment to nucleosomes and activity at a genome-wide scale are not known.

This work aimed to provide further insight into the roles of Gcn5 and Esa1 on RSC recruitment/activity, in vivo, at a genome-wide scale. To this end, RSC and H3 ChIP-seq was performed in wild-type (WT) *S. cerevisiae* cells and in cells lacking Gcn5 (*gcn5Δ*), functional Esa1 (*esa1*), both HATs (*gcn5Δ/esa1*) or the bromodomain in the RSC catalytic subunit Sth1 (*sth1ΔBrD*, lacks C-terminal 1270-1359 residues), since bromodomains recognize acetylated histones (Dhalluin et al., 1999; Zeng and Zhou, 2002). Esa1 is essential for cell viability, so strains containing a conditional temperature-sensitive allele of *ESA1* (*esa1L254P*) were used (Ginsburg et al., 2009). To inactivate Esa1, the *esa1* and *gcn5Δ/esa1* strains were heat shocked at 37°C for 1 hour before harvesting. This chapter focuses primarily on how the loss of HATs impacts RSC localization at a genome-wide level and how these changes in RSC localization impact chromatin organization. This chapter also presents a novel acetylation-independent role of Esa1 in recruiting RSC to promoter nucleosomes.

4.2 RSC Accumulates in the Promoters of HAT Mutants

To determine how HATs promote RSC recruitment to chromatin at a genome-wide level, RSC ChIP-seq was performed using sonicated chromatin from WT cells and from *sth1Δ*BrD*, gcn5Δ*, *esa1*, and *gcn5/esa1* mutants. These mutants contained a copy of

myc-tagged Sth1, allowing for the ChIP of RSC using an antibody specific to the myc tag. Because heat shock might induce indirect effects on RSC recruitment, WT cells were also heat shocked (HS-WT) and subjected to RSC ChIP-seq. The DNA isolated from the RSC ChIP was then sequenced and the resulting reads were aligned to the *S. cerevisiae* genome before being used for analysis. Heatmaps were generated showing RSC occupancies for WT cells, HS-WT cells, and in *sth1Δ*BrD*, gcn5Δ*, *esa1*, and *gcn5/esa1* mutants at all genes, as well as the changes in RSC occupancy compared to WT or HS-WT cells for greater clarity in determining the differences in RSC occupancies in the mutant compared to WT cells (Figure 4.1). Genes were sorted by decreasing Pol II occupancies, which were determined by separate Pol II ChIP-seq experiments. The RSC occupancies are centered at and extend +/- 1000 bp from the TSS. RSC was localized to the CDSs of transcribed genes for all strains, as indicated by the red hues after the TSS towards the top of the heatmaps (top panels), consistent with the findings of this work (Figures 3.4 – 3.5) and of previous studies (Spain et al., 2014). Just upstream of the TSS, the occupancy profiles look very similar to the WT heatmap except for *esa1* and *gcn5Δ/esa1*, where RSC levels are higher than in the WT cells. The heatmaps showing the changes in RSC occupancy compared to WT or HS-WT cells provides greater clarity regarding how RSC levels change in the mutants (bottom panels). There is a modest increase in RSC in the promoters in HS-WT cells compared to non-heat-shocked cells, as indicated by the yellow hues upstream of the TSS in the HS-WT ΔRSC occ. profile. This is consistent with studies that show that RSC redistributes from CDSs to promoters during heat shock (Vinayachandran et al., 2018), and in addition to the increase in RSC at promoters, there is also a slight reduction in RSC in the CDSs of HS-WT cells, as

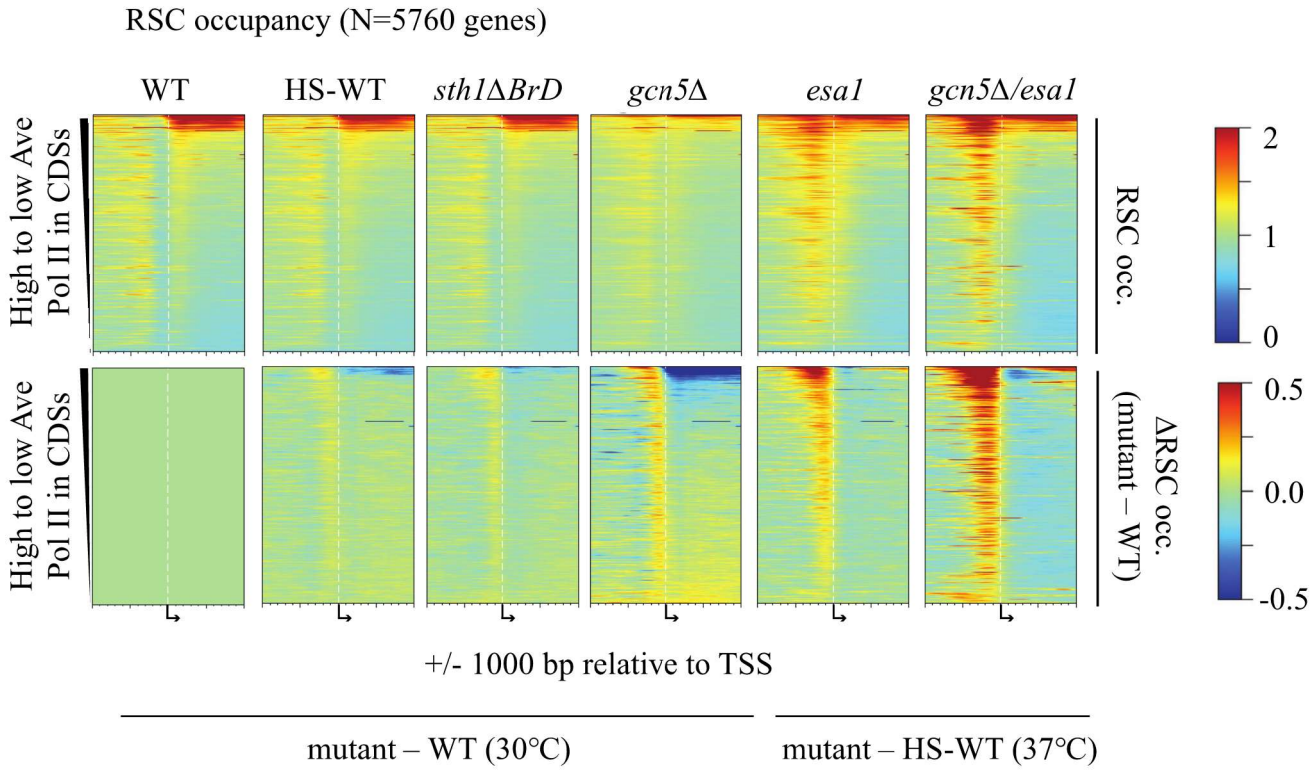

Figure 4.1. RSC accumulates in the promoters of HAT mutants. Heatmaps showing RSC occupancies (RSC occ., top panels) and the changes in RSC occupancies compared to WT or HS-WT cells (ΔRSC occ., bottom panels) at all genes (N=5760) for WT cells, heat-shocked WT cells (HS-WT), *gcn5Δ, esa1*, and *gcn5Δ/esa1*. Genes were sorted by decreasing average Pol II (Rpb3) occupancies in their CDSs and are centered at the transcription start site (TSS).

indicated by the blue hues towards the top of the HS-WT ΔRSC occ. heatmap.

Because RSC bromodomains have been shown to bind to acetylated histones (Chen et al., 2020; Kasten et al., 2004), it was expected that loss of either the Sth1 bromodomain (BrD) or the HATs would result in decreased RSC occupancies wherever RSC localized. In the CDS regions of the mutants, a slight reduction in RSC could be overserved at highly transcribed genes (Figure 4.1, blue hues at very top of ΔRSC occ. heatmaps). Surprisingly, a modest increase in RSC was observed at the promoters in *sth1ΔBrD* compared to WT cells, genome-wide, and resembled the profile of HS-WT cells. RSC accumulation at promoters was even greater in the HAT mutants, with the greatest increases observed in *esa1* and *gcn5Δ/esa1* (Figure 4.1, compare red/yellow hues upstream of the TSS in bottom panels). These changes can also be seen in the metagene profiles for the changes in RSC occupancy (Figure 4.2), where peaks of varying sizes corresponding to RSC increases can be seen in the NDRs of these strains (the profile for WT nucleosomes has been included to show the locations of the -1 nucleosome, NDR, and +1 nucleosome). The RSC accumulation observed in the *esa1*-containing mutants is likely not solely due to the effects of heat shock, as the changes in RSC occupancies for these strains were calculated against HS-WT cells, and the accumulation of RSC within these mutants was much higher than that observed for HS-WT cells (Figures 4.1 and 4.2). Plotting the RSC occupancy changes along with the MNase-seq (nucleosome) profile revealed that RSC predominantly accumulates in the nucleosome-depleted regions (NDRs) of the mutants (Figure 4.2). Additionally, RSC increases at the -1 nucleosome position in *gcn5Δ/esa1* (henceforth known as HAT double mutant) (Figure 4.2, righthand panel, compare dotted and black traces). Contrary to the expectation that RSC would

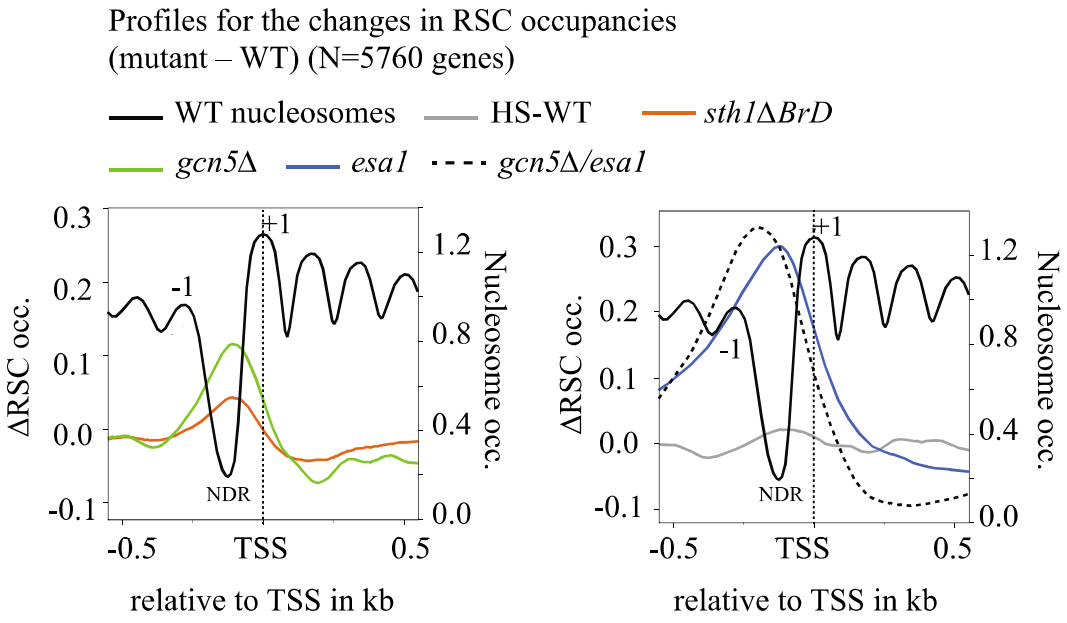

Figure 4.2. RSC accumulates at NDRs of HAT mutants and *sth1ΔBrD*. Metagene profiles depicting the changes in RSC occupancies (ΔRSC occ.) at all genes (N=5760) in the indicated strains. The lefthand y-axis displays the Δ RSC occ. and the righthand y-axis displays nucleosome occupancies. The profile for WT nucleosomes is included to easily find the location of the NDR and -1 and +1 nucleosomes, which are indicated on the profile. Profiles are centered at the TSS.

decrease in cells lacking the Sth1 bromodomain or HATs, the data shows an increase in RSC at the promoter regions in these mutants, indicating that Gcn5 and Esa1 prevent the accumulation of RSC at promoter regions genome-wide.

4.3 RSC Accumulation in Promoters Correlates with NDR Width in Mutants Lacking Functional Esa1

Given the surprising results that RSC accumulates in NDRs in cells lacking HATs, which are contrary to the slight RSC reduction in CDSs of transcribed genes and to the expectations set forth by previous studies (Chen et al., 2020; Kasten et al., 2004), it is possible that NDRs might contain certain characteristics or factors that might impact the role of Gcn5 and Esa1 in regulating RSC recruitment at promoters. Nucleosome-Depleted Regions (NDRs) are typically wider than the spaces in between nucleosomes located within CDSs and vary in length, where genes with higher levels of transcription display wider NDRs than moderately- or lowly-transcribed genes (Weiner et al., 2010). Because the accumulation of RSC seemed to be greatest in genes with the highest Pol II occupancies in the mutants (Figure 4.1, compare intense red/yellow hues at top of ΔRSC occ. heatmaps to the fainter yellow hues towards the bottom of the heatmap), the changes in RSC occupancies in the promoters of the mutants relative to WT cells was compared to NDR width to determine if NDR width correlated with RSC accumulation (Figure 4.3). To find the RSC occupancy changes at promoters, the RSC occupancies were calculated for 350 bp upstream of the TSS for each gene before the differences in RSC occupancies between each mutant and WT cells at each gene were found and plotted against the NDR width for that gene. *sth1ΔBrD, gcn5Δ,* and heat-shocked WT cells showed little to no significant correlation between NDR widths and the changes in RSC

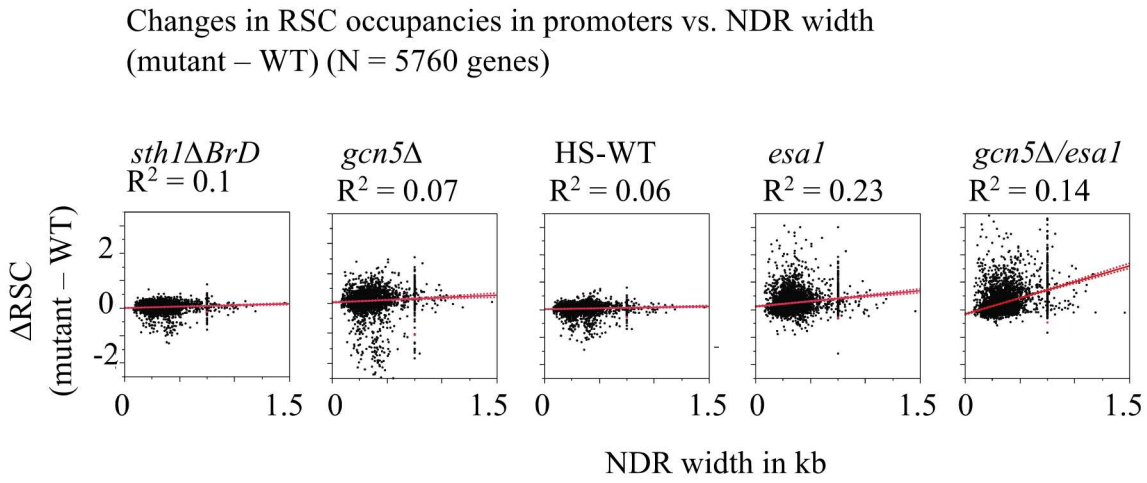

Figure 4.3. RSC accumulations in the promoters of *esa1*-containing HAT mutants slightly correlate with NDR width. Scatterplots depicting the correlations of NDR width and the changes in RSC occupancies (ΔRSC) in the promoters of *sth1ΔBrD* and the HAT mutants compared to WT cells. RSC occupancies were calculated for 350 bp upstream of the TSS for each gene.

occupancies. However, slightly higher correlations were observed for the *esa1* and *gcn5Δ/esa1* mutants, suggesting that wider NDRs might be more prone to RSC accumulation in these mutants.

4.4 RSC Accumulates in NDRs of Genes Suspected to Contain Fragile Nucleosomes in Cells Lacking Functional HATs

The finding that NDR width was slightly correlated with RSC accumulation in the *esa1*-containing mutants raises the intriguing possibility that the accumulation might be occurring in genes that are suspected of containing fragile nucleosomes (FNs) (Kubik et al., 2015). Fragile nucleosomes were initially proposed to explain a signal that appeared in the NDRs of ~1/3 of yeast genes under low MNase-digestion conditions but disappeared when chromatin was digested with high amounts of MNase (Brahma and Henikoff, 2019; Kubik et al., 2015; Schlichter et al., 2020; Xi et al., 2011). These complexes are thought to be highly susceptible to MNase and are bound by RSC (Kubik et al., 2015; Schlichter et al., 2020). The existence of fragile nucleosomes is highly controversial. While it is generally thought that a complex exists in the NDRs of these genes, some researcher question if it is indeed a nucleosome, as histone ChIP-seq and MNase-ChIP-seq did not show the presence of histones at these complex locations (Chereji et al., 2017). However, other MNase-based methods such as CUT&RUN have been able to detect fragile nucleosomes while not suffering from some of the drawbacks of conventional MNase digestion, and others were able to detect histones using ChIP-seq (Brahma and Henikoff, 2019; Kubik et al., 2017). However, more research is being conducted to confirm that these complexes (referred to in this work henceforth as fragile nucleosomes for simplicity) are indeed fragile nucleosomes, as well as to analyze the

biochemical properties of these complexes.

Because RSC has been associated with fragile nucleosome complexes and because RSC accumulation was observed in genes containing wide NDRs in the *esa1*-containing mutants, RSC might be accumulating in the NDRs of genes suspected of containing fragile nucleosomes in cells lacking either one or both HATs. To determine if RSC was accumulating in NDRs containing fragile nucleosomes in the HAT mutants, genes were categorized based on the suspected presence of FNs within their promoters (FN_NDRs) or stable nucleosomes at their -1 positions (SN_NDRs) and the RSC ChIP-seq data were analyzed using these subsets of genes. A list of these genes was used from previous studies (Kubik et al., 2015), where 1887 genes were identified as FN_NDR genes and 2974 genes were part of the SN_NDR gene subset. The NDR width for each of these genes was determined to compare the median NDR width for each gene subset. It was found that FN_NDRs had wider NDRs than SN_NDRs (Figure 4.4), consistent with previous studies (Kubik et al., 2015). The heatmaps generated from the RSC ChIP-seq data showed that RSC accumulation was significantly greater in FN_NDRs than in SN_NDRs (Figure 4.5, compare the top panel of each mutant to the corresponding bottom panel). The differences between RSC accumulation in SN_NDRs versus FN_NDRs were most striking in the *esa1* and HAT double mutants, where the greatest increase in RSC accumulation was observed, though *sth1ΔBrD* and *gcn5Δ* also showed greater RSC accumulation at FN_NDRs than SN_NDRs (compare bottom panels with each other). This suggests that RSC is more prone to accumulation in NDRs thought to contain fragile nucleosomes than those containing stable nucleosomes in cells lacking the H4 HAT Esa1.

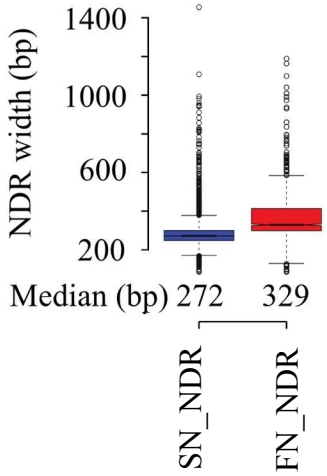

Figure 4.4. Genes containing fragile nucleosomes at NDRs have wider NDRs than genes containing stable nucleosomes. Boxplot showing NDR widths for genes thought to contain fragile nucleosomes within their NDRs (FN_NDRs, N = 1887) and for genes containing stable nucleosomes at the -1 position (SN_NDRs, N = 2974). The median NDR width is shown for each gene subset. Notches on the boxplot represent the 95% confidence interval for each median.

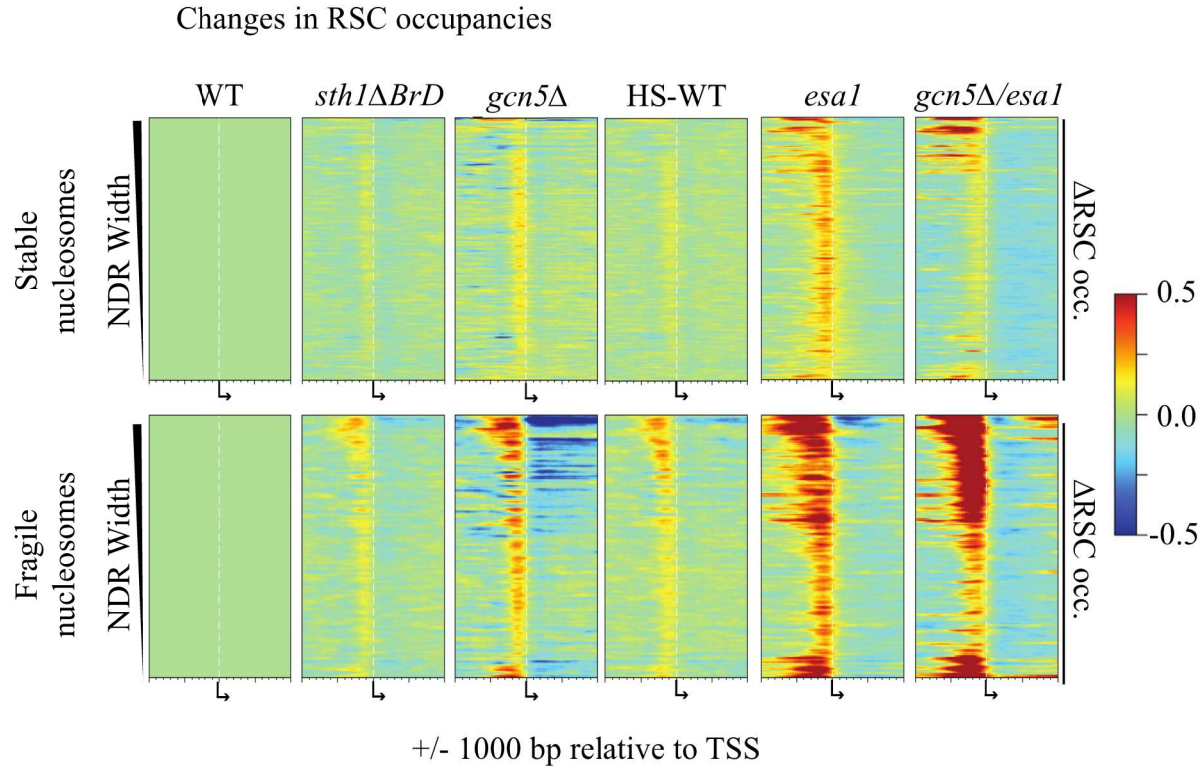

Figure 4.5. RSC accumulates more in the promoters of HAT mutants in genes containing fragile nucleosomes. Heatmaps showing the changes in RSC occupancies compared to WT or HS-WT cells (ΔRSC occ.) at genes containing fragile nucleosomes (bottom panels) or stable nucleosomes (top panels) in WT cells, heat-shocked WT cells (HS-WT), *gcn5Δ, esa1*, and *gcn5Δ/esa1*. Genes were sorted by decreasing NDR width and are centered at the transcription start site (TSS).

To better visualize the RSC accumulations observed in the heatmaps, metagene profiles depicting the changes in RSC occupancy (ΔRSC) occupancies compared to WT cells in FN_NDRs (FN profile) and in SN_NDRs (SN profile) in HS- WT cells, *sth1ΔBrD*, and in the HAT mutants were generated (Figure 4.6). The profiles corroborated the findings observed in the heatmaps (Figure 4.5). The profiles showed that the changes in RSC occupancies were predominantly within the NDRs for both SNs and FNs, reinforcing the idea that RSC accumulates in the NDRs for these mutants (Figure 4.6, compare peaks of each colored line to the solid and dashed traces that show WT nucleosomes occupancies of SNs and FNs, respectively). All of the mutants displayed more RSC accumulation at FN_NDRs than in SN_NDRs, though *esa1* and *gcn5Δ/esa1* displayed greater differences in RSC accumulations between FN_NDRs and SN_NDRs than the other mutants (compare solid-colored traces to dashed traces of the same color). This is unlikely due to heat shock, as RSC accumulation at SN_NDRs and FN_NDRs were relatively similar to each other (compare gray traces to each other), and the accumulation at FN_NDRs observed in HS-WT cells was minor compared to *esa1*-containing cells (compare traces in the righthand panel). The *gcn5Δ/esa1* mutant showed the most striking difference in RSC accumulation between FN_NDRs and SN_NDRs. The ΔRSC profiles show that the increase in RSC seen in SN_NDRs was smaller in the HAT double mutant compared to *esa1* and was comparable to the accumulation seen in HS-WT cells. In contrast, RSC accumulation in FN_NDRs was highest in *gcn5Δ/esa1* compared to HS-WT cells and the other mutants. These results support the findings that RSC binds to the proposed fragile nucleosome complexes (Kubik et al., 2015; Schlichter

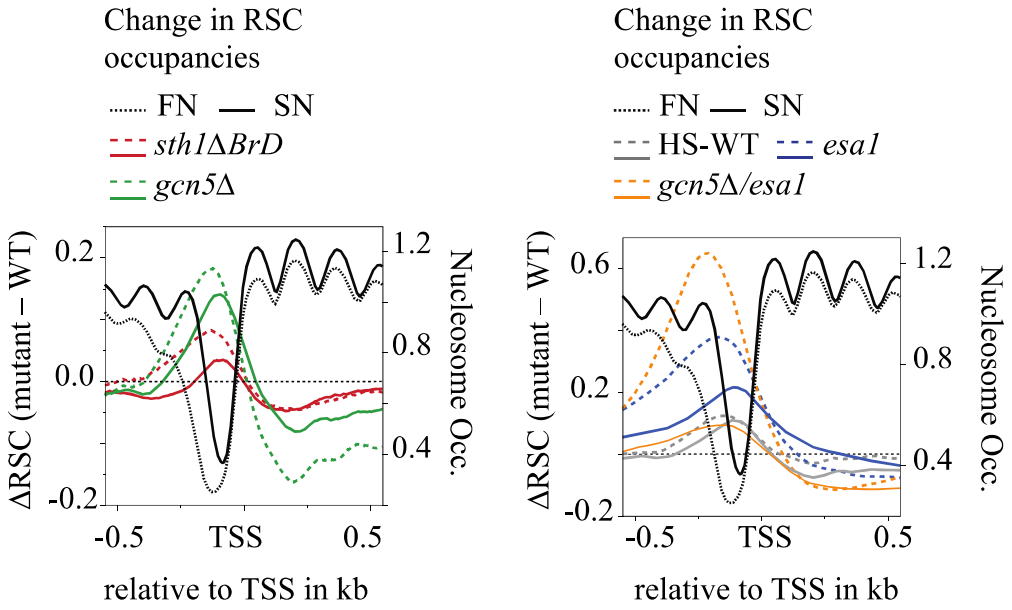

Figure 4.6. RSC accumulates in NDRs in genes containing fragile or stable nucleosomes. Metagene profiles showing the changes in RSC occupancies (ΔRSC) compared to WT cells in HS-WT cells and in *sth1ΔBrD*, *gcn5Δ*, *esa1*, and *gcn5Δ/esa1* mutants at genes containing fragile nucleosomes (FNs) and at genes containing stable nucleosomes (SNs). Solid lines represent ΔRSC changes in SNs, and dashed lines show ΔRSC changes for FNs. Black lines show the WT nucleosome profiles for FNs and SNs to show the location of NDR (deep valley upstream of TSS). Profiles are centered at the TSS, and the lefthand y-axis shows ΔRSC, whereas the righthand y-axis shows the WT nucleosome occupancies.

et al., 2020) and suggests that HATs, especially Esa1, help to regulate RSC buildup at NDRs, particularly at NDRs containing fragile nucleosomes.

4.5 RSC Accumulates in NDRs containing Fragile Nucleosomes of Genes Activated by Transcription Factors in a HAT-Dependent Manner

Since RSC accumulates in FN_NDRs more so than in SN_NDRs when HATs are lost, it is possible that fragile nucleosome complexes or the promoters they occupy might possess characteristics that help retain RSC in those NDRs. NDRs that contain these complexes have also been shown to interact with general regulatory factors (GRFs) such as Rap1, Reb1, and Abf1 (Kubik et al., 2018). These factors bind to their promoters and interact with RSC to maintain NDR width, as depletion of these factors is associated with NDR narrowing at their respective promoters (Kubik et al., 2017; Kubik et al., 2018). To determine if GRFs might play a role in retaining RSC at FN_NDRs when HATs are absent, the RSC ChIP-seq data were analyzed according to several transcription factors known to bind to FN_NDRs. Genes were categorized based on which transcription factor (Abf1, Fkh1, Rap1, or Reb1) bound to them. Genes in which these transcription factors did not bind were categorized under the NDR label. A boxplot was then generated based on the RSC occupancies of these gene sets for WT cells, HS-WT cells, *gcn5Δ*, and *esa1* (Figure 4.7). The boxplot revealed that RSC occupancies were higher in the HAT mutants than in WT or HS-WT cells at the NDRs of these gene sets. The differences between RSC levels relative to WT cells were greater for *esa1* than *gcn5Δ* (compare distances between notches of HAT mutant and WT/HS-WT cells of each respective gene set between the top and bottom panels), supporting the idea that the H4 HAT may be more important in preventing RSC accumulation at FN_NDRs than the H3 HAT. Even

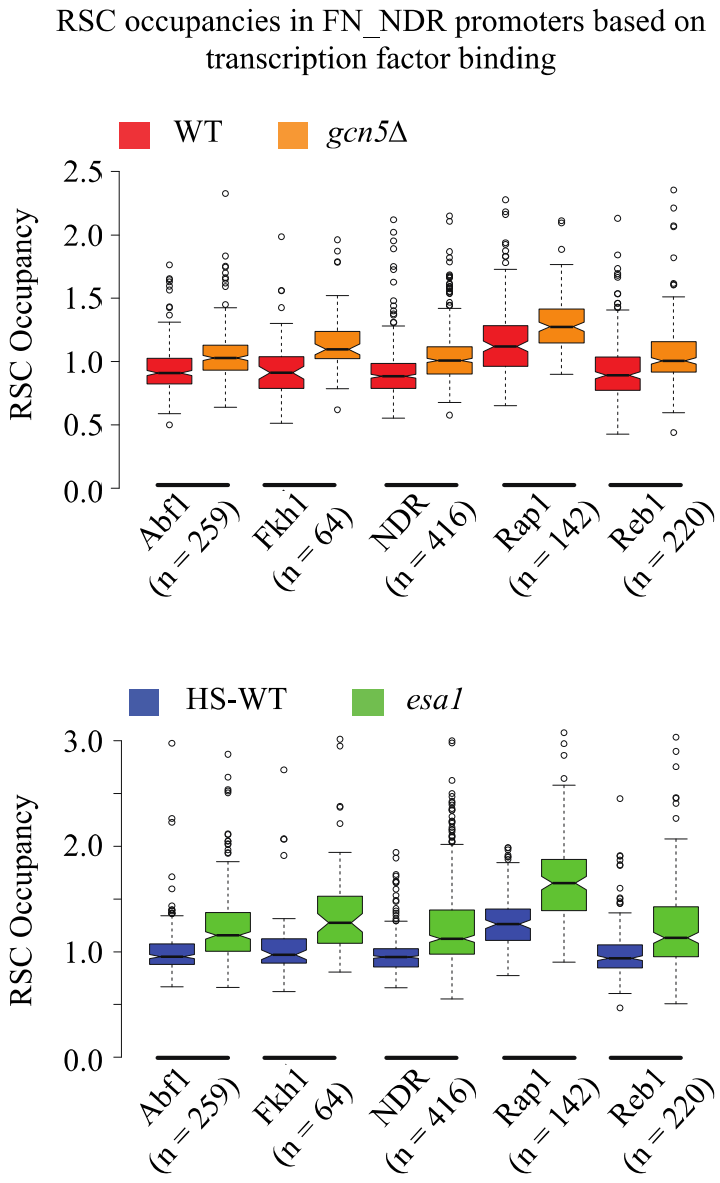

Figure 4.7. RSC accumulates at FN_NDRs containing transcription factors. Boxplots showing RSC occupancies at FN_NDRs based on transcription factor (TF) binding at their promoters. Notches represent the 95% confidence interval of each median.

though the increases were higher in *esa1* than *gcn5Δ*, the relative pattern between the gene sets remained the same for each HAT mutant: the increases observed in Abf1 and Reb1 were very similar to the increase seen in genes that did not contain these transcription factors (NDR). Fkh1 and Rap1 displayed increases greater than NDR genes, with the greatest increase in RSC occupancy observed for *esa1* at Rap1-containing genes. This suggests that GRFs might play a role with HATs in maintaining RSC at these genes, especially Rap1 in regard to the H4 HAT. However, the effects might not be direct, as these factors have been shown to act independently but coordinately with RSC to maintain NDR regions. RSC/GRF double depletion experiments have not revealed a fully epistatic relationship that would suggest that GRFs recruit RSC to NDRs or vice versa (Kubik et al., 2018), and no direct evidence has been found to implicate GRFs in recruiting or retaining RSC at promoters. While these findings do not rule out a potential role of GRFs in regulating RSC recruitment/retention to FN_NDRs in a HAT-dependent manner, since Gcn5 and Esa1 are part of larger complexes that interact with other coactivators, other factors might be at play that help retain RSC to promoters when HATs, especially Esa1, are absent.

4.6 Histone Acetylation is Absent in the HAT Mutants

While the SAGA (Gcn5) and NuA4 (Esa1) complexes have been shown to interact with many other coactivators to regulate DNA-dependent processes, their HAT modules are responsible for acetylating histones H3 and H4, respectively (Ginsburg et al., 2009; Govind et al., 2007; Marmorstein, 2001; Roth et al., 2001). Since histone acetylation is lost in the HAT mutants and RSC accumulates more in FN_NDRs than in SN_NDRs in these mutants, we wondered if hypoacetylation of fragile nucleosomes

might play a role in recruiting or retaining RSC to FN_NDRs. To this end, a western blot was performed by fellow lab member Uzair Khan to confirm that histone acetylation was reduced in the HAT mutants compared to WT cells. An antibody specific to H3 acetylation (H3Ac) was used to determine relative H3Ac levels in WT cells and *gcn5Δ*, and an antibody specific to H4 acetylation (H4Ac) was used to determine relative H4Ac levels in HS-WT cells and *esa1*. The Western blot confirmed that the HAT mutants displayed little to no histone acetylation (Figure 4.8). The H3Ac levels for *gcn5Δ* were reduced compared to WT cells, and *esa1* showed little to no H4Ac levels compared to HS-WT cells. An antibody specific to Rpb3 was used as a loading control, and it was found that the Rpb3 bands for each strain were very similar to each other, suggesting that the reduction in histone acetylation was not simply due to lower protein levels being used for the HAT mutants compared to WT cells. These results confirm that the loss of Gcn5 or Esa1 in the HAT mutants leads to the loss of H3 or H4 acetylation, respectively, supporting the possibility that histone acetylation may play a role in RSC accumulation at FN_NDRs in the HAT mutants.

4.7 Gcn5, Esa1, and the Sth1 Bromodomain Stimulate Histone Eviction at NDRs

Considering that histone acetylation is mostly absent in *gcn5Δ* and *esa1* (Figure 4.8) and that RSC accumulates in NDRs when cells lack Gcn5 or functional Esa1 (Figures 4.1 and 4.2), it is possible that RSC might be accumulating on hypoacetylated histones in promoters, leading to increased histone occupancies at promoters. To determine if RSC is accumulating on histones in promoters, histone H3 ChIP-seq was performed. An antibody specific to H3 was used, and the same chromatin that was used for RSC ChIP-seq was also used to prevent any variation in ChIP signals due to the

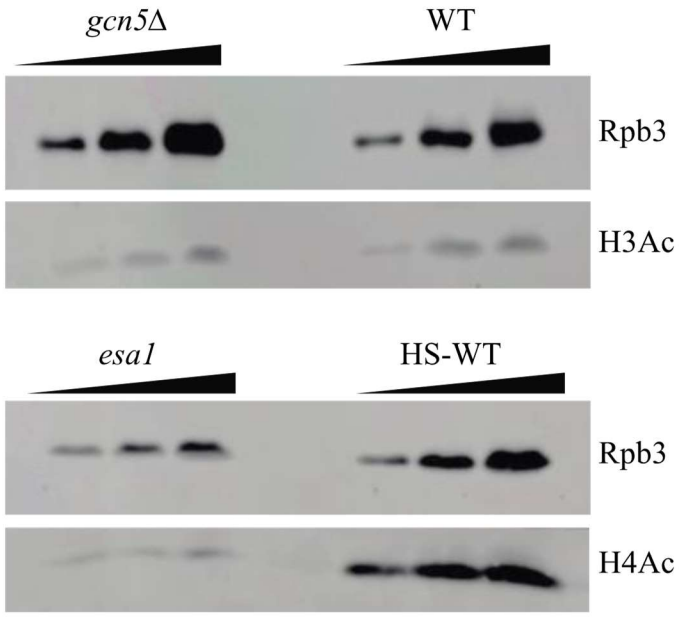

Figure 4.8. Histone acetyltransferases Gcn5 and Esa1 acetylate histones. Western Blot showing that histone H3 acetylation (H3Ac) is reduced in cells lacking Gcn5 compared to WT cells, and that histone H4 acetylation (H4Ac) is largely absent in cells with inactivated Esa1, compared to HS-WT cells. Antibodies specific to Rpb3 were used as a loading control for these experiments, and the black triangles indicate increasing amounts of total protein were used for each strain from left to right. Western Blot data courtesy of Uzair Khan of the Govind Lab.

extent of sonication. The data were aligned to the *S. cerevisiae* genome after sequencing, and heatmaps were generated depicting the changes in H3 occupancies in *sth1ΔBrD*, *gcn5Δ*, *esa1,* and *gcn5Δ/esa1* compared to WT or HS-WT cells (Figure 4.9). H3 occupancies increased genome-wide at the promoters in all of the mutants, though the accumulation was not as striking as the RSC accumulation observed in these mutants (compare yellow hues upstream of the TSS in Figure 4.9 to red hues in bottom panels of Figure 4.1). *sth1ΔBrD* and *gcn5Δ* both displayed similar increases in H3, whereas *esa1* and *gcn5Δ/esa1* showed larger increases, with the greatest increase displayed in the HAT double mutant (compare the intensity of yellow hues in heatmaps). In contrast, the HS-WT cells showed a very slight increase in H3 at its promoters, though not to the extent of *esa1* or the HAT double mutant, indicating that the H3 accumulation is not primarily due to heat shock.

To gain further insight into where the increases in H3 were located, metagene profiles depicting the changes in H3 occupancies (ΔH3 occ.) in the mutants compared to WT cells at all genes were generated (Figure 4.10A). The results seen in the heatmaps were confirmed in the profiles (Figures 4.9 and 4.10A). H3 occupancies increased relative to WT cells in all of the mutants, with the greatest increase in H3 observed in the HAT double mutant (compare traces at NDRs in Figure 4.10A). In the *esa1*-containing mutants, the accumulations were not restricted to NDRs but extended further upstream and downstream of the NDRs (compare broad traces of *esa1* and *gcn5Δ/esa1* to sharp peaks of *gcn5Δ* and *sth1ΔBrD*). To determine if these H3 increases at promoters were significant, a boxplot was generated depicting H3 occupancies at promoters (defined here

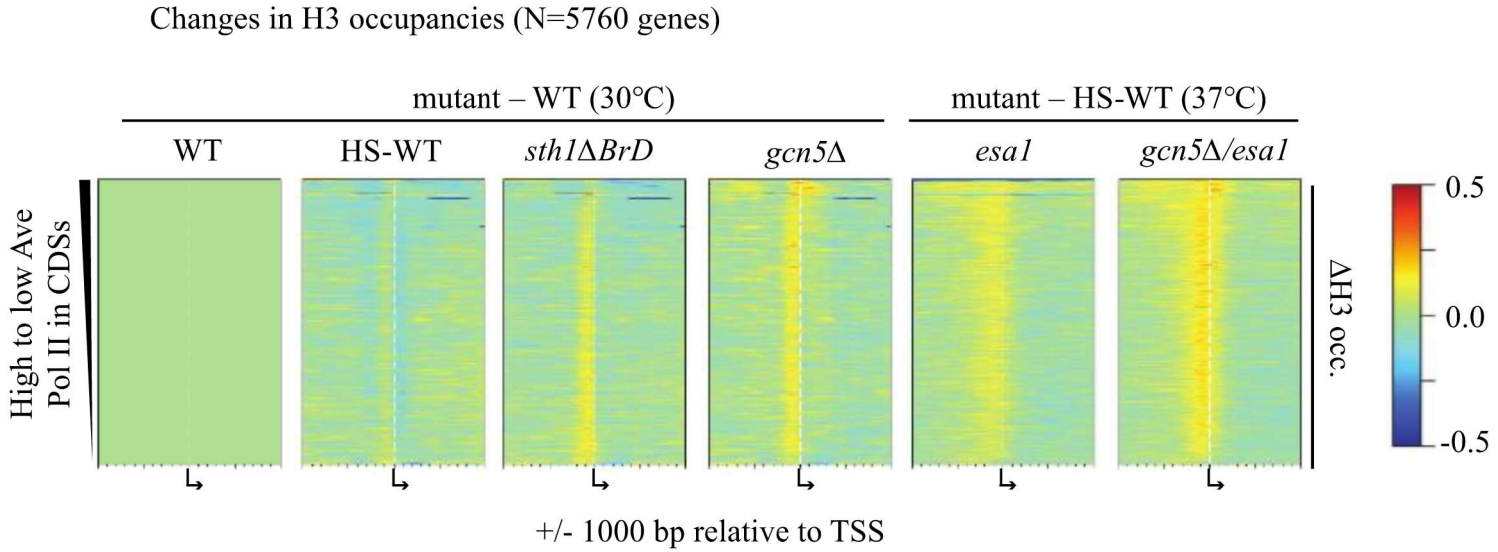

Figure 4.9. H3 accumulates in the promoter regions of the bromodomain and HAT mutants. Heatmaps showing the changes in H3 occupancies compared to WT or HS-WT cells (ΔH3 occ.) genome-wide (N = 5760 genes) in WT cells, heat-shocked WT cells (HS-WT), *gcn5Δ, esa1*, and *gcn5Δ/esa1*. Genes were sorted by decreasing Pol II in CDSs and are centered at the transcription start site (TSS. indicated by a dotted white line at the center of the heatmap).

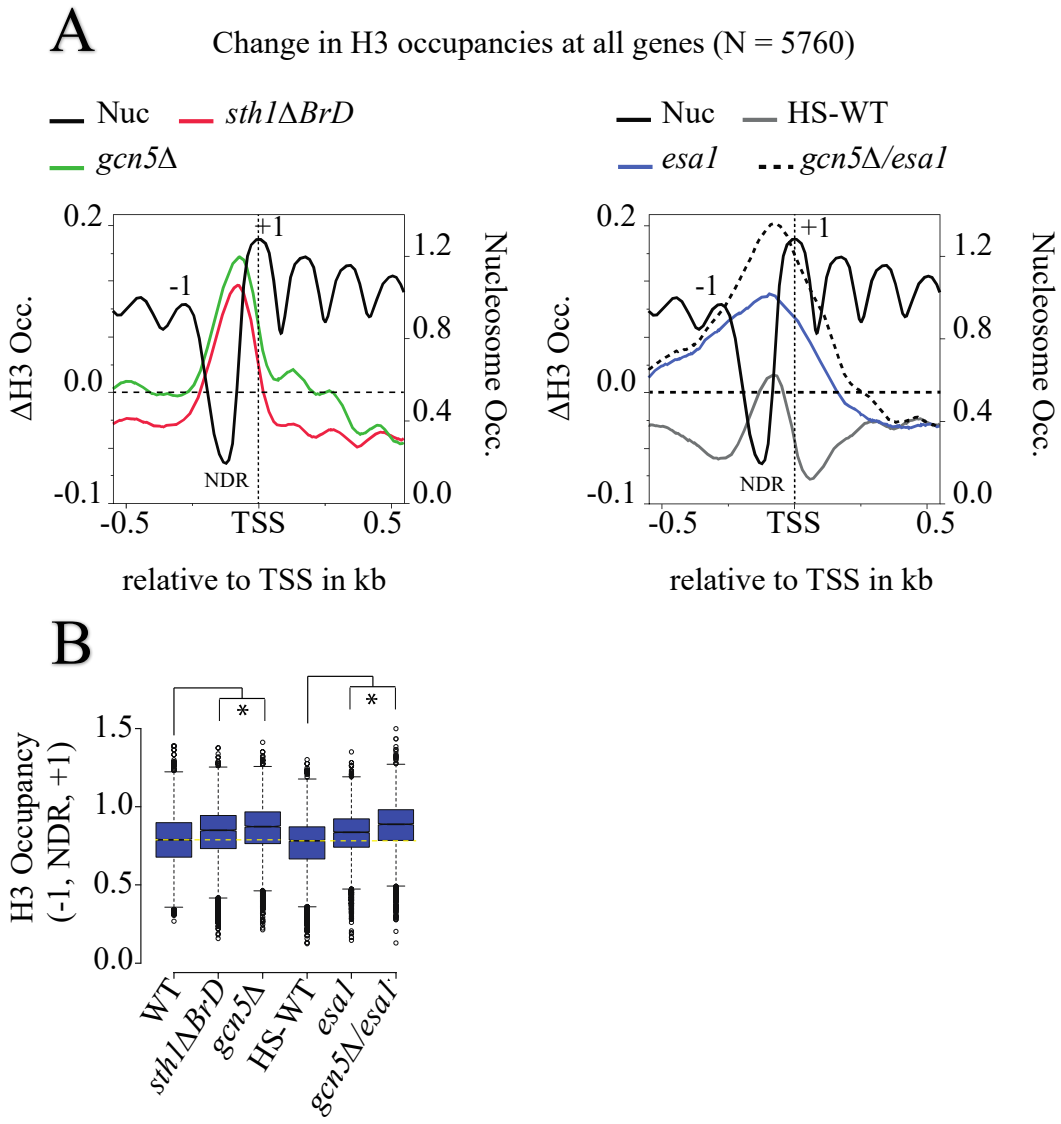

Figure 4.10. Loss of HATs results in increased H3 occupancies at promoters genome-wide. A) Metagene profiles showing the changes in H3 occupancies (ΔH3) compared to WT cells in HS-WT cells and in *sth1ΔBrD*, *gcn5Δ*, *esa1*, and *gcn5Δ/esa1* mutants at all genes. Black lines show the WT nucleosome profiles to show the location of NDR (deep valley upstream of TSS) and the -1 and +1 nucleosomes indicated on the profiles. Profiles are centered at the TSS, and the lefthand y-axis shows ΔH3, whereas the righthand y-axis shows the WT nucleosome occupancies. B) Boxplot showing the normalized H3 occupancies at promoters (-1_Nuc, NDR, and +1_Nuc positions) in WT cells, HS-WT cells, and the mutants. The dotted yellow line represents the median of WT and HS-WT H3 occupancies, and the asterixis represent significant (p-value < 0.05) increases compared to WT cells. p values were determined by the Welch t-test.

as the -1 nucleosome, NDR, and +1 nucleosome locations) for WT cells, HS-WT cells, and the HAT and BrD mutants. Welch student t-tests were performed to calculate the p-value of each mutant-WT H3 change, and the changes were deemed significant if the p-value were less than 0.05 (Figure 4.10B). The mutants showed significant increases in H3 occupancies at promoters compared to WT or HS-WT cells, with the greatest occurring for the HAT double mutant. Overall, the data suggest that the Sth1 bromodomain and the HATs Gcn5 and Esa1 each play a role in evicting histones that may be assembled in promoters.

While the metagene profiles show that the H3 increases were within NDRs, the peaks for each mutant were not centered firmly within the NDR, but were skewed towards the +1 nucleosome location (Figure 4.10A). Additionally, the *esa1*-containing mutants had broad profiles encompassing the -1 and +1 nucleosome locations (Figure 4.10A), indicating that increases in H3 might also occur at the -1 and +1 nucleosome positions. To determine the extent of the H3 increases at the -1 and +1 positions for each mutant, the H3 occupancies were calculated at the -1 position, NDR, and +1 nucleosome position at all genes for WT cells, HS-WT cells, *sth1ΔBrD, gcn5Δ, esa1,* and *gcn5Δ/esa1* and the data was used to generate a boxplot for comparison (Figure 4.11). All mutants showed significantly higher H3 occupancies at NDRs compared to WT or HS-WT cells (significant increases were defined as the increases having a p-value < 0.05). Interestingly, *sth1ΔBrD* showed an increase similar to *gcn5Δ* at NDRs (compare notches on the red box with notches on the orange box, representing the 95% confidence that two medians differ from each other). Thus, both the Sth1 bromodomain and HATs play important roles in maintaining nucleosome-depleted regions genome-wide. At the -1 and

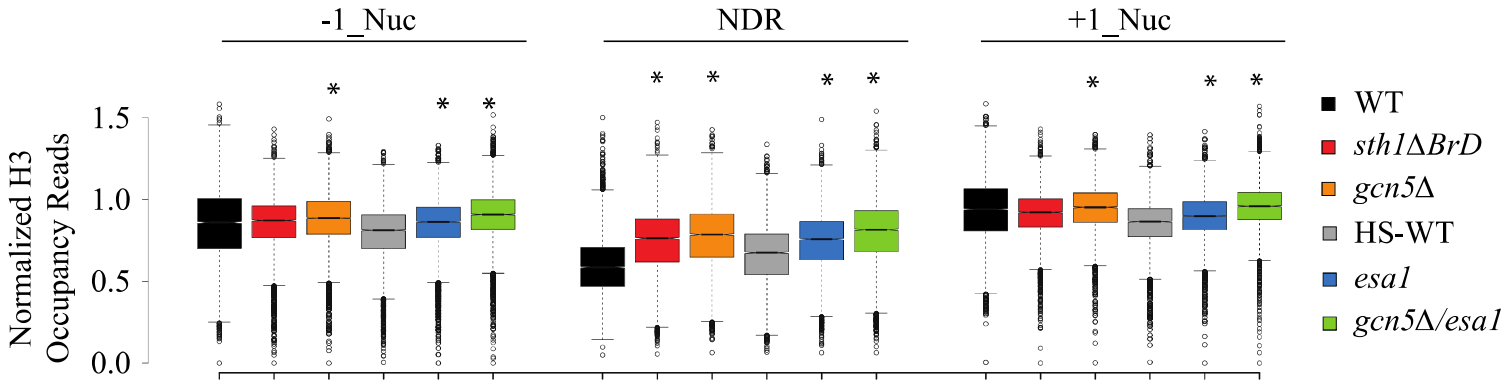

Figure 4.11. H3 increased at the NDRs and the -1 and +1 nucleosome positions in the HAT mutants. Boxplot comparing the H3 occupancies at the -1 nucleosome (-1_Nuc) position, NDR, and the +1 nucleosome (+1_Nuc) position for all genes (N = 5760) in WT cells, HS-WT cells, and in the *sth1ΔBrD*, *gcn5Δ*, *esa1,* and *gcn5Δ/esa1* mutants. Asterixis indicate significant changes in the mutant relative to WT cells (or HS-WT for the *esa1*-containing mutants). Changes were deemed significant if their p-values were less than 0.05 and were determined by the Welch student t-test.

+1 nucleosome positions, the overall H3 occupancies in all strains were higher than in the NDRs, indicating that HATs are important for maintaining histone levels at these positions. The HAT mutants all showed significant increases in H3 occupancies compared to WT cells. Surprisingly, *sth1ΔBrD* showed similar or slightly reduced H3 levels compared to WT cells, though this reduction does not appear significant.

It has been shown that the SAGA and NuA4 complexes interact with and are recruited by other coactivators to promote histone eviction and transcription of their target genes (Govind et al., 2010; Govind et al., 2007; Qiu et al., 2016; Rawal et al., 2018). Additionally, histone eviction from promoters has been shown to expose the TBP binding site, which is important for transcription initiation (Kubik et al., 2019). Considering that the HAT mutants show increased histone levels at promoters, it is possible that the HAT mutants might show more substantial H3 increases at promoters of highly transcribed genes. To this end, H3 occupancies in NDRs and at the +1 nucleosome positions (+1_Nuc) were found for the top and bottom 10% Pol II-occupied genes (Pol II-T10 and Pol II-B10, respectively) in WT cells, HS-WT cells, *sth1ΔBrD*, and in the HAT mutants and plotted on a boxplot for comparison (Figure 4.12). The H3 occupancies at both the NDRs and +1_Nuc were higher in the Pol II-B10 genes than in the Pol II-T10 genes. At Pol II-T10 NDRs, H3 occupancies were higher in *gcn5Δ, esa1,* and *gcn5Δ/esa1* compared to WT cells, HS-WT cells, or even *sth1ΔBrD* (compare medians of each strain to each other), indicating that HATs play a more crucial role in evicting histones at NDRs of highly transcribed genes than the Sth1 bromodomain. At Pol II-B10 NDRs, all mutants showed significantly higher histone levels compared to WT or HS-WT cells (compare the notches indicating a 95% confidence that two medians of the indicated strains differ from

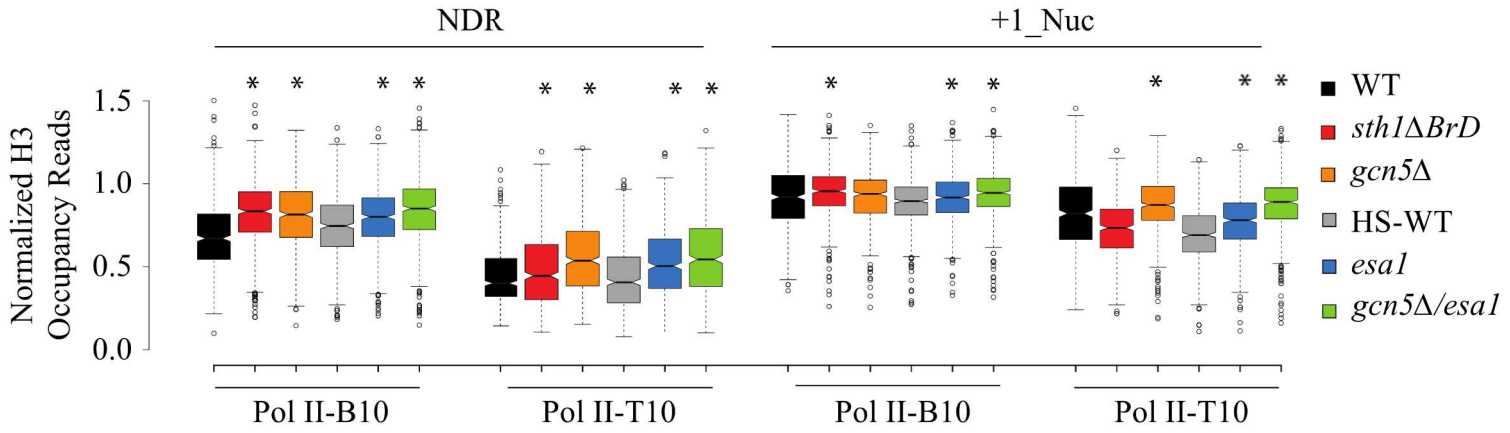

Figure 4.12. The HAT mutants show increased H3 at the NDRs and the +1 nucleosome position at Pol II-occupied genes. Boxplot depicting the H3 occupancies at the NDR and the +1 nucleosome (+1_Nuc) position for the top and bottom 10% Pol II-occupied genes (Pol II-T10 and Pol II-B10 genes, respectively) in WT cells, HS-WT cells, and in the *sth1ΔBrD*, *gcn5Δ*, *esa1,* and *gcn5Δ/esa1* mutants. Asterixis indicate significant changes in the mutant relative to WT cells (or HS-WT for the *esa1*-containing mutants). Changes were deemed significant if their p-values were less than 0.05 and were determined by the Welch student t-test.

each other). In Pol II-B10 genes, the H3 occupancy increases at +1_Nuc were less pronounced than the increases seen at NDRs, and only *sth1ΔBrD*, *esa1*, and the HAT double mutant showed significant increases (compare Pol II-B10 NDR boxplots with Pol II-B10 +1_Nuc boxplots). At Pol II-T10 genes, H3 occupancies at +1_Nuc were higher in *gcn5Δ* than in *esa1*, and the greatest increase was observed for the HAT double mutant. Surprisingly, H3 occupancies at +1_Nuc in the Pol II_T10 genes were reduced in *sth1ΔBrD.* Overall, the data suggest that HATs are important for H3 eviction at NDRs and the +1 nucleosome position at transcribed genes, whereas *sth1ΔBrD* plays a greater role in evicting nucleosomes from lowly-transcribed genes. Indeed, when the H3 ChIP-seq data is separated into quartiles based on Pol II occupancies in CDSs, it is revealed that loss of the Sth1 bromodomain results in significant H3 occupancy increases in promoters at all but the top 25% of transcribed genes (Figure 4.13, compare H3 increases in *sth1*ΔBrD seen in Q2-Q4 versus the similar levels between WT and *sth1ΔBrD* in Q1). In contrast, H3 occupancies increase in promoters in the HAT mutants at both RPGs and the top 20% Pol II-occupied genes excluding RPGs, with the greatest increase observed for the HAT double mutant (Figure 4.14).

Taken together, the data show that H3 increases in cells lacking Gcn5 or Esa1, suggesting that HATs play a role in evicting histones from promoters. At transcribed genes, HATs play a particularly important role in evicting histones in NDRs (Figures 4.12 and 4.14). The increase in H3 occupancies largely coincided with the RSC accumulation observed at NDRs (Figures 4.1, 4.2, 4.5, 4.6, 4.9, and 4.10). Since the HAT mutants are deficient in histone acetylation, these data strongly support the possibility of RSC binding to acetylated nucleosomes in promoters and possibly to fragile

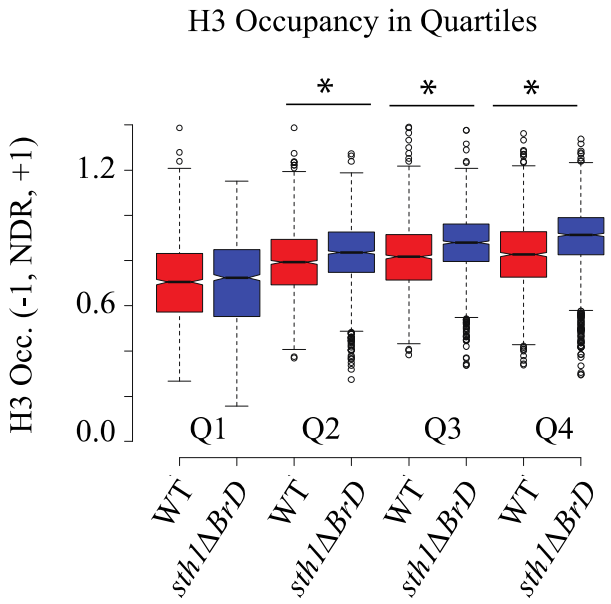

Figure 4.13. The Sth1 bromodomain is important for histone eviction at the majority of genes. Boxplot showing the H3 occupancies at promoters (-1_Nuc, NDR, and +1_Nuc positions) of WT and *sth1ΔBrD*. Genes are separated into quartiles based on average Pol II occupancies in CDSs determined from a separate Rpb3 ChIP, where genes in Q1 harbor the most Pol II and genes in Q4 harbor the least. H3 significantly increases in *sth1ΔBrD* compared to WT cells for quartiles Q2 to Q4. Changes were deemed significant if their p-values were < 0.05, and were determined by the Welch student t-test.

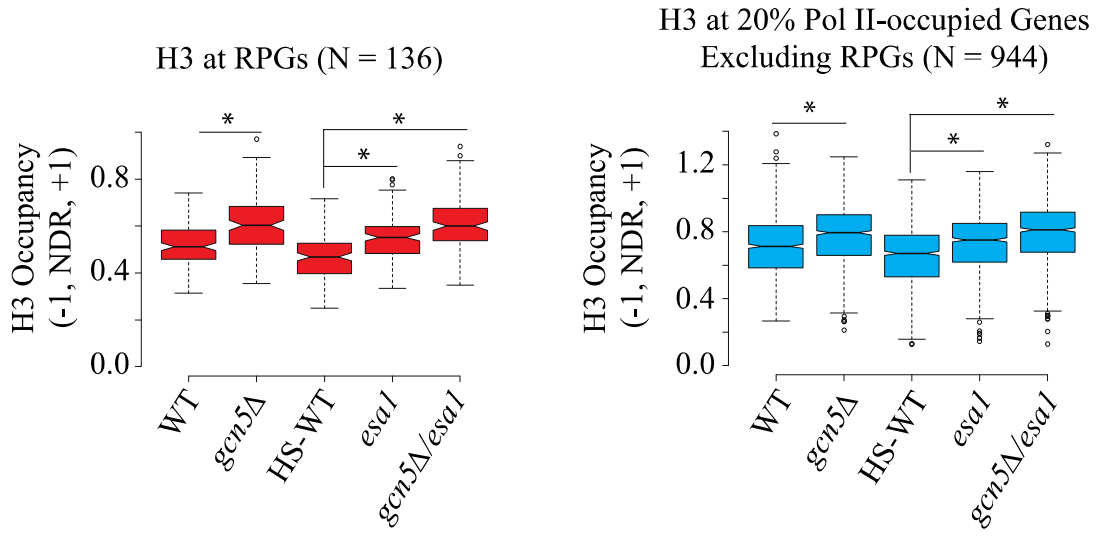

Figure 4.14. Gcn5 and Esa1 are important for H3 eviction at RPGs and other Pol II-occupied genes. Boxplots comparing H3 occupancies in the promoters (-1_Nuc, NDR, and +1_Nuc positions) of RPGs (left boxplot) and of the top 20% of Pol II-occupied genes excluding RPGs (right boxplot) in WT cells, HS-WT cells, and in the HAT mutants. Changes were deemed significant if their p-values were < 0.05, and were determined by the Welch student t-test.

nucleosomes.

4.8 NDRs that contain Fragile Nucleosomes show Comparable Histone Occupancy Increases to NDRs containing Stable Nucleosomes in the HAT Mutants

Considering that the HAT mutants showed increased H3 and RSC occupancies compared to WT cells at promoters (Figures 4.1 – 4.2, 4.9 – 4.10) and that the RSC accumulation was greater at FN_NDRs than SN_NDRs (Figures 4.5 – 4.6), it is possible that the mutants might also show greater H3 increases at FN_NDRs than at SN_NDRs in the mutants, especially if RSC is trapping histones underneath it, or if RSC is accumulating on fragile nucleosomes. The H3 ChIP-seq data were analyzed for average histone occupancies at the -1, NDR, +1 positions (promoters) of SN_NDR and FN_NDR genes for WT cells, HS-WT cells, *sth1ΔBrD, gcn5Δ, esa1,* and *gcn5Δ/esa1,* and the data was used to generate a boxplot (Figure 4.15). Overall, H3 occupancies in WT cells were higher in SN_NDRs than in FN_NDRs (Figure 4.15, compare black boxplots at Stable Nuc. and Fragile Nuc.). Both *sth1ΔBrD* and *gcn5Δ* showed higher increases than WT cells at both FN_NDRs and SN_NDRs, though the H3 increase was higher in *gcn5Δ* cells than the BrD mutant for both gene sets. Both *esa1* and *gcn5Δ/esa1* showed higher H3 occupancies at promoters than HS-WT cells, with the greatest increases being observed for the HAT double mutant at both gene sets. The greater increases observed for *gcn5Δ/esa1* indicate that both Gcn5 and Esa1 are important for histone eviction at promoters, despite the differences in H3 occupancies for the HAT single mutants. For *gcn5Δ* and *sth1ΔBrD*, the H3 increases at SN_NDR promoters were a little higher than the increases observed at FN_NDRs, whereas the H3 increases observed at FN_NDRs were slightly higher than the increases observed at SN_NDRs for *esa1* and the HAT

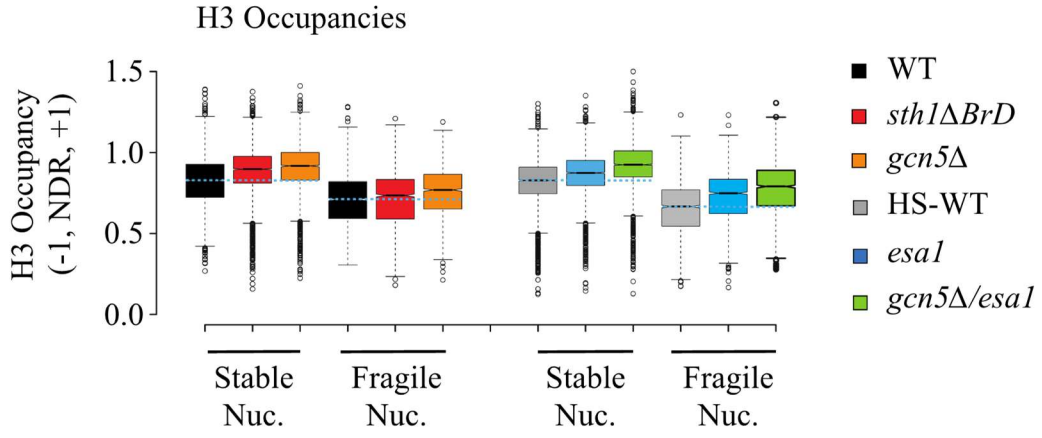

Figure 4.15. H3 increases in the promoters of genes containing Fragile or Stable nucleosomes (Nuc) in the HAT mutants. Boxplots comparing normalized H3 occupancies in the promoters (-1_Nuc, NDR, and +1_Nuc positions) of Stable and Fragile Nucleosome containing genes in WT cells, HS-WT cells, and in the HAT mutants. Changes were deemed significant if their p-values were < 0.05 and were determined by the Welch student t-test. The dotted blue line indicates the median of either WT or HS-WT cells for easier comparison of the medians of mutants to those of WT cells.

double mutant (Figure 4.15, compare the distances between the median of each mutant and WT or HS-WT cells at both Stable Nuc. genes and Fragile Nuc. genes).

To get a clearer look as to where the H3 occupancies were increasing for each gene, heatmaps were generated showing the change in H3 occupancies compared to WT or HS-WT cells at genes containing fragile or stable nucleosomes for HS-WT cells, *sth1ΔBrD*, and the HAT mutants (Figure 4.16). The overall patterns of the H3 increases were very similar to the RSC increases observed for the mutants (compare the heatmaps for each mutant in Figure 4.16 to the heatmaps for the respective mutant in Figure 4.5). For *gcn5Δ* and *sth1ΔBrD*, H3 increases at FN_NDRs were less pronounced than the changes observed at SN_NDRs (Figure 4.16, compare top panels with the corresponding bottom panels), consistent with the trend observed in Figure 4.15. The *esa1*-containing mutants show a greater H3 increase at FN_NDRs than at SN_NDRs, though the increase is not as pronounced at the RSC accumulation seen at FN_NDRs of these mutants (Figures 4.5 and 4.16).

The mixed results regarding the H3 increases of the *sth1ΔBrD, gcn5Δ,* and the *esa1*-containing mutants lend to some intriguing possibilities. The higher H3 increases at SN_NDRs observed in the *sth1ΔBrD* and *gcn5Δ* mutants suggest that there is more RSC in those NDRs simply due to the presence of more histones for RSC to interact with. However, the RSC increases observed at FN_NDRs were more substantial in the *sth1ΔBrD* and HAT mutants than the increases in H3 (compare the bottom panels in Figure 4.5 with the bottom panels of Figure 4.16). The higher RSC levels might indicate that fragile nucleosomes might recruit or retain RSC more than stable nucleosomes. Since FN_NDRs display lower H3 occupancies at promoters than SN_NDRs, it is possible that

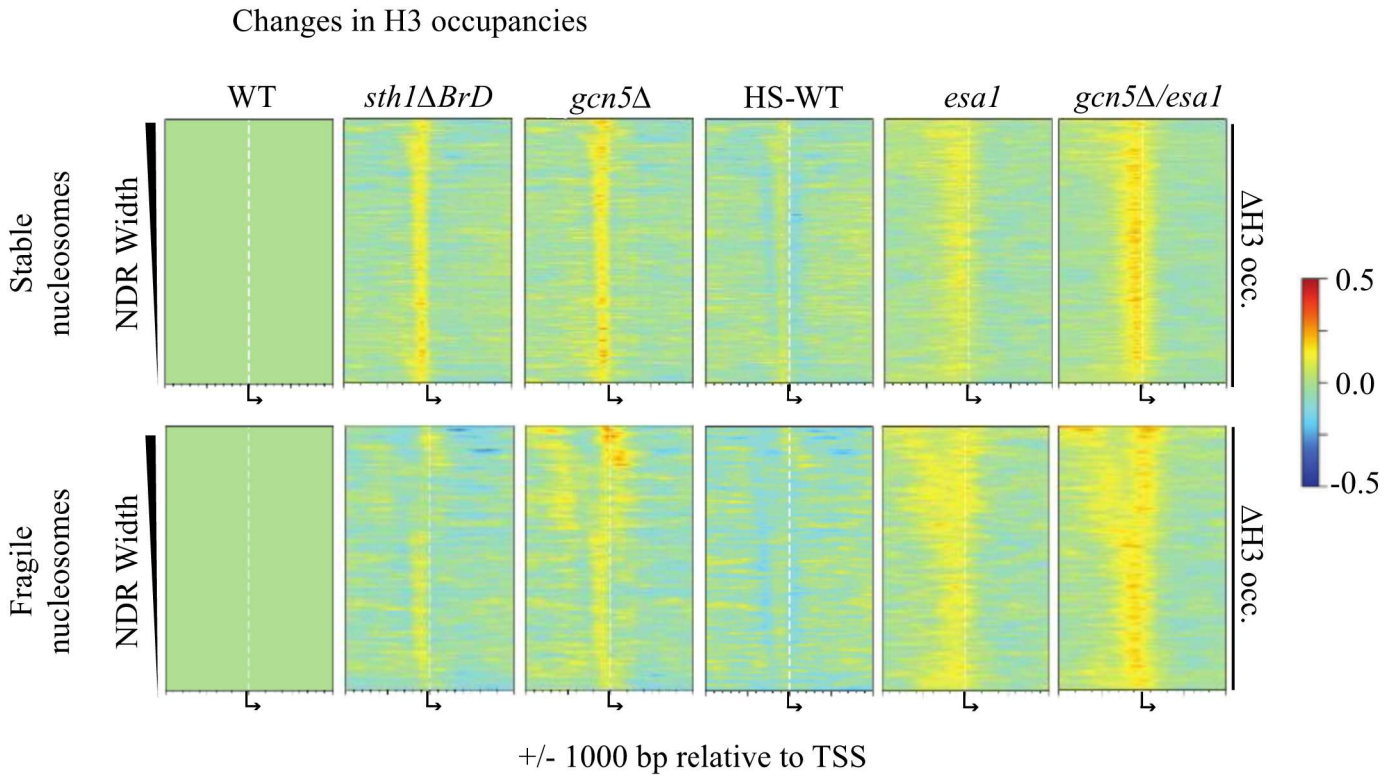

Figure 4.16. Histone occupancies increase in genes containing fragile or stable nucleosomes in the Sth1 bromodomain and HAT mutants. Heatmaps showing the changes in H3 occupancies (ΔH3 occ.) compared to WT cells (or HS-WT cells for esa1-containing mutants) at promoters containing fragile (bottom panels) or stable nucleosomes (top panels) in WT cells, heat-shocked WT cells (HS-WT), *gcn5Δ, esa1*, and *gcn5Δ/esa1*. Genes were sorted by decreasing NDR width and are centered at the transcription start site (TSS, indicated by a dotted white line at the center of the heatmap). Control heatmaps depicting WT-WT (i.e. no change) are included for reference.

the ability of fragile nucleosome complexes to recruit or retain RSC more efficiently might also help in maintaining lower histone occupancies at FN_NDRs compared to SN_NDRs.

4.9 Nucleosomes at Promoters are Stabilized in the HAT Mutants

The possibility of RSC accumulating on promoter nucleosomes in the HAT mutants raises questions regarding the overall stability and accessibility of nucleosomes within these regions. Because RSC has been shown to slide, evict, and remodel nucleosomes in vitro (Clapier et al., 2017; Harada et al., 2016; Lorch and Kornberg, 2017; Saha et al., 2002; Shukla et al., 2019; Shukla et al., 2010), it is possible that the increased RSC at promoters in the HAT mutants might remodel any nucleosomes RSC may be interacting with, resulting in nucleosomes that are more susceptible to MNase digestion. However, RSC might also confer protective qualities to the nucleosome if it is stuck or retained on the nucleosome (Shukla et al., 2010), or it might be bound in such a way that RSC activity is less efficient on these retained nucleosomes. Either of these scenarios could result in nucleosomes being less accessible and therefore less susceptible to MNase digestion. To determine the stability of promoter nucleosomes in the HAT mutants, MNase digestion was performed in WT cells and *gcn5Δ, esa1,* and *gcn5Δ/esa1*. The resulting chromatin was then sequenced and used to generate heatmaps depicting nucleosome occupancies at all genes, as well as the changes in nucleosome occupancies compared to WT cells at all genes, FN_NDRs, and SN_NDRs for the HAT mutants (Figure 4.17). The heatmap showing WT nucleosome occupancies at all genes (top left panel of Figure 4.17A) largely coincides with the profile observed for the nucleosome dyad densities (Figure 3.7C): for each gene, there is a region of blue upstream of the TSS,

indicating the NDR, and flanking the NDR are two yellow regions representing the -1 and +1 nucleosomes. When the genes are stacked together to form the heatmap, the result is a blue column just upstream of the TSS representing the NDR, a faint yellow column upstream of the NDR representing the -1 nucleosome, and a more intense yellow column downstream of the NDR and TSS representing the +1 nucleosome (Figure 4.17A). Yellow columns downstream of the +1 nucleosome represent nucleosomes in the CDSs. The heatmaps depicting nucleosome occupancies in the HAT mutants show greater nucleosome occupancies predominately at the -1 and +1 nucleosome positions than in the WT cells, with the greatest increase being observed in the HAT double mutant (Figure 4.17A, top panels, compare red/yellow hues in WT and HAT mutants). The changes are more apparent in the heatmaps depicting the changes in nucleosome occupancy compared to WT cells (Figure 4.17A, bottom panels), where an increase in nucleosome occupancies can be observed at the -1 and +1 nucleosome positions for the HAT mutants. These results suggest that nucleosomes are stabilized when HATs are lost, and the stabilization is greatest in the HAT double mutant, indicating that both Gcn5 and Esa1 contribute to nucleosome accessibility within these regions. Since RSC accumulates more in FN_NDRs than SN_NDRs (Figures 4.5 and 4.6), the changes in nucleosome occupancies compared to WT cells were examined for FN_NDRs and SN_NDRs (Figure 4.17B). The increases in nucleosome occupancies at SN_NDRs and FN_NDRs were comparable (Figure 4.17B, compare the top panel of each mutant with the bottom panel). Increases in nucleosome occupancies at the -1 and +1 positions were observed for *gcn5Δ* and *esa1*, with the greatest increase in the HAT double mutant. These increases suggest that nucleosomes at promoters are stabilized when HATs are absent or inactivated, despite the

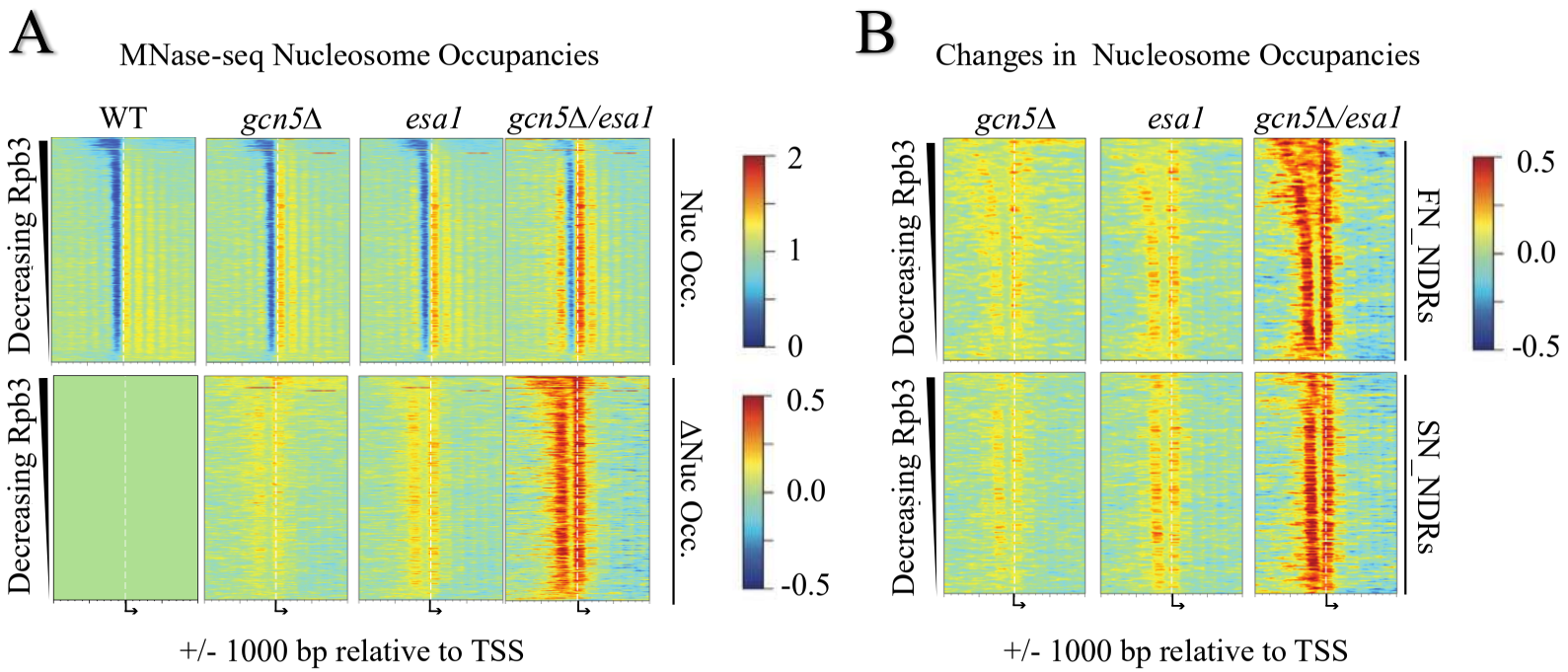

Figure 4.17. Nucleosomes are stabilized genome-wide in the HAT mutants. A) Heatmap showing nucleosome occupancies (top panels) and changes in nucleosome occupancies compared to WT cells (ΔNuc; bottom panels) at 5760 genes for WT cells and the HAT mutants. B) Heatmap depicting the changes in nucleosome occupancies and at FN_NDRs and SN_NDRs. For each heatmap, fragment sizes 130-160 bp were included in the analysis. Genes were sorted by decreasing Pol II in CDSs and are centered at the TSS.

increased RSC presence. It could be that RSC may indeed be stuck on these nucleosomes and cannot efficiently remodel or evict them, resulting in nucleosomes that are less accessible to MNase and yielding a stronger signal at the -1 and +1 positions. It is interesting to note that at the highest Pol II-occupied FN_NDR genes in the HAT double mutant (Figure 4.17B, top of FN_NDR heatmap), a signal is detected between the -1 and +1 nucleosomes. This signal is also present in the HAT single mutants, though it is not as strong or as clearly visible as in the HAT double mutant. While the signal could be indicative of NDR filling or narrowing, it is possible that it could represent fragile nucleosomes within the NDRs of those genes and that RSC buildup at FN_NDRs may have further stabilized these possible fragile nucleosomes in the HAT mutants. Further investigation is needed to determine if the signal detected in between the -1 and +1 positions is indeed a fragile nucleosome. Nevertheless, the data shows that promoter nucleosomes are stabilized in the HAT mutants, despite the increased presence of RSC.

4.10 The Accumulation of RSC in Promoters of HAT Mutants is Histone Tail-Dependent

Several studies have shown that histone acetyltransferases acetylate lysine residues on histone tails (Dhalluin et al., 1999; Zeng and Zhou, 2002). In *S. cerevisiae*, Gcn5 acetylates lysine residues at positions 9, 14, 18, 23, and 27 on the histone H3 tail (Carre et al., 2005; Cheon et al., 2020; Eberharter et al., 1999; Haque et al., 2021; Marmorstein, 2001), whereas Esa1 acetylates lysine residues at positions 5, 8, 12 and 16 on the H4 tail (Marmorstein, 2001). Considering that histone acetylation is largely absent in the HAT mutants (Figure 4.8) and that RSC accumulates in the NDRs of the HAT mutants (Figures 4.1 – 4.2), it is possible that the RSC accumulation is dependent on histone tails, specifically hypoacetylated histone tails. To determine if histone tails are

important for RSC accumulation observed in the HAT mutants, RSC ChIP-seq was performed in cells containing WT H3 tails and mutants lacking either the histone H3 tail (*H3Δ1-28*) or the H4 tail (*H4Δ1-16*). The deleted regions contain the lysine residues that could otherwise be acetylated by Gcn5 or Esa1, meaning that nucleosomes that were missing these histones would be hypoacetylated compared to WT cells and might mirror the RSC accumulation seen in the HAT mutants. The heatmaps depicting RSC occupancies at all genes for cells containing WT H3 tails (WT (H3)), *H3Δ1-28,* and *H4Δ1-16* do not show an accumulation of RSC in the promoters of WT cells or the tail deletion mutants, as the heatmaps of WT cells and mutants look very similar to each other upstream of the TSS (Figure 4.18A). The changes in RSC occupancies in the tail deletion mutants compared to WT cells were calculated and used to generate heatmaps to further clarify the differences in RSC occupancies between WT cells and the histone tail mutants (Figure 4.18B). The heatmaps revealed that RSC occupancies decreased in both tail deletion mutants, though the decrease was greater in *H3Δ1-28* than in *H4Δ1-16* (Figure 4.18B). To better visualize the differences between the HAT mutants and tail deletion mutants in regards to RSC levels in the promoters, metagene profiles depicting the changes in RSC occupancies compared to WT cells (ΔRSC) were generated for the HAT mutants *gcn5Δ* and *esa1* and the tail deletion mutants *H3Δ1-28* and *H4Δ1-16* (Figure 4.19). Because RSC accumulation was greater at FN_NDRs than SN_NDRs in the HAT mutants, the ΔRSC profiles were generated for both FN_NDR genes (lefthand panel) and at SN_NDR genes (righthand panel) to compare the differences observed between HAT and tail deletion mutants at both gene sets. Comparing the ΔRSC profiles

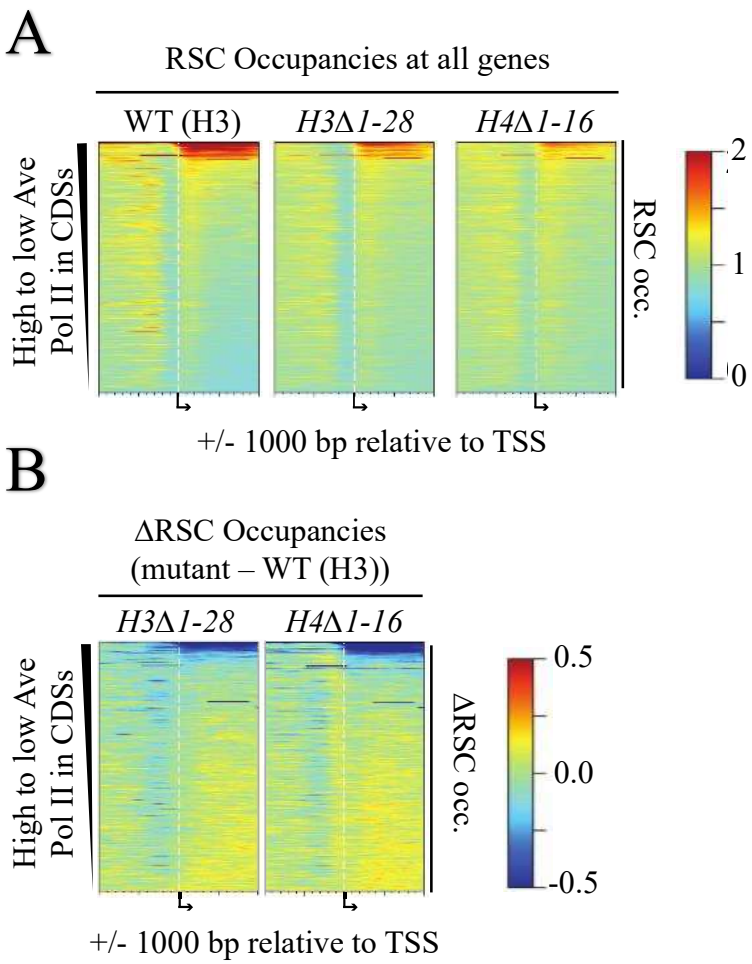

Figure 4.18. RSC does not accumulate at promoters in cells lacking histone N-terminal tails. A) Heatmaps showing RSC occupancies for cells containing WT histone H3 tails, as well as for cells lacking either the H3 tail (*H3Δ1-28*) or H4 tail (*H4Δ1-16*) at all genes. B) Heatmaps showing the changes in RSC occupancies in the tail deletion mutants compared to cells containing WT H3 tails at all genes. For all heatmaps, genes are sorted by decreasing Pol II occupancies and are centered at the TSS.

of *gcn5Δ* and *H3Δ1-28* and the ΔRSC profiles of *esa1* and *H4Δ1-16* reveal that the increases in RSC observed in the NDRs of the HAT mutants were largely absent in the NDRs of the tail deletion mutants (Figure 4.19, compare solid traces to dotted traces). Moreover, the differences between the HAT mutants and the histone tail mutants were larger at FN_NDRs than at SN_NDRs (compare solid traces to dotted traces and note the changes in the lefthand y-axis for each panel). Overall, differences between the ΔRSC profiles of *esa1* and *H4Δ1-16* were more striking than those between the ΔRSC profiles of *gcn5Δ* and *H3Δ1-28* (compare solid traces to dotted traces of the same color).

The findings that RSC does not accumulate in the NDRs of tail deletion mutants, though initially surprising, make sense if RSC is accumulating on hypoacetylated tails, as the complete loss of the tail should result in RSC being unable to be retained on histones. The differences between the metagene profiles of the HAT and tail deletion mutants indicate that the H4 tail might play a larger role in retaining RSC to the promoters than the H3 tail. Nonetheless, the H3 tail might play some role in recruiting or retaining RSC to promoters, as *H3Δ1-28* did not show the RSC accumulation observed in *gcn5Δ*.

4.11 RSC Accumulates in the Promoters of Mutants Containing Hypoacetylated H4 Tails

Because the H3 or H4 tails were lacking in the tail deletion mutants, RSC did not accumulate in the promoters of the tail deletion mutants as they did for the HAT mutants. However, while the tail deletion mutants yielded insights into how histone tails play a role in retaining or recruiting RSC to promoters, they did not provide any information regarding the roles that hypoacetylated tails play in retaining RSC to promoters. To gain further insight into the roles hypoacetylated tails play in recruiting or retaining RSC to promoter nucleosomes, RSC ChIP-seq was performed for the *H3K14A* and *H4K16A*

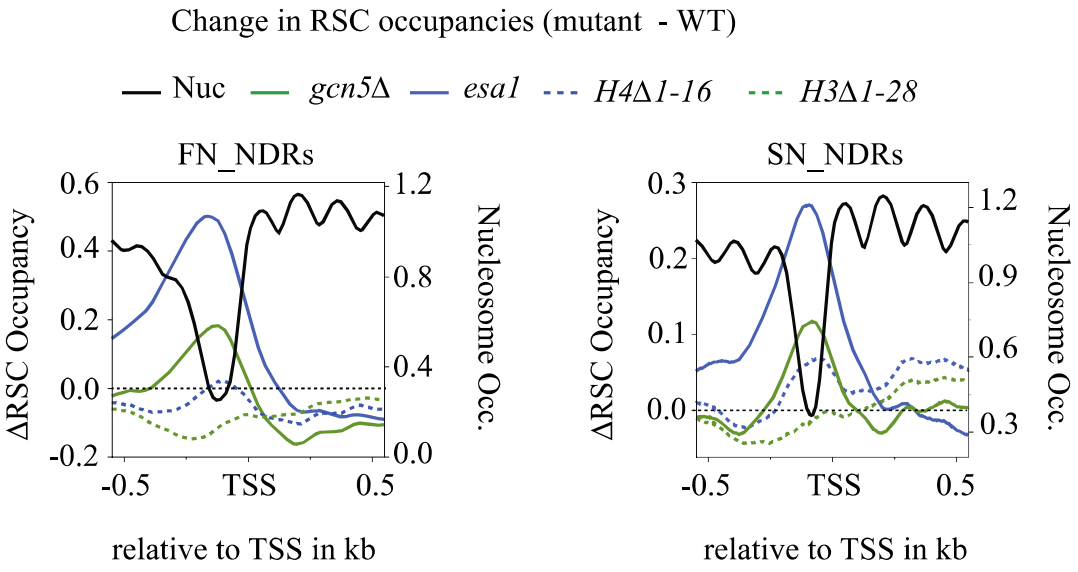

Figure 4.19. RSC accumulates in the NDRs of HAT mutants, but not in histone tail mutants. Metagene profiles depicting the changes in RSC occupancies (Δ RSC Occupancy) at FN_NDRs (lefthand panel) and at SN_NDRs (righthand panel) in HAT mutants *gcn5*Δ and esa1, as well as in the H3 and H4 N-terminal tail mutants. The lefthand y-axis displays ΔRSC and the righthand y-axis displays nucleosome occupancies. The profile for WT nucleosomes is included to easily find the location of the NDR and -1 and +1 nucleosomes. Profiles are centered at the TSS.

mutants. The replacement of the lysine residue with alanine prevents the residues at those locations from being acetylated. *H3K14A* and *H4K16A* mutants were initially selected since the Sth1 bromodomain has been shown to preferentially bind to acetylated H3K14 (Chen et al., 2020; Jain et al., 2020), and H4K16 acetylation is important for chromatin decompaction (Robinson et al., 2008) and recruits Gcn5 in a bromodomain-dependent manner (Owen et al., 2000). Additionally, these mutants already contained myc-tagged Sth1, so these mutants underwent RSC ChIP-seq while other K→A mutants (H3K9,14,18,23→A, H4K5,8,12,16→Q, and H4K5,8,12,16→R [K→A mutations of all lysine residues on H4 is lethal]) were subjected to transformations to tag Sth1 with myc. Heatmaps depicting the changes in RSC occupancies compared to WT cells at all genes were generated for the *H3K14A* and *H4K16A* tail mutants and compared to the heatmaps for the tail deletion mutants (*H3Δ1-28* and *H4Δ1-16*) and the HAT mutants (*gcn5Δ* and *esa1*) (Figure 4.20). Surprisingly, the *H3K14A* mutant displayed slightly higher RSC levels in the promoter regions compared to the H3 deletion mutant, but showed very little change compared to WT cells, and did not show any recapitulation of RSC accumulation at promoters exhibited by the H3 HAT (Figure 4.20A). In contrast, *H4K16A* showed increased RSC occupancies at the promoter compared to WT cells, recapitulating some of the accumulation observed in the H4 HAT mutant (Figure 4.20B). This suggests that the hypoacetylated H4 tail might be important for recruiting or retaining RSC to promoter nucleosomes. To gain further insight as to whether the accumulation in the H4 tail mutant is more prominent at FN_NDRs than SN_NDRs, metagene profiles were generated depicting the changes in RSC occupancies at FN_NDRs (left panels) and SN_NDRs (righthand panels) for *gcn5Δ, H3K14A,* and *H3Δ1-28* mutants (Figure 4.21A), as well as

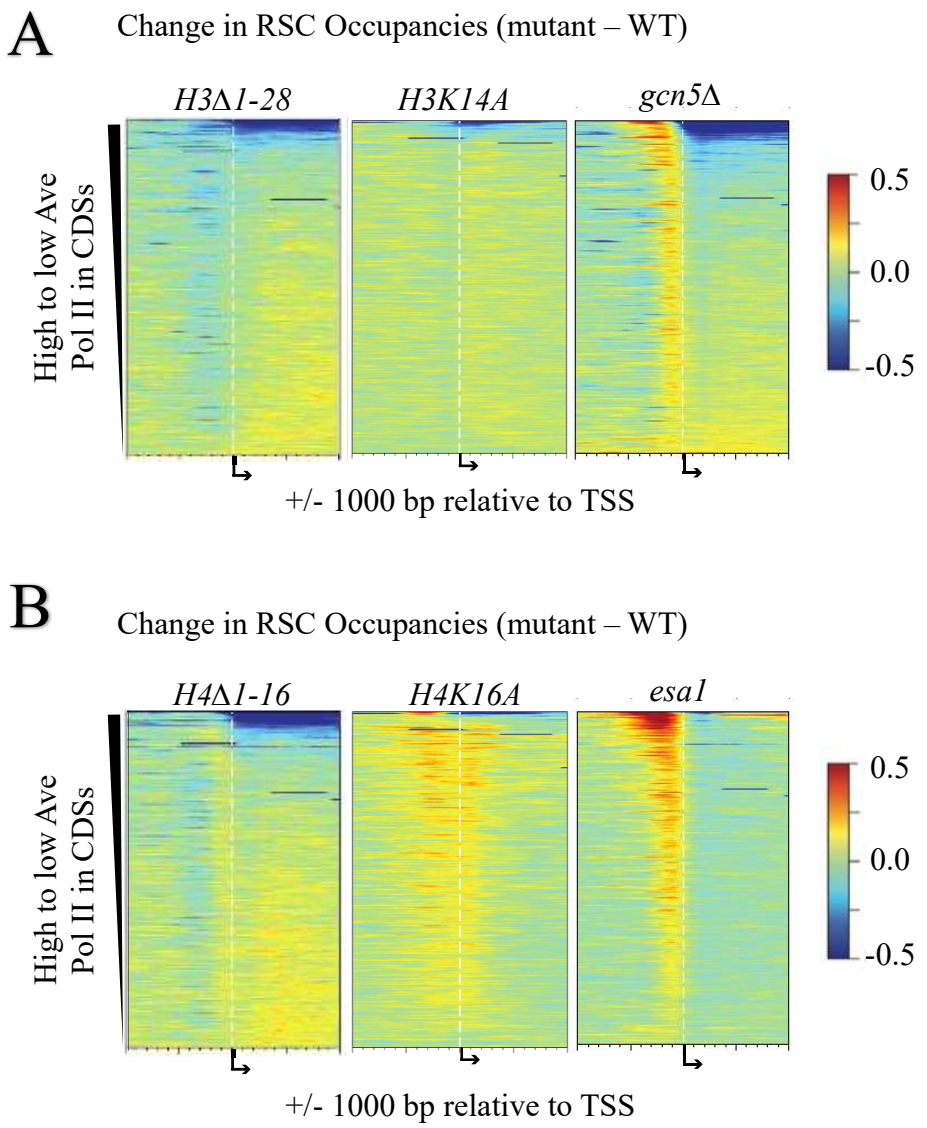

Figure 4.20. RSC accumulates in the promoters of mutants containing hypoacetylated H4 tails, but not in mutants containing hypoacetylated H3 tails. A-B) Heatmaps depicting the change in RSC occupancies compared to WT cells at all genes in *H3Δ1-28, H3K14A,* and *gcn5*Δ (A), as well as *H4Δ1-16, H4K16A,* and the *esa1* mutants (B). The K to A mutations prevent the residue from being acetylated in the mutants. Genes are sorted by decreasing Pol II occupancies and are centered at the TSS.

for the *H4K14A, esa1,* and *H4Δ1-16* mutants (Figure 4.21B). The *H3K14A* mutant did show higher accumulations of RSC at both FN_NDRs and SN_NDRs than *H3Δ1-28*, though the overall RSC levels in the *H3K14A* mutant did not change significantly compared to WT cells (Figure 4.21A), suggesting that loss of acetylation at this individual residue does not result in RSC accumulation. This is surprising, given the in vitro and in vivo evidence that RSC preferentially binds acetylated H3K14 (Chen et al., 2020; Cheon et al., 2020; Jain et al., 2020; Marmorstein, 2001). It is possible that while RSC recognizes H3K14 for recruitment, acetylation of other H3 or H4 lysine residues might help RSC to dissociate from the nucleosome, and the absence of acetylation at those other lysine residues might be responsible for retaining RSC on nucleosomes, leading to the accumulation of RSC observed in the HAT mutants. Indeed, the *H4K16*A mutant did show some accumulation of RSC at NDRs, though the accumulation was not as great as that observed in *esa1* (Figure 4.21B). Since the H4 tail could still be acetylated at other lysine residues in the *H4K16A* mutant, it is possible that mutations at one or all of these other residues might fully recapitulate the RSC accumulation seen in *esa1*. These results indicate that RSC might be retained on hypoacetylated H4 tails.

The differences between the RSC accumulations in the *H3K14A* and *H3Δ1-28* mutants were very similar at both FN_NDRs and SN_NDRs (Figure 4.21A, compare dotted and dashed traces and scales of the lefthand y-axis of both panels. In contrast, while the *H4K16A* mutant exhibited similar changes compared to WT cells at both FN_NDRs and SN_NDRs, the differences between the *H4K16A* mutant and the *H4Δ1-16* mutant were larger at FN_NDRs than at SN_NDRs, (Figure 4.21B, compare dotted and dashed traces and scales of the lefthand y-axis in both panels), indicating that

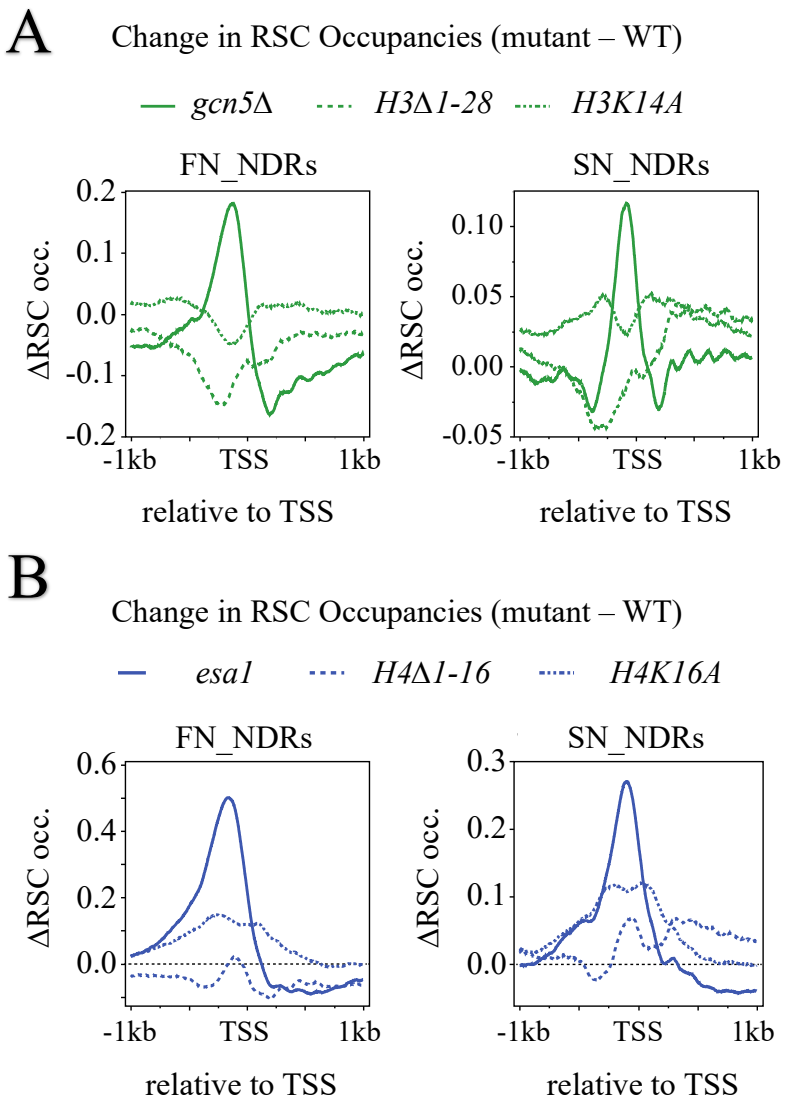

Figure 4.21. The H4 hypoacetylated tail mutant recapitulates some of the RSC accumulation seen in the H4 HAT mutant. A-B) Metagene profiles depicting the changes in RSC occupancies at FN_NDRs and at SN_NDRs in the indicated H3 (A) and H4 (B) HAT and histone tail mutants. In *H3K14A* and *H4K16A*, the K to A mutations prevent the residue from being acetylated in the mutants. Profiles are centered at the TSS.

hypoacetylated H4K16 residues might play more of a role in retaining RSC at FN_NDRs than at SN_NDRs. This also suggests that RSC might accumulate on fragile nucleosome complexes in a hypoacetylated H4 tail-dependent manner.

Overall, the observation that RSC accumulates in the HAT mutants but not in the tail deletion mutants suggests a role for unacetylated or hypoacetylated nucleosomes in retaining RSC at promoters. Recent cryo-EM structures of RSC bound to a nucleosome revealed that the H4 tail interacts with Sth1, where it binds to the interface of the SnAC and ATPase domains of the subunit (Wagner et al., 2020). Since the H4 tail is unacetylated in this structure, it is reasonable to speculate that the binding of the unacetylated H4 tail to RSC could stabilize the interaction of RSC with the nucleosome. This enhancement of the RSC-nucleosome interaction would explain why RSC accumulates in HAT mutants or *H4K14A* but not in WT cells or *H4Δ1-16.* In WT cells, acetylation of the H4 tail might alter the H4 tail binding so that the RSC-nucleosome interaction is weakened, providing a mechanism for RSC disengagement from promoter nucleosomes. Since RSC did not accumulate in *H3Δ1-28* like that observed for *gcn5Δ*, the H3 tail might also contribute to RSC retention in NDRs, though the lack of RSC accumulation in the *H3K14A* mutant casts some doubt on this possibility. While further investigation is needed using substitutions for other H3 and H4 lysine tail residues to confirm these possibilities, the data tentatively suggests that hypoacetylated histone tails retain RSC at FN_NDRs and that acetylation by HATs allows RSC to dissociate from nucleosomes to fine-tune histone eviction and NDR maintenance.

4.12 Histone Occupancies Do Not Increase in the NDRs of the Tail Mutants

Considering that RSC accumulation at promoters is only partially recapitulated in the *H4K14A* mutant but not in the other tail mutants, there might be some histone accumulation at promoters in the *H4K16A* mutant. Additionally, in the tail deletion mutants (*H3Δ1-28* and *H4Δ1-16*), it is also possible that histone occupancies could be elevated compared to WT cells, since RSC is involved in positioning the -1 and +1 nucleosomes and evicting nucleosomes within NDRs to maintain NDRs (Clapier et al., 2017; Ganguli et al., 2014; Harada et al., 2016; Krietenstein et al., 2016; Lorch and Kornberg, 2017; Rawal et al., 2018). To determine the organization of chromatin in the histone tail mutants, H3 ChIP-seq was performed using sonicated chromatin from cells containing WT H3 tails, as well as from *H3Δ1-28, H3K14A, H4Δ1-16,* and *H4K16A*. The sequenced data were then aligned to the *S. cerevisiae* genome and used to generate heatmaps depicting the changes in H3 occupancies in the tail mutants compared to WT cells (Figure 4.22) at FN_NDRs and SN_NDRs. The changes observed in each mutant were similar at both FN_NDR genes and at SN_NDR genes, and except for *H3Δ1-28*, the tail mutants showed a slight reduction of H3 around the TSS and slight increases in CDSs farther upstream of the TSS, though these changes are modest compared to the H3 increases observed in the HAT mutants (compare heatmaps in Figures 4.16 and 4.22). The *H3Δ1-28* mutant showed increased H3 occupancies compared to WT cells throughout the genes, despite having reduced RSC levels at promoters (Figures 4.16 - 4.21). Unlike the HAT mutants, which showed increased H3 occupancies at a more constricted area around the TSS, the H3 signal is more spread out throughout the genes (compare yellow hues in *H3Δ1-28* heatmaps in Figure 4.22 to yellow columns in Figure

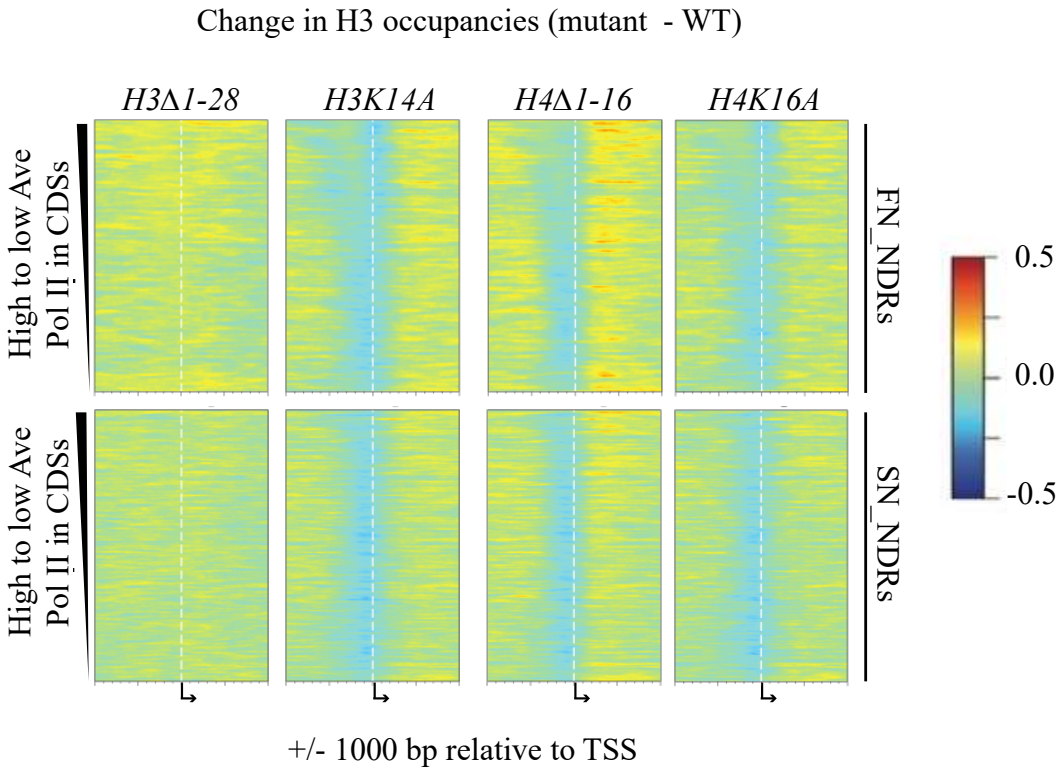

Figure 4.22. Histones do not accumulate in the promoters of the histone tail mutants, except for the H3 tail deletion mutant. Heatmaps showing the changes in H3 occupancies compared to WT cells at FN_NDRs (top panels) and at SN_NDRs (bottom panels) in the indicated histone tail mutants. Genes are sorted by decreasing Pol II occupancies and are centered at the TSS.

4.16 heatmaps). This suggests that the H3 tail may play a role in the positioning of nucleosomes in promoters, possibly by being recognized by RSC. Since the *H3K14A* mutant did not show similar effects, other residues within the H3 tail, or even the H3 tail as a whole, might be important for proper nucleosome positioning. Since the H4 tail mutants did not show these H3 changes despite the slight accumulation of RSC observed in the *H4K16A* mutant (Figures 4.16-4.22), it is likely that the H4 tail does not play a major role in nucleosome occupancies, but instead is needed to retain RSC to promoter nucleosomes and to promote nucleosome stability (Figure 4.17). Taken together, the RSC and H4 ChIP-seq data for the tail mutants suggest distinct roles of the H3 and H4 N-terminal tails in nucleosome positioning and RSC recruitment or retainment on promoter nucleosomes.

4.13 Gcn5 and Esa1 Promote RSC Recruitment to Transcribed CDSs

It has been shown that, in addition to promoters, RSC is enriched in the CDSs of many transcribed genes in a HAT-dependent manner (Ganguli et al., 2014; Rawal et al., 2018; Spain et al., 2014; Vinayachandran et al., 2018). To determine the effects of the HAT mutants on RSC occupancies in the CDSs of highly transcribed genes, the RSC ChIP-seq data for the top 20% of Pol II-occupied genes (Pol II-T20, N = 1092) was analyzed for WT cells, *sth1ΔBrD*, and for each of the HAT mutants (*gcn5Δ, esa1, gcn5Δ/esa1*). The heatmap depicting the changes in RSC occupancies in the BrD and HAT mutants compared to WT cells at the Pol II-T20 genes revealed substantial RSC reductions in the CDSs of the *gcn5Δ* mutant (Figure 4.23, note the dark blue hues after the TSS), indicating that the H3 HAT is needed to recruit or retain RSC to transcribed CDSs. In contrast, the reductions in RSC in the CDSs of transcribed genes were minor in

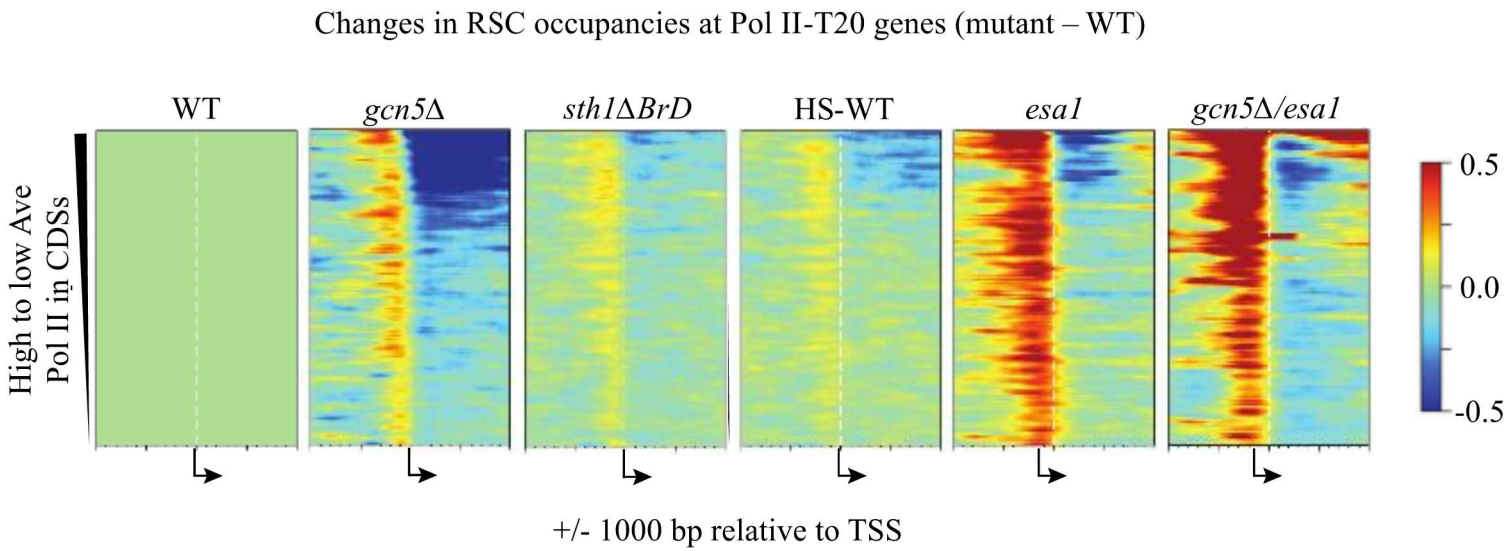

Figure 4.23. RSC is reduced in the CDSs of transcribed genes in the Sth1 bromodomain and HAT mutants. Heatmaps showing the changes in RSC occupancies compared to WT or HS-WT cells at the top 20% of Pol II-occupied genes (Pol II-T20) in WT cells, heat-shocked WT cells (HS-WT), *gcn5Δ, esa1*, and *gcn5Δ/esa1*. Genes were sorted by decreasing Pol II in CDSs and are centered at the transcription start site (TSS. indicated by a dotted white line at the center of the heatmap). The WT-WT heatmap is included as the far left panel for reference to no-change conditions

the *sth1ΔBrD* mutant compared to *gcn5Δ*, despite previous studies showing that acetylated H3K14 enhances Sth1 binding to nucleosomes (Blus et al., 2019; Chen et al., 2020; Jain et al., 2020). This discrepancy between the RSC ChIP-seq results and previous studies suggests that other RSC bromodomains might act redundantly to recruit RSC to transcribed CDSs. For instance, the Rsc4 tandem bromodomains have also been shown to bind to acetylated H3K14 (Kasten et al., 2004; VanDemark et al., 2007; Wagner et al., 2020). RSC occupancies were also reduced in the CDSs of transcribed genes in *esa1* and *gcn5Δ/esa1*, though these reductions were more modest compared to the reductions observed in the CDSs of *gcn5Δ* (Figure 4.23, compare greenish/blue hues after the TSS in the *esa1*-containing mutants to the dark hues of *gcn5Δ*). It is possible that the RSC recruitment defects observed in the CDSs of the *esa1*-containing mutants might be dampened by the increased interactions of the hypoacetylated H4 tails of CDS nucleosomes with RSC, similar to what was observed at NDRs (Figures 4.1-4.21). Nevertheless, the data shows that Gcn5 and Esa1 promote RSC enrichment to transcribed CDSs.

Because Ribosomal Protein Genes (RPGs) are highly expressed (Petibon et al., 2021), boxplots were generated to compare the RSC occupancies in CDSs of RPGs for WT cells, HS-WT cells, *sth1ΔBrD*, and the HAT mutants (Figure 4.24). RSC occupancies were higher in the CDSs of RPGs compared to the CDSs of the bottom 10% of Pol II-occupied genes (Pol II-B10), consistent with the finding that RSC localizes to the CDSs of highly transcribed genes (Figure 3.4). The median RSC occupancies for WT cells and *sth1ΔBrD* were nearly identical to each other (2.19 vs. 2.18), indicating that the

Sth1 bromodomain is not required to recruit or retain RSC to the CDSs of RPGs (Figure 4.24). RSC occupancies were significantly reduced in *gcn5Δ* compared to WT cells, in sharp contrast with *sth1ΔBrD*. RSC occupancies at RPGs were also significantly reduced in the *esa1* and HAT double mutants compared to HS-WT cells, though the reduction is not as pronounced as in *gcn5Δ*. The HAT double mutant also showed a greater RSC reduction than the *esa1* single mutant, suggesting that the H3 and H4 HATs contribute to RSC recruitment in RPGs in a manner independent from each other. It is worth noting that even though RSC occupancies were reduced in the HAT mutants, the RSC occupancies were still higher in these mutants at RPGs than that observed for lowly-transcribed genes (Figure 4.24, compare RSC occupancies of the HAT mutants with the occupancies observed at the Pol II-B10 genes). The residual binding of RSC in the CDSs of RPGs in the HAT mutants indicates the existence of additional mechanisms for recruiting RSC to the CDSs of transcribed genes. For instance, RSC might bind to CDS nucleosomes by recognizing accessible nucleosomes present in transcribed CDSs (Figure 3.12), similar to how RSC might recognize and accumulate on hypoacetylated fragile nucleosomes in promoters of the HAT mutants. The existence and prevalence of these mechanisms might help to explain the differences between RSC occupancies in the promoters and CDSs of the HAT mutants.

RPGs represent a small subset of highly transcribed genes (129 vs. 1092 Pol II-T20 genes). Therefore, to gain further insight into the differences in the RSC reductions in CDSs of RPGs in the HAT mutants vs. the RSC reduction seen in the CDSs of other Pol II-T20 genes, metagene profiles were generated showing RSC occupancies in WT cells, HS-WT cells, *sth1ΔBrD, gcn5Δ, esa1,* and *gcn5Δ/esa1* at RPGs and Pol II-T20

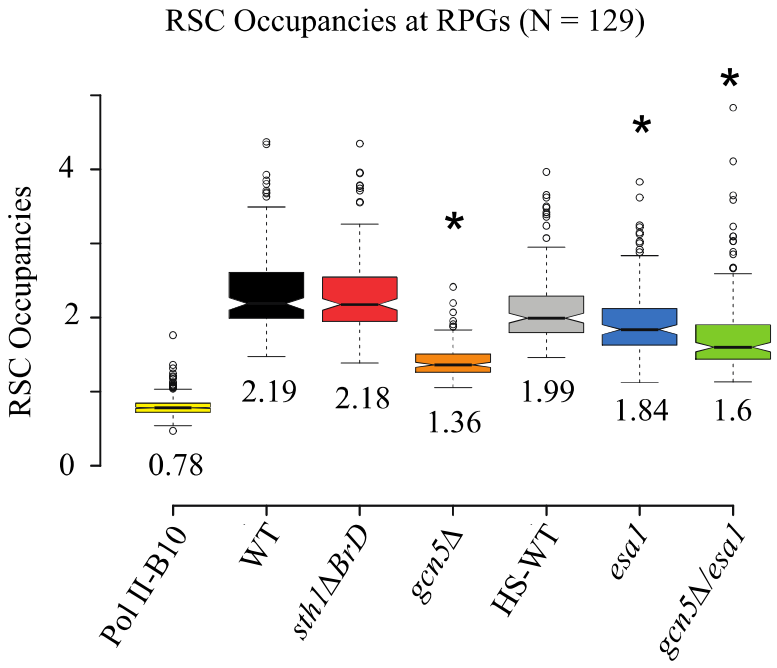

Figure 4.24. RSC is reduced in the CDSs of RPGs in the HAT mutants. Boxplot depicting the normalized RSC occupancies in CDSs at Ribosomal Protein Genes (RPGs) in WT, HS-WT, *sth1ΔBrD, gcn5Δ, esa1,* and *gcn5Δ/esa1.* Increases in median mutant RSC occupancies relative to WT or HS-WT cells (for *esa1*-containing mutants) were deemed significant if their p-values were < 0.05, and were determined by the Welch student t-test and denoted with an Asterix. RSC occupancies for the bottom 10% Pol II-occupied genes (Pol II-B10) are shown for comparison. The median RSC occupancies for each strain are also shown below each boxplot.

genes excluding RPGs (Figure 4.25). The profiles for the HAT mutants were similar to the findings observed in the boxplots (Figures 4.24 and 4.25A). The *gcn5Δ* mutant showed substantially lower RSC occupancies in CDSs compared to WT cells, and *sth1ΔBrD* showed no change compared to WT cells (Figure 4.25A). Both *esa1* and the HAT double mutant showed lower RSC occupancies than WT and HS-WT cells, though the reductions were more modest than in *gcn5Δ*. The patterns in RSC occupancies in CDSs for the Pol II-T20 genes excluding RPGs for the mutants were largely similar to those observed in RPGs, except for the HAT double mutant (Figure 4.25B). The *gcn5Δ* mutant showed the most substantial decrease in RSC at CDSs compared to WT cells, while the RSC occupancies in the CDSs of WT cells and *sth1ΔBrD* were very similar to each other. RSC levels in the CDSs of *esa1* were still lower than those of WT or HS-WT cells, but the reductions were still modest compared to those in *gcn5Δ*. Surprisingly, the HAT double mutant showed an increase of RSC in the CDSs of Pol II-T20 genes excluding RPGs, with the increases becoming greater farther away from the TSS and towards the 3' end of the metagene (Figure 4.25B, compare dotted trace to blue and green traces). This increase is inconsistent with the RSC reduction seen in the HAT single mutants. It is possible that the presence of both hypoacetylated H3 and H4 tails in the HAT double mutant stabilizes the RSC-nucleosome interactions to a much higher degree than in the HAT single mutants, masking the actual RSC occupancy defects present in the CDSs of *gcn5Δ/esa1*. Altogether, the data implicate HATs, especially Gcn5, in maintaining high levels of RSC in transcribed CDSs. Since RSC contains multiple bromodomains in multiple subunits that recognize acetylated histones (Dhalluin et al.,

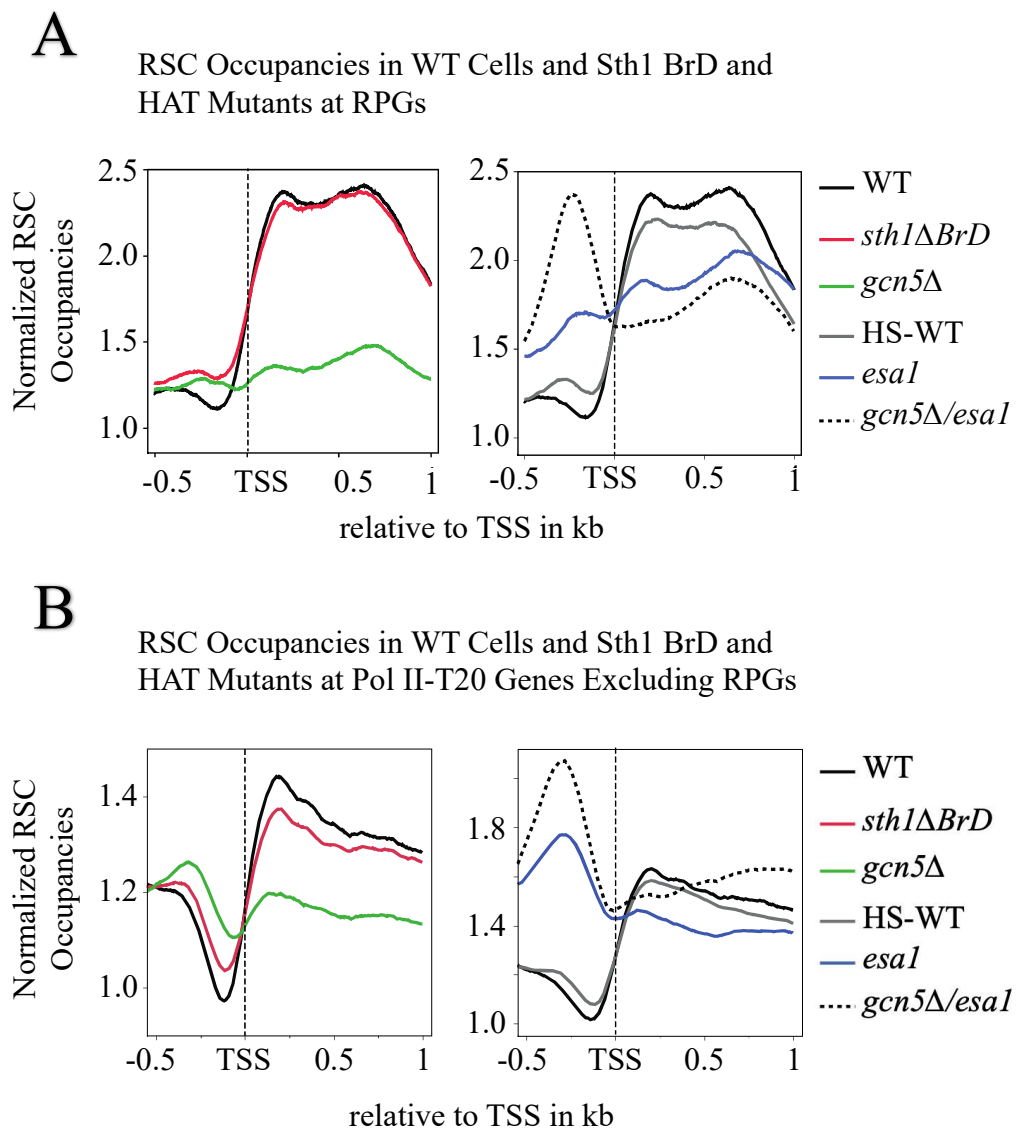

Figure 4.25. Gcn5 and Esa1 recruit RSC to the CDSs of transcribed genes. A-B) Metagene profiles depicting RSC occupancies in WT cells, HS-WT cells, *gcn5Δ, esa1,* and *gcn5Δ/esa1* at Ribosomal Protein Genes (RPGs, N = 129) (A) and at the top 20% Pol II-Occupied Genes (Pol II-T10, N = 963) excluding RPGs. The vertical dotted line indicates the TSS.

1999; Patel et al., 2019; Wagner et al., 2020; Zeng and Zhou, 2002), the data suggest that Gcn5 and Esa1 might play a role in recruiting RSC to transcribed CDSs via the acetylation of the H3 and H4 N-terminal tails.

4.14 RSC Recruitment to Transcribed CDSs is Dependent on H3 and H4 Tails

To determine if histone tails play a role in recruiting RSC to transcribed CDS, RSC occupancies in the CDSs of Pol II-T20 genes were analyzed in cells containing WT H3 tails (WT(H3)) and in the *H3Δ1-28* and *H4Δ1-16* mutants (Figure 4.26). The mutants showed reduced RSC occupancies in the CDSs of the Pol II-T20 genes compared to WT cells, with the H4 tail deletion mutant showing a greater reduction in RSC than the H3 tail mutant (compare red/yellow hues in the left three heatmaps, as well as the dark blue hues after the TSS in the right two heatmaps in Figure 4.26). To gain further clarity into the extent of RSC reduction at distinct subsets of highly transcribed genes, metagene profiles were generated depicting RSC occupancies at RPGs and Pol II-T20 genes excluding RPGs for WT cells and the tail deletion mutants (Figure 4.27). Both *H3Δ1-28* and *H4Δ1-16* had lower RSC occupancies compared to WT cells in the CDSs of RPGs (Figure 4.27A) and at other highly-transcribed genes (Figure 4.27B), where the H4 tail deletion mutant also showed a greater reduction in RSC than the H3 tail deletion mutant. Intriguingly, the RSC occupancies were reduced to a greater extent in the coding sequences of the H4 tail deletion mutant than in the H4 HAT mutant (compare the *esa1* profiles after the TSS in Figure 4.25 to the *H4Δ1*-16 profiles in Figure 4.27). These results raise the strong possibility that the RSC occupancy defects in *esa1*-containing mutants are masked by hypoacetylated tails that enhance RSC-nucleosome interactions. Indeed, the highest Pol II-occupied genes in the *H4K16A* mutant show reduced RSC

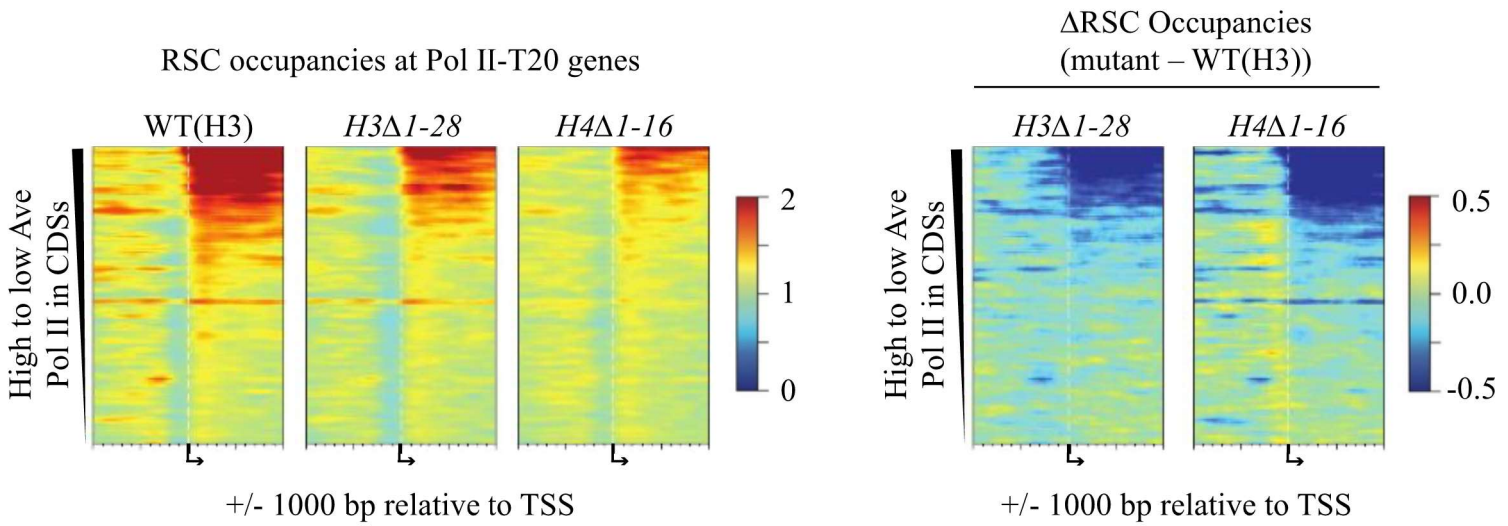

Figure 4.26. RSC is also reduced in the CDSs of the histone tail deletion mutants. Heatmaps depicting the RSC occupancies of WT histone H3 cells (WT(H3)), *H3Δ1-28,* and *H4Δ1-16* (left three panels), as well as the changes in RSC occupancies (ΔRSC, mutant – WT(H3)) in *H3Δ1-28* and *H4Δ1-16* (right two panels) at the top 20% of Pol II-occupied genes (Pol II-T20). Genes were sorted by decreasing Pol II in CDSs and are centered at the transcription start site (TSS. indicated by a dotted white line at the center of the heatmap).

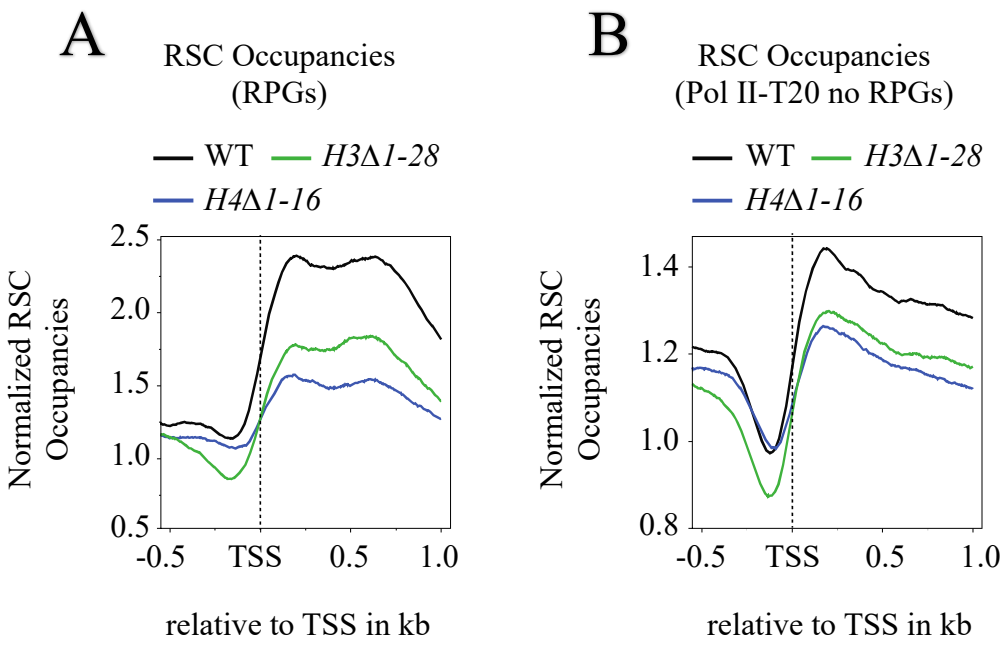

Figure 4.27. RSC recruitment to transcribed CDSs depends on H3 and H4 tails. A-B) Metagene profiles showing RSC occupancies for WT cells, *H3Δ1-28,* and *H4Δ1-16* at Ribosomal Protein Genes (RPGs) (A), and at the top 20% Pol II-occupied genes excluding RPGs (Pol II-T20 no RPGs) (B). The vertical line represents the location of the TSS.

occupancies in their CDSs, and though the reduction is less than that in *H4Δ1-16*, the reduction is similar to or even slightly more reduced than that observed for *esa1* (compare the very tops of the heatmaps in Figure 4.20B). This makes sense, since there should only be one hypoacetylated residue in *H4K16A,* whereas most lysine residues in the H4 tail should be hypoacetylated in *esa1*, which could lead to a stronger interaction of the H4 tail with RSC in *esa1* than in *H4K16A*. In contrast, RSC reductions were less pronounced in the *H3Δ1-28* and *H3K14A* mutants than in the *gcn5Δ* mutant (compare the very top of heatmaps in Figure 4.20A). It is possible that the acetylation of lysine residues at positions other than 1-28 on the H3 tail, such as H3K36, might also contribute to RSC recruitment. For instance, H3K36 can also be acetylated by Gcn5 (Morris et al., 2007; Pai et al., 2014) and could contribute to RSC recruitment. Taken together, the data strongly implies that acetylation of the H3 and H4 tails promotes RSC recruitment/retention to the CDSs of highly transcribed genes.

4.15 The Increase in RSC Occupancies at Promoters in HAT Mutants is Independent of the RSC Reduction in Transcribed CDSs

Since RSC increased in the promoters yet decreased in transcribed CDSs in the HAT mutants, it is possible that RSC might migrate from the promoters to the CDSs of transcribed genes in a HAT-dependent manner, and that the loss of Gcn5 and/or Esa1 in the HAT mutants might have prevented this migration from occurring. To determine if the reductions in RSC within CDSs correlated with the increase in RSC occupancies at promoters, a scatterplot was generated showing the correlation between Pol II ChIP-seq reads (determined by Rpb3 ChIP-seq using sonicated chromatin) and RSC occupancy changes at CDSs and promoters for the top 20% of transcribed genes in the *gcn5Δ* mutant

(Figure 4.28). Since *gcn5Δ* showed the greatest RSC reduction in the CDSs of transcribed genes, the correlations were compared in this mutant. The reduction in RSC occupancies in CDSs correlated with Pol II occupancies ($R^2 = 0.67$, Figure 4.28). However, the RSC occupancy increases at promoters did not correlate with Pol II occupancies ($R^2 = 0.00$). If the increases in RSC at promoters correlated with the RSC reductions in CDSs, then the changes in RSC occupancies at promoters should correlate with Pol II occupancies at transcribed genes since the reductions in CDSs correlated with Pol II occupancies. Because the increases at promoters did not correlate with Pol II, this suggests that RSC does not migrate from promoters to CDSs, at least in *gcn5Δ*. To be certain that this correlation was not specific to just the H3 HAT mutant, scatterplots depicting the correlations between the changes in RSC occupancies at promoters with the changes in RSC occupancies in CDSs were generated for HS-WT cell, *sth1ΔBrD*, *gcn5Δ*, and *esa1* (Figure 4.29). In HS-WT cells and all mutants, the RSC accumulation at promoters was weakly correlated with the changes in RSC occupancies in CDSs. Taken together, the data suggest that the accumulation seen in the promoters of HAT mutants is not likely to be due to RSC failing to migrate to CDSs of transcribed genes when HATs are lost, or at least it is not occurring at a large scale. It is more likely that other factors, one of which being hypoacetylated histone tails, contribute to the differences in promoter and CDS RSC levels in the HAT mutants.

4.16 Discussion

The work in this chapter investigated the importance of histone acetyltransferases (HATs) Gcn5 and Esa1 in regulating the occupancy of the essential chromatin remodeler RSC. The data revealed contrasting roles of these HATs in regulating RSC occupancies

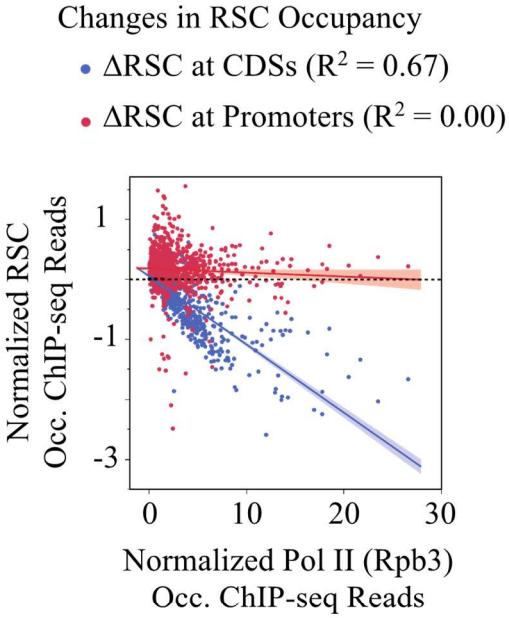

Figure 4.28. RSC increases in promoters are not correlated with Pol II occupancies in *gcn5*Δ. Scatterplot showing the comparing the changes in RSC occupancies (ΔRSC, mutant – WT) in CDSs and promoters of *gcn5*Δ with WT Pol II occupancies in the CDS of the top 20% of Pol II-occupied genes (N = 1092).

Correlation between changes in RSC Occupancies in promoters and CDSs of the Bromodomain and HAT mutants

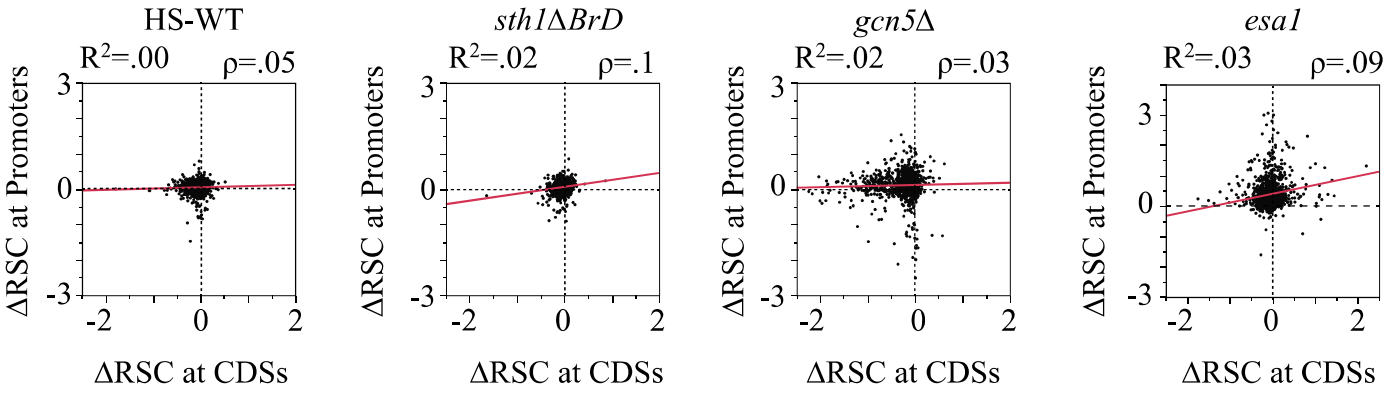

Figure 4.29. RSC accumulation at promoters does not correlate with RSC reduction in CDSs in the HAT and bromodomain mutants. Scatterplots showing RSC occupancy changes (ΔRSC) in promoters and in CDSs for HS-WT cells and for the Sth1 bromodomain and HAT single mutants. The R-squared and Spearman correlation (ρ) are shown for each comparison.

at promoters and CDSs of genes. RSC occupancies were substantially reduced at transcribed CDSs in cells lacking Gcn5, functional Esa1, or the H3 or H4 N-terminal tails (Figures 4.23 – 4.27). These results support the idea that histone tail acetylation by HATs is important for recruiting or retaining RSC in transcribed sequences. Surprisingly, substantial RSC accumulation was observed at promoters of the HAT mutants, which initially suggested that histone acetylation precludes RSC binding in promoters (Figures 4.1 – 4.2). However, RSC accumulation was not observed in the H3 or H4 N-terminal tail mutants (Figures 4.18 – 4.19). Considering this, the findings collectively suggest that hypoacetylated or unacetylated histone tails enhance RSC retention in NDRs and that the acetylation of these tails might help RSC to disengage from the chromatin. In addition to the RSC accumulation observed in NDRs, H3 occupancies were also increased in the HAT mutants (Figure 4.9), suggesting a global role of HATs in evicting histones from NDRs.

4.16.1 Hypoacetylated Tails Promote RSC Binding to Nucleosomes in NDRs

The results from this project show that RSC accumulates in the promoters in cells lacking the H3 HAT Gcn5 or in cells where the H4 HAT Esa1 is inactivated (Figures 4.1 – 4.2). These results were surprising, considering that RSC has been shown to bind to acetylated histones in vitro (Carey et al., 2006; Chatterjee et al., 2015). Since HATs acetylate histones (Marmorstein, 2001; Shahbazian and Grunstein, 2007), RSC occupancies at promoters should have decreased, not increased, as histone acetylation is decreased within these mutants (Figure 4.8). In addition to the RSC increases, histone H3 occupancies also increased in the NDRs of the HAT mutants, suggesting that RSC may be accumulating on nucleosomes within NDRs. Not all NDRs are completely free of

histones, as demonstrated by the low but nonzero H3 occupancies detected at NDRs (Figure 4.11, compare the median of the black boxplot to the y-axis scale). Indeed, MNase-sensitive complexes have been detected in the NDRs of ~2000 genes (Brahma and Henikoff, 2019; Chereji et al., 2017; Kubik et al., 2015; Schlichter et al., 2020). While the exact nature of these complexes is disputed (Chereji et al., 2017; Kubik et al., 2017), multiple studies support the idea that these are fragile nucleosomes and have shown that many of these fragile nucleosomes are RSC-bound (Brahma and Henikoff, 2019; Klein et al., 2023; Kubik et al., 2015; Schlichter et al., 2020). Thus, the RSC and H3 increases at NDRs in the HAT mutants might suggest that: 1) fragile nucleosomes might be stabilized in the HAT mutants such that their nucleosomal DNA is less accessible, resulting in higher H3 occupancies in the HAT mutants, and 2) RSC binds more efficiently to fragile nucleosomes than to stable nucleosomes. It is likely that both increased nucleosome occupancies and nucleosome stabilization contribute to the higher RSC occupancies found in NDRs. It was also observed that the RSC and H3 occupancy increases at NDRs containing stable nucleosomes in the HAT mutants were similar to each other (Figures 4.5 and 4.16), suggesting that the RSC accumulation may be due to the greater presence of nucleosomes within these NDRs. However, in NDRs containing fragile nucleosomes, RSC accumulated to a greater extent than in NDRs containing stable nucleosomes. At the same time, the H3 increases were more moderate compared to the increases observed in NDRs containing stable nucleosomes. These findings suggest that fragile nucleosomes (more accessible nucleosomes) retain RSC better than stable (canonical) nucleosomes.

Since histone acetylation is reduced in the HAT mutants (Figure 4.8),

nucleosomes within the HAT mutants should contain histone N-terminal tails that are hypoacetylated compared to nucleosomes in WT cells. If hypoacetylated tails help stabilize RSC occupancy in the HAT mutants, then nucleosomes that lack the tails should not be able to retain RSC, and RSC levels should be reduced. Indeed, RSC accumulation was not observed in the NDRs of cells lacking H3 or H4 N-terminal tails (Figures 4.18 – 4.19). Additionally, RSC accumulation was observed in the NDRs of cells that contained the H4 tail but lacked H4K16 acetylation (Figures 4.20 – 4.21), further supporting the idea that RSC is retained on hypoacetylated tails. The RSC accumulation observed in the *H4K16A* mutant was not as pronounced as the accumulation seen in the H4 HAT mutant, suggesting that acetylation at other lysine residues in the H4 tail might play a role in regulating RSC retainment to NDRs. Overall, the data within this chapter indicate that hypoacetylated tails promote RSC recruitment/binding to nucleosomes within promoters and that the acetylation of these tails weakens this binding. This is surprising, given that RSC contains multiple bromodomains that have been shown to recognize and bind to acetylated nucleosomes (Dhalluin et al., 1999; Kasten et al., 2004; VanDemark et al., 2007; Wagner et al., 2020; Zeng and Zhou, 2002).

Cryo-EM structures depicting RSC interacting with nucleosomes have revealed that several RSC subunits, including the catalytic subunit Sth1, interact with the nucleosome at several different points (Patel et al., 2019; Wagner et al., 2020; Ye et al., 2019). One such interaction was the binding of the H4 tail to the interface between the SnAC and ATPase domains of Sth1 (Wagner et al., 2020). Since the H4 tail in this structure was unacetylated, it is possible that acetylation could weaken the interaction of the H4 tail with RSC, which would help RSC in dissociating from the nucleosome. The

finding that RSC and H3 occupancies increase in the NDRs of the HAT mutants (Figures 4.1 – 4.2 and 4.9 – 4.10) provides in vivo evidence for this. Since RSC accumulates to a greater extent in NDRs containing fragile nucleosomes than in NDRs containing stable nucleosomes (Figures 4.5 – 4.6), it is possible that the more accessible fragile nucleosomes might allow for better association of the H4 tail with the Sth1 interface than the less accessible stable nucleosomes. In WT cells, the hypoacetylated tails of fragile nucleosomes might recruit more RSC to facilitate the sliding and eviction of promoter nucleosomes to allow these genes to obtain higher transcription levels. A recent study showed that RSC binds to NDRs in quiescent cells and that this binding was critical for rapid transcription during quiescence exit (Cucinotta et al., 2021). Given these findings, it is possible that the ability of fragile nucleosomes to recruit RSC to NDRs in an acetylation-independent manner might prime these promoters to rapidly respond to recover from stress.

4.16.2 HATs Prevent Histone Accumulation at NDRs Genome-wide

Chromatin remodelers have been implicated in the formation and maintenance of canonical chromatin structure in NDRs (Krietenstein et al., 2016; Ramachandran and Henikoff, 2016; Yen et al., 2012). RSC has been shown to position the flanking -1 and +1 nucleosomes to maintain NDRs genome-wide (Klein-Brill et al., 2019; Krietenstein et al., 2016; Kubik et al., 2019; Kubik et al., 2018; Rawal et al., 2018). It is widely accepted that histones are evicted from promoters during transcription induction (Boeger et al., 2004; Reinke et al., 2001; Reinke and Horz, 2003; Sanz et al., 2016). For instance, studies have shown that deletion of the *GCN5* gene results in increased histone at the NDRs of genes that are induced by sulfometuron methyl (SM) (Govind et al., 2007; Qiu

et al., 2016), a compound that causes amino acid starvation stress by inhibiting isoleucine/valine biosynthesis and triggers the transcriptional activation of amino acid stress response genes. This work shows that H3 levels increased in most NDRs of the HAT mutants, even those of lowly transcribed genes (Figures 4.9 – 4.16). The global histone occupancy increases in the HAT mutants suggest that both RSC and HATs play important roles in evicting nucleosomes from NDRs. Interestingly, the Sth1 bromodomain mutant also displayed increased H3 occupancies within NDRs that were comparable to the increases seen in *gcn5Δ* at all but the top 25% of transcribed genes (Figures 4.12 – 4.13). This makes sense, considering that the Sth1 bromodomain preferentially recognizes acetylated H3K14, a target for Gcn5 (Jain et al., 2020; Neumann and Wilkins, 2021).

The observations that both RSC and histone occupancies are increased in the HAT mutants makes it tempting to speculate that the hypoacetylated histones are not as efficiently evicted in the HAT mutants, despite the increased presence of RSC within NDRs. This makes sense since biochemical studies have shown that the acetylation of histone tails stimulates RSC catalytic activity in vitro (Chatterjee et al., 2015; Chatterjee et al., 2011). Indeed, the increased nucleosome occupancies in the HAT mutants suggest that nucleosomes within promoters are stabilized despite RSC presence, indicating that these nucleosomes are not efficiently remodeled by RSC (Figure 4.17). Thus, fragile nucleosomes might recruit RSC in an acetylation-independent but tail-dependent manner, and subsequent acetylation of the tails by HATs might stimulate RSC to remove those histones more efficiently, priming these genes for efficient transcription (Chatterjee et al., 2015; Chatterjee et al., 2011; Jain et al., 2020; Neumann and Wilkins, 2021).

4.16.3 Acetylated H3 and H4 Tails Promote RSC Recruitment/Retention in Transcribed CDSs

Historically, acetylation has been thought to promote transcription by weakening the interaction between nucleosomal DNA and histone tails (Berndsen and Denu, 2008; Lee and Workman, 2007). However, a recent study has challenged this notion by showing that transcription promotes the acetylation of histone tails (Martin et al., 2021). Histone tail acetylation is also thought to promote the binding of bromodomain-containing complexes such as RSC to relieve the nucleosome barrier for transcription (Hassan et al., 2007; Hassan et al., 2001; Kasten et al., 2004). The findings of this chapter support the idea that acetylation recruits RSC by showing that HATs are important for RSC enrichment in the CDSs of transcribed genes. RSC was severely reduced in transcribed CDSs of cells lacking Gcn5 (Figures 4.23 – 4.25). RSC reductions were also seen in the CDSs of *esa1* and *gcn5Δ/esa1*, though to a more moderate extent. Despite the modest decreases in the *esa1*-containing mutants, substantial reductions of RSC in transcribed CDSs were also observed in cells lacking either the H3 or H4 N-terminal tail (Figures 4.26 – 4.27), providing strong support for histone tails in mediating RSC recruitment/retention in CDSs. As such, the data strongly suggest that one of the functions of transcription-dependent acetylation of nucleosomes within CDSs is to recruit or maintain high levels of RSC in transcribed CDSs. RSC recruitment to CDSs might make nucleosomes more accessible to elongating polymerases, as discussed in Chapter 3 (Figure 3.14).

Overall, the data suggest that HATs are important for regulating RSC levels at promoters and in transcribed CDSs. The findings support a model where hypoacetylated

tails might recruit RSC to NDRs, and the subsequent acetylation of these tails by HATs Gcn5 and Esa1 leads to efficient histone eviction by RSC from NDRs, which promotes PIC assembly and transcription (Figure 4.30). When cells lack these HATs, RSC is still recruited to the NDRs, but histones are evicted less efficiently, resulting in increased histone occupancies at promoters. In transcribed CDSs, histone acetylation promotes RSC recruitment, which may render nucleosomes in transcribed CDSs more accessible to elongating Pol II to promote efficient transcription elongation.

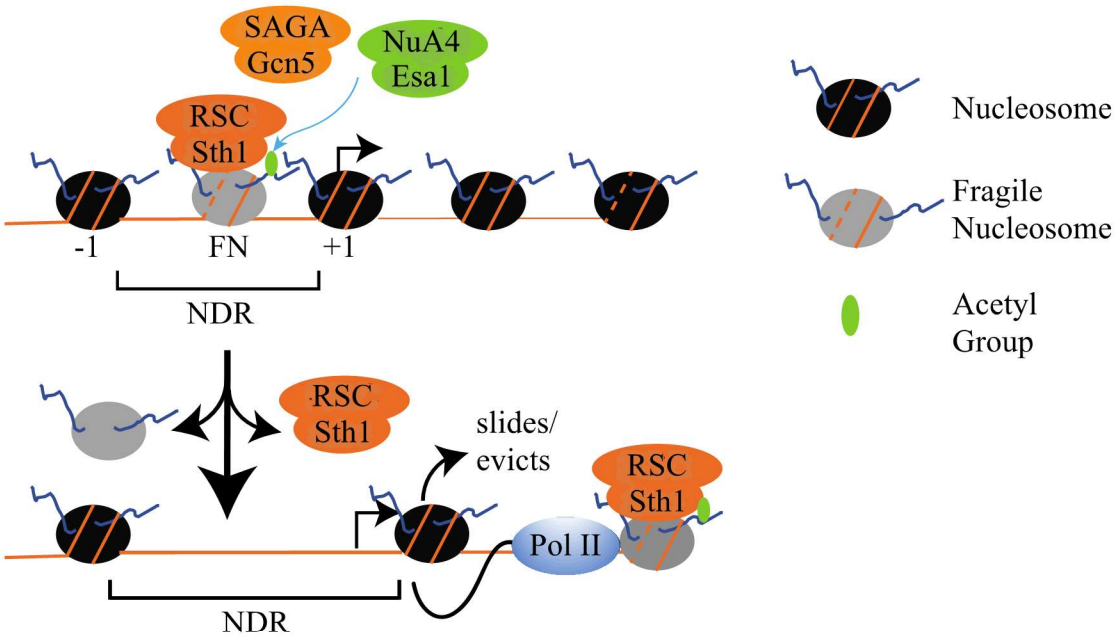

Figure 4.30. Model depicting the roles of Gcn5 and Esa1 in regulating chromatin structure at promoters and in CDSs. At a typical gene, the nucleosome-depleted region (NDR) is flanked by the -1 and +1 nucleosomes. Certain genes also harbor complexes termed fragile nucleosomes (FN) within their NDRs, which have been shown to be RSC-bound and sensitive to MNase digestion. In WT cells, nucleosomes such as the +1 nucleosome can be evicted or repositioned by RSC, which could be transiently recruited to NDRs via transcription activators, histone acetylation by Gcn5 of Esa1, or by recognizing DNA sequences within the promoter. Repositioning/remodeling of the +1 nucleosome by RSC can then facilitate TBP recruitment and transcription. Acetylation by Esa1 or Gcn5 may also promote RSC activity and inhibit RSC retention on histone tails, allowing RSC to dissociate from the chromatin to allow for efficient remodeling and transcription. In CDSs, RSC is recruited to chromatin in an acetylation-dependent manner, where it can remodel nucleosomes in transcribed CDSs (Figure 3.14).

CHAPTER FIVE

RSC COORDINATES WITH GCN5 AND ESA1 TO PROMOTE TRANSCRIPTION

5.1 Introduction

Given that RSC and HATs modify chromatin structure and chromatin can impair transcription, it is important to understand how RSC and HATs promote transcription. Previous studies have shown that RSC is important for the transcription of Pol II genes. At promoters, RSC helps to position the -1 and +1 nucleosomes to maintain NDR width genome-wide (Krietenstein et al., 2016), as depletion of RSC results in NDR filling and reduced pre-initiation complex (PIC) assembly and transcription (Badis et al., 2008; Brahma and Henikoff, 2019; Ganguli et al., 2014; Klein-Brill et al., 2019; Kubik et al., 2018; Rawal et al., 2018), implicating RSC in promoting PIC formation and transcription initiation. RSC is also thought to be involved in transcription elongation. In vitro experiments have shown that RSC promotes Pol II transcription through the chromatin template (Carey et al., 2006), whereas in vivo experiments showed altered Pol II distribution through the coding regions upon Rsc8 depletion (Ocampo et al., 2019). Importantly, RSC has also been shown to localize to transcribed coding sequences (CDSs) of Gcn4-activated genes in a Gcn5- and Esa1-dependent manner, leading to reduced Pol II occupancies under Gcn4-activating conditions (Rawal et al., 2018; Spain et al., 2014). Given these findings, as well as the results of this project that have shown that HATs Gcn5 and Esa1 prevent RSC accumulation in promoters yet recruit RSC to CDSs of transcribed genes (Chapter 4), it is possible that HATs coordinate with RSC to regulate chromatin structure and transcription. To test the impacts of the Sth1

bromodomain, Gcn5, and Esa1 on transcription, TBP and Pol II ChIP-seq were performed in WT cells, *sth1ΔBrD, gcn5Δ, esa1,* and the HAT double mutant *gcn5Δ/esa1*. Tata-binding protein (TBP) can exist independently or as part of the TFIID complex and is the first component of the PIC recruited to the promoter (Greber and Nogales, 2019). Given the TBP and Pol II defects observed upon Sth1 depletion, any reduction in TBP levels in the mutants compared to WT cells would likely represent PIC assembly defects, and aberrant Pol II levels would represent transcriptional defects (Kubik et al., 2018; Ocampo et al., 2019). In addition to the HAT mutants, TBP and Pol II ChIP-seq data from various RSC depletion experiments (Klein-Brill et al., 2019; Kubik et al., 2018; Ocampo et al., 2019) were analyzed to determine the impacts of RSC and RSC activity alone on PIC assembly and transcription, in order to tease out the interplay between RSC and HATs on transcription.

5.2 RSC Depletion Differentially Affects TBP and Pol II Occupancies at Highly-Transcribed Genes

The findings from Chapter 3 suggest that RSC might remodel nucleosomes in CDSs, which might facilitate Pol II elongation. To assess the role of RSC in regulating Pol II elongation, data was analyzed from several studies in which RSC subunits were depleted, and the changes in TBP and Pol II occupancies compared to WT cells were examined for the RSC-depleted samples. Because RSC contains multiple essential subunits, including Rsc8 and the catalytic subunit Sth1 (Clapier et al., 2016; Wagner et al., 2020), deletion of the genes encoding for these essential subunits results in a lethal phenotype. As such, depletion experiments such as anchor away (Haruki et al., 2008) or auxin-induced degradation (AID) (Morawska and Ulrich, 2013; Nishimura et al., 2009)

were employed to study the effects of RSC loss. The two main studies used for analysis (Kubik et al., 2018; Ocampo et al., 2019) employed two different methods to deplete RSC to study its effect on transcription, both of which will be discussed in detail below.

5.2.1 Pol II Levels are Reduced in Rsc8-Depleted Cells

To determine the impact of RSC on Pol II occupancies, Pol II ChIP-seq and MNase-seq data using chromatin from WT and RSC-depleted cells were analyzed from (Ocampo et al., 2019). To deplete RSC, the researchers used a mutant yeast strain that encoded a *RSC8* gene on a plasmid under the control of the *GAL1* promoter. The *GAL1* promoter is induced by galactose and is repressed by glucose or dextrose. The cells were grown in synthetic complete media containing 2% galactose, then switched to media containing 2% glucose to inhibit transcription of *RSC8*. Cells were then allowed to grow until growth plateaued to allow for the depletion of the protein reservoir of Rsc8 (Ganguli et al., 2014; Ocampo et al., 2019). Once Rsc8 was depleted, chromatin was then extracted and used by the researchers for either MNase-seq or Pol II ChIP-seq. Figures 5.1-5.2 show genome browser snapshots for Pol II ChIP-seq and MNase-seq data in WT and Rsc8-depleted (*rsc8*) cells at the indicated ribosomal protein genes (RPGs) and metabolism genes. The MNase-seq tracks in the WT and *rsc8* cells were similar, indicating very few changes in chromatin structure. However, Pol II levels were lower in the *rsc8* cells than in the WT cells at the indicated genes (Figures 5.1-5.2), suggesting that RSC is needed for sufficient levels of Pol II at these highly transcribed genes.

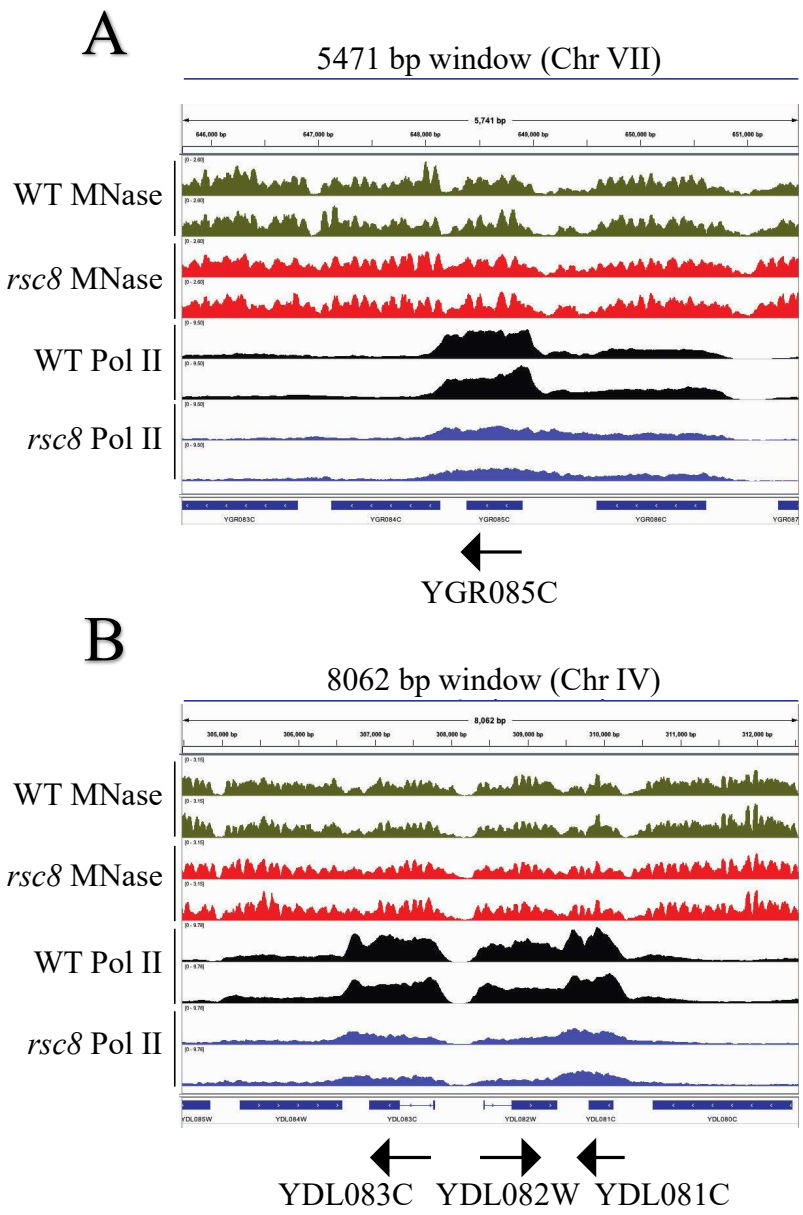

Figure 5.1. Pol II is reduced in RPGs when RSC is depleted. (A-B) Genome browser snapshots showing Pol II levels in WT cells (black tracks) and in cells depleted of the Rsc8 subunit (*rsc8,* blue tracks) at RPGs YGR085C, YDL083C, YDL082W, and YDL081C. Green and red tracks show the reads for MNase inputs for WT and *rsc8* cells, respectively. Arrows denote the 5'→ 3' direction of the gene. Data was obtained from (Ocampo et al, 2019).

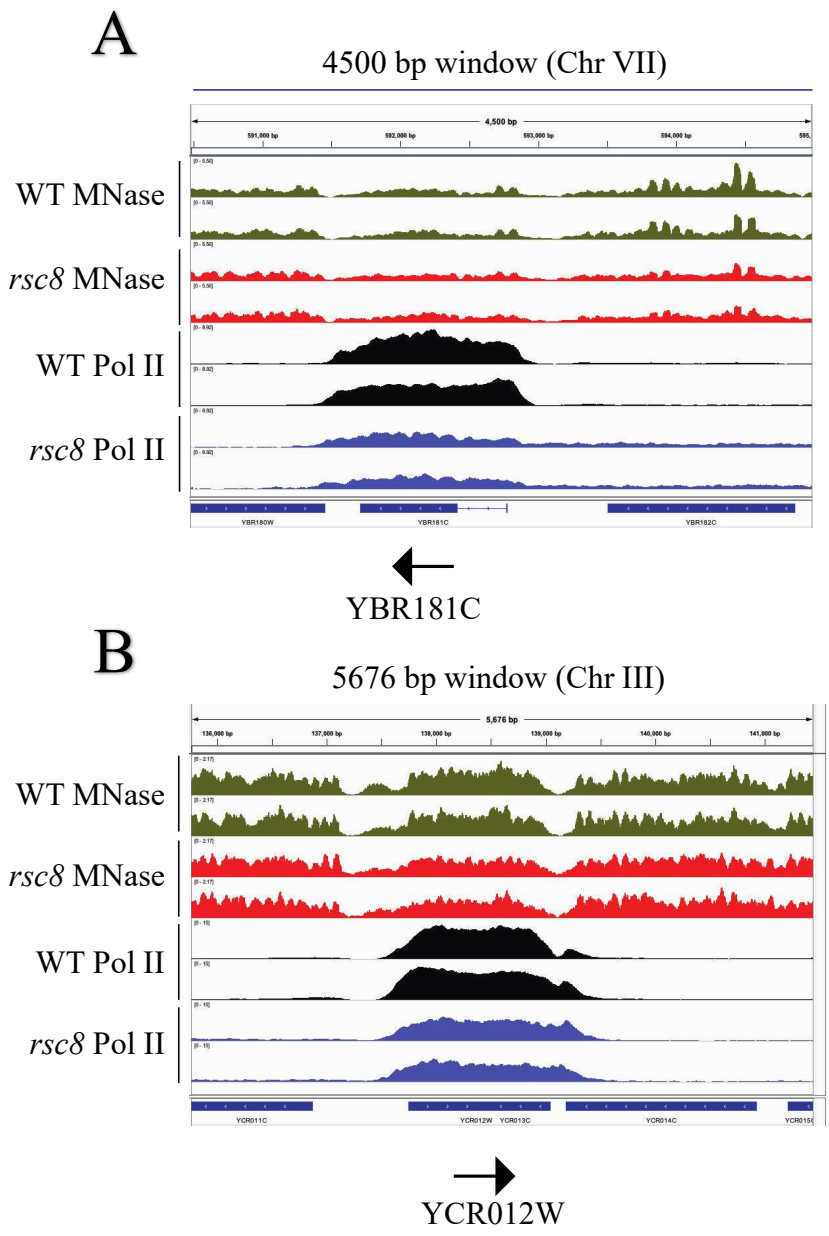

Figure 5.2. Pol II is reduced in RPGs and metabolic genes when RSC is depleted. (A-B) Genome browser snapshots showing Pol II levels in WT cells (black tracks) and in cells depleted of the Rsc8 subunit (*rsc8,* blue tracks) at RPG YBR181C and at YCR012W (involved in glucose metabolism). Green and red tracks show the reads for MNase inputs for WT and *rsc8* cells, respectively. Arrows denote the 5'→ 3' direction of the gene. Data was obtained from (Ocampo et al. 2019).

5.2.2 Pol II and TBP Occupancies are Differentially Affected at Different Gene Sets when RSC is Depleted

While the results from (Ocampo et al., 2019) are intriguing, these six genes are a very small sample size of the entire yeast genome. Additionally, Rsc8 is not the catalytic subunit of RSC; so it would be difficult to tweeze out the indirect structural effects of Rsc8 depletion from effects due to the loss of RSC activity. To determine the impact of RSC on TBP and Pol II occupancies at a genome-wide scale, TBP and Pol II ChIP-seq data from WT and Sth1-depleted cells were analyzed from (Kubik et al., 2018). To deplete Sth1, the researchers employed the anchor-away method to rapidly deplete Sth1 (Haruki et al., 2008). The anchor away strain encodes for both an FKBP12-tagged ribosomal protein and an FRB-tagged Sth1 (Haruki et al., 2008; Kubik et al., 2018). Upon the addition of rapamycin (Rapa), the FRB-tagged Sth1 forms a complex with the FKBP12-tagged ribosomal proteins, which are located in the nucleus to be assembled into pre-ribosomal subunits (Panse and Johnson, 2010). When the ribosomal subunits are transported into the cytoplasm for maturation, the FRB-tagged Sth1 protein is shuttled along with the pre-ribosome, depleting Sth1 from the nucleus.

While the study found that both Pol II and TBP were significantly reduced in Sth1 anchor-away cells (Kubik et al., 2018), they did not fully assess the role of RSC in potentially regulating transcription elongation. Since RSC might remodel nucleosomes in CDSs to make them more accessible to elongating polymerase, the data was divided into deciles based on WT Pol II occupancies to identify the genes where RSC function might be attributed to Pol II elongation in a way that was distinct from the role of RSC in transcription initiation. The boxplot showing the changes in Pol II and TBP occupancies

in Sth1 anchor-away (*sth1AA*) cells compared to WT cells revealed that TBP occupancies were reduced in all genes except for the decile containing the lowest levels of Pol II occupancies (Figure 5.3). These results suggest that TBP is strongly dependent on RSC function. Pol II levels were also reduced in Deciles 3-9, consistent with a study that showed a strong relationship between PIC assembly (TBP) and Pol II occupancies genome-wide (Petrenko et al., 2019).

Interestingly, in Deciles 1, 2, and 10, Pol II levels either did not change or were actually increased in the Sth1-depleted cells, in contrast to the other deciles and the genes shown in Figures 5.1-5.2. The genes in Deciles 1 and 2 showed the expected decreases in Pol II when TBP was depleted instead of Sth1 (Petrenko et al., 2019) (Figure 5.4), indicating that the Pol II increases observed in the *sth1AA* cells is more likely due to loss of RSC rather than a different response to TBP loss. To clarify where the increases in Pol II were occurring when Sth1 was depleted, metagene profiles were generated depicting the Pol II and TBP occupancies for the top 10% of Pol II-occupied genes (Decile 1), as well as for the top 10% of genes that showed the greatest TBP defects in *sth1AA* cell for comparison (Figure 5.5). At the top 10% of Pol II-occupied genes, TBP was reduced when Sth1 was depleted, whereas Pol II increased when Sth1 was depleted, especially in the CDSs of these genes (Figure 5.5, lefthand panel, compare solid traces to dotted traces). In contrast, the 10% of genes showing the greatest TBP defects upon Sth1 depletion displayed reduced TBP and Pol II occupancies throughout the metagene (compare solid and dotted traces in the righthand panel). Genome browser snapshots of several of these genes from Decile 1 reveal increases in Pol II throughout the gene when Sth1 is depleted (Figures 5.6 and 5.7, compare light green to respective dark green

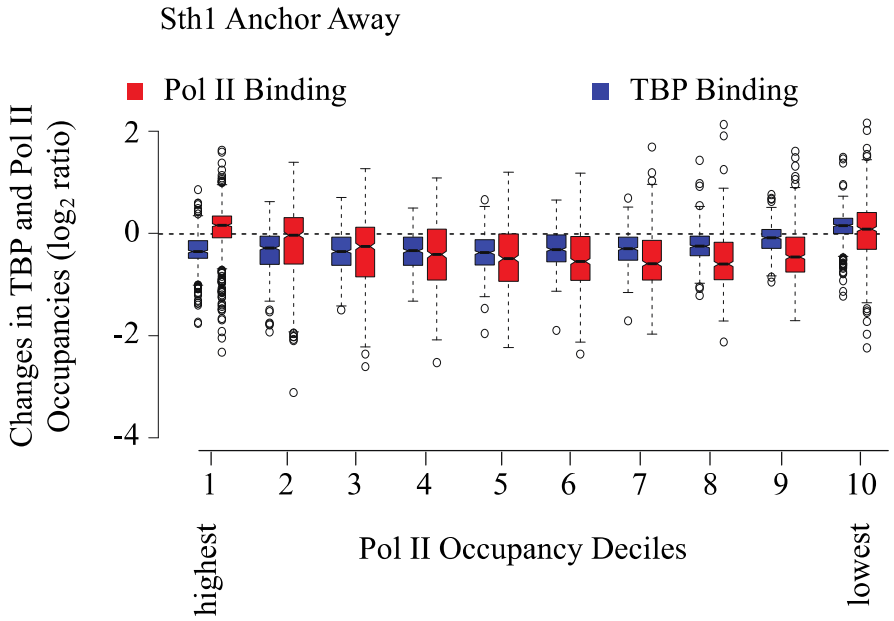

Figure 5.3. Pol II and TBP levels at all but high and low transcribed genes are reduced when Sth1 is depleted. Boxplot depicting the changes in TBP and Pol II Occupancies in Sth1 anchor-away cells (+ Rapa) compared to WT cells (- Rapa) in genes categorized into deciles. Decile 1 contains the genes with the highest Pol II occupancies in WT CDSs, whereas Decile 10 contains genes with the lowest Pol II occupancies. Rapa, rapamycin; CDSs, coding sequences. Data was obtained from (Kubik et al., 2018).

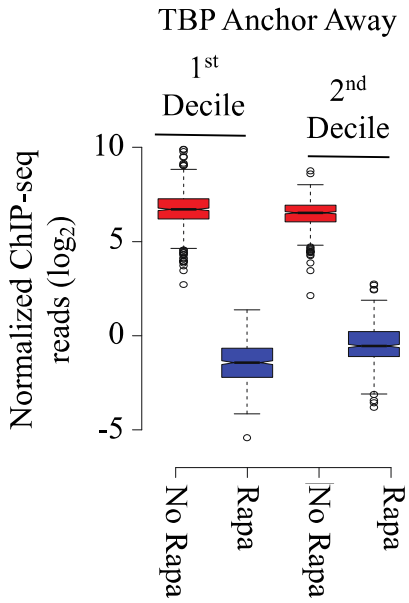

Figure 5.4. Pol II decreases at highly transcribed genes when TBP is depleted. Boxplot showing the Pol II occupancies for the top 2 deciles of Pol II-occupied genes in WT (No Rapa) and TBP-depleted (Rapa) cells. Data was obtained from (Petrenko et al., 2019), where TBP was depleted via anchor away.

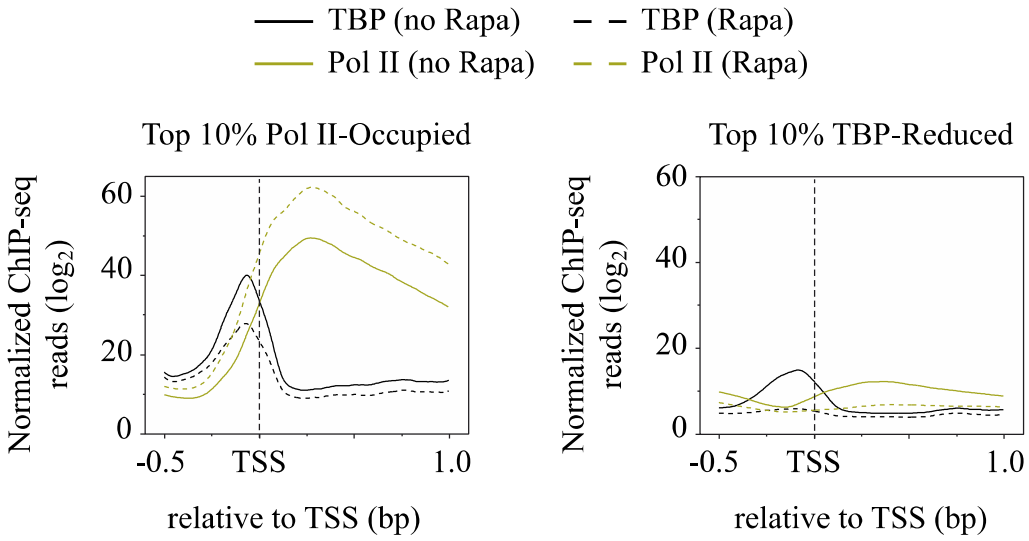

Figure 5.5. Pol II increases in the CDSs of the top 10% Pol II-Occupied genes when Sth1 is depleted. Metagene profiles depicting TBP and Pol II occupancies for the top 10% of Pol II-Occupied genes (Decile 1, lefthand panel) and the top 10% of genes showing the highest reductions in TBP (righthand panel) in untreated (WT, no Rapa) cells and Rapa-treated (*sth1AA,* Rapa) Sth1 anchor-away cells. The vertical dotted line represents TSS. Data from (Kubik et al., 2018).

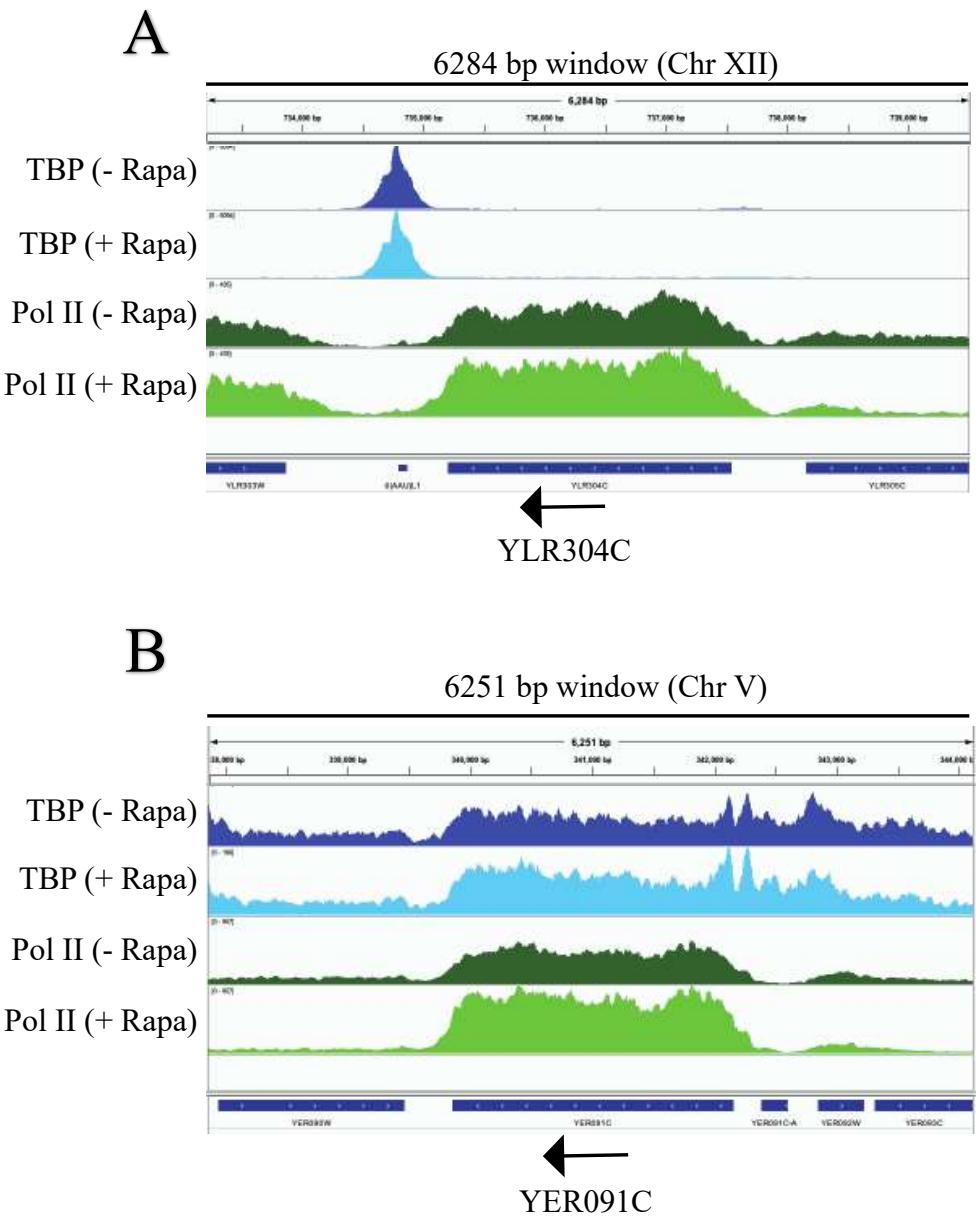

Figure 5.6. Pol II Occupancies are increased in metabolic genes upon Sth1 depletion. (A-B) Genome browser snapshots showing TBP and Pol II ChIP-seq occupancies of YLR304C (involved in the citric acid cycle) and YER091C (involved in methionine biosynthesis) before (-Rapa) and after (+Rapa) Sth1 anchor away. These genes show increases in Pol II after Sth1 depletion. Arrows denote the 5'→ 3' direction of the gene. Data from (Kubik et al, 2018).

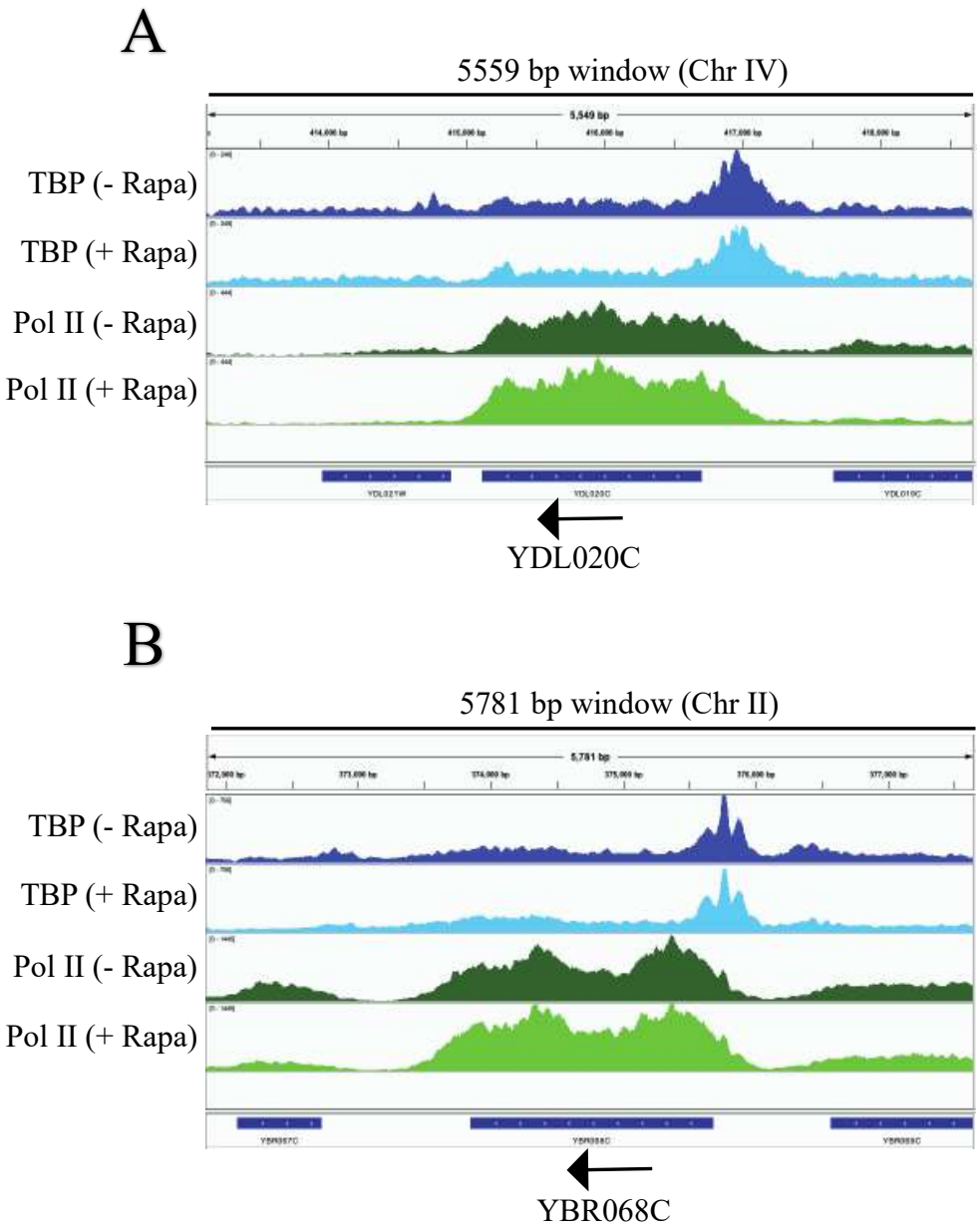

Figure 5.7. Pol II Occupancies are increased in genes involved in transcription and nutrient uptake upon Sth1 anchor away. (A-B) Genome browser snapshots showing TBP and Pol II ChIP-seq occupancies of YDL020C (transcription factor) and YBR068C (involved in amino acid uptake) before (-Rapa) and after (+Rapa) Sth1 anchor away. These genes show increases in Pol II after Sth1 depletion. Arrows denote the 5'→ 3' direction of the gene. Data from (Kubik et al, 2018).

tracks), following the Pol II trend observed in the metagene profile (Figure 5.5, lefthand panel). Thus, it appears that genes that harbor high levels of Pol II in their CDSs respond differently to RSC depletion than the majority of genes in that they are less responsive to the presumed initiation defects (as indicated by the reduced TBP binding) at their promoters.

It is possible that a subset of genes within the first two deciles may contribute to the discrepancy observed between TBP and Pol II levels when Sth1 is depleted. Previous studies have shown that the nucleosome occupancies in RPGs, which are present in Decile 1, were largely unaffected by Sth1 depletion (Kubik et al., 2018). Thus, the presence of RPGs in these deciles might account for the increases in Pol II observed in Deciles 1 and 2 upon Sth1 depletion. To address this concern, the genes within Deciles 1 and 2 were further divided into gene subsets based on whether Pol II increased or decreased upon Sth1 depletion and were analyzed based on Pol II and TBP occupancies (Figure 5.8). TBP was reduced for all gene subsets in Deciles 1 and 2, though the extent of reduction varied for each gene subset. For Decile 1, genes were also divided into RPGs and non-RPGs that displayed an increase in Pol II (lefthand panel in Figure 5.8). Pol II was reduced in 191 out of 570 genes in the first decile upon Sth1 depletion, accounting for 34% of the total genes in this decile. The majority of genes (66%), including 107 RPGs, showed increased Pol II upon Sth1 depletion. Increased Pol II was evident and even higher in the 296 non-RPGs that showed increased Pol II in Decile 1. While Decile 2 contained a higher proportion of genes where Pol II occupancies reduced upon Sth1 depletion, there was a subset that showed an increase in Pol II when Sth1 was depleted (227 out of 570 genes, 40%). Thus, while many genes in these deciles do show reduced

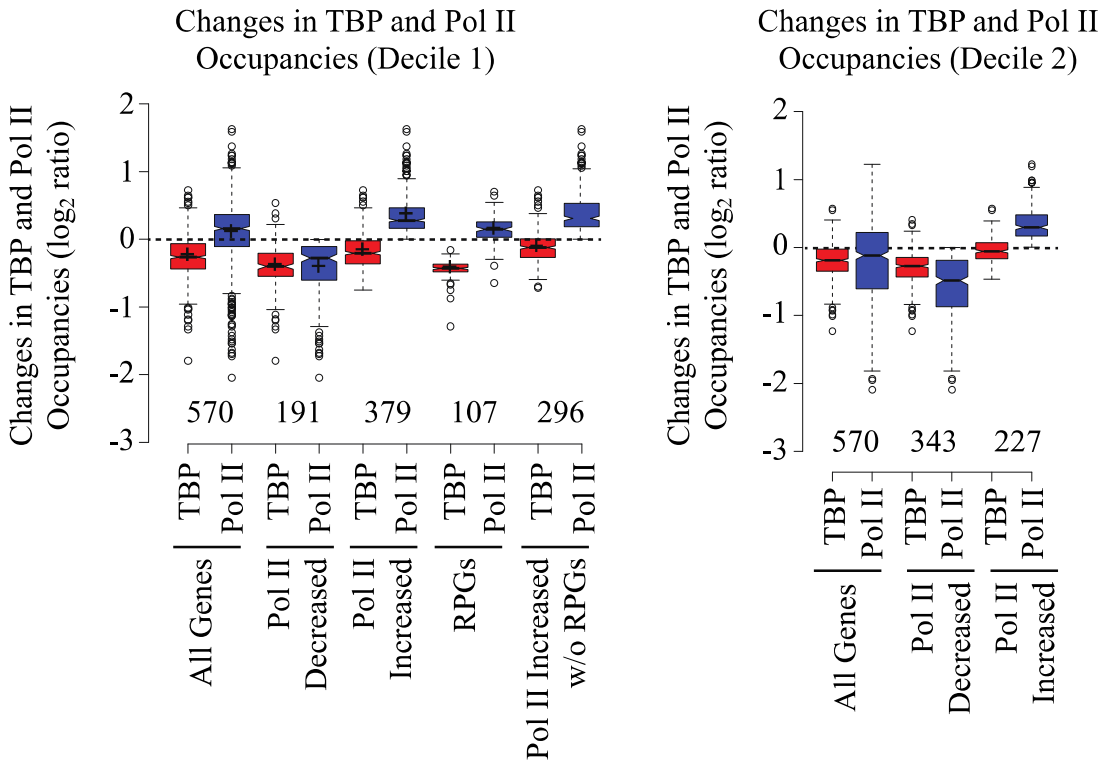

Figure 5.8. Nuclear depletion of RSC differentially affects Pol II occupancies at highly expressed genes. A-B) Boxplots depicting the changes in TBP and Pol II occupancies for deciles 1 (A) and 2 (B). Each of the figures shows all genes for that decile, as well as for the genes within that decile that show a reduction in Pol II (Pol II decreased) or an increase in Pol II occupancies (Pol II increased) upon Sth1 depletion are shown. For (A), RPGs and the Pol II increased genes excluding RPGs are also shown. The number of genes for each gene set is shown below each boxplot. Data from (Kubik et al., 2018).

Pol II occupancies, a substantial number of genes within these deciles show an increase in Pol II when Sth1 is depleted, despite a reduction in TBP. Given that nucleosomes within the CDSs of RPGs and other highly transcribed genes are less accessible upon Sth1 depletion (Figure 3.13) and that RSC is highly enriched in transcribed CDSs (Spain et al., 2014), it is possible that the reduced nucleosome accessibility may contribute to a decreased rate of Pol II elongation at these genes such that the dwell time for elongating Pol II is increased, leading to increased crosslinking and the subsequent enrichment of Pol II in the CDSs of these genes. As such, the increased Pol II may not indicate enhanced Pol II elongation but rather transcription elongation defects due to the loss of RSC and its remodeling activity.

5.2.3 RSC Catalytic Activity Promotes TBP Occupancies

While depletion of Sth1 using the anchor away strategy provides great insights as to how RSC impacts Pol II and TBP occupancies, there are several drawbacks to using this method. It is a concern that nuclear depletion may result in the loss of the entire RSC complex from the nucleus instead of only the Sth1 subunit, rendering it difficult to discern the effects of the absence of Sth1 from the absence of other subunits within the RSC complex. As such, it is difficult to identify the impact of Sth1 catalytic activity from the effects of other Sth1 subunits on transcription. Moreover, since transcription regulation involves multiple chromatin remodelers, other remodelers could compensate for the loss of Sth1 activity, which could mask or confound the direct effects of the loss of RSC catalytic activity. To gain further insight into the impact of RSC catalytic activity on transcription, Pol II and TBP ChIP-seq were performed in cells depleted of Sth1 (*Sth1-AID)* and in cells expressing a catalytic inactive copy of Sth1 (*STH1*^{K501R}, *sth1-KR*

henceforth) (Du et al., 1998). Since the *STH1*^{K501R} mutation is lethal, a modified version of protein depletion using an auxin-inducible degron (AID) was employed (Haruki et al., 2008; Munoz et al., 2019). In this strategy, the endogenous Sth1 protein is tagged with an auxin-inducible degron (*Sth1-AID*). In addition to the AID-tagged endogenous Sth1, the *sth1-KR* strain contains a copy of the *STH1*^{K501R} gene integrated into the *TRP1* locus. When *Sth1-AID* and *sth1-KR* cells are treated with the plant hormone auxin (3-IAA), the endogenous copy of Sth1 is degraded by the 26S proteasome, leaving cells that are either depleted of Sth1 or cells only expressing a catalytic inactive copy of Sth1, respectively. Untreated and auxin-treated *Sth1-AID* cells and *sth1-KR* cells were subjected to TBP and Pol II ChIP-seq. We then compared the effects of catalytic inactive RSC to the effects observed upon Sth1 depletion on transcription.

To examine the effects of RSC activity on TBP occupancies at highly transcribed genes, heatmaps were generated showing the TBP occupancies at the top 25% of Pol II-occupied genes (Q1 genes) before (Aux -) and after (Aux +) endogenous Sth1 depletion in *Sth1-AID* (Figure 5.9A) and *sth1-KR* (Figure 5.9B). TBP was slightly reduced in Sth1-AID after Sth1 depletion compared to untreated cells (Figure 5.9A, compare red/yellow hues of the two heatmaps), indicating that Sth1 is important for the efficient recruitment of TBP to promoters. TBP occupancies were also reduced in cells expressing only catalytic dead Sth1 after endogenous Sth1 was depleted (Figure 5.9B, compare red/yellow hues of the two heatmaps), supporting the idea that RSC catalytic activity is important for TBP recruitment to promoters. Interestingly, the reduction in TBP was greater in *sth1-KR* upon auxin treatment (expresses only catalytic inactive RSC) than in *Sth1-AID* upon auxin treatment (cells deficient of Sth1 subunit), even though both strains

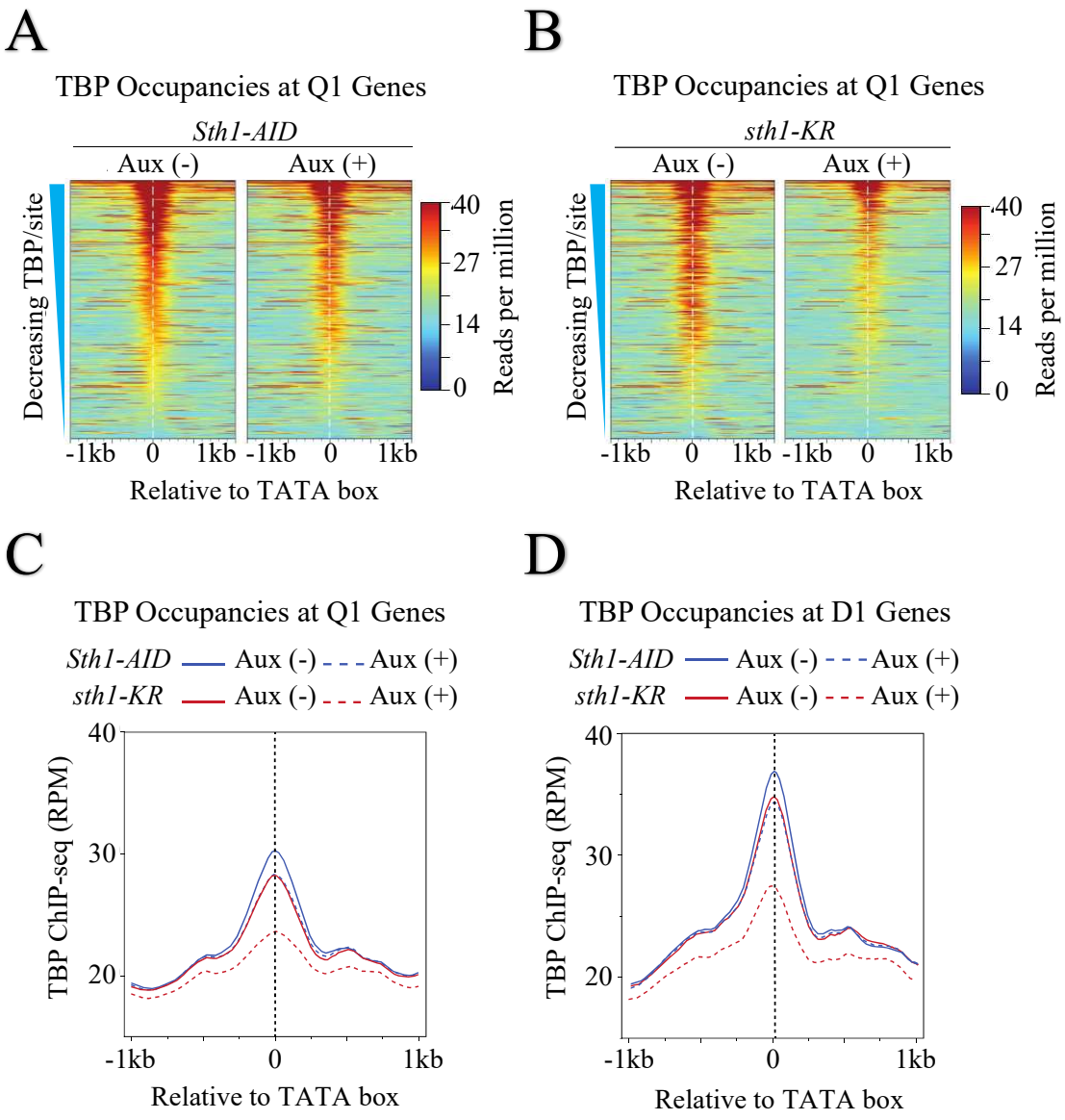

Figure 5.9. Loss of RSC activity results in reduced TBP binding. A-B) Heatmaps showing TBP occupancies before and after treatment with auxin (Aux) in *Sth1-AID* (A) and *sth1-KR* (B) cells treatment at the top 25% of Pol II-occupied genes (Q1). Genes are sorted by decreasing TBP levels at each gene's TATA-like sequence. C-D) Metagene profiles depicting TBP occupancies for *Sth1-AID* and *sth1-KR* cells before and after auxin treatment at Q1 genes (C) and at the top 10% of Pol II-occupied genes (D1, D). Heatmaps and profiles are centered at the TATA-box or TATA-like elements.

should be deficient for Sth1 activity after depletion and show similar TBP reductions. This pattern in TBP reduction was also observed in the metagene profiles showing TBP occupancies for untreated and auxin-treated *Sth1-AID* and *sth1-KR* cells at Q1 genes (Figure 5.9C, compare solid traces to dotted traces), as well as for the top 10% Pol II-occupied genes (D1 genes, Figure 5.9D). One possibility for the discrepancy between Sth1-depleted cells and cells only expressing catalytic inactive Sth1 is that the depletion of endogenous Sth1 might be incomplete in both cell types. After auxin treatment, the residual Sth1 in Sth1-AID cells might be sufficient to recruit most of the TBP to its target genes, resulting in a modest TBP reduction. In contrast, the remaining Sth1 present in *sth1-KR* after auxin treatment would have to compete with catalytic dead Sth1 copies also present within the mutant, dampening the effects seen of the remaining functional Sth1 copies and resulting in a greater TBP reduction. Nevertheless, the reductions in TBP are consistent with the TBP reductions observed upon Sth1 anchor away (Figures 5.3 and 5.8). These TBP reductions in cells with deficient RSC function are consistent with the idea that RSC evicts nucleosomes from promoters and positions the +1 nucleosome to expose TATA boxes and TSSs to the transcriptional machinery, facilitating transcription initiation (Hartley and Madhani, 2009; Klein-Brill et al., 2019; Kubik et al., 2018; Rawal et al., 2018).

5.2.4 Pol II Accumulated in the CDSs of Transcribed Genes in Cells Expressing Catalytic Inactive RSC

Considering that TBP occupancies were reduced in cells expressing only catalytic inactive RSC, Pol II ChIP-seq was performed in *Sth1-AID* and *sth1-KR* cells before and after auxin treatment. Since defects in Pol II occupancies within CDSs should be

representative of transcription initiation, elongation, and termination defects, comparing the Pol II occupancies in Sth1-depleted cells to cells expressing catalytic-inactive RSC would provide further insights into how RSC activity impacts transcription at multiple steps. Upon depletion of endogenous Sth1, Pol II occupancies were significantly reduced in CDSs in *Sth1-AID*, whereas Pol II levels were significantly elevated in *sth1-KR*, especially at highly transcribed genes (Figures 5.10A and 5.10B). To better visualize these changes in Pol II at highly transcribed genes, the Pol II metagene profiles were generated depicting Pol II occupancies at Q1 genes, D1 genes, and RPGs in untreated and auxin-treated *Sth1-AID* cells (Figure 5.11A) and in *sth1-KR* cells (Figure 5.11B). Similar to that observed in the boxplots, Pol II occupancies were reduced within transcribed CDSs in cells depleted of Sth1 (Figure 5.11A, compare solid traces to dotted traces after TSS). In contrast, Pol II accumulated in transcribed CDSs in cells expressing only catalytic inactive Sth1 (Figure 5.11B, compare solid to dashed traces). This is surprising, given that cells depleted of Sth1 and cells containing catalytic inactive RSC are both deficient in RSC function and should yield similar changes in Pol II occupancies. It is important to note that Sth1 contains domains such as the SnAC domain that interact with histones (Sen et al., 2013; Wagner et al., 2020) and that structural data has shown that Sth1 contacts histone tails (Wagner et al., 2020), which may enhance RSC-nucleosome interactions (Chapter 4). It is possible that cells depleted of Sth1 might harbor RSC complexes that lack Sth1 and can bind to nucleosomes less efficiently than complete RSC complexes. In contrast, cells containing catalytic inactive Sth1 would harbor RSC complexes that would still be able to interact with nucleosomes efficiently but would be unable to remodel them. As such, in auxin-treated *sth1-KR*, the catalytic inactive RSC

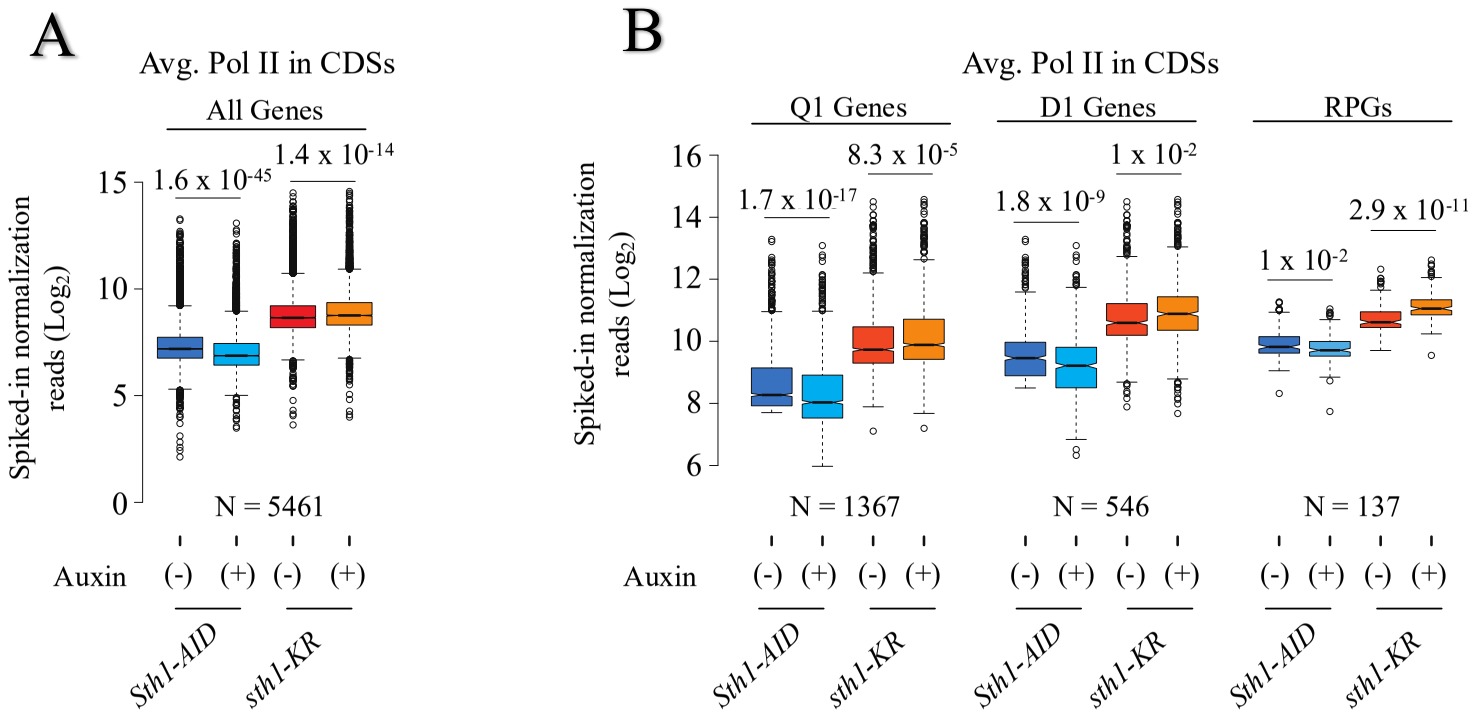

Figure 5.10. Depletion of endogenous Sth1 leads to Pol II defects in *Sth1-AID* and *sth1-KR*. A-B) Boxplots showing Pol II occupancies in CDSs for all genes (A), as well as for Q1 genes, D1 genes, and RPGs (B) for the indicated untreated and auxin-treated strains. The significance between the untreated and treated cells for each strain is shown above the boxplots and was determined using the Welch t-test. Reads were normalized using spiked-in reads from *S. pombe*.

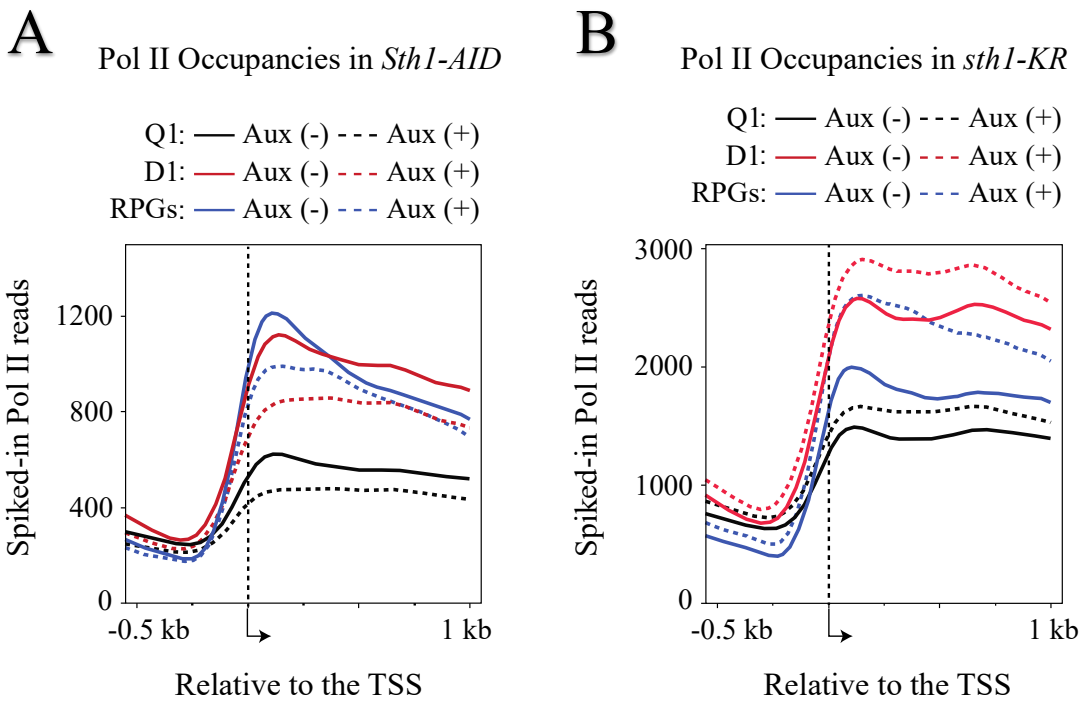

Figure 5.11. Depletion of endogenous Sth1 lead to reduced Pol II in the CDSs of highly-transcribed genes in *Sth1-AID,* and increased Pol II in *sth1-KR*. A-B) Metagene profiles showing Pol II occupancies in untreated and auxin-treated *Sth1-AID* cells (A) and in *sth1-KR* cells (B) at Q1 genes, D1 genes, and RPGs. Pol II reads were normalized using spiked-in reads from *S. pombe*.

could be binding to and getting stuck on nucleosomes since it is unable to remodel them. The non-remodeled nucleosomes could then hinder the elongation of Pol II through DNA, resulting in the accumulation of Pol II in CDSs upon endogenous Sth1 depletion and masking the true reduction in Pol II in these cells. In contrast, RSC binding might be reduced in the *Sth1-AID* cells upon Sth1 depletion, allowing other remodelers to interact with those nucleosomes and compensate for the loss of RSC function, facilitating the traversal of the recruited Pol II through CDSs. In this scenario, both the reduction of Pol II in *Sth1-AID* and the accumulation of Pol II in *sth1-KR* would be indicative of Pol II elongation defects, supporting the idea proposed in previous studies that RSC activity is important for transcription elongation (Ganguli et al., 2014; Spain et al., 2014).

The accumulation of Pol II observed in cells expressing catalytic dead RSC is consistent with the accumulation seen at transcribed CDSs of the Sth1 anchor away data (Figures 5.3 and 5.8. However, Pol II occupancies were reduced in *Sth1-AID* after Sth1 depletion (Figure 5.10), whereas Pol II was increased only at highly transcribed genes in Sth1 anchor-away cells (Figures 5.3 and 5.8). The study from which the Sth1 anchor away data did not use an *S. pombe* spike-in control (Kubik et al., 2018), so the data was normalized to the total reads, which cannot detect genome-wide changes. This issue is mitigated by spiked-in normalization, which reflects absolute changes vs. only relative changes inferred from read-normalization. Thus, the increases in Pol II observed upon Sth1 anchor away might not represent the absolute changes in Pol II levels when Sth1 was depleted. It is possible that reductions might have been observed upon Sth1 anchor away had an *S. pombe* spike-in control been used. Nevertheless, Pol II was reduced at the majority of genes upon Sth1 anchor away (Figure 5.3), consistent with the Pol II

reductions observed genome-wide in auxin-treated *Sth1-AID* cells (Figures 5.10 and 5.11A). Taken together, the data suggest that RSC activity is important for Pol II recruitment and elongation, implicating RSC activity in facilitating transcription at multiple steps.

5.3 HATs Gcn5 and Esa1 Promote Pol II Occupancies

Given that RSC was recruited to transcribed CDSs in a HAT-dependent manner (Spain et al., 2014) and that the loss of Esa1 or Gcn5 results in increased RSC and histone occupancies at promoters, it is possible that these increases might affect transcription. To determine the impact of the coordination between RSC and HATs on transcription, Rpb3 (Pol II) ChIP-seq was performed in WT cells, HS-WT cells, and in the *sth1ΔBrD, gcn5Δ, esa1,* and *gcn5Δ/esa1* mutants. Since Pol II occupancies increased when RSC was depleted at some highly transcribed genes but not at other genes (Figure 5.3), and since cells expressing catalytic inactive RSC showed increased Pol II occupancies at highly transcribed genes (Figures 5.10B and 5.11B), the Pol II ChIP-seq data for WT and the mutants were divided into deciles of genes based on WT Pol II occupancies (D1 genes have highest WT Pol II occupancies, D10 genes have the lowest) and analyzed (Figures 5.12 and 5.13). The *sth1ΔBrD* mutant showed modest changes in Pol II occupancies except for a small reduction in Pol II observed in Decile 2 (Figure 5.12, D2). The lower transcribed genes (D6-D10) showed Pol II increases compared to WT cells for the BrD mutant. In contrast, significant reductions compared to WT cells could be observed for *gcn5Δ* in the top transcribed genes (Figure 5.12, D1-D3). The greatest reduction was observed for the D1 genes (Top 10% Pol II-occupied genes). Since the top 10% Pol II-occupied genes also showed increased histone H3 occupancies within

NDRs and at the +1 nucleosome position in the *gcn5Δ* mutant (Figure 4.12), it could be that the reduction in transcription may be due to increased histone occupancies at these genes. Similar to the Sth1 bromodomain mutant, the *gcn5Δ* mutant showed increased Pol II occupancies at lower transcribed genes (D5-D10) (Figure 5.12). Since Gcn5 promotes RSC recruitment to the CDSs of transcribed genes (Figures 4.23 – 4.25), the increase in Pol II occupancies at these genes might indicate an elongation defect due to inefficient chromatin remodeling in CDSs. Nevertheless, Pol II occupancies were reduced at highly expressed genes in the *gcn5Δ* mutant, consistent with earlier studies showing that Gcn5 promotes transcription (Baptista et al., 2017; Qiu et al., 2016).

In contrast to cells lacking Gcn5, the median Pol II occupancies of D1 genes decreased slightly in the *esa1* mutant (Figure 5.13). However, Pol II occupancies were substantially reduced in deciles D2-D9, suggesting that Esa1 is important for transcription at the majority of genes. Furthermore, *gcn5Δ/esa1* showed Pol II reductions in D1-D9 that were greater than those observed for *esa1*. The exception for both mutants was the lowest transcribed genes (D10), which showed little/no change in Pol II occupancies for *esa1* and an increase in Pol II in the HAT double mutant. These results show that HATs Gcn5 and Esa1 are important for robust transcription of all genes, where Gcn5 might play a larger role in the transcription of highly-transcribed genes. It is possible that Gcn5 suppresses Pol II occupancy defects in the *esa1* mutant, since the *gcn5Δ/esa1* double mutant showed a more substantial reduction at D1 genes than either of the single mutants.

To determine where Pol II was reduced in highly transcribed genes, heatmaps were generated showing the changes in Pol II occupancies compared to WT or HS-WT

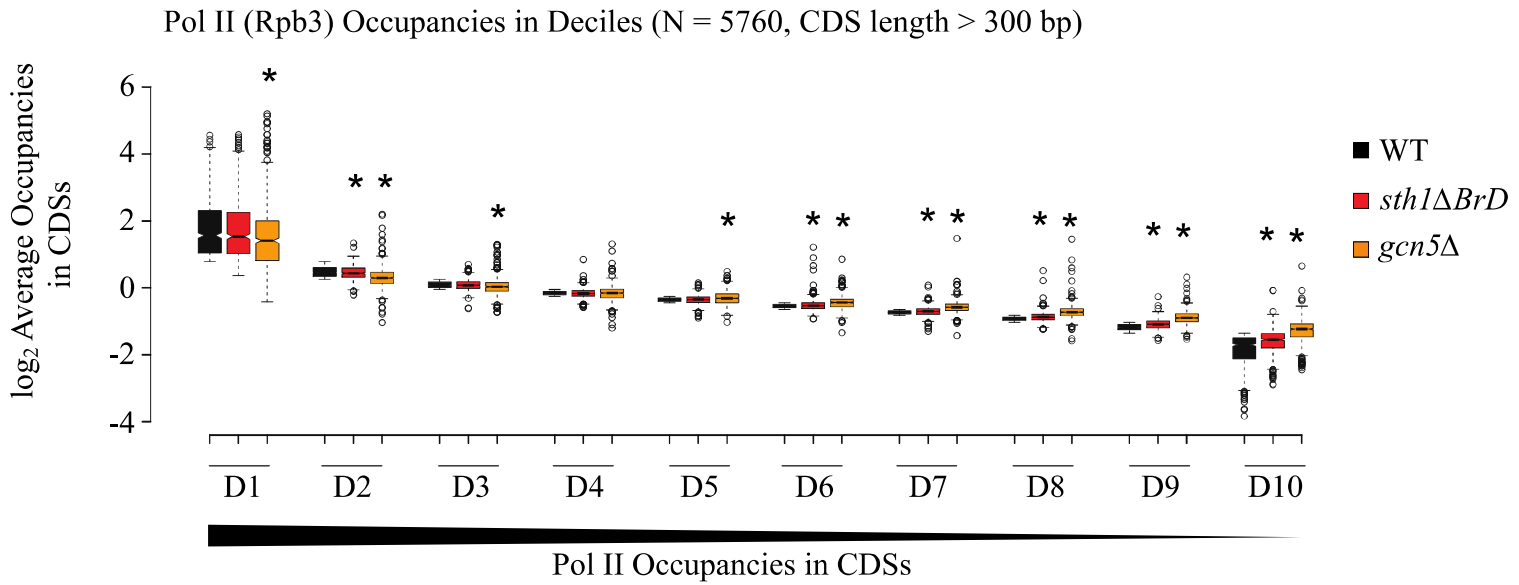

Figure 5.12. Pol II is reduced at highly transcribed genes in cells lacking Gcn5. Boxplot showing the average Pol II occupancies in WT cells and in the *sth1ΔBrD* and *gcn5Δ* mutants. Genes were sorted based on average Pol II occupancies in CDSs and separated into deciles (D, N = 576 per decile) such that the highest Pol II-occupied genes were in D1 and the lowest in D10. Asterixis indicate significant changes in the mutant relative to WT cells. Changes were deemed significant if their p-values were less than 0.05, and were determined by the Welch student t-test.

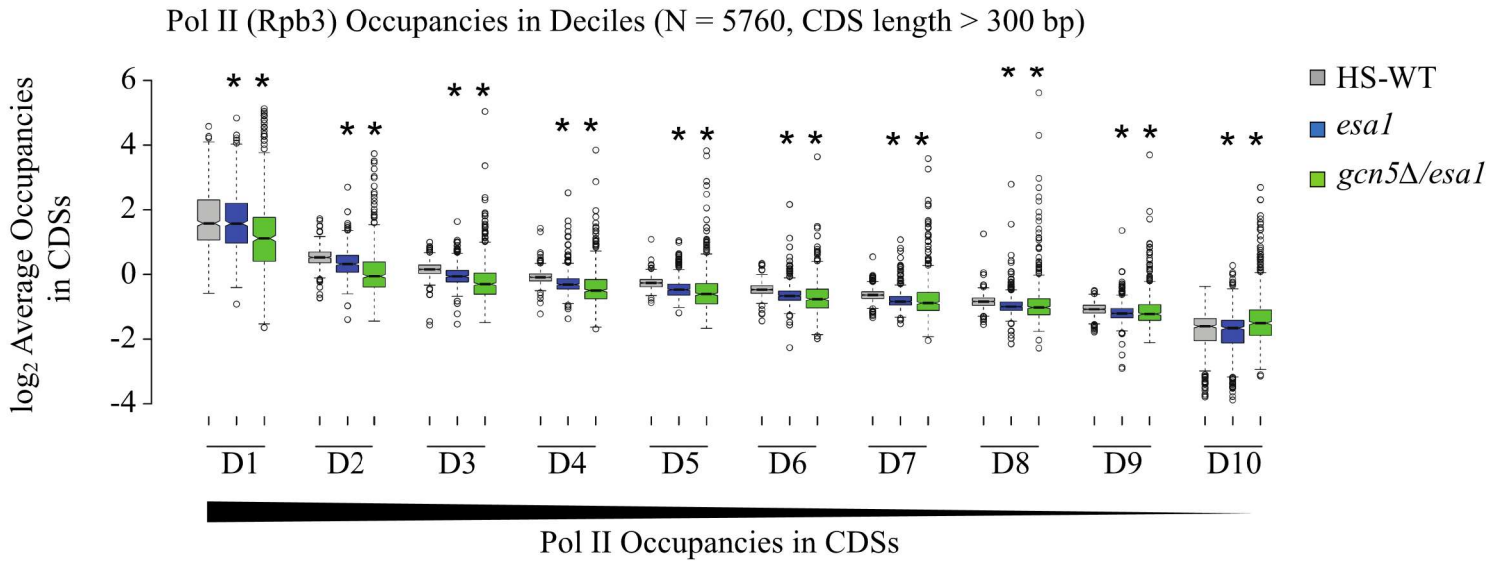

Figure 5.13. Pol II is reduced at the majority of genes in cells lacking either Esa1 or both HATs. Boxplot showing the average Pol II occupancies in HS-WT cells and in the *esa1* and *gcn5Δ/esa1* mutants. Genes were sorted based on average Pol II occupancies in CDSs and separated into deciles (D, N = 576 per decile) such that the highest Pol II-occupied genes were in D1 and the lowest in D10. Asterixis indicate significant changes in the mutant relative to WT cells. Changes were deemed significant if their p-values were less than 0.05 and were determined by the Welch student t-test.

cells (ΔRpb3) in the top 20% of Pol II (Deciles D1 and D2) of the HAT mutants (Figure 5.14). In cells lacking Gcn5, the greatest reduction in Pol II was observed at the TSS (Figure 5.14A, see blue hues around the TSS of the right heatmap), likely representing an initiation defect (Baptista et al., 2017). However, the genes also show an increase in Pol II farther downstream of the TSS, within their CDSs (note red hues at the very top of the right heatmap). This pattern of Pol II occupancies was also observed in *esa1,* though to a lesser extent (Figure 5.14B, compare blue hues near the TSS of the middle panel to light yellows farther downstream). These findings are similar to the Pol II accumulation observed in the CDSs of highly transcribed genes when Sth1 was depleted (Figures 5.5 - 5.8), indicating that the elongation rate of any residual Pol II that was able to begin transcription at these genes w slower in the HAT mutants compared to WT cells. The HAT double mutant showed the greatest reductions not only at the TSS but throughout the CDSs (Figure 5.14B, righthand panel), indicating that both HATs are important for Pol II transcription.

When Sth1 was depleted in Sth1 anchor away and cells expressing catalytic inactive Sth1, there was an increase in Pol II at RPGs despite a reduction in TBP occupancies at these same genes (Figures 5.8, 5.9, 5.10B, and 5.11B). Given that *gcn5Δ* and *esa1* also displayed RSC accumulations in the CDSs of highly transcribed genes (Figure 5.14), RPGs might also show increased Pol II in the HAT mutants. To compare the Pol II occupancies at RPGs in the HAT mutants with WT cells, boxplots were generated showing Pol II occupancies in the CDSs of RPGs for WT cells, HS-WT cells, *sth1ΔBrD, gcn5Δ, esa1,* and *gcn5Δ/esa1* (Figure 5.15). While *sth1ΔBrD* showed little/no change compared to WT cells, *gcn5Δ* and *esa1* displayed reductions in Pol II at RPGs.

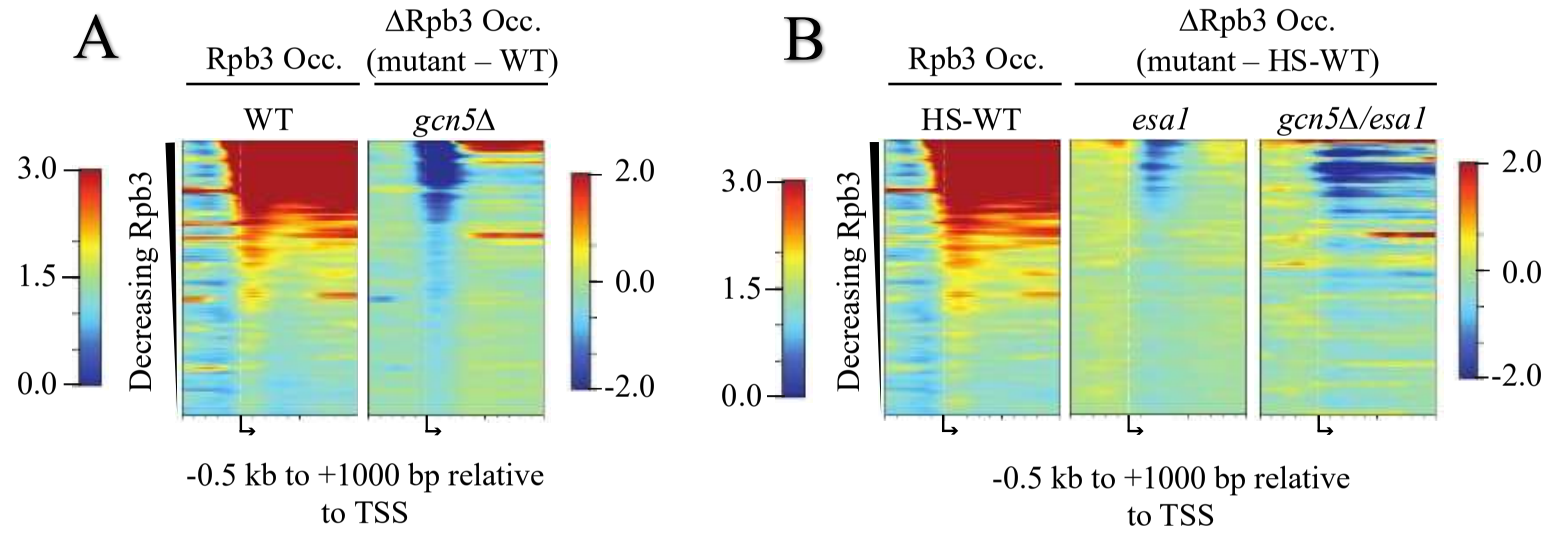

Figure 5.14. The HAT mutants display defects in Pol II occupancies. A-B) Heatmaps showing Rpb3 occupancies (Rpb3) and changes in Rpb3 occupancies compared to WT or HS-WT cells (ΔRpb3)at the top 20% of Pol II-occupied genes (D1 + D2, excluding RPGs) of *gcn5Δ, esa1*, and *gcn5Δ/esa1*. Genes were sorted by decreasing Pol II occupancies in WT cells. The scales for Rpb3 occupancies are shown on the lefthand side of the heatmaps and the scales for ΔRpb3 are on the righthand side. The transcription start site (TSS) is indicated by the vertical dotted white line on the heatmaps.

The HAT double mutant showed significantly greater Pol II reductions than either of the single mutants, displaying additive effects similar to those observed in the heatmaps of highly transcribed non-RPGs (Figures 5.14 and 5.15). Collectively, the data suggest that HATs are important for Pol II occupancies at highly transcribed genes, including RPGs.

5.4 Gcn5 and Esa1 Promote TBP Occupancies

Since H3 occupancies increased at promoters in the HAT mutants, specifically at the +1 nucleosome position (Figure 4.12), the HAT mutants might also show defects in TBP binding, as its recognition site is often occluded by the +1 nucleosome (Kubik et al., 2018). To determine the impacts of the HAT mutants on TBP binding, TBP ChIP-seq was performed using sonicated chromatin from WT cells, *gcn5Δ, esa1,* and *gcn5Δ/esa1*. Since the TBP data were similar between the HAT mutants, the heatmaps depicting RSC occupancies in WT cells and the changes in RSC occupancies compared to WT cells for the *gcn5Δ/esa1* mutant were shown (Figure 5.16). TBP occupancies were higher at RPGs than at Pol II-T20 (Top 20% of Pol II-occupied genes) genes in WT cells. However, TBP was substantially reduced in the HAT double mutant compared to WT cells, with a greater reduction observed at RPGs. This reduction in TBP is consistent with the increase in H3 occupancies observed in the NDRs of highly transcribed genes in the HAT mutants, implicating roles for Gcn5 and Esa1 in proper PIC assembly.

5.5 Discussion

5.5.1 RSC Plays a Role in Both Transcription Initiation and Elongation

Overall, the data suggest that RSC, in coordination with HATs Gcn5 and Esa1, regulates transcription. Cells depleted of RSC, as well as cells expressing catalytic inactive RSC, showed reduced TBP in all but the lowly transcribed genes (Figures 5.3,

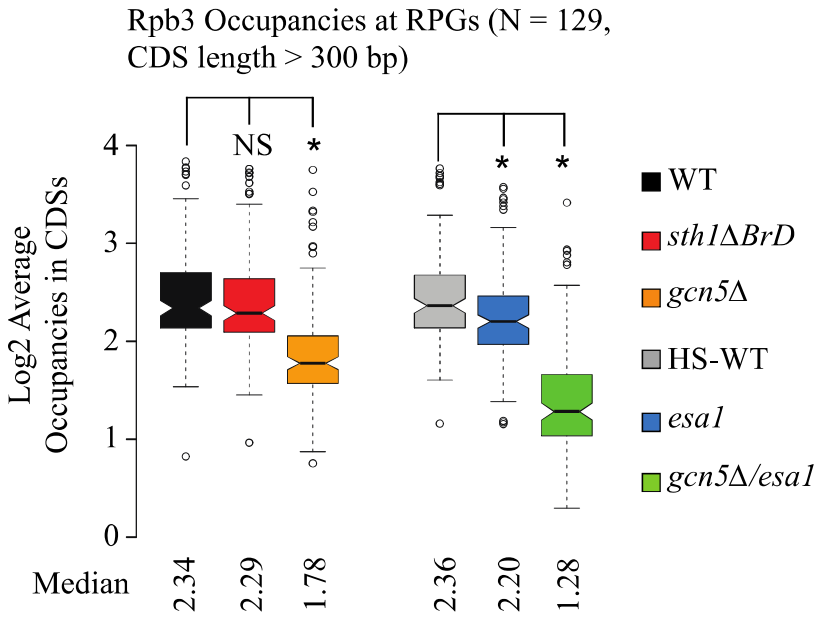

Figure 5.15. Pol II occupancies are reduced at RPGs in the HAT mutants. Boxplot depicting average Pol II (Rpb3) occupancies (Log2) at RPGs in WT cells, HS-WT cells, and in the *sth1ΔBrD, gcn5Δ, esa1,* and *gcn5Δ/esa1* mutants. Differences in the medians between the mutants and WT cells (HS-WT cells for *esa1*-containing mutants) were denoted as significant (*) or non-significant (NS), based on the p-values of those differences. P-values were calculated using the Welch t-test, and those < 0.05 were considered significant.

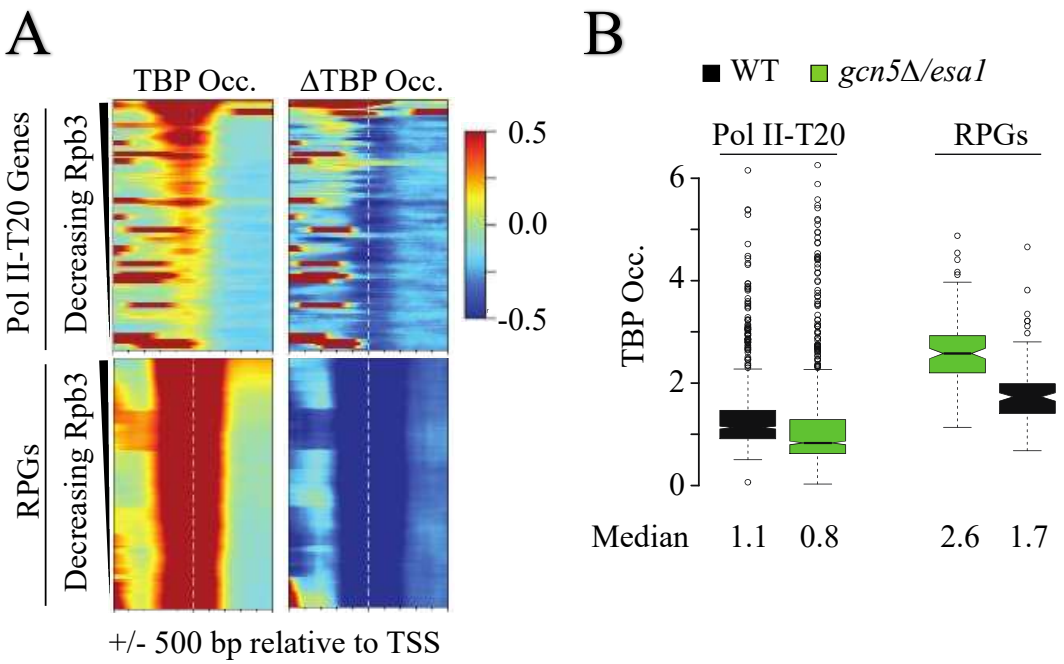

Figure 5.16. RSC recruitment to transcribed CDSs depends on H3 and H4 tails. A) Heatmaps showing TBP occupancies (TBP Occ., lefthand panels) and the changes in TBP occupancies compared to WT cells (ΔTBP Occ., righthand panels) at RPGs and the top 20% of Pol II-Occupied genes excluding RPGs (Pol II-T20) for WT cells and *gcn5Δ/esa1*. B) Boxplots showing TBP occupancies at RPGs and Pol II-T20 genes in WT cells and in the HAT double mutant.

5.8, and 5.9). Since RSC has been shown to position the -1 and +1 nucleosomes to maintain NDRs and the +1 nucleosome has been shown to occlude the binding site for TBP (Klein-Brill et al., 2019; Krietenstein et al., 2016; Kubik et al., 2018; Rawal et al., 2018), it makes sense that cells deficient in RSC or RSC activity would also exhibit TBP defects. As TBP is regarded as an indicator for PIC assembly, the results implicate RSC in facilitating PIC assembly, consistent with other studies (Klein-Brill et al., 2019; Krietenstein et al., 2016; Kubik et al., 2018; Rawal et al., 2018). In addition to PIC assembly defects, these studies also observed reduced TSS selection within RSC-depleted cells. Taken together, these findings support a role for RSC in facilitating transcription initiation.

RSC is recruited to CDSs of transcribed genes (Rawal et al., 2018; Spain et al., 2014) and potentially makes nucleosomes more accessible (Figures 3.4, 3.5, 3.9, and 3.10). Since Pol II is also associated with accessible nucleosomes in transcribed CDSs (Figure 3.12), it is extremely difficult to separate the distinct effects of RSC and Pol II on nucleosome structure. However, the analyses within this project also point towards a potential role for RSC in genic nucleosome accessibility and transcription. Depletion of RSC elicited reduced Pol II occupancies in all but the lowest and highest transcribed genes, consistent with previous findings that RSC depletion results in lower TBP and Pol II occupancies (Petrenko et al., 2019) (Figures 5.3, 5.10, and 5.11A). However, Pol II levels increased in some of the highly transcribed genes for Sth1 anchor away cells, including at RPGs (Figures 5.3 and 5.8), despite a concurrent reduction of TBP at these genes. Furthermore, cells expressing catalytic inactive RSC also showed Pol II accumulations in the CDSs of genes, including highly transcribed genes (Figures 5.10

and 5.11A). Considering that TBP is indicative of PIC assembly defects and that the PIC recruits Pol II for transcription, Pol II occupancies should decrease in these genes, not increase. One explanation for the Pol II increase in cells expressing catalytic inactive RSC could be that, in the absence of RSC-mediated remodeling of nucleosomes within CDSs, elongating Pol II could have a difficult time traversing through the less accessible chromatin, thereby increasing the dwell time of Pol II and leading to increased Pol II ChIP enrichment. For Sth1-depleted cells, other remodelers could compensate for the loss of RSC recruitment and remodeling to nucleosomes, mitigating the Pol II accumulation observed when only RSC catalytic activity was lost. However, in both cases, Pol II recruitment would be reduced due to the loss of Sth1 functions. One way to test this idea would be to compare the Pol II occupancies from ChIP-seq to nascent RNA levels in RSC-depleted cells and cells expressing catalytic inactive RSC. A reduction in nascent transcripts upon endogenous Sth1 depletion in *Sth1-AID* and in *sth1-KR* would provide stronger support for the role of RSC in promoting transcription elongation.

Considering that RSC is present in both promoters and in CDSs (Kubik et al., 2019; Rawal et al., 2018; Spain et al., 2014), the data suggest that, in addition to regulating PIC assembly and transcription initiation, RSC may also remodel nucleosomes in CDSs to promote Pol II elongation. The idea that RSC also promotes elongation is supported by in vitro experiments showing that RSC-remodeled nucleosomes promote transcription elongation in an acetylation-dependent manner (Carey et al., 2006).

5.5.2 Histone Acetyltransferases Gcn5 and Esa1 Promote Transcription

Analyses of Pol II occupancies in cells lacking Gcn5 or functional Esa1 reveal that HATs have a differential effect on Pol II levels. Cells lacking Gcn5 showed

reductions of Pol II at highly transcribed genes, whereas the *esa1* mutant showed Pol II reductions at the majority of genes, excluding the top and bottom 10% of Pol II-occupied genes (Figures 5.12 and 5.13). This suggests that Esa1 is more broadly required for Pol II occupancies than the H3 HAT, consistent with previous studies (Baptista et al., 2017; Bruzzone et al., 2018; Donczew et al., 2020). The HAT double mutant showed the greatest reduction of Pol II occupancies, where Pol II was substantially reduced at all but the lowest transcribed genes (Figure 5.13). The findings that the HAT double mutant elicited a greater effect than the single mutants at the highly transcribed genes (D1 genes) suggests that Gcn5 might be able to compensate for the loss of Esa1 at some genes but not at others. Additionally, the HAT double mutant revealed a role for Gcn5 at genes other than the highly expressed genes since the double mutant exhibited greater Pol II reductions than those seen in *esa1* for the majority of genes. Considering that both HATs are important for RSC enrichment in transcribed CDSs (Spain et al., 2014), Pol II might migrate slower in the HAT mutants due to reduced RSC remodeling of nucleosomes in CDSs, resulting in the dampening of the actual transcription defects in the HAT mutants. The double mutant also showed a substantial reduction in TBP occupancies for RPGs and for the top 20% of transcribed genes excluding RPGs (Figure 5.16), suggesting that increased histone occupancies observed in the NDRs of the HAT mutants might interfere with TBP binding and possibly PIC formation.

Overall, the data suggest that RSC is important for proper PIC assembly and transcription initiation and that RSC plays a role in transcription elongation. Due to the similarities in TBP and Pol II occupancies between the HAT mutants and RSC-depleted cells, there is strong support that RSC and HATs coordinate with each other to regulate

chromatin structure and transcription. As such, the model introduced in Figure 4.30 can be further refined to show that RSC is recruited to NDRs via hypoacetylated histone tails, and the subsequent acetylation by Gcn5 and/or Esa1 leads to efficient histone eviction from NDRs. This histone eviction then allows TBP to bind and for PIC assembly to occur, promoting transcription initiation. However, in cells lacking these HATs, RSC is still recruited to NDRs by mechanisms other than histone acetylation (Badis et al., 2008; Cairns et al., 1999; Ferreira et al., 2011; Kubik et al., 2018; Soutourina et al., 2006; Wagner et al., 2020), but histone eviction is reduced, leading to reduced TBP and Pol II recruitment, and ultimately dampened transcription (Figure 5.17). Within transcribed CDSs, the data suggest that the lack of histone acetylation by HATs results in decreased RSC recruitment, which leads to reduced nucleosome accessibility and Pol II processivity, ultimately leading to the accumulation of Pol II in the CDSs further downstream of the TSS.

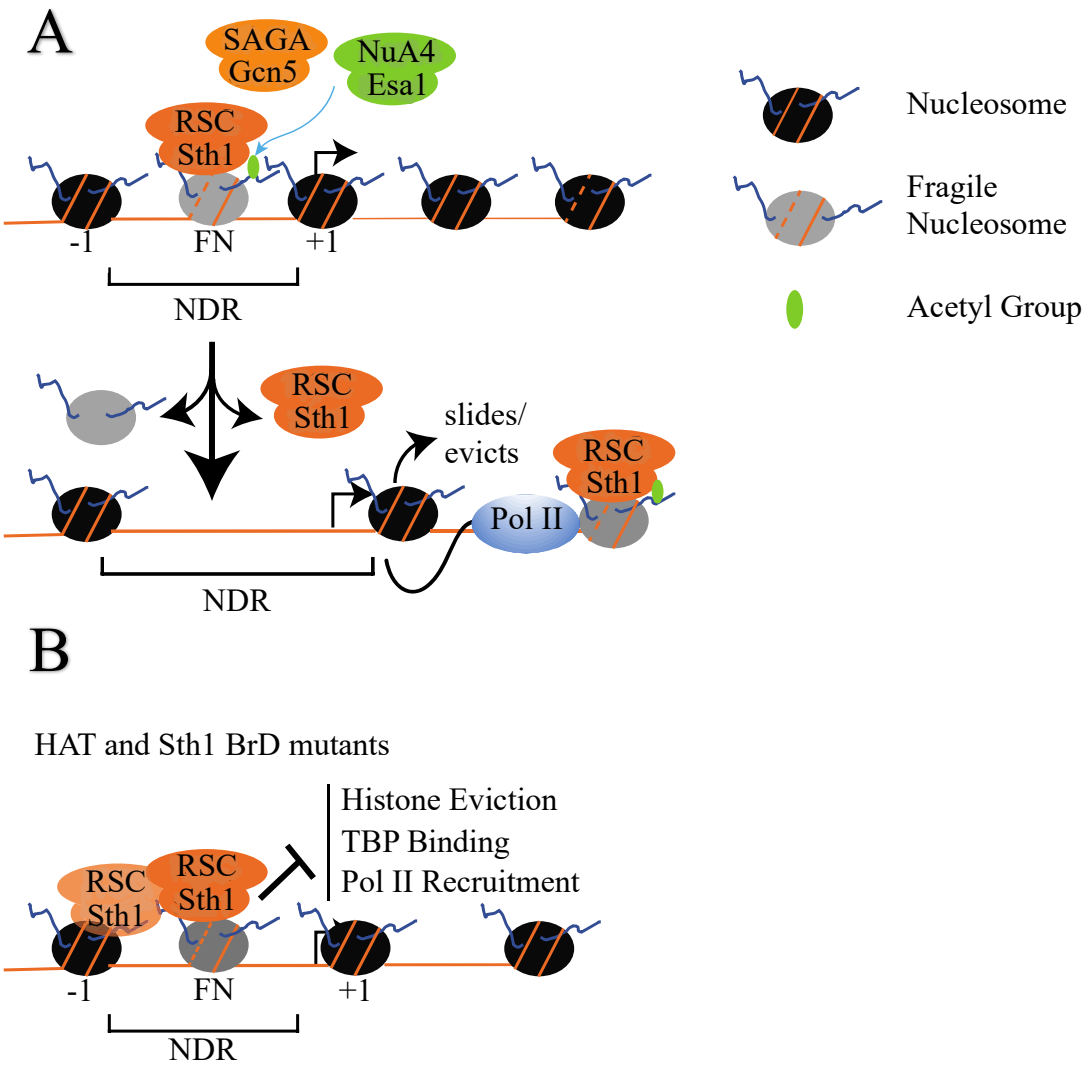

Figure 5.17. RSC coordinates with Gcn5 and Esa1 to regulate chromatin structure and transcription. A) Model depicting the roles of Gcn5 and Esa1 in regulating chromatin structure at promoters and in CDSs (Figure 4.30). In WT cells, nucleosomes such as the +1 nucleosome can be evicted or repositioned by RSC, which could be transiently recruited to NDRs via transcription activators, histone acetylation by Gcn5 of Esa1, or by recognizing DNA sequences within the promoter. Repositioning/remodeling of the +1 nucleosome by RSC can then facilitate TBP recruitment and transcription. B) When Esa1 and/or Gcn5 are absent, RSC is able to accumulate on hypoacetylated tails of promoter nucleosomes, and possibly those of fragile nucleosomes. The hypoacetylated nucleosomes are not as efficiently removed, resulting in reduced TBP and Pol II recruitment. In CDSs, RSC is not as efficiently recruited to the chromatin, resulting in less accessible nucleosomes and possible Pol II elongation defects.

APPENDIX A

LIST OF STRAINS USED IN THIS STUDY

TABLE 1. LIST OF STRAINS USED IN THIS STUDY

Name	Parent	Genotype	Reference
F729	BY4741	*MATa his3Δ1 leu2Δ0 met15Δ0 ura3Δ0*	Research Genetics
CGY 2	BY4741	*MATa his3Δ1 leu2Δ0 met15Δ0 ura3Δ0 STH1-myc13::HIS3*	This study
DG 265	7285	*MATa his3Δ leu2Δ met15Δ ura3Δ gcn5Δ::kanMX4 STH1-myc13::HIS3*	(Ginsburg et al., 2009)
DG 259	DG150	*MATa his3Δ leu2Δ met15Δ ura3Δ esa1L254P STH1-myc13::HIS3*	(Ginsburg et al., 2009)
DG 271	DG154	*MATa his3Δ leu2Δ met15Δ ura3Δ gcn5Δ::kanMX4 esa1L254P STH1-myc13::HIS3*	(Ginsburg et al., 2009)
YPE468	W303	*MATa ade2-1can1-100his3-11,15leu2-3,112trp1-1ura3-1RAD5+rsc8::KanMX-GALp-HA3-RSC8*	(Ocampo et al. 2019)
EBY 1	BY4741	*MATa his3Δ1 leu2Δ0 met15Δ0 ura3Δ0 STH1ΔBrD(1270-1359)-myc13::HIS3*	This study
JDY 86	S288C	*MATa his3Δ200 leu2Δ0 lys2Δ0 trp1Δ63 ura3Δ0 met15Δ0 hht1-hhf1::NatMX4 can1::MFA1pr-HIS3 [pJP11, HHT1-HHF1 CEN-LYS2]*	(Dai et al., 2008)
SJY 1	JDY 86	*MATa his3Δ200 leu2Δ0 lys2Δ0 trp1Δ63 ura3Δ0 met15Δ0 can1::MFA1pr-HIS3 hht1-hhf1::NatMX4 hht2-hhf2::H3-URA3 STH1-myc13::TRP1*	This study
SJY 2	JDY 86	*MATa his3Δ200 leu2Δ0 lys2Δ0 trp1Δ63 ura3Δ0 met15Δ0 can1::MFA1pr-HIS3 hht1-hhf1::NatMX4 hht2-hhf2::[H3Δ1-28]-URA3 STH1-myc13::TRP1*	This study
EBY 11	JDY 86	*MATa his3Δ200 leu2Δ0 lys2Δ0 trp1Δ63 ura3Δ0 met15Δ0 can1::MFA1pr-HIS3 hht1-hhf1::NatMX4 hht2-hhf2::[H4Δ1-16]-URA3 STH1-myc13::TRP1*	This study

TABLE 1. – *Continued*

Name	Parent	Genotype	Reference
EC 1	JDY 86	*MATa his3Δ200 leu2Δ0 lys2Δ0 trp1Δ63 ura3Δ0 met15Δ0 can1::MFA1pr-HIS3 hht1-hhf1::NatMX4 hht2-hhf2::[H3K14A]-URA3 STH1-myc13::TRP1*	This study
EBY 10	JDY 86	*MATa his3Δ200 leu2Δ0 lys2Δ0 trp1Δ63 ura3Δ0 met15Δ0 can1::MFA1pr-HIS3 hht1-hhf1::NatMX4 hht2-hhf2::[H4K16A]-URA3 STH1-myc13::TRP1*	This study
YSK111	W303	*MATa tor1-1 fpr1::NAT RPL13A-2XFKB12::TRP1 STH1-FRB-KanMX*	(Kubik et al. 2018)
KHW76	W303	*MATalpha, tor1-1, fpr1::NAT, RPL13TAB-2Px (FSKpBt1152):*	(Petrenko et al. 2019)
NF198	BY4742	*MATa his3-Δ200, leu2-3,2-112, lys2-801, trp1-1(am), URA3::TIR-9Myc, STH1-44AID9Flag::hphNT*	(Klein-Brill et al. 2019)
Y4810	4796	*MATa trp1Δ1 can1Δ100 leu2Δ3-112 his3Δ11-15 ura3Δ0 GAL psi+ pADH1-OsTIR1-9myc::ADE2 URA2::pMET3::STH1-IAA17::KanMX6*	Gift from Dr. Frank Uhlmann
Y4855	4810	*MATa trp1Δ1 can1Δ100 leu2Δ3-112 his3Δ11-15 ura3Δ0 GAL psi+ pADH1-OsTIR1-9myc::ADE2 URA2::pMET3::STH1-IAA17::KanMX6 STH1K501R-PK3::TRP1*	Gift from Dr. Frank Uhlmann
YP606	*S. pombe*	*h-, leu1; ura4; dis2::ura4+*	National BioResource Project (NBRP), Japan

APPENDIX B

LIST OF PLASMIDS AND OLIGONUCLEOTIDES USED TO GENERATE MYC-TAGGED STRAINS

TABLE 2. LIST OF PLASMIDS USED IN THIS STUDY

Name of bacterial strain	Plasmid Genotype	Tag	Selectable Marker	Reference
B3214	pFA6a-13myc-HIS3MX6	13XMyc	HIS3	(Longtine et al., 1998)
B3213	pFA6a-13myc-TRP1	13XMyc	TRP1	(Longtine et al., 1998)

TABLE 3. LIST OF PRIMERS USED FOR MYC TAGGING

Gene	Primer Name	Primer Type (Forward or Reverse)	Sequence (5'→3')
STH1	STH1-13myc-593	Forward	ATCCTGGGTTTACGTTGATGCTGACA
STH1	STH1-13myc-594	Reverse	CTAGAAAGAGTATTAGAGGGGAAAGG
STH1	STH1 BD 1270-1359 myc (F)	Forward	CCCACGGTGGAAAAATTGGTGGAAGAAATGCGCGAACAGTTAGATGAGGTACGGATC

APPENDIX C

LIST OF ANTIBODIES AND KEY REAGENTS USED IN THIS STUDY

TABLE 4. LIST OF ANTIBODIES USED IN THIS STUDY

Antibody	Manufacturer	Catalog #
Anti-myc	Roche	11667203001
Anti-Rpb3	Neoclone	W0012
Anti-H3	Abcam	ab1791
Anti-TBP	gift from Dr. Joseph Reese	not applicable

TABLE 5. LIST OF KEY REAGENTS USED IN THIS STUDY

Reagent	Manufacturer	Catalog #
Proteinase K	Ambion	AM2546
Micrococcal Nuclease	Worthington Biochemical	LS004798
Pan Mouse IgG (Anti-mouse) Dynabeads	Thermofisher Scientific	11-041
M-280 Sheep (Anti-rabbit) Dynabeads	Thermofisher Scientific	11-204-D
RNase A	Fisher Scientific	12091-021
AMPure XP beads	Beckman Coulter	A63881
NEBNext Ultra II DNA Library Kit	New England Biolabs	E7645S
NEXTFlex DNA Barcodes	PerkinElmer	514104
Qiaex II Gel Extraction Kit	Qiagen	20051

APPENDIX D

PERMISSIONS

Parts of this work were published in the following article:

1. Biernat, E., Kinney, J., Dunlap, K., Rizza, C., and Govind, C.K. (2021). The RSC complex remodels nucleosomes in transcribed coding sequences and promotes transcription in Saccharomyces cerevisiae. Genetics *217*.

License Details

This Agreement between Emily Biernat ("You") and Oxford University Press ("Oxford University Press") consists of your license details and the terms and conditions provided by Oxford University Press and Copyright Clearance Center.

Print Copy

License Number	5587180770336
License date	Jul 13, 2023
Licensed Content Publisher	Oxford University Press
Licensed Content Publication	Genetics
Licensed Content Title	The RSC complex remodels nucleosomes in transcribed coding sequences and promotes transcription in *Saccharomyces cerevisiae*
Licensed Content Author	Biernat, Emily; Kinney, Jeena
Licensed Content Date	Feb 11, 2021
Licensed Content Volume	217
Licensed Content Issue	4
Type of Use	Thesis/Dissertation
Requestor type	Author of this OUP content
Format	Print
Portion	Full article
Will you be translating?	No
Title	ANALYZING THE IN VIVO ROLES OF HISTONE ACETYLTRANSFERASES GCN5 AND ESA1 IN RSC RECRUITMENT AND REMODELING ACTIVITY GENOME-WIDE IN SACCHAROMYCES CEREVISIAE
Institution name	Oakland University
Expected presentation date	Jul 2023
Order reference number	2011
Requestor Location	Emily Biernat 334 Mathematics and Science Center 118 Library Drive ROCHESTER, MI 48309 United States Attn: Oakland University
Publisher Tax ID	GB125506730
Total	**0.00 USD**

REFERENCES

1. Adkins, M.W., Howar, S.R., and Tyler, J.K. (2004). Chromatin disassembly mediated by the histone chaperone Asf1 is essential for transcriptional activation of the yeast PHO5 and PHO8 genes. Mol Cell *14*, 657-666.

2. Akhtar, A., Faye, G., and Bentley, D.L. (1996). Distinct activated and non-activated RNA polymerase II complexes in yeast. EMBO J *15*, 4654-4664.

3. Andrews, A.J., Chen, X., Zevin, A., Stargell, L.A., and Luger, K. (2010). The histone chaperone Nap1 promotes nucleosome assembly by eliminating nonnucleosomal histone DNA interactions. Mol Cell *37*, 834-842.

4. Andrews, F.H., Strahl, B.D., and Kutateladze, T.G. (2016). Insights into newly discovered marks and readers of epigenetic information. Nat Chem Biol *12*, 662-668.

5. Angus-Hill, M.L., Schlichter, A., Roberts, D., Erdjument-Bromage, H., Tempst, P., and Cairns, B.R. (2001). A Rsc3/Rsc30 zinc cluster dimer reveals novel roles for the chromatin remodeler RSC in gene expression and cell cycle control. Mol Cell *7*, 741-751.

6. Arimbasseri, A.G., Rijal, K., and Maraia, R.J. (2014). Comparative overview of RNA polymerase II and III transcription cycles, with focus on RNA polymerase III termination and reinitiation. Transcription *5*, e27639.

7. Avcilar-Kucukgoze, I., and Kashina, A. (2020). Hijacking tRNAs From Translation: Regulatory Functions of tRNAs in Mammalian Cell Physiology. Front Mol Biosci *7*, 610617.

8. Avvakumov, N., Nourani, A., and Cote, J. (2011). Histone chaperones: modulators of chromatin marks. Mol Cell *41*, 502-514.

9. Badis, G., Chan, E.T., van Bakel, H., Pena-Castillo, L., Tillo, D., Tsui, K., Carlson, C.D., Gossett, A.J., Hasinoff, M.J., Warren, C.L.*, et al.* (2008). A library of yeast transcription factor motifs reveals a widespread function for Rsc3 in targeting nucleosome exclusion at promoters. Mol Cell *32*, 878-887.

10. Bannister, A.J., and Kouzarides, T. (2011). Regulation of chromatin by histone modifications. Cell Res *21*, 381-395.

11. Baptista, T., Grunberg, S., Minoungou, N., Koster, M.J.E., Timmers, H.T.M., Hahn, S., Devys, D., and Tora, L. (2017). SAGA Is a General Cofactor for RNA Polymerase II Transcription. Mol Cell *68*, 130-143 e135.

12. Bataille, A.R., Jeronimo, C., Jacques, P.E., Laramee, L., Fortin, M.E., Forest, A., Bergeron, M., Hanes, S.D., and Robert, F. (2012). A universal RNA polymerase II CTD cycle is orchestrated by complex interplays between kinase, phosphatase, and isomerase enzymes along genes. Mol Cell *45*, 158-170.

13. Belda, I., Ruiz, J., Santos, A., Van Wyk, N., and Pretorius, I.S. (2019). Saccharomyces cerevisiae. Trends Genet *35*, 956-957.

14. Belotserkovskaya, R., Oh, S., Bondarenko, V.A., Orphanides, G., Studitsky, V.M., and Reinberg, D. (2003). FACT facilitates transcription-dependent nucleosome alteration. Science *301*, 1090-1093.

15. Berndsen, C.E., and Denu, J.M. (2008). Catalysis and substrate selection by histone/protein lysine acetyltransferases. Curr Opin Struct Biol *18*, 682-689.

16. Blus, B.J., Hashimoto, H., Seo, H.S., Krolak, A., and Debler, E.W. (2019). Substrate Affinity and Specificity of the ScSth1p Bromodomain Are Fine-Tuned for Versatile Histone Recognition. Structure *27*, 1460-1468 e1463.

17. Boeger, H., Griesenbeck, J., Strattan, J.S., and Kornberg, R.D. (2004). Removal of promoter nucleosomes by disassembly rather than sliding in vivo. Mol Cell *14*, 667-673.

18. Bogershausen, N., and Wollnik, B. (2018). Mutational Landscapes and Phenotypic Spectrum of SWI/SNF-Related Intellectual Disability Disorders. Front Mol Neurosci *11*, 252.

19. Bohm, K.A., Hodges, A.J., Czaja, W., Selvam, K., Smerdon, M.J., Mao, P., and Wyrick, J.J. (2021). Distinct roles for RSC and SWI/SNF chromatin remodelers in genomic excision repair. Genome Res *31*, 1047-1059.

20. Bondarenko, V.A., Steele, L.M., Ujvari, A., Gaykalova, D.A., Kulaeva, O.I., Polikanov, Y.S., Luse, D.S., and Studitsky, V.M. (2006). Nucleosomes can form a polar barrier to transcript elongation by RNA polymerase II. Mol Cell *24*, 469-479.

21. Bourgeois, C.F., Kim, Y.K., Churcher, M.J., West, M.J., and Karn, J. (2002). Spt5 cooperates with human immunodeficiency virus type 1 Tat by preventing premature RNA release at terminator sequences. Mol Cell Biol *22*, 1079-1093.

22. Bradner, J.E., Hnisz, D., and Young, R.A. (2017). Transcriptional Addiction in Cancer. Cell *168*, 629-643.

23. Braglia, P., Percudani, R., and Dieci, G. (2005). Sequence context effects on oligo(dT) termination signal recognition by Saccharomyces cerevisiae RNA polymerase III. J Biol Chem *280*, 19551-19562.

24. Brahma, S., and Henikoff, S. (2019). RSC-Associated Subnucleosomes Define MNase-Sensitive Promoters in Yeast. Mol Cell *73*, 238-249 e233.

25. Brahma, S., Udugama, M.I., Kim, J., Hada, A., Bhardwaj, S.K., Hailu, S.G., Lee, T.H., and Bartholomew, B. (2017). INO80 exchanges H2A.Z for H2A by translocating on DNA proximal to histone dimers. Nat Commun *8*, 15616.

26. Briggs, S.D., Bryk, M., Strahl, B.D., Cheung, W.L., Davie, J.K., Dent, S.Y., Winston, F., and Allis, C.D. (2001). Histone H3 lysine 4 methylation is mediated by Set1 and required for cell growth and rDNA silencing in Saccharomyces cerevisiae. Genes Dev *15*, 3286-3295.

27. Bruzzone, M.J., Grunberg, S., Kubik, S., Zentner, G.E., and Shore, D. (2018). Distinct patterns of histone acetyltransferase and Mediator deployment at yeast protein-coding genes. Genes Dev *32*, 1252-1265.

28. Buratowski, S. (2009). Progression through the RNA polymerase II CTD cycle. Mol Cell *36*, 541-546.

29. Buratowski, S., Hahn, S., Guarente, L., and Sharp, P.A. (1989). Five intermediate complexes in transcription initiation by RNA polymerase II. Cell *56*, 549-561.

30. Burugula, B.B., Jeronimo, C., Pathak, R., Jones, J.W., Robert, F., and Govind, C.K. (2014). Histone deacetylases and phosphorylated polymerase II C-terminal domain recruit Spt6 for cotranscriptional histone reassembly. Mol Cell Biol *34*, 4115-4129.

31. Butler, J.E., and Kadonaga, J.T. (2002). The RNA polymerase II core promoter: a key component in the regulation of gene expression. Genes Dev *16*, 2583-2592.

32. Cabart, P., and Luse, D.S. (2012). Inactivated RNA polymerase II open complexes can be reactivated with TFIIE. J Biol Chem *287*, 961-967.

33. Cairns, B.R. (2007). Chromatin remodeling: insights and intrigue from single-molecule studies. Nat Struct Mol Biol *14*, 989-996.

34. Cairns, B.R., Lorch, Y., Li, Y., Zhang, M., Lacomis, L., Erdjument-Bromage, H., Tempst, P., Du, J., Laurent, B., and Kornberg, R.D. (1996). RSC, an essential, abundant chromatin-remodeling complex. Cell *87*, 1249-1260.

35. Cairns, B.R., Schlichter, A., Erdjument-Bromage, H., Tempst, P., Kornberg, R.D., and Winston, F. (1999). Two functionally distinct forms of the RSC nucleosome-remodeling complex, containing essential AT hook, BAH, and bromodomains. Mol Cell *4*, 715-723.

36. Cakiroglu, A., Clapier, C.R., Ehrensberger, A.H., Darbo, E., Cairns, B.R., Luscombe, N.M., and Svejstrup, J.Q. (2019). Genome-wide reconstitution of chromatin transactions reveals that RSC preferentially disrupts H2AZ-containing nucleosomes. Genome Res *29*, 988-998.

37. Campsteijn, C., Wijnands-Collin, A.M., and Logie, C. (2007). Reverse genetic analysis of the yeast RSC chromatin remodeler reveals a role for RSC3 and SNF5 homolog 1 in ploidy maintenance. PLoS Genet *3*, e92.

38. Cao, Y., Cairns, B.R., Kornberg, R.D., and Laurent, B.C. (1997). Sfh1p, a component of a novel chromatin-remodeling complex, is required for cell cycle progression. Mol Cell Biol *17*, 3323-3334.

39. Carey, M., Li, B., and Workman, J.L. (2006). RSC exploits histone acetylation to abrogate the nucleosomal block to RNA polymerase II elongation. Mol Cell *24*, 481-487.

40. Carninci, P., Sandelin, A., Lenhard, B., Katayama, S., Shimokawa, K., Ponjavic, J., Semple, C.A., Taylor, M.S., Engstrom, P.G., Frith, M.C.*, et al.* (2006). Genome-wide analysis of mammalian promoter architecture and evolution. Nat Genet *38*, 626-635.

41. Carre, C., Szymczak, D., Pidoux, J., and Antoniewski, C. (2005). The histone H3 acetylase dGcn5 is a key player in Drosophila melanogaster metamorphosis. Mol Cell Biol *25*, 8228-8238.

42. Carrozza, M.J., Li, B., Florens, L., Suganuma, T., Swanson, S.K., Lee, K.K., Shia, W.J., Anderson, S., Yates, J., Washburn, M.P.*, et al.* (2005). Histone H3 methylation by Set2 directs deacetylation of coding regions by Rpd3S to suppress spurious intragenic transcription. Cell *123*, 581-592.

43. Chatterjee, N., North, J.A., Dechassa, M.L., Manohar, M., Prasad, R., Luger, K., Ottesen, J.J., Poirier, M.G., and Bartholomew, B. (2015). Histone Acetylation near the Nucleosome Dyad Axis Enhances Nucleosome Disassembly by RSC and SWI/SNF. Mol Cell Biol *35*, 4083-4092.

44. Chatterjee, N., Sinha, D., Lemma-Dechassa, M., Tan, S., Shogren-Knaak, M.A., and Bartholomew, B. (2011). Histone H3 tail acetylation modulates ATP-dependent remodeling through multiple mechanisms. Nucleic Acids Res *39*, 8378-8391.

45. Chen, G., Li, W., Yan, F., Wang, D., and Chen, Y. (2020). The Structural Basis for Specific Recognition of H3K14 Acetylation by Sth1 in the RSC Chromatin Remodeling Complex. Structure *28*, 111-118 e113.

46. Chen, H., and Pugh, B.F. (2021). What do Transcription Factors Interact With? J Mol Biol *433*, 166883.

47. Cheon, Y., Kim, H., Park, K., Kim, M., and Lee, D. (2020). Dynamic modules of the coactivator SAGA in eukaryotic transcription. Exp Mol Med *52*, 991-1003.

48. Chereji, R.V., Bryson, T.D., and Henikoff, S. (2019). Quantitative MNase-seq accurately maps nucleosome occupancy levels. Genome Biol *20*, 198.

49. Chereji, R.V., Ocampo, J., and Clark, D.J. (2017). MNase-Sensitive Complexes in Yeast: Nucleosomes and Non-histone Barriers. Mol Cell *65*, 565-577 e563.

50. Chereji, R.V., Ramachandran, S., Bryson, T.D., and Henikoff, S. (2018). Precise genome-wide mapping of single nucleosomes and linkers in vivo. Genome Biol *19*, 19.

51. Cheung, A.C.M., and Diaz-Santin, L.M. (2019). Share and share alike: the role of Tra1 from the SAGA and NuA4 coactivator complexes. Transcription *10*, 37-43.

52. Cheung, V., Chua, G., Batada, N.N., Landry, C.R., Michnick, S.W., Hughes, T.R., and Winston, F. (2008). Chromatin- and transcription-related factors repress transcription from within coding regions throughout the Saccharomyces cerevisiae genome. PLoS Biol *6*, e277.

53. Chittuluru, J.R., Chaban, Y., Monnet-Saksouk, J., Carrozza, M.J., Sapountzi, V., Selleck, W., Huang, J., Utley, R.T., Cramet, M., Allard, S.*, et al.* (2011). Structure and nucleosome interaction of the yeast NuA4 and Piccolo-NuA4 histone acetyltransferase complexes. Nat Struct Mol Biol *18*, 1196-1203.

54. Chu, Y., Simic, R., Warner, M.H., Arndt, K.M., and Prelich, G. (2007). Regulation of histone modification and cryptic transcription by the Bur1 and Paf1 complexes. EMBO J *26*, 4646-4656.

55. Churchman, L.S., and Weissman, J.S. (2011). Nascent transcript sequencing visualizes transcription at nucleotide resolution. Nature *469*, 368-373.

56. Cianfrocco, M.A., Kassavetis, G.A., Grob, P., Fang, J., Juven-Gershon, T., Kadonaga, J.T., and Nogales, E. (2013). Human TFIID binds to core promoter DNA in a reorganized structural state. Cell *152*, 120-131.

57. Clancy, S. (2008). DNA Transcription. Nature Education *1*, 41.

58. Clapier, C.R., and Cairns, B.R. (2009). The biology of chromatin remodeling complexes. Annu Rev Biochem *78*, 273-304.

59. Clapier, C.R., Iwasa, J., Cairns, B.R., and Peterson, C.L. (2017). Mechanisms of action and regulation of ATP-dependent chromatin-remodelling complexes. Nat Rev Mol Cell Biol *18*, 407-422.

60. Clapier, C.R., Kasten, M.M., Parnell, T.J., Viswanathan, R., Szerlong, H., Sirinakis, G., Zhang, Y., and Cairns, B.R. (2016). Regulation of DNA Translocation Efficiency within the Chromatin Remodeler RSC/Sth1 Potentiates Nucleosome Sliding and Ejection. Mol Cell *62*, 453-461.

61. Conaway, J.W., Shilatifard, A., Dvir, A., and Conaway, R.C. (2000). Control of elongation by RNA polymerase II. Trends Biochem Sci *25*, 375-380.

62. Cormack, B.P., and Struhl, K. (1992). The TATA-binding protein is required for transcription by all three nuclear RNA polymerases in yeast cells. Cell *69*, 685-696.

63. Cox, P.M., and Goding, C.R. (1991). Transcription and cancer. Br J Cancer *63*, 651-662.

64. Cramer, P. (2002). Multisubunit RNA polymerases. Curr Opin Struct Biol *12*, 89-97.

65. Cramer, P., Bushnell, D.A., and Kornberg, R.D. (2001). Structural basis of transcription: RNA polymerase II at 2.8 angstrom resolution. Science *292*, 1863-1876.

66. Cucinotta, C.E., Dell, R.H., Braceros, K.C., and Tsukiyama, T. (2021). RSC primes the quiescent genome for hypertranscription upon cell-cycle re-entry. Elife *10*.

67. Cui, F., Cole, H.A., Clark, D.J., and Zhurkin, V.B. (2012). Transcriptional activation of yeast genes disrupts intragenic nucleosome phasing. Nucleic Acids Res *40*, 10753-10764.

68. Dauden, M.I., Kosinski, J., Kolaj-Robin, O., Desfosses, A., Ori, A., Faux, C., Hoffmann, N.A., Onuma, O.F., Breunig, K.D., Beck, M.*, et al.* (2017). Architecture of the yeast Elongator complex. EMBO Rep *18*, 264-279.

69. Dhalluin, C., Carlson, J.E., Zeng, L., He, C., Aggarwal, A.K., and Zhou, M.M. (1999). Structure and ligand of a histone acetyltransferase bromodomain. Nature *399*, 491-496.

70. Dhoondia, Z., Elewa, H., Malik, M., Arif, Z., Pique-Regi, R., and Ansari, A. (2021). A termination-independent role of Rat1 in cotranscriptional splicing. Nucleic Acids Res *49*, 5520-5536.

71. Donczew, R., Warfield, L., Pacheco, D., Erijman, A., and Hahn, S. (2020). Two roles for the yeast transcription coactivator SAGA and a set of genes redundantly regulated by TFIID and SAGA. Elife *9*.

72. Dover, J., Schneider, J., Tawiah-Boateng, M.A., Wood, A., Dean, K., Johnston, M., and Shilatifard, A. (2002). Methylation of histone H3 by COMPASS requires ubiquitination of histone H2B by Rad6. J Biol Chem *277*, 28368-28371.

73. Drouin, S., Laramee, L., Jacques, P.E., Forest, A., Bergeron, M., and Robert, F. (2010). DSIF and RNA polymerase II CTD phosphorylation coordinate the recruitment of Rpd3S to actively transcribed genes. PLoS Genet *6*, e1001173.

74. Du, J., Nasir, I., Benton, B.K., Kladde, M.P., and Laurent, B.C. (1998). Sth1p, a Saccharomyces cerevisiae Snf2p/Swi2p homolog, is an essential ATPase in RSC and differs from Snf/Swi in its interactions with histones and chromatin-associated proteins. Genetics *150*, 987-1005.

75. Durant, M., and Pugh, B.F. (2006). Genome-wide relationships between TAF1 and histone acetyltransferases in Saccharomyces cerevisiae. Mol Cell Biol *26*, 2791-2802.

76. Dvir, A. (2002). Promoter escape by RNA polymerase II. Biochim Biophys Acta *1577*, 208-223.

77. Dvir, A., Conaway, R.C., and Conaway, J.W. (1997a). A role for TFIIH in controlling the activity of early RNA polymerase II elongation complexes. Proc Natl Acad Sci U S A *94*, 9006-9010.

78. Dvir, A., Tan, S., Conaway, J.W., and Conaway, R.C. (1997b). Promoter escape by RNA polymerase II. Formation of an escape-competent transcriptional intermediate is a prerequisite for exit of polymerase from the promoter. J Biol Chem *272*, 28175-28178.

79. Eberharter, A., Sterner, D.E., Schieltz, D., Hassan, A., Yates, J.R., 3rd, Berger, S.L., and Workman, J.L. (1999). The ADA complex is a distinct histone acetyltransferase complex in Saccharomyces cerevisiae. Mol Cell Biol *19*, 6621-6631.

80. Egloff, S. (2012). Role of Ser7 phosphorylation of the CTD during transcription of snRNA genes. RNA Biol *9*, 1033-1038.

81. Egloff, S., and Murphy, S. (2008). Cracking the RNA polymerase II CTD code. Trends Genet *24*, 280-288.

82. Egly, J.M., and Coin, F. (2011). A history of TFIIH: two decades of molecular biology on a pivotal transcription/repair factor. DNA Repair (Amst) *10*, 714-721.

83. Ehara, H., Yokoyama, T., Shigematsu, H., Yokoyama, S., Shirouzu, M., and Sekine, S.I. (2017). Structure of the complete elongation complex of RNA polymerase II with basal factors. Science *357*, 921-924.

84. Eitoku, M., Sato, L., Senda, T., and Horikoshi, M. (2008). Histone chaperones: 30 years from isolation to elucidation of the mechanisms of nucleosome assembly and disassembly. Cell Mol Life Sci *65*, 414-444.

85. Eriksson, P.R., Ganguli, D., Nagarajavel, V., and Clark, D.J. (2012). Regulation of histone gene expression in budding yeast. Genetics *191*, 7-20.

86. Farnung, L., Vos, S.M., and Cramer, P. (2018). Structure of transcribing RNA polymerase II-nucleosome complex. Nat Commun *9*, 5432.

87. Ferreira, M.E., Flaherty, K., and Prochasson, P. (2011). The Saccharomyces cerevisiae histone chaperone Rtt106 mediates the cell cycle recruitment of SWI/SNF and RSC to the HIR-dependent histone genes. PLoS One *6*, e21113.

88. Finch, J.T., and Klug, A. (1976). Solenoidal model for superstructure in chromatin. Proc Natl Acad Sci U S A *73*, 1897-1901.

89. Fish, R.N., and Kane, C.M. (2002). Promoting elongation with transcript cleavage stimulatory factors. Biochim Biophys Acta *1577*, 287-307.

90. Fishburn, J., and Hahn, S. (2012). Architecture of the yeast RNA polymerase II open complex and regulation of activity by TFIIF. Mol Cell Biol *32*, 12-25.

91. Florio, C., Moscariello, M., Ederle, S., Fasano, R., Lanzuolo, C., and Pulitzer, J.F. (2007). A study of biochemical and functional interactions of Htl1p, a putative component of the Saccharomyces cerevisiae, Rsc chromatin-remodeling complex. Gene *395*, 72-85.

92. Fuchs, S.M., Laribee, R.N., and Strahl, B.D. (2009). Protein modifications in transcription elongation. Biochim Biophys Acta *1789*, 26-36.

93. Fussner, E., Strauss, M., Djuric, U., Li, R., Ahmed, K., Hart, M., Ellis, J., and Bazett-Jones, D.P. (2012). Open and closed domains in the mouse genome are configured as 10-nm chromatin fibres. EMBO Rep *13*, 992-996.

94. Ganguli, D., Chereji, R.V., Iben, J.R., Cole, H.A., and Clark, D.J. (2014). RSC-dependent constructive and destructive interference between opposing arrays of phased nucleosomes in yeast. Genome Res *24*, 1637-1649.

95. Garcia-Molinero, V., Garcia-Martinez, J., Reja, R., Furio-Tari, P., Antunez, O., Vinayachandran, V., Conesa, A., Pugh, B.F., Perez-Ortin, J.E., and Rodriguez-Navarro, S. (2018). The SAGA/TREX-2 subunit Sus1 binds widely to transcribed genes and affects mRNA turnover globally. Epigenetics Chromatin *11*, 13.

96. Geng, F., and Laurent, B.C. (2004). Roles of SWI/SNF and HATs throughout the dynamic transcription of a yeast glucose-repressible gene. EMBO J *23*, 127-137.

97. Ginsburg, D.S., Govind, C.K., and Hinnebusch, A.G. (2009). NuA4 lysine acetyltransferase Esa1 is targeted to coding regions and stimulates transcription elongation with Gcn5. Mol Cell Biol *29*, 6473-6487.

98. Gnatt, A.L., Cramer, P., Fu, J., Bushnell, D.A., and Kornberg, R.D. (2001). Structural basis of transcription: an RNA polymerase II elongation complex at 3.3 A resolution. Science *292*, 1876-1882.

99. Govind, C.K., Ginsburg, D., and Hinnebusch, A.G. (2012). Measuring dynamic changes in histone modifications and nucleosome density during activated transcription in budding yeast. Methods Mol Biol *833*, 15-27.

100. Govind, C.K., Qiu, H., Ginsburg, D.S., Ruan, C., Hofmeyer, K., Hu, C., Swaminathan, V., Workman, J.L., Li, B., and Hinnebusch, A.G. (2010). Phosphorylated Pol II CTD recruits multiple HDACs, including Rpd3C(S), for methylation-dependent deacetylation of ORF nucleosomes. Mol Cell *39*, 234-246.

101. Govind, C.K., Yoon, S., Qiu, H., Govind, S., and Hinnebusch, A.G. (2005). Simultaneous recruitment of coactivators by Gcn4p stimulates multiple steps of transcription in vivo. Mol Cell Biol *25*, 5626-5638.

102. Govind, C.K., Zhang, F., Qiu, H., Hofmeyer, K., and Hinnebusch, A.G. (2007). Gcn5 promotes acetylation, eviction, and methylation of nucleosomes in transcribed coding regions. Mol Cell *25*, 31-42.

103. Greber, B.J., and Nogales, E. (2019). The Structures of Eukaryotic Transcription Pre-initiation Complexes and Their Functional Implications. Subcell Biochem *93*, 143-192.

104. Grunberg, S., Henikoff, S., Hahn, S., and Zentner, G.E. (2016). Mediator binding to UASs is broadly uncoupled from transcription and cooperative with TFIID recruitment to promoters. EMBO J *35*, 2435-2446.

105. Grunberg, S., Warfield, L., and Hahn, S. (2012). Architecture of the RNA polymerase II preinitiation complex and mechanism of ATP-dependent promoter opening. Nat Struct Mol Biol *19*, 788-796.

106. Grzechnik, P., Gdula, M.R., and Proudfoot, N.J. (2015). Pcf11 orchestrates transcription termination pathways in yeast. Genes Dev *29*, 849-861.

107. Hahn, S., and Young, E.T. (2011). Transcriptional regulation in Saccharomyces cerevisiae: transcription factor regulation and function, mechanisms of initiation, and roles of activators and coactivators. Genetics *189*, 705-736.

108. Haque, M.E., Jakaria, M., Akther, M., Cho, D.Y., Kim, I.S., and Choi, D.K. (2021). The GCN5: its biological functions and therapeutic potentials. Clin Sci (Lond) *135*, 231-257.

109. Harada, B.T., Hwang, W.L., Deindl, S., Chatterjee, N., Bartholomew, B., and Zhuang, X. (2016). Stepwise nucleosome translocation by RSC remodeling complexes. Elife *5*.

110. Hartley, P.D., and Madhani, H.D. (2009). Mechanisms that specify promoter nucleosome location and identity. Cell *137*, 445-458.

111. Hartzog, G.A., Wada, T., Handa, H., and Winston, F. (1998). Evidence that Spt4, Spt5, and Spt6 control transcription elongation by RNA polymerase II in Saccharomyces cerevisiae. Genes Dev *12*, 357-369.

112. Haruki, H., Nishikawa, J., and Laemmli, U.K. (2008). The anchor-away technique: rapid, conditional establishment of yeast mutant phenotypes. Mol Cell *31*, 925-932.

113. Hassan, A.H., Awad, S., Al-Natour, Z., Othman, S., Mustafa, F., and Rizvi, T.A. (2007). Selective recognition of acetylated histones by bromodomains in transcriptional co-activators. Biochem J *402*, 125-133.

114. Hassan, A.H., Neely, K.E., and Workman, J.L. (2001). Histone acetyltransferase complexes stabilize swi/snf binding to promoter nucleosomes. Cell *104*, 817-827.

115. He, Y., Yan, C., Fang, J., Inouye, C., Tjian, R., Ivanov, I., and Nogales, E. (2016). Near-atomic resolution visualization of human transcription promoter opening. Nature *533*, 359-365.

116. He, Z., Chen, K., Ye, Y., and Chen, Z. (2021). Structure of the SWI/SNF complex bound to the nucleosome and insights into the functional modularity. Cell Discov *7*, 28.

117. Henikoff, J.G., Belsky, J.A., Krassovsky, K., MacAlpine, D.M., and Henikoff, S. (2011). Epigenome characterization at single base-pair resolution. Proc Natl Acad Sci U S A *108*, 18318-18323.

118. Hieb, A.R., Gansen, A., Bohm, V., and Langowski, J. (2014). The conformational state of the nucleosome entry-exit site modulates TATA box-specific TBP binding. Nucleic Acids Res *42*, 7561-7576.

119. Hilton, T.L., Li, Y., Dunphy, E.L., and Wang, E.H. (2005). TAF1 histone acetyltransferase activity in Sp1 activation of the cyclin D1 promoter. Mol Cell Biol *25*, 4321-4332.

120. Hinnebusch, A.G. (2014). The scanning mechanism of eukaryotic translation initiation. Annu Rev Biochem *83*, 779-812.

121. Hoagland, M.B., Stephenson, M.L., Scott, J.F., Hecht, L.I., and Zamecnik, P.C. (1958). A soluble ribonucleic acid intermediate in protein synthesis. J Biol Chem *231*, 241-257.

122. Hsu, J.M., Huang, J., Meluh, P.B., and Laurent, B.C. (2003). The yeast RSC chromatin-remodeling complex is required for kinetochore function in chromosome segregation. Mol Cell Biol *23*, 3202-3215.

123. Huisinga, K.L., and Pugh, B.F. (2004). A genome-wide housekeeping role for TFIID and a highly regulated stress-related role for SAGA in Saccharomyces cerevisiae. Mol Cell *13*, 573-585.

124. Imamura, Y., Yu, F., Nakamura, M., Chihara, Y., Okane, K., Sato, M., Kanai, M., Hamada, R., Ueno, M., Yukawa, M.*, et al.* (2015). RSC Chromatin-Remodeling Complex Is Important for Mitochondrial Function in Saccharomyces cerevisiae. PLoS One *10*, e0130397.

125. Ivanovska, I., Jacques, P.E., Rando, O.J., Robert, F., and Winston, F. (2011). Control of chromatin structure by spt6: different consequences in coding and regulatory regions. Mol Cell Biol *31*, 531-541.

126. Izban, M.G., and Luse, D.S. (1991). Transcription on nucleosomal templates by RNA polymerase II in vitro: inhibition of elongation with enhancement of sequence-specific pausing. Genes Dev *5*, 683-696.

127. Izumi, K. (2016). Disorders of Transcriptional Regulation: An Emerging Category of Multiple Malformation Syndromes. Mol Syndromol *7*, 262-273.

128. Jain, N., Tamborrini, D., Evans, B., Chaudhry, S., Wilkins, B.J., and Neumann, H. (2020). Interaction of RSC Chromatin Remodeling Complex with Nucleosomes Is Modulated by H3 K14 Acetylation and H2B SUMOylation In Vivo. iScience *23*, 101292.

129. Jaiswal, D., Turniansky, R., and Green, E.M. (2017). Choose Your Own Adventure: The Role of Histone Modifications in Yeast Cell Fate. J Mol Biol *429*, 1946-1957.

130. Jenuwein, T., and Allis, C.D. (2001). Translating the histone code. Science *293*, 1074-1080.

131. Jeong, S.W., Lang, W.H., and Reeder, R.H. (1995). The release element of the yeast polymerase I transcription terminator can function independently of Reb1p. Mol Cell Biol *15*, 5929-5936.

132. Jeronimo, C., Bataille, A.R., and Robert, F. (2013). The writers, readers, and functions of the RNA polymerase II C-terminal domain code. Chem Rev *113*, 8491-8522.

133. Jeronimo, C., Watanabe, S., Kaplan, C.D., Peterson, C.L., and Robert, F. (2015). The Histone Chaperones FACT and Spt6 Restrict H2A.Z from Intragenic Locations. Mol Cell *58*, 1113-1123.

134. Jiang, C., and Pugh, B.F. (2009). Nucleosome positioning and gene regulation: advances through genomics. Nat Rev Genet *10*, 161-172.

135. Joshi, A.A., and Struhl, K. (2005). Eaf3 chromodomain interaction with methylated H3-K36 links histone deacetylation to Pol II elongation. Mol Cell *20*, 971-978.

136. Kadoch, C., Hargreaves, D.C., Hodges, C., Elias, L., Ho, L., Ranish, J., and Crabtree, G.R. (2013). Proteomic and bioinformatic analysis of mammalian SWI/SNF complexes identifies extensive roles in human malignancy. Nat Genet *45*, 592-601.

137. Kanin, E.I., Kipp, R.T., Kung, C., Slattery, M., Viale, A., Hahn, S., Shokat, K.M., and Ansari, A.Z. (2007). Chemical inhibition of the TFIIH-associated kinase Cdk7/Kin28 does not impair global mRNA synthesis. Proc Natl Acad Sci U S A *104*, 5812-5817.

138. Kaplan, C.D. (2013). Basic mechanisms of RNA polymerase II activity and alteration of gene expression in Saccharomyces cerevisiae. Biochim Biophys Acta *1829*, 39-54.

139. Kaplan, C.D., Laprade, L., and Winston, F. (2003). Transcription elongation factors repress transcription initiation from cryptic sites. Science *301*, 1096-1099.

140. Karakas, D., and Ozpolat, B. (2021). The Role of LncRNAs in Translation. Noncoding RNA *7*.

141. Kasten, M., Szerlong, H., Erdjument-Bromage, H., Tempst, P., Werner, M., and Cairns, B.R. (2004). Tandem bromodomains in the chromatin remodeler RSC recognize acetylated histone H3 Lys14. EMBO J *23*, 1348-1359.

142. Keller, W., and Minvielle-Sebastia, L. (1997). A comparison of mammalian and yeast pre-mRNA 3'-end processing. Curr Opin Cell Biol *9*, 329-336.

143. Keogh, M.C., Kurdistani, S.K., Morris, S.A., Ahn, S.H., Podolny, V., Collins, S.R., Schuldiner, M., Chin, K., Punna, T., Thompson, N.J.*, et al.* (2005). Cotranscriptional set2 methylation of histone H3 lysine 36 recruits a repressive Rpd3 complex. Cell *123*, 593-605.

144. Kim, H., Erickson, B., Luo, W., Seward, D., Graber, J.H., Pollock, D.D., Megee, P.C., and Bentley, D.L. (2010). Gene-specific RNA polymerase II phosphorylation and the CTD code. Nat Struct Mol Biol *17*, 1279-1286.

145. Kim, M., Ahn, S.H., Krogan, N.J., Greenblatt, J.F., and Buratowski, S. (2004). Transitions in RNA polymerase II elongation complexes at the 3' ends of genes. EMBO J *23*, 354-364.

146. Kim, T., and Buratowski, S. (2007). Two Saccharomyces cerevisiae JmjC domain proteins demethylate histone H3 Lys36 in transcribed regions to promote elongation. J Biol Chem *282*, 20827-20835.

147. Kim, T., and Buratowski, S. (2009). Dimethylation of H3K4 by Set1 recruits the Set3 histone deacetylase complex to 5' transcribed regions. Cell *137*, 259-272.

148. Kim, T., Xu, Z., Clauder-Munster, S., Steinmetz, L.M., and Buratowski, S. (2012). Set3 HDAC mediates effects of overlapping noncoding transcription on gene induction kinetics. Cell *150*, 1158-1169.

149. Kim, T.K., Ebright, R.H., and Reinberg, D. (2000). Mechanism of ATP-dependent promoter melting by transcription factor IIH. Science *288*, 1418-1422.

150. Kireeva, M.L., Walter, W., Tchernajenko, V., Bondarenko, V., Kashlev, M., and Studitsky, V.M. (2002). Nucleosome remodeling induced by RNA polymerase II: loss of the H2A/H2B dimer during transcription. Mol Cell *9*, 541-552.

151. Kizer, K.O., Phatnani, H.P., Shibata, Y., Hall, H., Greenleaf, A.L., and Strahl, B.D. (2005). A novel domain in Set2 mediates RNA polymerase II interaction and couples histone H3 K36 methylation with transcript elongation. Mol Cell Biol *25*, 3305-3316.

152. Klein, D.C., Troy, K., Tripplehorn, S.A., and Hainer, S.J. (2023). The esBAF and ISWI nucleosome remodeling complexes influence occupancy of overlapping dinucleosomes and fragile nucleosomes in murine embryonic stem cells. BMC Genomics *24*, 201.

153. Klein-Brill, A., Joseph-Strauss, D., Appleboim, A., and Friedman, N. (2019). Dynamics of Chromatin and Transcription during Transient Depletion of the RSC Chromatin Remodeling Complex. Cell Rep *26*, 279-292 e275.

154. Klopf, E., Schmidt, H.A., Clauder-Munster, S., Steinmetz, L.M., and Schuller, C. (2017). INO80 represses osmostress induced gene expression by resetting promoter proximal nucleosomes. Nucleic Acids Res *45*, 3752-3766.

155. Knezetic, J.A., Jacob, G.A., and Luse, D.S. (1988). Assembly of RNA polymerase II preinitiation complexes before assembly of nucleosomes allows efficient initiation of transcription on nucleosomal templates. Mol Cell Biol *8*, 3114-3121.

156. Knezetic, J.A., and Luse, D.S. (1986). The presence of nucleosomes on a DNA template prevents initiation by RNA polymerase II in vitro. Cell *45*, 95-104.

157. Koerber, R.T., Rhee, H.S., Jiang, C., and Pugh, B.F. (2009). Interaction of transcriptional regulators with specific nucleosomes across the Saccharomyces genome. Mol Cell *35*, 889-902.

158. Komarnitsky, P., Cho, E.J., and Buratowski, S. (2000). Different phosphorylated forms of RNA polymerase II and associated mRNA processing factors during transcription. Genes Dev *14*, 2452-2460.

159. Korber, P., Barbaric, S., Luckenbach, T., Schmid, A., Schermer, U.J., Blaschke, D., and Horz, W. (2006). The histone chaperone Asf1 increases the rate of histone eviction at the yeast PHO5 and PHO8 promoters. J Biol Chem *281*, 5539-5545.

160. Krietenstein, N., Wal, M., Watanabe, S., Park, B., Peterson, C.L., Pugh, B.F., and Korber, P. (2016). Genomic Nucleosome Organization Reconstituted with Pure Proteins. Cell *167*, 709-721 e712.

161. Krogan, N.J., Dover, J., Wood, A., Schneider, J., Heidt, J., Boateng, M.A., Dean, K., Ryan, O.W., Golshani, A., Johnston, M.*, et al.* (2003). The Paf1 complex is required for histone H3 methylation by COMPASS and Dot1p: linking transcriptional elongation to histone methylation. Mol Cell *11*, 721-729.

162. Kubik, S., Bruzzone, M.J., Albert, B., and Shore, D. (2017). A Reply to "MNase-Sensitive Complexes in Yeast: Nucleosomes and Non-histone Barriers," by Chereji et al. Mol Cell *65*, 578-580.

163. Kubik, S., Bruzzone, M.J., Challal, D., Dreos, R., Mattarocci, S., Bucher, P., Libri, D., and Shore, D. (2019). Opposing chromatin remodelers control transcription initiation frequency and start site selection. Nat Struct Mol Biol *26*, 744-754.

164. Kubik, S., Bruzzone, M.J., Jacquet, P., Falcone, J.L., Rougemont, J., and Shore, D. (2015). Nucleosome Stability Distinguishes Two Different Promoter Types at All Protein-Coding Genes in Yeast. Mol Cell *60*, 422-434.

165. Kubik, S., O'Duibhir, E., de Jonge, W.J., Mattarocci, S., Albert, B., Falcone, J.L., Bruzzone, M.J., Holstege, F.C.P., and Shore, D. (2018). Sequence-Directed Action of RSC Remodeler and General Regulatory Factors Modulates +1 Nucleosome Position to Facilitate Transcription. Mol Cell *71*, 89-102 e105.

166. Kujirai, T., Ehara, H., Fujino, Y., Shirouzu, M., Sekine, S.I., and Kurumizaka, H. (2018). Structural basis of the nucleosome transition during RNA polymerase II passage. Science *362*, 595-598.

167. Kulaeva, O.I., Hsieh, F.K., Chang, H.W., Luse, D.S., and Studitsky, V.M. (2013). Mechanism of transcription through a nucleosome by RNA polymerase II. Biochim Biophys Acta *1829*, 76-83.

168. Kuryan, B.G., Kim, J., Tran, N.N., Lombardo, S.R., Venkatesh, S., Workman, J.L., and Carey, M. (2012). Histone density is maintained during transcription mediated by the chromatin remodeler RSC and histone chaperone NAP1 in vitro. Proc Natl Acad Sci U S A *109*, 1931-1936.

169. Lai, W.K.M., and Pugh, B.F. (2017). Understanding nucleosome dynamics and their links to gene expression and DNA replication. Nat Rev Mol Cell Biol *18*, 548-562.

170. Langst, G., and Manelyte, L. (2015). Chromatin Remodelers: From Function to Dysfunction. Genes (Basel) *6*, 299-324.

171. Laribee, R.N., Krogan, N.J., Xiao, T., Shibata, Y., Hughes, T.R., Greenblatt, J.F., and Strahl, B.D. (2005). BUR kinase selectively regulates H3 K4 trimethylation and H2B ubiquitylation through recruitment of the PAF elongation complex. Curr Biol *15*, 1487-1493.

172. Larschan, E., and Winston, F. (2001). The S. cerevisiae SAGA complex functions in vivo as a coactivator for transcriptional activation by Gal4. Genes Dev *15*, 1946-1956.

173. Laurent, B.C., Yang, X., and Carlson, M. (1992). An essential Saccharomyces cerevisiae gene homologous to SNF2 encodes a helicase-related protein in a new family. Mol Cell Biol *12*, 1893-1902.

174. Lee, D.H., Gershenzon, N., Gupta, M., Ioshikhes, I.P., Reinberg, D., and Lewis, B.A. (2005). Functional characterization of core promoter elements: the downstream core element is recognized by TAF1. Mol Cell Biol *25*, 9674-9686.

175. Lee, J.B., and Keung, A.J. (2018). Chromatin Immunoprecipitation in Human and Yeast Cells. Methods Mol Biol *1767*, 257-269.

176. Lee, K.K., and Workman, J.L. (2007). Histone acetyltransferase complexes: one size doesn't fit all. Nat Rev Mol Cell Biol *8*, 284-295.

177. Leppek, K., Das, R., and Barna, M. (2018). Functional 5' UTR mRNA structures in eukaryotic translation regulation and how to find them. Nat Rev Mol Cell Biol *19*, 158-174.

178. Lercher, L., Danilenko, N., Kirkpatrick, J., and Carlomagno, T. (2018). Structural characterization of the Asf1-Rtt109 interaction and its role in histone acetylation. Nucleic Acids Res *46*, 2279-2289.

179. Li, B., Carey, M., and Workman, J.L. (2007). The role of chromatin during transcription. Cell *128*, 707-719.

180. Li, H.J. (1975). A model for chromatin structure. Nucleic Acids Res *2*, 1275-1289.

181. Li, Y., Flanagan, P.M., Tschochner, H., and Kornberg, R.D. (1994). RNA polymerase II initiation factor interactions and transcription start site selection. Science *263*, 805-807.

182. Liao, G.B., Li, X.Z., Zeng, S., Liu, C., Yang, S.M., Yang, L., Hu, C.J., and Bai, J.Y. (2018). Regulation of the master regulator FOXM1 in cancer. Cell Commun Signal *16*, 57.

183. Lickwar, C.R., Rao, B., Shabalin, A.A., Nobel, A.B., Strahl, B.D., and Lieb, J.D. (2009). The Set2/Rpd3S pathway suppresses cryptic transcription without regard to gene length or transcription frequency. PLoS One *4*, e4886.

184. Lin, C.L., Chaban, Y., Rees, D.M., McCormack, E.A., Ocloo, L., and Wigley, D.B. (2017). Functional characterization and architecture of recombinant yeast SWR1 histone exchange complex. Nucleic Acids Res *45*, 7249-7260.

185. Lin, Y.C., Choi, W.S., and Gralla, J.D. (2005). TFIIH XPB mutants suggest a unified bacterial-like mechanism for promoter opening but not escape. Nat Struct Mol Biol *12*, 603-607.

186. Lindstrom, K.C., Vary, J.C., Jr., Parthun, M.R., Delrow, J., and Tsukiyama, T. (2006). Isw1 functions in parallel with the NuA4 and Swr1 complexes in stress-induced gene repression. Mol Cell Biol *26*, 6117-6129.

187. Liu, C.L., Kaplan, T., Kim, M., Buratowski, S., Schreiber, S.L., Friedman, N., and Rando, O.J. (2005). Single-nucleosome mapping of histone modifications in S. cerevisiae. PLoS Biol *3*, e328.

188. Longtine, M.S., McKenzie, A., 3rd, Demarini, D.J., Shah, N.G., Wach, A., Brachat, A., Philippsen, P., and Pringle, J.R. (1998). Additional modules for versatile and economical PCR-based gene deletion and modification in Saccharomyces cerevisiae. Yeast *14*, 953-961.

189. Lorch, Y., and Kornberg, R.D. (2017). Chromatin-remodeling for transcription. Q Rev Biophys *50*, e5.

190. Lorch, Y., Kornberg, R.D., and Maier-Davis, B. (2023). Role of the histone tails in histone octamer transfer. Nucleic Acids Res.

191. Lorch, Y., LaPointe, J.W., and Kornberg, R.D. (1987). Nucleosomes inhibit the initiation of transcription but allow chain elongation with the displacement of histones. Cell *49*, 203-210.

192. Loveland, A.B., Demo, G., Grigorieff, N., and Korostelev, A.A. (2017). Ensemble cryo-EM elucidates the mechanism of translation fidelity. Nature *546*, 113-117.

193. Lubliner, S., Regev, I., Lotan-Pompan, M., Edelheit, S., Weinberger, A., and Segal, E. (2015). Core promoter sequence in yeast is a major determinant of expression level. Genome Res *25*, 1008-1017.

194. Luger, K., Mader, A.W., Richmond, R.K., Sargent, D.F., and Richmond, T.J. (1997a). Crystal structure of the nucleosome core particle at 2.8 A resolution. Nature *389*, 251-260.

195. Luger, K., Rechsteiner, T.J., Flaus, A.J., Waye, M.M., and Richmond, T.J. (1997b). Characterization of nucleosome core particles containing histone proteins made in bacteria. J Mol Biol *272*, 301-311.

196. Luo, Z., Lin, C., and Shilatifard, A. (2012). The super elongation complex (SEC) family in transcriptional control. Nat Rev Mol Cell Biol *13*, 543-547.

197. Luse, D.S., and Jacob, G.A. (1987). Abortive initiation by RNA polymerase II in vitro at the adenovirus 2 major late promoter. J Biol Chem *262*, 14990-14997.

198. Mark, K.G., and Rape, M. (2021). Ubiquitin-dependent regulation of transcription in development and disease. EMBO Rep *22*, e51078.

199. Marmorstein, R. (2001). Structure and function of histone acetyltransferases. Cell Mol Life Sci *58*, 693-703.

200. Martin, B.J.E., Brind'Amour, J., Kuzmin, A., Jensen, K.N., Liu, Z.C., Lorincz, M., and Howe, L.J. (2021). Transcription shapes genome-wide histone acetylation patterns. Nat Commun *12*, 210.

201. Mas, G., de Nadal, E., Dechant, R., Rodriguez de la Concepcion, M.L., Logie, C., Jimeno-Gonzalez, S., Chavez, S., Ammerer, G., and Posas, F. (2009). Recruitment of a chromatin remodelling complex by the Hog1 MAP kinase to stress genes. EMBO J *28*, 326-336.

202. Mason, P.B., and Struhl, K. (2005). Distinction and relationship between elongation rate and processivity of RNA polymerase II in vivo. Mol Cell *17*, 831-840.

203. Maxon, M.E., Goodrich, J.A., and Tjian, R. (1994). Transcription factor IIE binds preferentially to RNA polymerase IIa and recruits TFIIH: a model for promoter clearance. Genes Dev *8*, 515-524.

204. Mayer, A., Heidemann, M., Lidschreiber, M., Schreieck, A., Sun, M., Hintermair, C., Kremmer, E., Eick, D., and Cramer, P. (2012). CTD tyrosine phosphorylation impairs termination factor recruitment to RNA polymerase II. Science *336*, 1723-1725.

205. Mayer, A., Lidschreiber, M., Siebert, M., Leike, K., Soding, J., and Cramer, P. (2010). Uniform transitions of the general RNA polymerase II transcription complex. Nat Struct Mol Biol *17*, 1272-1278.

206. Miller, T., Krogan, N.J., Dover, J., Erdjument-Bromage, H., Tempst, P., Johnston, M., Greenblatt, J.F., and Shilatifard, A. (2001). COMPASS: a complex of proteins associated with a trithorax-related SET domain protein. Proc Natl Acad Sci U S A *98*, 12902-12907.

207. Minakhin, L., Bhagat, S., Brunning, A., Campbell, E.A., Darst, S.A., Ebright, R.H., and Severinov, K. (2001). Bacterial RNA polymerase subunit omega and eukaryotic RNA polymerase subunit RPB6 are sequence, structural, and functional homologs and promote RNA polymerase assembly. Proc Natl Acad Sci U S A *98*, 892-897.

208. Mischo, H.E., Gomez-Gonzalez, B., Grzechnik, P., Rondon, A.G., Wei, W., Steinmetz, L., Aguilera, A., and Proudfoot, N.J. (2011). Yeast Sen1 helicase protects the genome from transcription-associated instability. Mol Cell *41*, 21-32.

209. Mischo, H.E., and Proudfoot, N.J. (2013). Disengaging polymerase: terminating RNA polymerase II transcription in budding yeast. Biochim Biophys Acta *1829*, 174-185.

210. Mitchell, L., Huard, S., Cotrut, M., Pourhanifeh-Lemeri, R., Steunou, A.L., Hamza, A., Lambert, J.P., Zhou, H., Ning, Z., Basu, A.*, et al.* (2013). mChIP-KAT-MS, a method to map protein interactions and acetylation sites for lysine acetyltransferases. Proc Natl Acad Sci U S A *110*, E1641-1650.

211. Montel, F., Castelnovo, M., Menoni, H., Angelov, D., Dimitrov, S., and Faivre-Moskalenko, C. (2011). RSC remodeling of oligo-nucleosomes: an atomic force microscopy study. Nucleic Acids Res *39*, 2571-2579.

212. Morawska, M., and Ulrich, H.D. (2013). An expanded tool kit for the auxin-inducible degron system in budding yeast. Yeast *30*, 341-351.

213. Morris, S.A., Rao, B., Garcia, B.A., Hake, S.B., Diaz, R.L., Shabanowitz, J., Hunt, D.F., Allis, C.D., Lieb, J.D., and Strahl, B.D. (2007). Identification of histone H3 lysine 36 acetylation as a highly conserved histone modification. J Biol Chem *282*, 7632-7640.

214. Mosley, A.L., Pattenden, S.G., Carey, M., Venkatesh, S., Gilmore, J.M., Florens, L., Workman, J.L., and Washburn, M.P. (2009). Rtr1 is a CTD phosphatase that regulates RNA polymerase II during the transition from serine 5 to serine 2 phosphorylation. Mol Cell *34*, 168-178.

215. Munoz, S., Jones, A., Bouchoux, C., Gilmore, T., Patel, H., and Uhlmann, F. (2022). Functional crosstalk between the cohesin loader and chromatin remodelers. Nat Commun *13*, 7698.

216. Munoz, S., Minamino, M., Casas-Delucchi, C.S., Patel, H., and Uhlmann, F. (2019). A Role for Chromatin Remodeling in Cohesin Loading onto Chromosomes. Mol Cell *74*, 664-673 e665.

217. Nagarajavel, V., Iben, J.R., Howard, B.H., Maraia, R.J., and Clark, D.J. (2013). Global 'bootprinting' reveals the elastic architecture of the yeast TFIIIB-TFIIIC transcription complex in vivo. Nucleic Acids Res *41*, 8135-8143.

218. Natarajan, K., Jackson, B.M., Rhee, E., and Hinnebusch, A.G. (1998). yTAFII61 has a general role in RNA polymerase II transcription and is required by Gcn4p to recruit the SAGA coactivator complex. Mol Cell *2*, 683-692.

219. Neumann, H., and Wilkins, B.J. (2021). Spanning the gap: unraveling RSC dynamics in vivo. Curr Genet *67*, 399-406.

220. Neuwald, A.F., and Landsman, D. (1997). GCN5-related histone N-acetyltransferases belong to a diverse superfamily that includes the yeast SPT10 protein. Trends Biochem Sci *22*, 154-155.

221. Ng, H.H., Robert, F., Young, R.A., and Struhl, K. (2002). Genome-wide location and regulated recruitment of the RSC nucleosome-remodeling complex. Genes Dev *16*, 806-819.

222. Nishimura, K., Fukagawa, T., Takisawa, H., Kakimoto, T., and Kanemaki, M. (2009). An auxin-based degron system for the rapid depletion of proteins in nonplant cells. Nat Methods *6*, 917-922.

223. Noguchi, C., Singh, T., Ziegler, M.A., Peake, J.D., Khair, L., Aza, A., Nakamura, T.M., and Noguchi, E. (2019). The NuA4 acetyltransferase and histone H4 acetylation promote replication recovery after topoisomerase I-poisoning. Epigenetics Chromatin *12*, 24.

224. Ocampo, J., Chereji, R.V., Eriksson, P.R., and Clark, D.J. (2016). The ISW1 and CHD1 ATP-dependent chromatin remodelers compete to set nucleosome spacing in vivo. Nucleic Acids Res *44*, 4625-4635.

225. Ocampo, J., Chereji, R.V., Eriksson, P.R., and Clark, D.J. (2019). Contrasting roles of the RSC and ISW1/CHD1 chromatin remodelers in RNA polymerase II elongation and termination. Genome Res *29*, 407-417.

226. Ohkuma, Y., Hashimoto, S., Wang, C.K., Horikoshi, M., and Roeder, R.G. (1995). Analysis of the role of TFIIE in basal transcription and TFIIH-mediated carboxy-terminal domain phosphorylation through structure-function studies of TFIIE-alpha. Mol Cell Biol *15*, 4856-4866.

227. Okuda, M., Horikoshi, M., and Nishimura, Y. (2007). Structural polymorphism of chromodomains in Chd1. J Mol Biol *365*, 1047-1062.

228. Oruba, A., Saccani, S., and van Essen, D. (2020). Role of cell-type specific nucleosome positioning in inducible activation of mammalian promoters. Nat Commun *11*, 1075.

229. Otero, G., Fellows, J., Li, Y., de Bizemont, T., Dirac, A.M., Gustafsson, C.M., Erdjument-Bromage, H., Tempst, P., and Svejstrup, J.Q. (1999). Elongator, a multisubunit component of a novel RNA polymerase II holoenzyme for transcriptional elongation. Mol Cell *3*, 109-118.

230. Owen, D.J., Ornaghi, P., Yang, J.C., Lowe, N., Evans, P.R., Ballario, P., Neuhaus, D., Filetici, P., and Travers, A.A. (2000). The structural basis for the recognition of acetylated histone H4 by the bromodomain of histone acetyltransferase gcn5p. EMBO J *19*, 6141-6149.

231. Pai, C.C., Deegan, R.S., Subramanian, L., Gal, C., Sarkar, S., Blaikley, E.J., Walker, C., Hulme, L., Bernhard, E., Codlin, S.*, et al.* (2014). A histone H3K36 chromatin switch coordinates DNA double-strand break repair pathway choice. Nat Commun *5*, 4091.

232. Panse, V.G., and Johnson, A.W. (2010). Maturation of eukaryotic ribosomes: acquisition of functionality. Trends Biochem Sci *35*, 260-266.

233. Papamichos-Chronakis, M., Watanabe, S., Rando, O.J., and Peterson, C.L. (2011). Global regulation of H2A.Z localization by the INO80 chromatin-remodeling enzyme is essential for genome integrity. Cell *144*, 200-213.

234. Parnell, T.J., Huff, J.T., and Cairns, B.R. (2008). RSC regulates nucleosome positioning at Pol II genes and density at Pol III genes. EMBO J *27*, 100-110.

235. Pascual-Garcia, P., Govind, C.K., Queralt, E., Cuenca-Bono, B., Llopis, A., Chavez, S., Hinnebusch, A.G., and Rodriguez-Navarro, S. (2008). Sus1 is recruited to coding regions and functions during transcription elongation in association with SAGA and TREX2. Genes Dev *22*, 2811-2822.

236. Patel, A.B., Louder, R.K., Greber, B.J., Grunberg, S., Luo, J., Fang, J., Liu, Y., Ranish, J., Hahn, S., and Nogales, E. (2018). Structure of human TFIID and mechanism of TBP loading onto promoter DNA. Science *362*.

237. Patel, A.B., Moore, C.M., Greber, B.J., Luo, J., Zukin, S.A., Ranish, J., and Nogales, E. (2019). Architecture of the chromatin remodeler RSC and insights into its nucleosome engagement. Elife *8*.

238. Pathak, R., Singh, P., Ananthakrishnan, S., Adamczyk, S., Schimmel, O., and Govind, C.K. (2018). Acetylation-Dependent Recruitment of the FACT Complex and Its Role in Regulating Pol II Occupancy Genome-Wide in Saccharomyces cerevisiae. Genetics *209*, 743-756.

239. Paule, M.R., and White, R.J. (2000). Survey and summary: transcription by RNA polymerases I and III. Nucleic Acids Res *28*, 1283-1298.

240. Pepenella, S., Murphy, K.J., and Hayes, J.J. (2014). Intra- and inter-nucleosome interactions of the core histone tail domains in higher-order chromatin structure. Chromosoma *123*, 3-13.

241. Perales, R., Erickson, B., Zhang, L., Kim, H., Valiquett, E., and Bentley, D. (2013). Gene promoters dictate histone occupancy within genes. EMBO J *32*, 2645-2656.

242. Petibon, C., Malik Ghulam, M., Catala, M., and Abou Elela, S. (2021). Regulation of ribosomal protein genes: An ordered anarchy. Wiley Interdiscip Rev RNA *12*, e1632.

243. Petrenko, N., Jin, Y., Dong, L., Wong, K.H., and Struhl, K. (2019). Requirements for RNA polymerase II preinitiation complex formation in vivo. Elife *8*.

244. Phelan, M.L., Sif, S., Narlikar, G.J., and Kingston, R.E. (1999). Reconstitution of a core chromatin remodeling complex from SWI/SNF subunits. Mol Cell *3*, 247-253.

245. Prajapati, H.K., Ocampo, J., and Clark, D.J. (2020). Interplay among ATP-Dependent Chromatin Remodelers Determines Chromatin Organisation in Yeast. Biology (Basel) *9*.

246. Pray-Grant, M.G., Daniel, J.A., Schieltz, D., Yates, J.R., 3rd, and Grant, P.A. (2005). Chd1 chromodomain links histone H3 methylation with SAGA- and SLIK-dependent acetylation. Nature *433*, 434-438.

247. Pugh, B.F., and Tjian, R. (1991). Transcription from a TATA-less promoter requires a multisubunit TFIID complex. Genes Dev *5*, 1935-1945.

248. Pulice, J.L., and Kadoch, C. (2016). Composition and Function of Mammalian SWI/SNF Chromatin Remodeling Complexes in Human Disease. Cold Spring Harb Symp Quant Biol *81*, 53-60.

249. Qiu, H., Biernat, E., Govind, C.K., Rawal, Y., Chereji, R.V., Clark, D.J., and Hinnebusch, A.G. (2020). Chromatin remodeler Ino80C acts independently of H2A.Z to evict promoter nucleosomes and stimulate transcription of highly expressed genes in yeast. Nucleic Acids Res *48*, 8408-8430.

250. Qiu, H., Chereji, R.V., Hu, C., Cole, H.A., Rawal, Y., Clark, D.J., and Hinnebusch, A.G. (2016). Genome-wide cooperation by HAT Gcn5, remodeler SWI/SNF, and chaperone Ydj1 in promoter nucleosome eviction and transcriptional activation. Genome Res *26*, 211-225.

251. Qiu, H., Hu, C., and Hinnebusch, A.G. (2009). Phosphorylation of the Pol II CTD by KIN28 enhances BUR1/BUR2 recruitment and Ser2 CTD phosphorylation near promoters. Mol Cell *33*, 752-762.

252. Qiu, H., Hu, C., Yoon, S., Natarajan, K., Swanson, M.J., and Hinnebusch, A.G. (2004). An array of coactivators is required for optimal recruitment of TATA binding protein and RNA polymerase II by promoter-bound Gcn4p. Mol Cell Biol *24*, 4104-4117.

253. Quan, T.K., and Hartzog, G.A. (2010). Histone H3K4 and K36 methylation, Chd1 and Rpd3S oppose the functions of Saccharomyces cerevisiae Spt4-Spt5 in transcription. Genetics *184*, 321-334.

254. Ramachandran, S., Ahmad, K., and Henikoff, S. (2017). Transcription and Remodeling Produce Asymmetrically Unwrapped Nucleosomal Intermediates. Mol Cell *68*, 1038-1053 e1034.

255. Ramachandran, S., and Henikoff, S. (2016). Nucleosome dynamics during chromatin remodeling in vivo. Nucleus *7*, 20-26.

256. Ramakrishnan, S., Pokhrel, S., Palani, S., Pflueger, C., Parnell, T.J., Cairns, B.R., Bhaskara, S., and Chandrasekharan, M.B. (2016). Counteracting H3K4 methylation modulators Set1 and Jhd2 co-regulate chromatin dynamics and gene transcription. Nat Commun *7*, 11949.

257. Ramakrishnan, V. (2002). Ribosome structure and the mechanism of translation. Cell *108*, 557-572.

258. Rando, O.J., and Winston, F. (2012). Chromatin and transcription in yeast. Genetics *190*, 351-387.

259. Rawal, Y., Chereji, R.V., Qiu, H., Ananthakrishnan, S., Govind, C.K., Clark, D.J., and Hinnebusch, A.G. (2018). SWI/SNF and RSC cooperate to reposition and evict promoter nucleosomes at highly expressed genes in yeast. Genes Dev *32*, 695-710.

260. Rawal, Y., Qiu, H., and Hinnebusch, A.G. (2022). Distinct functions of three chromatin remodelers in activator binding and preinitiation complex assembly. PLoS Genet *18*, e1010277.

261. Razin, S.V., and Gavrilov, A.A. (2014). Chromatin without the 30-nm fiber: constrained disorder instead of hierarchical folding. Epigenetics *9*, 653-657.

262. Reinke, H., Gregory, P.D., and Horz, W. (2001). A transient histone hyperacetylation signal marks nucleosomes for remodeling at the PHO8 promoter in vivo. Mol Cell *7*, 529-538.

263. Reinke, H., and Horz, W. (2003). Histones are first hyperacetylated and then lose contact with the activated PHO5 promoter. Mol Cell *11*, 1599-1607.

264. Rimel, J.K., and Taatjes, D.J. (2018). The essential and multifunctional TFIIH complex. Protein Sci *27*, 1018-1037.

265. Robert, F., Pokholok, D.K., Hannett, N.M., Rinaldi, N.J., Chandy, M., Rolfe, A., Workman, J.L., Gifford, D.K., and Young, R.A. (2004). Global position and recruitment of HATs and HDACs in the yeast genome. Mol Cell *16*, 199-209.

266. Robinson, P.J., An, W., Routh, A., Martino, F., Chapman, L., Roeder, R.G., and Rhodes, D. (2008). 30 nm chromatin fibre decompaction requires both H4-K16 acetylation and linker histone eviction. J Mol Biol *381*, 816-825.

267. Robzyk, K., Recht, J., and Osley, M.A. (2000). Rad6-dependent ubiquitination of histone H2B in yeast. Science *287*, 501-504.

268. Roeder, R.G., and Rutter, W.J. (1969). Multiple forms of DNA-dependent RNA polymerase in eukaryotic organisms. Nature *224*, 234-237.

269. Roeder, R.G., and Rutter, W.J. (1970). Specific nucleolar and nucleoplasmic RNA polymerases. Proc Natl Acad Sci U S A *65*, 675-682.

270. Romeo, M.J., Angus-Hill, M.L., Sobering, A.K., Kamada, Y., Cairns, B.R., and Levin, D.E. (2002). HTL1 encodes a novel factor that interacts with the RSC chromatin remodeling complex in Saccharomyces cerevisiae. Mol Cell Biol *22*, 8165-8174.

271. Roth, S.Y., Denu, J.M., and Allis, C.D. (2001). Histone acetyltransferases. Annu Rev Biochem *70*, 81-120.

272. Roy, A.L., and Singer, D.S. (2015). Core promoters in transcription: old problem, new insights. Trends Biochem Sci *40*, 165-171.

273. Ryu, H.Y., Zhao, D., Li, J., Su, D., and Hochstrasser, M. (2020). Histone sumoylation promotes Set3 histone-deacetylase complex-mediated transcriptional regulation. Nucleic Acids Res *48*, 12151-12168.

274. Saha, A., Wittmeyer, J., and Cairns, B.R. (2002). Chromatin remodeling by RSC involves ATP-dependent DNA translocation. Genes Dev *16*, 2120-2134.

275. Sainsbury, S., Bernecky, C., and Cramer, P. (2015). Structural basis of transcription initiation by RNA polymerase II. Nat Rev Mol Cell Biol *16*, 129-143.

276. Sainsbury, S., Niesser, J., and Cramer, P. (2013). Structure and function of the initially transcribing RNA polymerase II-TFIIB complex. Nature *493*, 437-440.

277. Sandelin, A., Carninci, P., Lenhard, B., Ponjavic, J., Hayashizaki, Y., and Hume, D.A. (2007). Mammalian RNA polymerase II core promoters: insights from genome-wide studies. Nat Rev Genet *8*, 424-436.

278. Santisteban, M.S., Kalashnikova, T., and Smith, M.M. (2000). Histone H2A.Z regulats transcription and is partially redundant with nucleosome remodeling complexes. Cell *103*, 411-422.

279. Sanz, A.B., Garcia, R., Rodriguez-Pena, J.M., Nombela, C., and Arroyo, J. (2016). Cooperation between SAGA and SWI/SNF complexes is required for efficient transcriptional responses regulated by the yeast MAPK Slt2. Nucleic Acids Res *44*, 7159-7172.

280. Saunders, A., Core, L.J., and Lis, J.T. (2006). Breaking barriers to transcription elongation. Nat Rev Mol Cell Biol *7*, 557-567.

281. Schlichter, A., Kasten, M.M., Parnell, T.J., and Cairns, B.R. (2020). Specialization of the chromatin remodeler RSC to mobilize partially-unwrapped nucleosomes. Elife *9*.

282. Schneider, J., Bajwa, P., Johnson, F.C., Bhaumik, S.R., and Shilatifard, A. (2006). Rtt109 is required for proper H3K56 acetylation: a chromatin mark associated with the elongating RNA polymerase II. J Biol Chem *281*, 37270-37274.

283. Schreieck, A., Easter, A.D., Etzold, S., Wiederhold, K., Lidschreiber, M., Cramer, P., and Passmore, L.A. (2014). RNA polymerase II termination involves C-terminal-domain tyrosine dephosphorylation by CPF subunit Glc7. Nat Struct Mol Biol *21*, 175-179.

284. Schuster, S.L., and Hsieh, A.C. (2019). The Untranslated Regions of mRNAs in Cancer. Trends Cancer *5*, 245-262.

285. Schwabish, M.A., and Struhl, K. (2004). Evidence for eviction and rapid deposition of histones upon transcriptional elongation by RNA polymerase II. Mol Cell Biol *24*, 10111-10117.

286. Sen, P., Vivas, P., Dechassa, M.L., Mooney, A.M., Poirier, M.G., and Bartholomew, B. (2013). The SnAC domain of SWI/SNF is a histone anchor required for remodeling. Mol Cell Biol *33*, 360-370.

287. Sermwittayawong, D., and Tan, S. (2006). SAGA binds TBP via its Spt8 subunit in competition with DNA: implications for TBP recruitment. EMBO J *25*, 3791-3800.

288. Shahbazian, M.D., and Grunstein, M. (2007). Functions of site-specific histone acetylation and deacetylation. Annu Rev Biochem *76*, 75-100.

289. Shi, Y., Shen, H.M., Gopalakrishnan, V., and Gordon, N. (2021). Epigenetic Regulation of Autophagy Beyond the Cytoplasm: A Review. Front Cell Dev Biol *9*, 675599.

290. Shim, E.Y., Ma, J.L., Oum, J.H., Yanez, Y., and Lee, S.E. (2005). The yeast chromatin remodeler RSC complex facilitates end joining repair of DNA double-strand breaks. Mol Cell Biol *25*, 3934-3944.

291. Shukla, M.S., Syed, S.H., Boopathi, R., Simon, E.B., Nahata, S., Ramos, L., Dalkara, D., Moskalenko, C., Travers, A., Angelov, D.*, et al.* (2019). Generation of Remosomes by the SWI/SNF Chromatin Remodeler Family. Sci Rep *9*, 14212.

292. Shukla, M.S., Syed, S.H., Montel, F., Faivre-Moskalenko, C., Bednar, J., Travers, A., Angelov, D., and Dimitrov, S. (2010). Remosomes: RSC generated non-mobilized particles with approximately 180 bp DNA loosely associated with the histone octamer. Proc Natl Acad Sci U S A *107*, 1936-1941.

293. Simic, R., Lindstrom, D.L., Tran, H.G., Roinick, K.L., Costa, P.J., Johnson, A.D., Hartzog, G.A., and Arndt, K.M. (2003). Chromatin remodeling protein Chd1 interacts with transcription elongation factors and localizes to transcribed genes. EMBO J *22*, 1846-1856.

294. Sims, R.J., 3rd, Chen, C.F., Santos-Rosa, H., Kouzarides, T., Patel, S.S., and Reinberg, D. (2005). Human but not yeast CHD1 binds directly and selectively to histone H3 methylated at lysine 4 via its tandem chromodomains. J Biol Chem *280*, 41789-41792.

295. Sklar, V.E., Schwartz, L.B., and Roeder, R.G. (1975). Distinct molecular structures of nuclear class I, II, and III DNA-dependent RNA polymerases. Proc Natl Acad Sci U S A *72*, 348-352.

296. Slaughter, M.J., Shanle, E.K., Khan, A., Chua, K.F., Hong, T., Boxer, L.D., Allis, C.D., Josefowicz, S.Z., Garcia, B.A., Rothbart, S.B.*, et al.* (2021). HDAC inhibition results in widespread alteration of the histone acetylation landscape and BRD4 targeting to gene bodies. Cell Rep *34*, 108638.

297. Smith, E.R., Eisen, A., Gu, W., Sattah, M., Pannuti, A., Zhou, J., Cook, R.G., Lucchesi, J.C., and Allis, C.D. (1998). ESA1 is a histone acetyltransferase that is essential for growth in yeast. Proc Natl Acad Sci U S A *95*, 3561-3565.

298. Smolle, M., Venkatesh, S., Gogol, M.M., Li, H., Zhang, Y., Florens, L., Washburn, M.P., and Workman, J.L. (2012). Chromatin remodelers Isw1 and Chd1 maintain chromatin structure during transcription by preventing histone exchange. Nat Struct Mol Biol *19*, 884-892.

299. Smolle, M., and Workman, J.L. (2013). Transcription-associated histone modifications and cryptic transcription. Biochim Biophys Acta *1829*, 84-97.

300. Soutourina, J., Bordas-Le Floch, V., Gendrel, G., Flores, A., Ducrot, C., Dumay-Odelot, H., Soularue, P., Navarro, F., Cairns, B.R., Lefebvre, O.*, et al.* (2006). Rsc4 connects the chromatin remodeler RSC to RNA polymerases. Mol Cell Biol *26*, 4920-4933.

301. Spain, M.M., Ansari, S.A., Pathak, R., Palumbo, M.J., Morse, R.H., and Govind, C.K. (2014). The RSC complex localizes to coding sequences to regulate Pol II and histone occupancy. Mol Cell *56*, 653-666.

302. Spain, M.M., and Govind, C.K. (2011). A role for phosphorylated Pol II CTD in modulating transcription coupled histone dynamics. Transcription *2*, 78-81.

303. Spangler, L., Wang, X., Conaway, J.W., Conaway, R.C., and Dvir, A. (2001). TFIIH action in transcription initiation and promoter escape requires distinct regions of downstream promoter DNA. Proc Natl Acad Sci U S A *98*, 5544-5549.

304. Srivatsan, A., Li, B.Z., Szakal, B., Branzei, D., Putnam, C.D., and Kolodner, R.D. (2018). The Swr1 chromatin-remodeling complex prevents genome instability induced by replication fork progression defects. Nat Commun *9*, 3680.

305. Steinmetz, E.J., Warren, C.L., Kuehner, J.N., Panbehi, B., Ansari, A.Z., and Brow, D.A. (2006). Genome-wide distribution of yeast RNA polymerase II and its control by Sen1 helicase. Mol Cell *24*, 735-746.

306. Strahl, B.D., and Allis, C.D. (2000). The language of covalent histone modifications. Nature *403*, 41-45.

307. Strahl, B.D., Grant, P.A., Briggs, S.D., Sun, Z.W., Bone, J.R., Caldwell, J.A., Mollah, S., Cook, R.G., Shabanowitz, J., Hunt, D.F.*, et al.* (2002). Set2 is a nucleosomal histone H3-selective methyltransferase that mediates transcriptional repression. Mol Cell Biol *22*, 1298-1306.

308. Straight, A.F., and Murray, A.W. (1997). The spindle assembly checkpoint in budding yeast. Methods Enzymol *283*, 425-440.

309. Sun, Y., Hu, X., Qiu, D., Zhang, Z., and Lei, L. (2023). rDNA Transcription in Developmental Diseases and Stem Cells. Stem Cell Rev Rep *19*, 839-852.

310. Sun, Z.W., and Allis, C.D. (2002). Ubiquitination of histone H2B regulates H3 methylation and gene silencing in yeast. Nature *418*, 104-108.

311. Sutton, A., Shia, W.J., Band, D., Kaufman, P.D., Osada, S., Workman, J.L., and Sternglanz, R. (2003). Sas4 and Sas5 are required for the histone acetyltransferase activity of Sas2 in the SAS complex. J Biol Chem *278*, 16887-16892.

312. Svetlov, V., and Nudler, E. (2013). Basic mechanism of transcription by RNA polymerase II. Biochim Biophys Acta *1829*, 20-28.

313. Swanson, M.J., Qiu, H., Sumibcay, L., Krueger, A., Kim, S.J., Natarajan, K., Yoon, S., and Hinnebusch, A.G. (2003). A multiplicity of coactivators is required by Gcn4p at individual promoters in vivo. Mol Cell Biol *23*, 2800-2820.

314. Szerlong, H., Hinata, K., Viswanathan, R., Erdjument-Bromage, H., Tempst, P., and Cairns, B.R. (2008). The HSA domain binds nuclear actin-related proteins to regulate chromatin-remodeling ATPases. Nat Struct Mol Biol *15*, 469-476.

315. Takahashi, Y.H., Schulze, J.M., Jackson, J., Hentrich, T., Seidel, C., Jaspersen, S.L., Kobor, M.S., and Shilatifard, A. (2011). Dot1 and histone H3K79 methylation in natural telomeric and HM silencing. Mol Cell *42*, 118-126.

316. Tamaru, H. (2010). Confining euchromatin/heterochromatin territory: jumonji crosses the line. Genes Dev *24*, 1465-1478.

317. Tanguay, R.L., and Gallie, D.R. (1996). Translational efficiency is regulated by the length of the 3' untranslated region. Mol Cell Biol *16*, 146-156.

318. Tramantano, M., Sun, L., Au, C., Labuz, D., Liu, Z., Chou, M., Shen, C., and Luk, E. (2016). Constitutive turnover of histone H2A.Z at yeast promoters requires the preinitiation complex. Elife *5*.

319. Treutlein, B., Muschielok, A., Andrecka, J., Jawhari, A., Buchen, C., Kostrewa, D., Hog, F., Cramer, P., and Michaelis, J. (2012). Dynamic architecture of a minimal RNA polymerase II open promoter complex. Mol Cell *46*, 136-146.

320. Tsankov, A.M., Thompson, D.A., Socha, A., Regev, A., and Rando, O.J. (2010). The role of nucleosome positioning in the evolution of gene regulation. PLoS Biol *8*, e1000414.

321. Tsuchiya, E., Hosotani, T., and Miyakawa, T. (1998). A mutation in NPS1/STH1, an essential gene encoding a component of a novel chromatin-remodeling complex RSC, alters the chromatin structure of Saccharomyces cerevisiae centromeres. Nucleic Acids Res *26*, 3286-3292.

322. Tu, S., Bulloch, E.M., Yang, L., Ren, C., Huang, W.C., Hsu, P.H., Chen, C.H., Liao, C.L., Yu, H.M., Lo, W.S.*, et al.* (2007). Identification of histone demethylases in Saccharomyces cerevisiae. J Biol Chem *282*, 14262-14271.

323. Tyagi, M., Imam, N., Verma, K., and Patel, A.K. (2016). Chromatin remodelers: We are the drivers!! Nucleus *7*, 388-404.

324. Udugama, M., Sabri, A., and Bartholomew, B. (2011). The INO80 ATP-dependent chromatin remodeling complex is a nucleosome spacing factor. Mol Cell Biol *31*, 662-673.

325. Udvardy, A., and Schedl, P. (1984). Chromatin organization of the 87A7 heat shock locus of Drosophila melanogaster. J Mol Biol *172*, 385-403.

326. Ujvari, A., Hsieh, F.K., Luse, S.W., Studitsky, V.M., and Luse, D.S. (2008). Histone N-terminal tails interfere with nucleosome traversal by RNA polymerase II. J Biol Chem *283*, 32236-32243.

327. van Bakel, H., Tsui, K., Gebbia, M., Mnaimneh, S., Hughes, T.R., and Nislow, C. (2013). A compendium of nucleosome and transcript profiles reveals determinants of chromatin architecture and transcription. PLoS Genet *9*, e1003479.

328. Van de Vosse, D.W., Wan, Y., Lapetina, D.L., Chen, W.M., Chiang, J.H., Aitchison, J.D., and Wozniak, R.W. (2013). A role for the nucleoporin Nup170p in chromatin structure and gene silencing. Cell *152*, 969-983.

329. VanDemark, A.P., Kasten, M.M., Ferris, E., Heroux, A., Hill, C.P., and Cairns, B.R. (2007). Autoregulation of the rsc4 tandem bromodomain by gcn5 acetylation. Mol Cell *27*, 817-828.

330. Vannini, A. (2013). A structural perspective on RNA polymerase I and RNA polymerase III transcription machineries. Biochim Biophys Acta *1829*, 258-264.

331. Vannini, A., and Cramer, P. (2012). Conservation between the RNA polymerase I, II, and III transcription initiation machineries. Mol Cell *45*, 439-446.

332. Verrijzer, C.P., Chen, J.L., Yokomori, K., and Tjian, R. (1995). Binding of TAFs to core elements directs promoter selectivity by RNA polymerase II. Cell *81*, 1115-1125.

333. Vinayachandran, V., Reja, R., Rossi, M.J., Park, B., Rieber, L., Mittal, C., Mahony, S., and Pugh, B.F. (2018). Widespread and precise reprogramming of yeast protein-genome interactions in response to heat shock. Genome Res *28*, 357-366.

334. Voichek, Y., Bar-Ziv, R., and Barkai, N. (2016). Expression homeostasis during DNA replication. Science *351*, 1087-1090.

335. Wada, T., Takagi, T., Yamaguchi, Y., Ferdous, A., Imai, T., Hirose, S., Sugimoto, S., Yano, K., Hartzog, G.A., Winston, F.*, et al.* (1998). DSIF, a novel transcription elongation factor that regulates RNA polymerase II processivity, is composed of human Spt4 and Spt5 homologs. Genes Dev *12*, 343-356.

336. Wagner, F.R., Dienemann, C., Wang, H., Stutzer, A., Tegunov, D., Urlaub, H., and Cramer, P. (2020). Structure of SWI/SNF chromatin remodeller RSC bound to a nucleosome. Nature *579*, 448-451.

337. Wang, F., Ranjan, A., Wei, D., and Wu, C. (2016). Comment on "A histone acetylation switch regulates H2A.Z deposition by the SWR-C remodeling enzyme". Science *353*, 358.

338. Wang, S.L., and Cheng, M.Y. (2012). The defects in cell wall integrity and G2-M transition of the Δhtl1 mutant are interconnected. Yeast *29*, 45-57.

339. Wang, X., Ahmad, S., Zhang, Z., Cote, J., and Cai, G. (2018). Architecture of the Saccharomyces cerevisiae NuA4/TIP60 complex. Nat Commun *9*, 1147.

340. Wang, X., Spangler, L., and Dvir, A. (2003). Promoter escape by RNA polymerase II. Downstream promoter DNA is required during multiple steps of early transcription. J Biol Chem *278*, 10250-10256.

341. Weber, C.M., Ramachandran, S., and Henikoff, S. (2014). Nucleosomes are context-specific, H2A.Z-modulated barriers to RNA polymerase. Mol Cell *53*, 819-830.

342. Weiner, A., Hughes, A., Yassour, M., Rando, O.J., and Friedman, N. (2010). High-resolution nucleosome mapping reveals transcription-dependent promoter packaging. Genome Res *20*, 90-100.

343. Weinert, T.A., and Hartwell, L.H. (1988). The RAD9 gene controls the cell cycle response to DNA damage in Saccharomyces cerevisiae. Science *241*, 317-322.

344. Weinmann, R., and Roeder, R.G. (1974). Role of DNA-dependent RNA polymerase 3 in the transcription of the tRNA and 5S RNA genes. Proc Natl Acad Sci U S A *71*, 1790-1794.

345. Weis, L., and Reinberg, D. (1992). Transcription by RNA polymerase II: initiator-directed formation of transcription-competent complexes. FASEB J *6*, 3300-3309.

346. Werner-Allen, J.W., Lee, C.J., Liu, P., Nicely, N.I., Wang, S., Greenleaf, A.L., and Zhou, P. (2011). cis-Proline-mediated Ser(P)5 dephosphorylation by the RNA polymerase II C-terminal domain phosphatase Ssu72. J Biol Chem *286*, 5717-5726.

347. Whitehouse, I., Rando, O.J., Delrow, J., and Tsukiyama, T. (2007). Chromatin remodelling at promoters suppresses antisense transcription. Nature *450*, 1031-1035.

348. Wilson, B., Erdjument-Bromage, H., Tempst, P., and Cairns, B.R. (2006). The RSC chromatin remodeling complex bears an essential fungal-specific protein module with broad functional roles. Genetics *172*, 795-809.

349. Winkler, G.S., Kristjuhan, A., Erdjument-Bromage, H., Tempst, P., and Svejstrup, J.Q. (2002). Elongator is a histone H3 and H4 acetyltransferase important for normal histone acetylation levels in vivo. Proc Natl Acad Sci U S A *99*, 3517-3522.

350. Wolffe, A.P., and Hayes, J.J. (1999). Chromatin disruption and modification. Nucleic Acids Res *27*, 711-720.

351. Wood, A., Schneider, J., Dover, J., Johnston, M., and Shilatifard, A. (2003). The Paf1 complex is essential for histone monoubiquitination by the Rad6-Bre1 complex, which signals for histone methylation by COMPASS and Dot1p. J Biol Chem *278*, 34739-34742.

352. Wu, S.Y., Lee, C.F., Lai, H.T., Yu, C.T., Lee, J.E., Zuo, H., Tsai, S.Y., Tsai, M.J., Ge, K., Wan, Y.*, et al.* (2020). Opposing Functions of BRD4 Isoforms in Breast Cancer. Mol Cell *78*, 1114-1132 e1110.

353. Wyce, A., Xiao, T., Whelan, K.A., Kosman, C., Walter, W., Eick, D., Hughes, T.R., Krogan, N.J., Strahl, B.D., and Berger, S.L. (2007). H2B ubiquitylation acts as a barrier to Ctk1 nucleosomal recruitment prior to removal by Ubp8 within a SAGA-related complex. Mol Cell *27*, 275-288.

354. Xi, Y., Yao, J., Chen, R., Li, W., and He, X. (2011). Nucleosome fragility reveals novel functional states of chromatin and poises genes for activation. Genome Res *21*, 718-724.

355. Xiao, T., Hall, H., Kizer, K.O., Shibata, Y., Hall, M.C., Borchers, C.H., and Strahl, B.D. (2003). Phosphorylation of RNA polymerase II CTD regulates H3 methylation in yeast. Genes Dev *17*, 654-663.

356. Xu, M., and Zhu, B. (2010). Nucleosome assembly and epigenetic inheritance. Protein Cell *1*, 820-829.

357. Xu, Y., Zhang, S., Lin, S., Guo, Y., Deng, W., Zhang, Y., and Xue, Y. (2017). WERAM: a database of writers, erasers and readers of histone acetylation and methylation in eukaryotes. Nucleic Acids Res *45*, D264-D270.

358. Xu, Z., Wei, W., Gagneur, J., Perocchi, F., Clauder-Munster, S., Camblong, J., Guffanti, E., Stutz, F., Huber, W., and Steinmetz, L.M. (2009). Bidirectional promoters generate pervasive transcription in yeast. Nature *457*, 1033-1037.

359. Yan, Q., Moreland, R.J., Conaway, J.W., and Conaway, R.C. (1999). Dual roles for transcription factor IIF in promoter escape by RNA polymerase II. J Biol Chem *274*, 35668-35675.

360. Yang, X.J., and Gregoire, S. (2005). Class II histone deacetylases: from sequence to function, regulation, and clinical implication. Mol Cell Biol *25*, 2873-2884.

361. Yarrington, R.M., Yu, Y., Yan, C., Bai, L., and Stillman, D.J. (2020). A Role for Mediator Core in Limiting Coactivator Recruitment in Saccharomyces cerevisiae. Genetics *215*, 407-420.

362. Ye, Y., Wu, H., Chen, K., Clapier, C.R., Verma, N., Zhang, W., Deng, H., Cairns, B.R., Gao, N., and Chen, Z. (2019). Structure of the RSC complex bound to the nucleosome. Science *366*, 838-843.

363. Yen, K., Vinayachandran, V., Batta, K., Koerber, R.T., and Pugh, B.F. (2012). Genome-wide nucleosome specificity and directionality of chromatin remodelers. Cell *149*, 1461-1473.

364. Yen, K., Vinayachandran, V., and Pugh, B.F. (2013). SWR-C and INO80 chromatin remodelers recognize nucleosome-free regions near +1 nucleosomes. Cell *154*, 1246-1256.

365. Zeng, L., and Zhou, M.M. (2002). Bromodomain: an acetyl-lysine binding domain. FEBS Lett *513*, 124-128.

366. Zhang, H., Roberts, D.N., and Cairns, B.R. (2005). Genome-wide dynamics of Htz1, a histone H2A variant that poises repressed/basal promoters for activation through histone loss. Cell *123*, 219-231.

367. Zheng, Q., Qiu, H., Zhang, H., and Hinnebusch, A.G. (2023). Differential requirements for Gcn5 and NuA4 HAT activities in the starvation-induced versus basal transcriptomes. Nucleic Acids Res.

368. Zhu, W., Wada, T., Okabe, S., Taneda, T., Yamaguchi, Y., and Handa, H. (2007). DSIF contributes to transcriptional activation by DNA-binding activators by preventing pausing during transcription elongation. Nucleic Acids Res *35*, 4064-4075.